MATRIX ENGINEERING MANUAL

Well Performance

Section 200 July 1998

Page 1 of 168

WELL PERFORMANCE

1 Introductory Summary	7
1.1 NODAL* Analysis	9
2 Reservoir System	10
2.1 Inflow Performance Relationship	10
2.2 Single-Phase Flow	11
2.3 Productivity Index	12
2.4 Productivity Ratio	12
2.5 Sources of Information	16
2.6 Important Definitions	17
2.6.1 Permeability	17
2.6.2 Reservoir Thickness	18
2.6.3 Average Reservoir Pressure	18
2.6.4 Skin	18
2.7 Boundary Effects	24
2.8 Two-Phase Flow	28
2.9 Phase Behavior of Hydrocarbon Fluids	29
2.10 Vogel's IPR	29
2.11 Composite IPR	30
2.12 Standing's Extension of Vogel's IPR	31
2.13 Fetkovich Method	33
2.14 Multipoint or Backpressure Testing	33
2.15 Isochronal Tests	35
2.16 Horizontal Wells	38
2.17 Tight Formations	40
2.18 Type Curves	41
2.19 Homogeneous Reservoir Type Curve	41
2.20 Transient IPR	43
2.20.1 Infinite Homogeneous Reservoir	43

July 1998

Page 2 of 168

MATRIX ENGINEERING MANUAL



Well Performance

2.20.2 Homogeneous Reservoir With Induced Vertical Fracture	45
3 Completion System	47
3.1 Pressure Loss in Perforations	49
3.1.1 McLeod Method	49
3.1.2 Karakas and Tariq Method	53
3.1.3 Crushed-Zone Effect	57
3.1.4 Anisotropy Effects	57
3.1.5 Damaged-Zone Effects	57
3.2 Pressure Loss in Gravel Packs	59
4 Flow Through Tubing and Flowlines	62
4.1 Single-Phase Gas Flow in Pipes	63
4.2 Estimation of Static Bottomhole Pressure	65
4.3 Estimation of Flowing Bottomhole Pressure	66
4.4 Multiphase Flow	66
4.5 Liquid Holdup	67
4.6 No-Slip Liquid Holdup	67
4.7 Superficial Velocity	68
4.8 Mixture Velocity	68
4.9 Slip Velocity	68
4.10 Liquid Density	68
4.11 Two-Phase Density	69
4.12 Viscosity	69
4.13 Two-Phase Viscosity	69
4.14 Surface Tension	70
4.15 Multiphase-Flow Pressure Gradient Equations	70
4.16 Two-Phase Friction	71
4.17 Hydrostatic Component	72
4.18 Friction Component	72
4.19 Acceleration Component	72
4.20 Flow Patterns	73

MATRIX ENGINEERING MANUAL

Well Performance

Section 200

July 1998

Page 3 of 168

	4.21 Calculation of Pressure Traverses	77
	4.22 Gradient Curves	78
5	S Well Performance Evaluation Of Stimulated Wells	88
_	5.1 Artificial Lift	
	5.1.1 Pumping Wells	
	5.1.2 Gas-Lift Wells	90
	5.1.2.1 Effect of Stimulation of Gas Lift Wells	91
	5.2 Example Problem — Clay Consolidation	92
	5.3 Example Problem — Pre- and Post-Acid Evaluation	93
	5.4 Example Problem — Producing Well	110
	5.5 Example Problem — Varying Wellbore Radius	111
	5.6 Example Problem — Shot-Density Sensitivity Analysis	114
c	· Dragging Laga Caustians	116
O	6.1 Oil IPR Equations	
	6.1.1 Darcy's Law	
	•	
	6.1.2 Vogel Test Data $\left(\overline{P}_r \leq p_b\right)$	116
	6.1.3 Combination Vogel = Darcy Test Data $(\overline{P}_r > p_b)$	117
	6.1.4 Jones IPR	
	6.2 Gas IPR Equations	119
	6.2.1 Darcy's Law (Gas)	
	6.2.2 Jones' Gas IPR (General Form)	119
	6.3 Backpressure Equation	120
	6.4 Transient Period Equations	121
	6.4.1 Time to Pseudosteady State	121
	6.4.2 Oil IPR (Transient)	121
	6.4.3 Gas IPR (Transient)	121
	6.5 Completion Pressure Drop Equations	122
	6.5.1 Gravel-Packed Wells	122
	6.5.2 Open Perforation Pressure Drop	123

July 1998

Page 4 of 168

MATRIX ENGINEERING MANUAL



Well Performance

7 Fluid Physical Properties Correlations	125
7.1 Oil Properties	125
7.2 Gas Solubility	126
7.3 Formation Volume Factor of Oil	127
7.4 Oil Viscosity	130
7.5 Gas Physical Properties	134
7.6 Real Gas Deviation Factor	135
7.7 Gas Viscosity	138
7.8 Rock and Fluid Compressibility	140
7.9 Oil Compressibility (c_o)	140
7.10 Gas Compressibility	142
7.11 Rock Pore Volume Compressibility	144
8 Vertical Pressure Flowing Gradient Curves	148
9 Calculation Of Gas Velocity	164
10 Partial Penetration	166
	100
11 Prats' Correlation	
11 Prats' CorrelationFIGURES	
	168
Fig. 1. Possible pressure losses in the producing system for a flowing well	9
Fig. 1. Possible pressure losses in the producing system for a flowing well	910
Fig. 1. Possible pressure losses in the producing system for a flowing well	9101115
Fig. 1. Possible pressure losses in the producing system for a flowing well	910111517
Fig. 1. Possible pressure losses in the producing system for a flowing well	91011151719
Fig. 1. Possible pressure losses in the producing system for a flowing well	91011151719
Fig. 1. Possible pressure losses in the producing system for a flowing well	
Fig. 1. Possible pressure losses in the producing system for a flowing well	168910151719202323
Fig. 1. Possible pressure losses in the producing system for a flowing well	168101115171920232323
Fig. 1. Possible pressure losses in the producing system for a flowing well	168910151719202323232323
Fig. 1. Possible pressure losses in the producing system for a flowing well	16891015171920232329313234

MATRIX ENGINEERING MANUAL

Well Performance

Section 200

July 1998

Page 5 of 168

		$(\overline{p}^2 - p^2)$	
Fig.	17.	$(\overline{p}_r^2 - p_{wfs}^2)$ versus q for isochronal test	37
Fig.	18.	Graph of log C versus log t for isochronal test.	37
Fig.	19.	Modified isochronal test, flow rate and pressure diagrams	38
Fia	20	$(\overline{p}_r^2 - p_{wf}^2)$ versus q for isochronal test	38
rig. Fia	20.	Horizontal well drainage model.	
_		Homogeneous reservoir type curve.	
		Constant rate type curve for finite-conductivity fracture–closed square system	40
ı ıg.	20.	$(x_e/y_e = 1)$	46
Fia	24	Typical shaped charge.	48
		Jet/slug formation	
_		Approximate jet velocities and pressures.	
		Flow into a perforation	
		Plot of flow rate versus pressure drop for varying shot densities.	
		Perforation geometry	
_		Gravel pack schematic	
		Cross section of gravel pack across a perforation tunnel	
		Pipe friction factors for turbulent flow (modified after Moody, L.F., Trans. ASME,	
3		66, 671, 1944).	. 65
Fig.	31a	Flow patterns for 20.09-cp viscosity, 0.851-specific gravity oil, and water mixtures	
3		in a 1.04-in. pipe based on observations of Govier, Sullivan and Wood, 1961	74
Fig.	31b	Figure showing the liquid velocity profile in stratified flow.	. 75
		Predicted flow pattern transition lines superimposed on the observed flow pattern	
•		map for kerosene in vertical uphill flow	75
Fig.	33.	Predicted flow pattern transition lines superimposed on the observed flow pattern	
		map for kerosene in uphill 30° flow	76
Fig.	34.	Predicted flow pattern transition lines superimposed on the observed flow pattern	
		map for kerosene in horizontal flow	76
_		Vertical multiphase flow: How to find the flowing bottomhole pressure	
_		Vertical multiphase flow: How to find the flowing wellhead pressure	
_		Horizontal multiphase flow: How to find the flowing wellhead pressure	
		Vertical water injection: How to find discharge pressure	
		Vertical flowing pressure gradients.	84
Fig.	40.	This figure was used to determine $p_{wf} = 800$ psig for a rate of 400 BPD through	
		2-in. ID tubing.	85
Fig.	41.	This figure was used to determine $p_{wf} = 910$ psig for a rate of 600 BPD through	
			86
Fig.	42.	This figure was used to determine $P_{wfs} = 1080$ psig for a rate of 800 BPD through	
	4.0	2-in. ID tubing.	87
Fig.	43.	This figure shows a tubing intake or outflow performance curve for a wellhead	
		pressure of 100 psig.	88
Fig.		Net payout at any time = Extra revenue from oil or gas production due to	0.0
-: -		stimulation at any time, t - cost of stimulation.	
		Effect of subsurface pumps of well pressure profile	
rıg.	46.	Showing potential problems in a pumping well through IPR curves	90

July 1998

Page 6 of 168

MATRIX ENGINEERING MANUAL

Well Performance

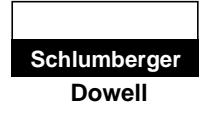


Fig. 47.	Unloading wells with gas lift	91
Fig. 48.	Effect of moving damage away from the wellbore	92
Fig. 49.	Pressure/flowrate history	98
Fig. 50.	Diagnostic plot.	99
Fig. 51.	Dimensionless superposition.	100
Fig. 52.	Production potential evaluation, Nodal plot	100
Fig. 53.	Production potential evaluation, rate versus wellhead pressure	101
Fig. 54.	Production potential evaluation, well performance rate versus shot density	101
Fig. 55.	Pressure/flowrate history.	105
Fig. 56.	Post-acid test validation, diagnostic plot	107
Fig. 57.	Post-acid test validation, dimensionless superposition	107
	Post-acid production evaluation, Nodal plot	
Fig. 59.	Post-acid production evaluation, rate versus wellhead pressure	108
	Example 5.3 IPR and tubing intake curve	
Fig. 61.	Plot of tubing intake versus production rates for different rw	112
Fig. 62.	Plot of flow rate versus effective wellbore radius	.113
Fig. 63.	Plot of flow rate versus pressure drop for varying shot densities	.114
	Plot of shot density versus flow rate.	
Fig. 65.	Variation of gas solubility with pressure and temperature	126
Fig. 66.	Variation of formation volume factor with pressure and temperature	127
Fig. 67.	Properties of natural mixtures of hydrocarbon gas and liquids, formation volume of	
	gas plus liquid phase (after Standing).	129
Fig. 68.	Properties of natural mixtures of hydrocarbon gas and liquids, bubble-point	
	pressure (after Standing)	
_	Variation of oil viscosity with pressure.	
•	Dead oil viscosity at reservoir temperature and atmospheric pressure (after Beal)	
_	Viscosity of gas-saturated crude oil at reservoir temperature and pressure	
_	Rate of increase of oil viscosity above bubble-point pressure (after Beal)	134
Fig. 73.	Correlation of pseudocritical properties of condensate well fluids and miscellaneous	
	natural gas with fluid gravity (after Brown et al.)	
Fig. 74.	Real gas deviation factor for natural gases as a function of pseudoreduced pressure	
	and temperature (after Standing and Katz).	137
	Viscosity of natural gases at 1 atm (after Carr, Kobayashi, and Burrows)	
Fig. 76.	Effect of temperature and pressure on gas viscosity: μ_{ga} (after Carr, Kobayashi, and	
		139
_	Correlation of pseudoreduced compressibility for an undersaturated oil (after Trube)	.141
Fig. 78.	Approximate correlation of liquid pseudocritical pressure and temperature with	
	specific gravity (after Trube).	
_	Effect of dissolved gas on water compressibility (after Dodson and Standing)	
_	Correlation of pseudoreduced compressibility for natural gases (after Trube)	
_	Correlation of pseudoreduced compressibility for natural gases (after Trube)	.144
Fig. 82.	Pore-volume compressibility at 75% lithostatic pressure versus initial sample	
- ! ••	porosity for limestones (after Newman)	145
Fig. 83.	Pore-volume compressibility at 75% lithostatic pressure versus initial sample	
	porosity for fiable sandstones (after Newman)	146

MATRIX ENGINEERING MANUAL

Well Performance

Section 200 July 1998

Page 7 of 168

Fig. 84. Pore-volume compressibility at 75% lithostatic pressure versus initial sample	
porosity for consolidated sandstones (after Newman)	147
Fig. 85. Vertical flowing pressure gradients. All oil - 1000 BPD	148
Fig. 86. Vertical flowing pressure gradients. All oil - 1500 BPD	149
Fig. 87. Vertical flowing pressure gradients. All oil - 2000 BPD	
Fig. 88. Vertical Flowing pressure gradients. 50% oil - 50% water - 500 BPD	151
Fig. 89. Vertical fowing presssure gradients. All oil - 500 BPD	152
Fig. 90. Vertical flowing pressure gradients. All oil - 800 BPD	153
Fig. 91. Vertical flowing pressure gradients. All oil - 1000 BPD	
Fig. 92. Vertical flowing pressure gradients. All oil - 1500 BPD	
Fig. 93. Vertical flowing pressure gradients. All oil - 2000 BPD	
Fig. 94. Vertical flowing pressure gradients. All oil - 3000 BPD.	
Fig. 95. Vertical flowing pressure gradients. All oil - 1000 BPD	
Fig. 96. Vertical flowing pressure gradients. All oil - 2000 BPD	
Fig. 97. Vertical flowing pressure gradients. All oil - 3000 BPD	
Fig. 98. Vertical flowing pressure gradients. All oil - 4000 BPD	
Fig. 99. Vertical flowing pressure gradients. All oil - 6000 BPD.	
Fig. 100. Vertical flowing pressure gradients. All oil - 8000 BPD	
Fig. 101. Partial penetration.	
Fig. 102. Pseudo-skin factor (S _R) nomograph	
Fig. 103. Dimensionless wellbore radius versus C _{fD} ·	168
TABLES	
Table 1. Factors For Different Shapes and Well Positions in a Drainage Area Where A =	
Drainage Area of System Shown and A ^{1/2} /r _e is Dimensionless	
Table 2. Dependence of σ_{θ} on Phasing	
Table 3. Variables C ₁ and C ₂	
Table 4. Vertical Skin Correlation Coefficients	
Table 5. Skin Due to Boundary Effect, 180° Phasing	57

1 Introductory Summary

A well can be defined as an interfacing conduit between the oil and gas reservoir and the surface handling facility. This interface is needed to produce reservoir fluid to the surface, making it a tangible asset. The physical description of a well is quite involved. For optimal production, a well design requires some complex engineering considerations. The optimal production refers to a maximum return on investment. The physical description of a typical oil or gas well is shown in Fig. 1.

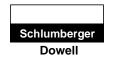
In the performance of a well the drainage volume of the reservoir draining to the well plays an important role. A well combined with the reservoir draining into it is normally called an oil or gas production system. A production system is thus composed of the following major components.

Section 200 July 1998

Page 8 of 168

MATRIX ENGINEERING MANUAL

Well Performance



- porous medium
- completion (stimulation, perforations, and gravel pack)
- vertical conduit with safety valves and chokes
- horizontal flowlines with chokes, and other piping components, for example, valves and elbows.

In an oil or gas production system, the fluids flow from the drainage in the reservoir to the separator at the surface. The average pressure within the drainage boundary is often called the average reservoir pressure. This pressure controls the flow through a production system and is assumed to remain constant over a fixed time interval during depletion. When this pressure changes, the well's performance changes and thus the well needs to be re-evaluated. The average reservoir pressure changes because of normal reservoir depletion or artificial pressure maintenance with water, gas, or other chemical injection.

The separator pressure at the surface is designed to optimize production and to retain lighter hydrocarbon components in the liquid phase. This pressure is maintained by using mechanical devices, for example, pressure regulators. As the well produces or injects, there is a continuous pressure gradient from the reservoir to the separator. It is common to use wellhead pressure for the separator pressure in production system analysis calculations assuming that the separator is at the wellhead or very near it. These assumptions imply negligible pressure loss in the flowline.

MATRIX ENGINEERING MANUAL

Well Performance

Section 200 July 1998

Page 9 of 168

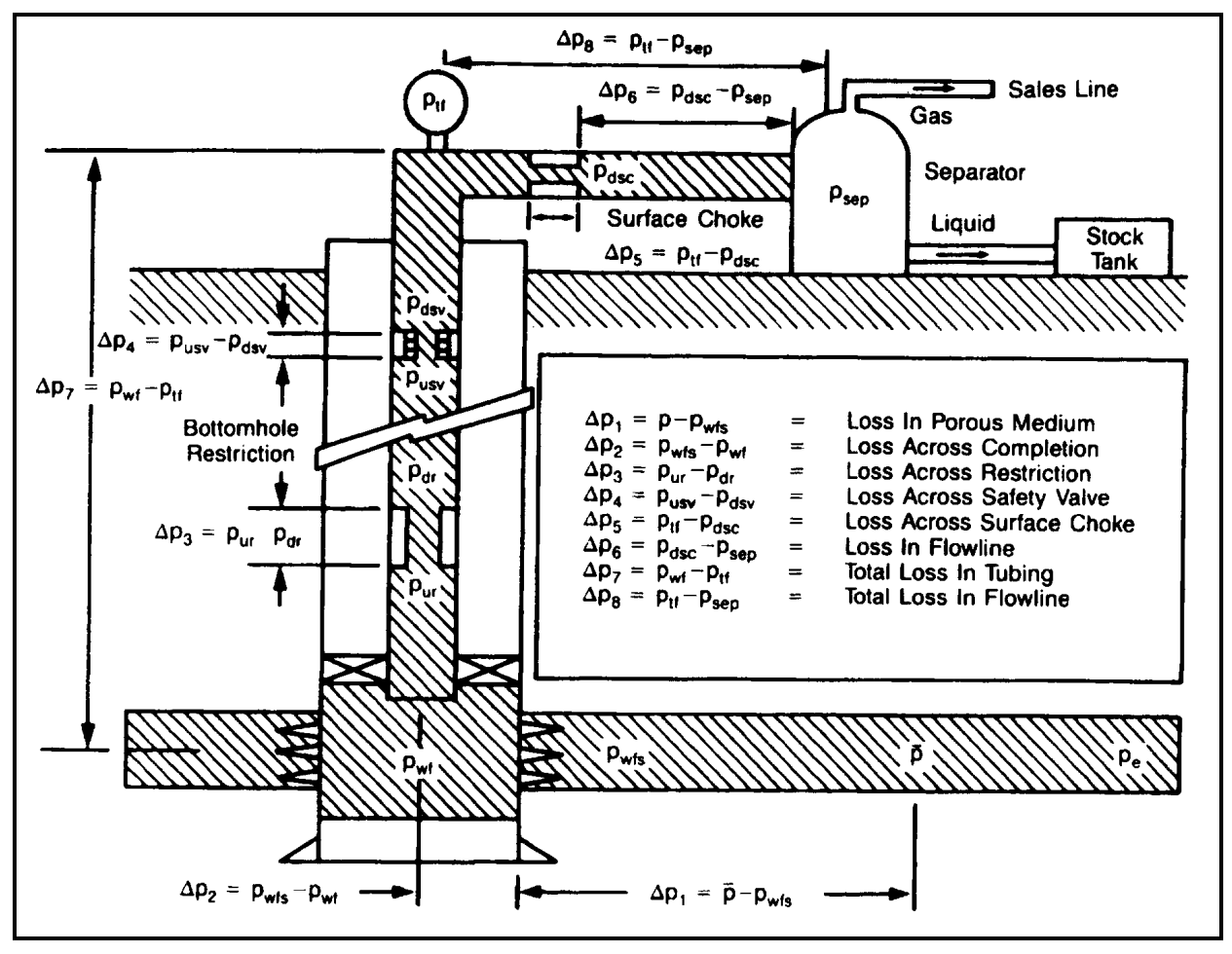


Fig. 1. Possible pressure losses in the producing system for a flowing well.

1.1 NODAL* Analysis

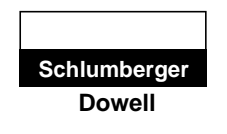
A node is any point in the production system (Fig. 2) between the drainage boundary and the separator, where the pressure can be calculated as a function of the flow rate. The two extreme nodes in the complex production system are the reservoir drainage boundary (8) and the separator (1). The pressures at these nodes are called the average reservoir pressure (\bar{p}_r) and the separator pressure (p_{sep}). The other two important nodes are the bottomhole (6), where the bottomhole flowing pressure (p_{vef}) is measured by a downhole gauge, and the wellhead (3) where the wellhead pressure (p_{vef}) is measured by a gauge attached to the Christmas tree or the flow arm. If the pressures are measured or calculated at each node, then the pressure loss between the nodes can be calculated as a function of the flow rate. Nodes (2, 4, and 5 in Fig. 2) where a pressure drop occurs across the node due to the presence of a choke, restrictions (safety valves), and other piping components are called the functional nodes. For each component in the production system, for

_

^{*} Mark of Schlumberger

Section 200		
July 1998		
Page 10 of 168		

Well Performance



example, the porous medium, completion, tubulars and chokes, the flow rate (q) is functionally related to the pressure differential (Δp) across the component (Eq. 1).

$$q = f(\Delta p) \tag{1}$$

The following sections establish mathematical relationships for different component segments of the production system. Based on these relationships, the parameters that are important for the optimization of production through these components are discussed. NODAL systems analysis is used as a method of combining all these component system design procedures to help design and optimize the total system.

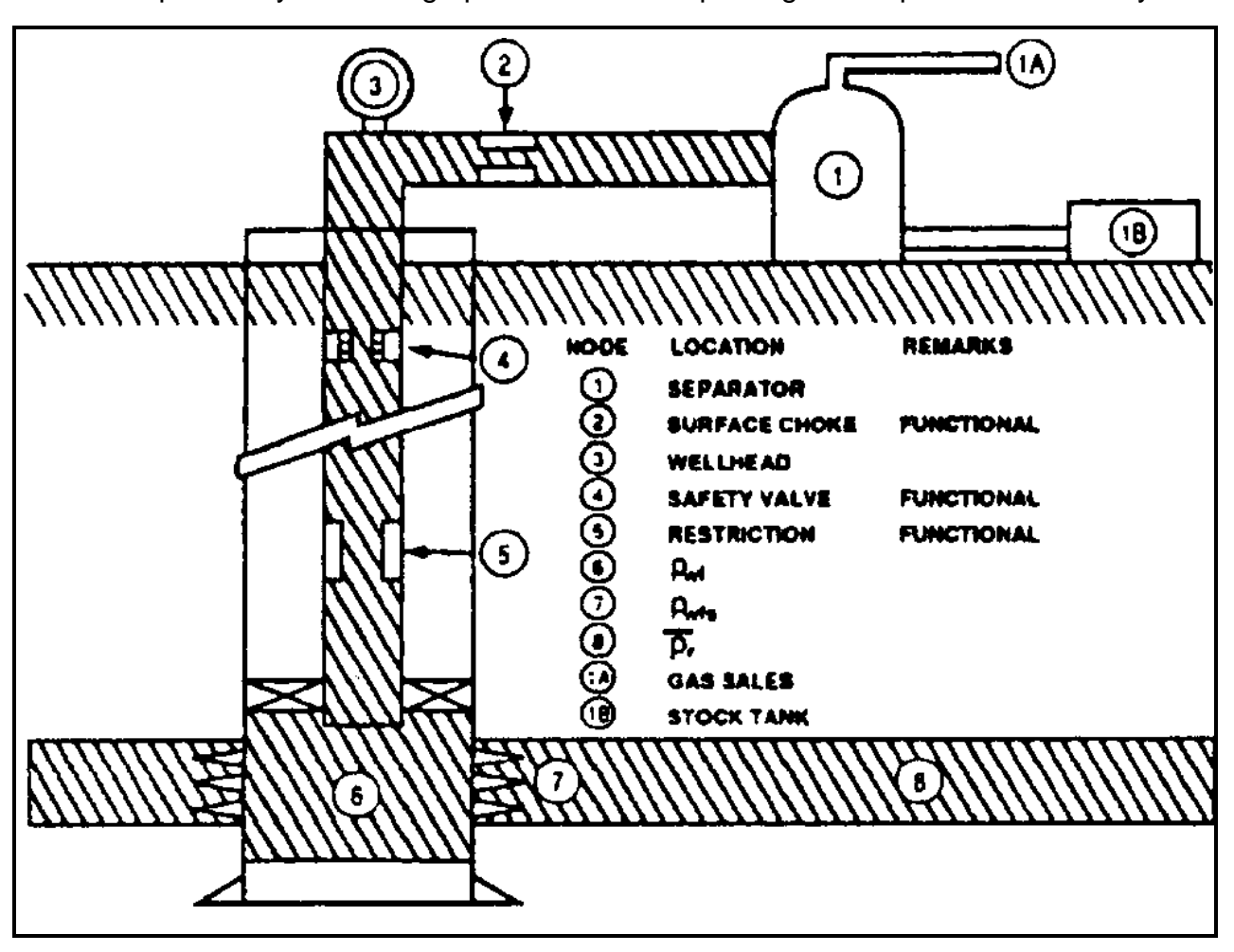


Fig. 2. Location of various nodes.

2 Reservoir System

2.1 Inflow Performance Relationship

The Inflow Performance Relationship (IPR) is defined as the functional relationship between the production rate and the bottomhole flowing pressure. Gilbert (1954) first proposed well analysis using this relationship. IPR is defined in the pressure range

MATRIX ENGINEERING MANUAL

Well Performance

Section 200
July 1998
Page 11 of 168

between the average reservoir pressure and atmospheric pressure. The flow rate corresponding to the atmospheric bottomhole flowing pressure is defined as the absolute open flow potential of the well, whereas the flow rate at the average reservoir pressure bottomhole is always zero. A typical inflow performance relationship is shown in Fig. 3.

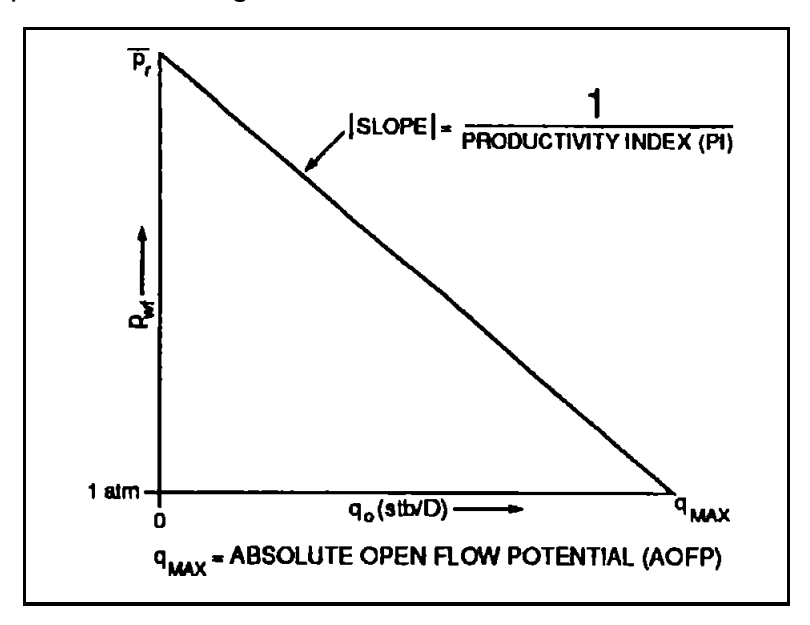


Fig. 3. A typical IPR curve.

2.2 Single-Phase Flow

For single-phase oil or liquids, the inflow performance relationship shown in Fig. 3 is stated by Darcy's law for radial flow (Eq. 2).

$$q_{o} = \frac{7.08 \times 10^{-3} \ k_{o} \ h \ (\overline{p}_{r} - p_{wf})}{\mu_{o} \ B_{o} \left[ln \left(\frac{r_{e}}{r_{w}} \right) - 0.75 + s_{t} + Dq_{o} \right]}$$
(2)

where:

 q_o = oil flow rate into the well (stb/D),

 B_o = formation volume factor of oil (bbl/stb) (defined in Section 7),

 μ_{o} = viscosity of oil (cp) (Section 7),

 k_o = permeability of the formation to oil (md),

h = net thickness of the formation (ft),

 \overline{p}_r = average reservoir pressure (psia),

 p_{wf} = bottomhole flowing pressure (psia),

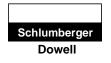
 r_e = radius of drainage (ft)

July 1998

Page 12 of 168

MATRIX ENGINEERING MANUAL

Well Performance



= $\sqrt{\frac{A}{\pi}}$ where A is area of circular drainage in sq ft,

 r_{w} = wellbore radius (ft),

 s_t = total skin,

 Dq_o = pseudo skin due to turbulence. In oil wells, this term is insignificant especially for low permeability reservoirs.

It can be shown that, for $r_e = 1466$ ft, $r_w = 0.583$ ft, $s_t = 0$ and no turbulence, Darcy's law simplifies to (Eq. 3)

$$q_o = \frac{kh}{\mu_o B_o} (\overline{p}_r - p_{wf}) (k \text{ in darcy})$$
 (3)

Eq. 3 is often used to estimate the flow rates of oil wells.

2.3 Productivity Index

An inflow performance relationship based on Darcy's law is a straight line relationship as shown in Fig. 3. Absolute open flow potential (AOFP) is the maximum flow rate the well can flow with atmospheric pressure at the bottomhole. The Productivity Index (PI) is the absolute value of the slope of the IPR straight line (Eq. 4).

$$PI = \frac{q}{(\overline{p}_r - p_{wf})} \tag{4}$$

Based on Darcy's law,

$$PI_{oil} = \frac{7.08 \times 10^{-3} k_o h}{\mu_o B_o \left[ln \left(\frac{r_e}{r_w} \right) - 0.75 + s_t \right]} = \frac{q_o}{(\overline{p}_r - p_{wf})}, \left(\frac{bbl}{psi - D} \right)$$
 (5)

The PI concept is not used for gas wells, as the IPR for a gas well is not a straight line but a curve.

2.4 Productivity Ratio

The productivity ratio is defined as the ratio of the actual Productivity Index to the ideal Productivity Index (total skin = 0).

Productivity Ratio =
$$\frac{PI(actual)}{PI(ideal, s = 0)}$$

MATRIX ENGINEERING MANUAL

Well Performance

Section	on	200
July	19	98

Page 13 of 168

$$= \frac{\left[ln\left(\frac{r_e}{r_w}\right) - 0.75\right]}{\left[ln\left(\frac{r_e}{r_w}\right) - 0.75 + s_t\right]}$$
$$= \frac{\overline{p}_r - p_{wf} - \Delta p_{skin}}{\overline{p}_r - p_{wf}}$$

where:

$$\Delta p_{skin} = 0.87 \text{m } s_t$$

$$= 0.87 \left(\frac{162.6 \ q\mu B}{kh} \right) s_t$$

m = slope of semilog straight line (Horner or MDH).

The productivity ratio is also called the flow efficiency, completion factor, or condition ratio.

Example

Darcy's Law is perhaps the most important relationship in petroleum reservoir engineering. It relates rate with the pressure drawdown and is often used to decide on an appropriate stimulation treatment. The following exercises illustrate uses of Darcy's Law:

Oil Well

$$q = \frac{kh \left(p_e - p_{wf}\right)}{141.2 \; B\mu \left(ln \frac{r_e}{r} + s\right)}$$

h (reservoir thickness) = 50 ft,

 p_e (initial reservoir pressure) = 3000 psi,

 p_{wf} (flowing bottomhole pressure) = 1000 psi,

B (formation volume factor) = 1.1 res bbl/stb,

 μ (viscosity) = 0.7 cp,

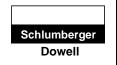
 r_{w} (well radius) = 0.328 ft (7-7/8 in. well)

Section 200 July 1998

Page 14 of 168

MATRIX ENGINEERING MANUAL

Well Performance



Impact of Drainage Area

A (acres)	r _e (ft)	$\ln (r_e/r_w)$	Rate Decrease ($s = 0$)
40	745	7.73	
80	1053	8.07	4%
160	1489	8.42	9%
640	2980	9.11	16%

Increasing the drainage area by a factor of 16 results in a maximum rate decrease by 16%. The drainage area for a steady state reservoir does not have a major impact on the rate; however, the drainage radius may have a profound effect on the cumulative recovery of the well.

Impact of Permeability and Skin

For the given variables
$$q = \frac{920 \text{ k}}{7.73 + \text{s}}$$

s = 0		s = 10		
<i>k</i> (md)	q (STB/D)	k (md)	q (STB/D)	
10.0	1190	10.0	519	
1.0	119	1.0	52	
0.1	12	0.1	5	
0.01	1.2	0.01	0.5	

If k = 10 md, elimination of skin from 10 to 0 would result in more than 600 STB/D increase (that is, candidate for matrix acidizing).

If k = 0.1 md, elimination of skin would lead to a maximum increase of 7 STB/D.

MATRIX ENGINEERING MANUAL

Well Performance

Section 200
July 1998
Page 15 of 168

Example

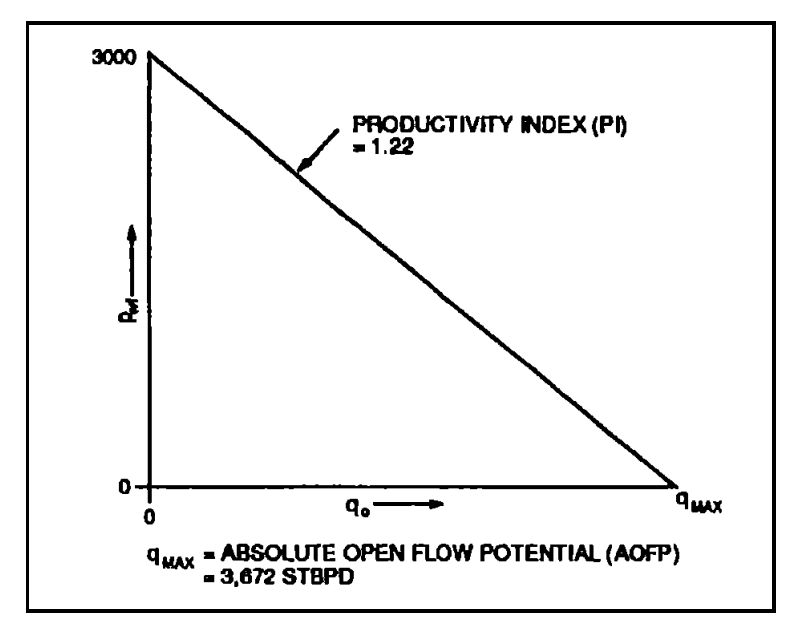


Fig. 4. IPR curve for the example problem.

For the following oil-well data:

- (a) calculate the absolute open flow potential and draw the inflow performance relationship curve
- (b) calculate the Productivity Index.

Data

Permeability, k_o = 30 md Pay thickness, h = 40 ft

Average reservoir pressure, $\overline{p}_r = 3000 \text{ psig}$

Reservoir temperature, T = 200° F

Well spacing, A = 160 acres $(43,560 \text{ ft}^2/\text{acre})$

Drilled hole size, D = 12-1/4 in. (open hole)

Formation volume factor, $B_o = 1.2 \text{ (bbl/STB)}$

Oil viscosity, μ_o = 0.8 cp

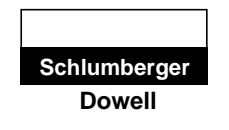
(assume skin = 0 and no turbulence)

July 1998

Page 16 of 168

MATRIX ENGINEERING MANUAL

Well Performance



Solution

(a) Drainage radius,
$$r_e = \sqrt{\frac{A \times 43,560}{\pi}} ft$$

= 1490 ft

Wellbore radius, $r_w = 0.51$ ft

Applying Darcy's law for radial flow,

$$q_o = \frac{7.08 \times 10^{-3} k h (\overline{p}_r - p_{wf})}{\mu_o B_o \left[ln \left(\frac{r_e}{r_w} \right) - 0.75 \right]}$$

Absolute open-flow potential,

$$q_o = \frac{7.08 \times 10^{-3} \; (30 \times 40) \; (3000 - 0)}{(0.8 \times 1.2) \left[ln \left(\frac{1.490}{0.51} \right) - 0.75 \right]}$$

$$q_o = \frac{26.550}{7.23} = 3672 \text{ stb}/D$$

(b) Productivity Index =
$$\frac{q}{\overline{p}_r - p_{wf}} = \frac{7.08 \times 10^{-3} \ k h}{\mu_o B_o \left[ln \left(\frac{r_e}{r_w} \right) - 0.75 \right]}$$
$$= 1.22 \left(\frac{bbl}{psi - D} \right)$$

2.5 Sources of Information

Transient Well Tests

A transient well test interpretation, for example, buildup, drawdown, and interference provides the permeability height/viscosity term, average reservoir pressure and total skin.

In injection wells, the buildup test is called a fall-off test, and the drawdown test is called an injectivity test.

Special Well Tests

Special well tests, that is, extended drawdown or reservoir limit tests, are used to determine the drainage shape and drainage radius.

Well Logs and Cores

Well logs and cores are also used to determine permeability and reservoir thickness.

MATRIX ENGINEERING MANUAL

Well Performance

Section 200
July 1998
Page 17 of 168

If properly conducted and interpreted, well test interpretation methods yield the most representative values of reservoir parameters such as permeability height/viscosity, average reservoir pressure and total skin. These values are normally the volumetric average values in the radius of investigation, whereas logs and cores determine the permeability value at discrete points around the wellbore.

2.6 Important Definitions

2.6.1 Permeability

The permeability (k) is a rock property that measures the transmissivity of fluids through the rock. In the simplest form, Darcy's law when applied to a rectangular slab of rock is:

$$q = \frac{kA(p_1 - p_2)}{\mu L}$$

where:

q = volumetric flow rate (cc/sec),

 μ = viscosity of fluid (cp),

k = permeability of the rock (darcy),

L = length of the rock (cm),

A = area of cross section of flow (cm²),

 p_1 - p_2 = pressure difference (atmosphere).

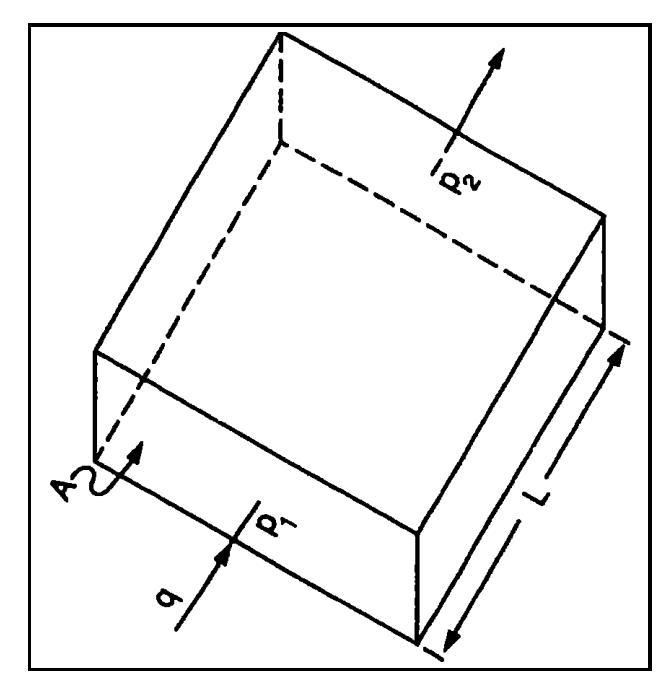
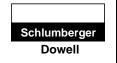


Fig. 5. Darcy's law for linear flow.

Section 200 July 1998

MATRIX ENGINEERING MANUAL

Well Performance



Page 18 of 168

From this equation, a permeability of one darcy of a porous medium is defined when a single-phase fluid of one centipoise viscosity that completely fills the voids of the medium will flow through it, under viscous flow at a rate of one cubic centimeter per second per square centimeter cross-sectional area under a pressure gradient of one atmosphere per centimeter. This definition applies mainly to matrix permeability. In carbonates, some sandstones, coals, or other formations that often contain solution channels and natural or induced fractures, these channels or fractures change the effective permeability of the total rock mass. It can be shown that in a low-permeability matrix, a few cracks or fractures can make an order of magnitude change in the effective permeability of the rock. It can also be shown that the permeability (in darcies) of a fracture of width "w" (in inches) per unit height is given by:

$$k = 54.4 \times 10^6 w^2$$
.

Consequently, a fracture of 0.01 in. width in a piece of rock will be equivalent to the rock having a permeability of 5400 darcies. Note that a few cracks in a low-permeability matrix may substantially increase the effective permeability of the bulk rock.

2.6.2 Reservoir Thickness

The net pay thickness (h) is the average thickness of the formation in the drainage area through which the fluid flows into the well. It is not just the perforated interval or the formation thickness encountered by the well.

2.6.3 Average Reservoir Pressure

If all the wells in the reservoir are shut in, the stabilized reservoir pressure is called the average reservoir pressure \overline{p}_r . The best method of obtaining an estimate of this pressure is by conducting a buildup test.

2.6.4 Skin

During drilling and completion, the permeability of the formation near the wellbore is often altered. This altered zone of permeability is called the damage zone. The invasion by drilling fluids, dispersion of clays, presence of mudcake and cement, and presence of high saturation of gas around the wellbore are some of the factors responsible for reduction in the permeability. However, a successful stimulation treatment results in an effective improvement of permeability near the wellbore, thus reducing the skin due to damage. The skin factor determined from a well test analysis reflects any near-wellbore mechanical or physical phenomena that restrict flow into the wellbore. The most common causes of these restrictions, in addition to damage, are due to the partial penetration of the well into the formation, limited perforations, plugging of perforations, and turbulence (Dq). These non-damage related skins are commonly known as the pseudoskin. It is important to note that the

MATRIX ENGINEERING MANUAL

Well Performance

Section 200 July 1998

Page 19 of 168

total skin including turbulence can be as high as 100 or even more in a poorly completed well; the minimum skin in a highly stimulated well is about -5.

The total skin factor (s_i) is a constant which relates the pressure drop in the skin to the flow rate and transmissivity of the formation (Fig. 6). Thus,

$$s_t = \frac{\Delta p_{skin}}{\left(\frac{141.2 \ q\mu_o \ B_o}{kh}\right)}$$

$$\Delta p_{skin} = 0.87 \text{ m } s_t$$
$$= (p'_{wf} - p_{wf}) \text{ in Fig. 6}$$

where:

 m = slope of semi-log straight line from Horner or Miller, Dyes and Hutchinson obtained from a buildup or drawdown test, respectively, (psi/log cycle).

$$S_t = S_d + S_p + S_{pp} + S_{turb} + S_o + S_s + \dots$$
,

where:

 s_t = total skin effect,

 s_d = skin effect due to formation damage (+ ve),

 S_{pp} = skin effect due to partial penetration (+ ve),

 s_p = skin effect due to perforation (+ ve) (Section),

 $S_{turb} = Dq$, skin effect due to turbulence or rate dependent skin (+ ve),

 s_a = skin effect due to slanting of well (- ve),

 s_s = skin effect due to stimulation (mostly - ve).

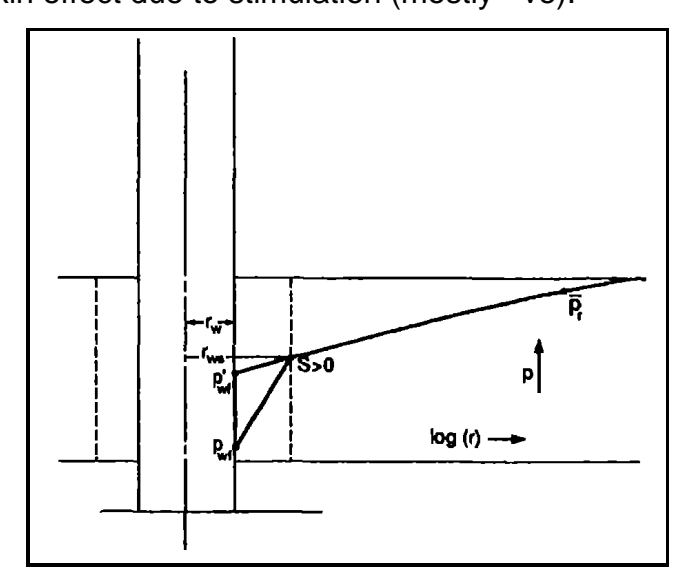


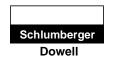
Fig. 6. Positive skin ≈ damaged wellbore or reduced wellbore radius.

July 1998

Page 20 of 168

MATRIX ENGINEERING MANUAL

Well Performance



Only positive skin can be treated in this manner. It is important to note that s_d can be at best reduced to zero by acidizing. However, induced fractures can impose a negative skin (s_s) in addition to rendering the damaged skin to zero.

Using the concept of skin as an annular area of altered permeability around a wellbore, Hawkins showed the well model in Fig. 7.

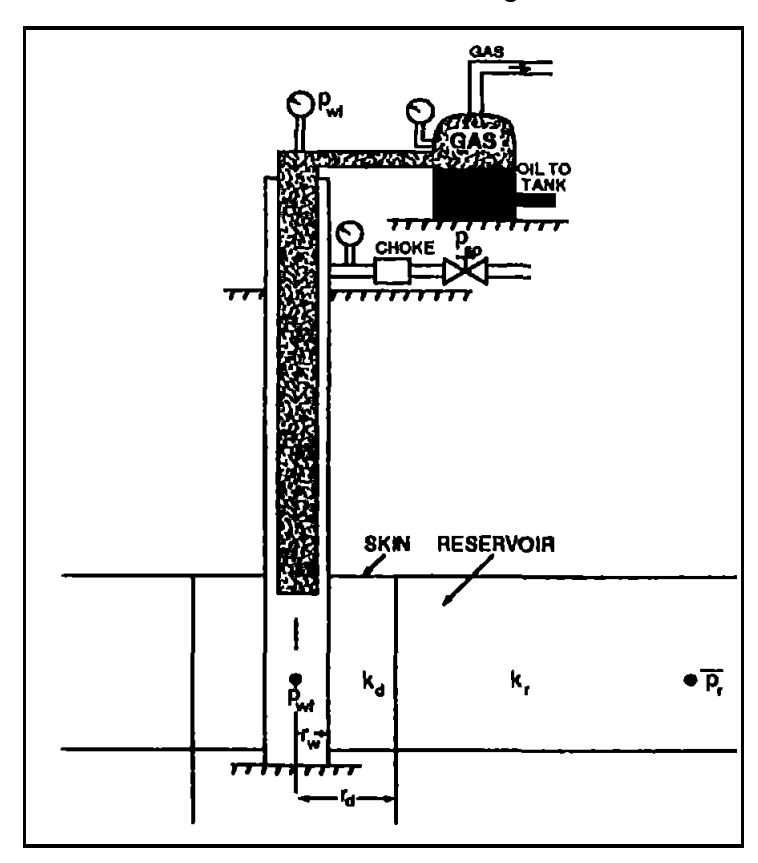


Fig. 7. Well and zone of damaged or altered permeability.

$$s_t = \left(\frac{k_r}{k_d} - I\right) \ln \frac{r_d}{r_w}$$

where:

 k_r = reservoir permeability,

 k_d = permeability of altered or damaged zone,

 r_d = radius of altered or damaged zone,

 r_w = wellbore radius.

This formula also suggests that when s_r is zero (the well is not damaged), the permeability of the altered zone (k_d) equals the reservoir permeability (k_r) or r_w equals r_d . A positive skin indicates a damaged well, whereas a negative skin implies stimulation.

MATRIX ENGINEERING MANUAL

Well Performance

Section 200
July 1998
Page 21 of 168

Darcy's law for a single-phase gas is (Eq. 6):

$$q_g = \frac{7.03 \times 10^{-4} \ k_g \ h\left(\overline{p}_r^2 - p_{wf}^2\right)}{\overline{\mu}_g \ \overline{z} \overline{T} \left[ln\left(\frac{r_e}{r_w}\right) - 0.75 + s_t + Dq_g \right]}$$
 (6)

where:

 q_s = gas flow rate (Mscf/D),

 k_{s} = permeability to gas (md),

 \overline{z} = gas deviation factor determined at average temperature and average pressure (fraction (Section 6))

 \overline{T} = average reservoir temperature (°R), °F + 460,

 $\overline{\mu}_g$ = gas viscosity (cp) (Section 6), calculated at average pressure and average temperature.

All other parameters are defined in Eq. 2. Note that the skin is reduced by a stimulation treatment only; the turbulence is reduced by increasing the shot density or perforation interval or a combination of these two.

Darcy's law for gas flow can be simplified by substituting:

$$z$$
 = 1, μ_s = 0.02 cp , t = 200°F or 660°R

$$ln\left(\frac{r_e}{r_w}\right) - 0.75 = 7.03$$

as,

$$q_g = 77 \times 10^{-7} \ kh \ (\overline{p}_r^2 - \overline{p}_{wf}^2),$$

where:

 q_s = gas flow rate (Mscf/D),

k = permeability (md),

h = reservoir thickness (ft).

This equation is used for a quick estimation of the gas flow rate from the well. Turbulence (Dq_s) in Eq. 6 is known as the skin due to turbulence. In gas wells this may be quite substantial and may need evaluation to decide the means to reduce it. In highly productive oil wells, this term may also be of significance. To evaluate the skin due to turbulence, Darcy's law can be rewritten as:

$$(\overline{p}_r - p_{wf}) = a_o q_o + b_o q_o^2$$

$$(\overline{p}_r^2 - p_{wf}^2) = a_g q_g + b_g q_g^2$$

July 1998

MATRIX ENGINEERING MANUAL

Schlumberger Dowell

Page 22 of 168

Well Performance

where:

$$a_{o} = \left[ln \left(\frac{r_{e}}{r_{w}} \right) - 0.75 + s_{t} \right] \frac{\mu_{o} B_{o}}{7.08 \times 10^{-3} k_{o} h}$$

$$b_{o} = \frac{\mu_{o} B_{o}}{7.08 \times 10^{-3} k_{o} h} D$$

$$a_{g} = \frac{\overline{\mu}_{g} \overline{z} \overline{T}}{7.03 \times 10^{-4} k_{g} h} \left[ln \left(\frac{r_{e}}{r_{w}} \right) - 0.75 + s_{t} \right]$$

$$b_{g} = \frac{\overline{\mu}_{g} \overline{z} \overline{T}}{7.03 \times 10^{-4} k_{o} h} D$$

These two equations can be linearized by dividing both sides by flow rates:

$$\frac{\overline{p}_r - p_{wf}}{q_o} = a_o = b_o q_o \quad oil$$

$$\frac{\overline{p_r^2 - p_{wf}^2}}{q_g} = a_g = b_g q_g \quad gas$$

Based on a four point test where the bottomhole flowing pressure is calculated for four stabilized flow rates, the following plots can be made on Cartesian graph paper and are shown in Fig. 8. The intercept and the slope of the straight line shown in Fig. 8, give the values of the constant a and b defining the straight line. The turbulence factor can be calculated from b. Diagnostics from a four-point plot are shown in Fig. 9. It is important to note that the well data in Case 1 does not show any turbulence because the slope of this line is zero, resulting in a value of zero for b. However, the turbulence or the skin due to it increases as the slopes increase as shown in Case 2 and Case 3.

Jones, Blount, and Glaze modified Darcy's law for radial flow with an analytical expression of the turbulence factor "D" as a function of the perforated interval and gas or oil turbulence coefficient in the rock (β). These equations are provided in Section 6.1.4 and Section 6.2.2.

MATRIX ENGINEERING MANUAL

Well Performance

Section 200 July 1998

Page 23 of 168

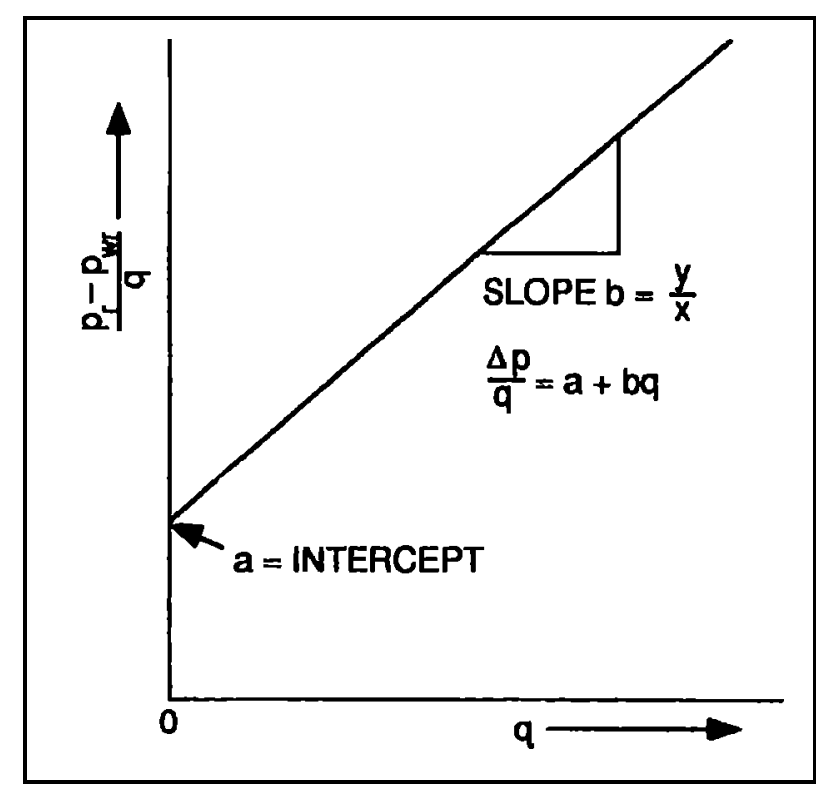


Fig. 8. Plots based on four point test.

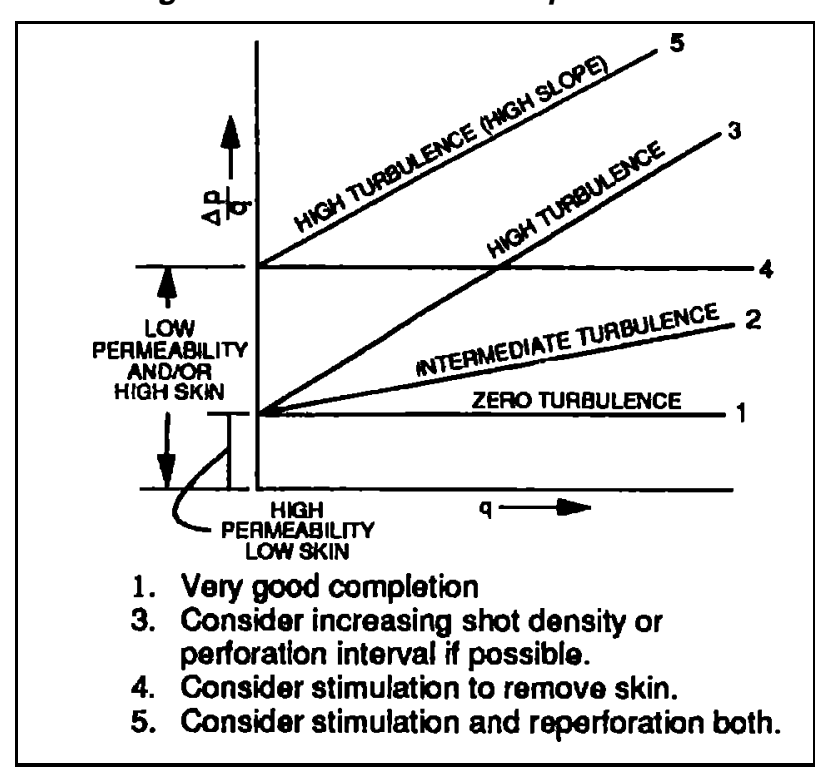
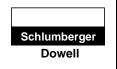


Fig. 9. Evaluation of four point test data (after Jones, Blount, and Glaze).

Section 200
July 1998
Page 24 of 168

MATRIX ENGINEERING MANUAL

Well Performance



2.7 Boundary Effects

Most reservoir engineering calculations assume radial flow geometry. Radial geometry implies that the drainage area of a well is circular and the well is located at the center of the drainage circle. In many cases, the drainage area of a well is rectangular, or some other noncircular shape. Applications of equations based on radial geometry to a noncircular drainage area could lead to substantial error. Darcy's law can be modified for a bounded drainage radius of different shapes of boundary as follows:

$$q_{o} = \frac{7.08 \times 10^{-3} \, kh \, (\overline{p}_{r} - p_{wf})}{B_{o} \, \mu_{o} \left[ln \, (x) - 0.75 + s \right]} \, for \, oil$$

$$703 \times 10^{-6} \, kh \, (\overline{p}_{r}^{2} - p_{wf}^{2})$$

$$q_{g} = \frac{703 \times 10^{-6} \, kh \, (\overline{p}_{r}^{2} - p_{wf}^{2})}{\mu_{g} Tz \left[ln \, (x) - 0.75 + s + Dq_{g} \right]} \, for \, gas$$

and

$$PI = \frac{q_o}{\overline{p}_r - p_{wf}} = \frac{7.08 \times 10^{-3} \, kh}{B_o \, \mu_o \, \left[\ln \left(x \right) - 0.75 + s \right]} \, for \, oil$$

where "x" is provided in Table 1 for various drainage areas and well locations.

Table 1. Factors For Different Shapes and Well Positions in a Drainage Area Where $A = D_{rainage}$ Area of System Shown and $A^{1/2}/r_e$ is Dimensionless

SYSTEM	Х	SYSTEM	Х
\odot	r _e r _₩	2	0.966A ^{1/2} r _w
	0.571A ^{1/2}	2	1.44A ^{1/2}
\odot	0,565A ^{1/2}	: -1	2.206A ^{1/2} r _w
\triangle	0.604A ^{1/2}	4	1.925A ^{1/2}
[-Xe0	0.610A ^{1/2}	4	6.59A ^{1/2}
**	0.678A ^{1/2}	4	9.36A ^{1/2}
**************************************	r _w 0.668A ^{1/2} r _w		1.724A ^{1/2}
<u>.</u>	1.368A ^{1/2}	2	1.794A ^{1/2}
	2.066A ^{1/2} (_w 0.884A ^{1/2}	2	4.072A ^{1/2}
	r _w	2	9.523A ^{1/2}
	1,485A ^{1/2} r _w		t -
		\triangle	10.135A ¹ / ²

MATRIX ENGINEERING MANUAL

Well Performance

Section 200	
July 1998	

Page 25 of 168

EXAMPLE

(a) A buildup test in a well after a constant rate production $(q_o) = 100$ BPD indicates

$$\frac{kh}{\mu} = 20 \frac{md - ft}{cp}$$

$$s_t = 2$$

Calculate the pressure loss due to skin for $B_o = 1$.

Solution

$$\Delta p_{skin} = 141.2 \times \frac{q\mu B_o}{kh} \times s_t = 141.2 \times \frac{100}{20} \times 2 = 141.2 \times 10 = 1412 \ psi$$

(b) Draw IPRs for the given well data and make a tabular presentation of skin versus absolute open flow potentials (AOFP).

Given:

Oil Well

$$k = 5 \text{ md}$$
 $\overline{p}_r = 2500 \text{ psig}$
 $h = 20 \text{ ft}$
 $s = -5, -1, 0, 1, 5, 10, 50$
 $\mu_o = 1.1 \text{ cp}$
 $B_o = 1.2 \text{ res bbl/STB}$
 $\text{spacing} = 80 \text{ acres}$
 $r_w = 0.365 \text{ ft}$

Solution

Drainage radius,
$$r_e = \sqrt{\frac{80 \times 43,560}{\pi}} = 1053 \text{ ft}$$

$$AOFP = q = \frac{7.08 \times 10^{-3} \text{ kh}\overline{p}_r}{\mu_o B_o \left[ln \left(\frac{r_e}{r_w} \right) - 0.75 + s \right]}$$

$$= \frac{7.08 \times 10^{-3} \times 5 \times 20 \times 2500}{1.1 \times 1.2 \left[ln \left(\frac{1053}{0.365} \right) - 0.75 + s \right]}$$

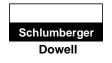
$$= \frac{1341}{7.97 - 0.75 + s}$$

Section 200	
July 1998	

Page 26 of 168

MATRIX ENGINEERING MANUAL

Well Performance



skin (s)	AOFP (STB/D)
-5	604
-1	216
0	186
1	163
5	110
10	78
50	23

For oil wells, since the PI is a straight line, the \bar{p}_r and AOFP will uniquely define the IPR.

(c) Draw the IPR curve for the following gas well data. Calculate the AOFP.

k = 1 md h = 20 ft

Reservoir temperature = 200° F

z = 1.1

 μ = 0.019 cp

spacing = 80 acres

 p_r = 3500 psig

skin, s = 1

 $r_w = 0.365 \text{ ft}$

Solution

From Section (b)

$$ln\frac{r_e}{r_w} - 0.75 = 7.22$$

From Darcy's law,

$$\begin{split} q_g \ (Mscf/D) &= \frac{7.03 \times 10^{-4} kh \left(\overline{p}_r^2 - p_{wf}^2\right)}{\overline{\mu}_g \ \overline{Z} \overline{T} \Bigg[ln \left(\frac{r_e}{r_w}\right) - 0.75 + s \Bigg]} (neglecting \ turbulence) \\ &= \frac{7.03 \times 10^{-4} \times 1 \times 200 (3500^2 - p_{wf}^2)}{0.019 \times 1.1 \times 660 (7.22 + 1)} \\ &= 1.24 \times 10^{-3} (3500^2 - p_{wf}^2) \end{split}$$

MATRIX ENGINEERING MANUAL

Well Performance

Section 200
July 1998
Page 27 of 168

$p_{\scriptscriptstyle wf}$ (psig)	Flow Rate (Msfc/D)
3500	0
3000	4,030
2500	7,440
2000	10,230
1500	12,400
1000	13,950
500	14,880
0	15,190

(d) Calculate the Absolute Flow Potential for problem (b) for a square drainage instead of a circular drainage and skin = 0.

Solution

$$AOFP = \frac{1341}{\ln x - 0.75 + s} = \frac{1341}{\ln x - 0.75}$$

From Table 1,

$$x = \frac{0.571\sqrt{80 \times 43,560}}{r_w} = \frac{1066}{0.365} = 2920$$

$$AOFP = \frac{1341}{\ln 2920 - 0.75} = \frac{1341}{7.98 - 0.75} = 185 \text{ (stb/D)}$$

EXAMPLE

The following data is from a four point (flow after flow) test conducted in an oil well.

Test No.	q (STB/D)	$p_{\scriptscriptstyle wf}$ (psia)
1	400	2820
2	1000	2175
3	1340	1606
4	1600	1080

 \overline{p}_r = 3000 psia

Using the Jones, Blount, and Glaze method, calculate

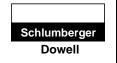
- 1) a and b, and
- 2) AOFP.

July 1998

Page 28 of 168

MATRIX ENGINEERING MANUAL

Well Performance



Solution

Plot q versus $\frac{\overline{p}_r - p_{wf}}{q}$ (Cartesian plot) based on the data provided. Prepare the following table.

q (STB/D)	p _{wf} (psia)	$\frac{\overline{p}_r - p_{wf}}{q}$
400	2820	0.45
1000	2175	0.825
1340	1606	1.0403
1600	1080	1.2000

A straight line is drawn through these points and the slope and intercept are determined. The equation of this straight line is:

$$\frac{\overline{p}_r - p_{wf}}{q} = 0.1997 + 0.000625 \ q$$

Intercept, a = 0.1997,

Slope, b = 0.000625,

AOFP = q for p_{wf} = 14.7 psia.

Solve the quadratic equation in *q*:

$$q = \frac{-0.1997 \pm \sqrt{(0.1997)^2 + (4 \times 0.000625 \times 2985.3)}}{2 \times 0.000625} = 2032 \text{ stb/D}$$

Therefore,

$$q = \frac{-0.1997 \pm \sqrt{7.5}}{1.25 \times 10^{-3}}$$

The positive root of this equation is:

$$q = \frac{-0.1997 \pm \sqrt{7.5}}{1.25 \times 10^{-3}} = 2031 (stb/D)$$

The absolute open flow potential of this well is 2031 STB/D.

2.8 Two-Phase Flow

Darcy's law is only applicable in single-phase flow within the reservoir. In the case of an oil reservoir, single-phase flow occurs when the bottomhole flowing pressure is above the bubblepoint pressure of the reservoir fluid at the reservoir temperature. During the depletion of a reservoir, the reservoir pressure continues to drop unless maintained by fluid injection or flooding. Consequently, during depletion the

MATRIX ENGINEERING MANUAL

Well Performance

Section 200
July 1998
Page 29 of 168

bottomhole flowing pressure falls below the bubblepoint pressure which results in the combination of single-phase and two-phase flow within the reservoir. This requires a composite IPR. Before discussing the composite IPR, a brief review of phase behavior is discussed.

2.9 Phase Behavior of Hydrocarbon Fluids

Reservoir fluid samples taken at the bottomhole pressure, when analyzed in Pressure- Volume,-Temperature (P-V-T) cells generate phase envelopes in the Pressure-Temperature (P-T) diagram. A typical black oil P-T diagram showing the physical state of fluid is shown in Fig. 10. Based on the average reservoir pressure, bottomhole flowing pressures, and the corresponding temperatures on this diagram, one can decide on the type of reservoir fluid; that is, single phase, two phase or a combination. This information is used to determine the type of IPR equation to be used.

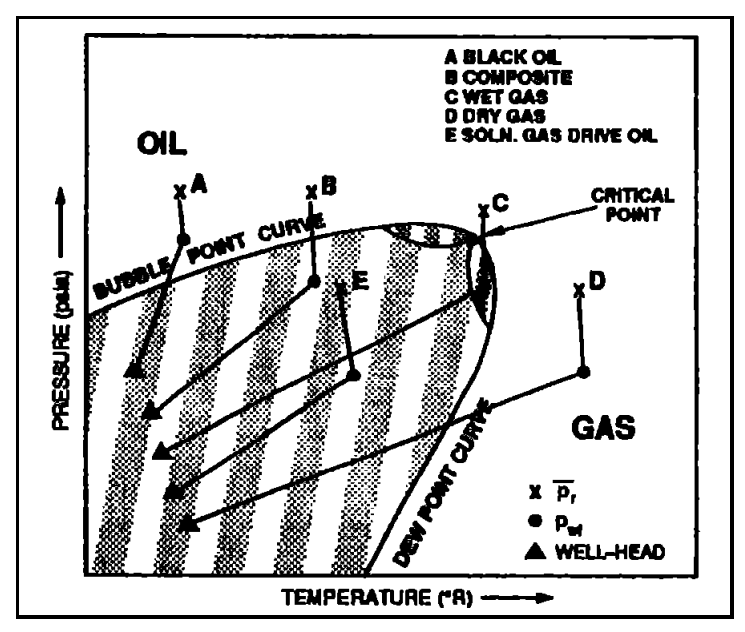


Fig. 10. Typical phase diagram for black oil.

2.10 Vogel's IPR

In the case of two-phase flow in the reservoir where the \overline{p}_r is below the bubblepoint pressure, the Vogel's inflow performance relationship is recommended (Fig. 11). This IPR equation (Eq. 7) is:

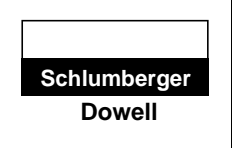
$$\frac{q_o}{q_{omax}} = 1 - 0.2 \left(\frac{p_{wf}}{\overline{p}_r}\right) - 0.8 \left(\frac{p_{wf}}{\overline{p}_r}\right)^2 \tag{7}$$

This IPR curve can be generated if either the absolute open flow potential (q_{omax}) and the reservoir pressure are known or the reservoir pressure and a flow rate and the

Section 200 July 1998 Page 30 of 168

MATRIX ENGINEERING MANUAL

Well Performance



corresponding bottomhole flowing pressure are known. For either case, a buildup test for the reservoir pressure and a flow test with a bottomhole gauge are required.

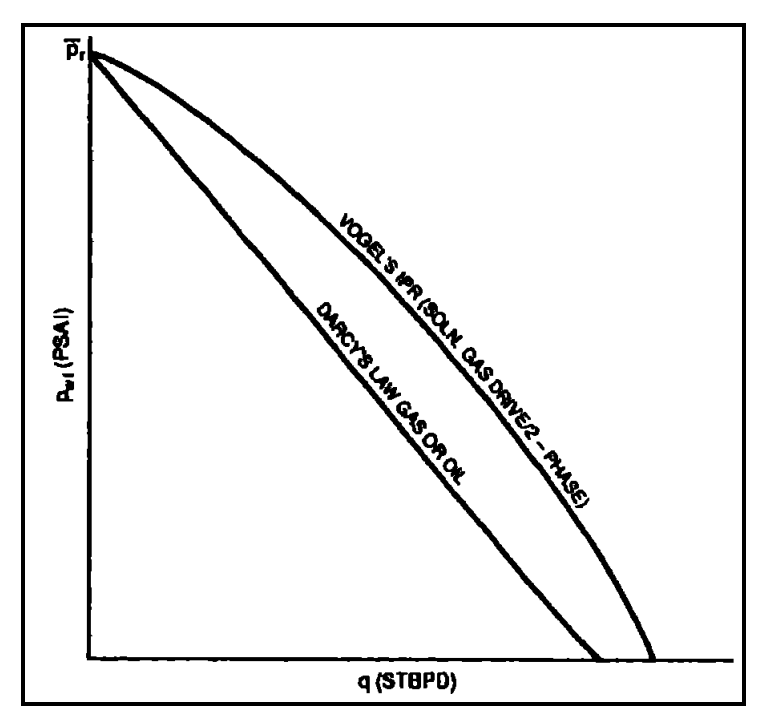


Fig. 11. Different forms of inflow performance relationships IPR.

2.11 Composite IPR

The composite IPR is a combination of the Productivity Index based on Darcy's law above the bubblepoint pressure and Vogel's IPR below the bubblepoint pressure. This IPR is particularly used when the reservoir pressure is above the bubblepoint pressure (p_b) and the bottomhole flowing pressure (p_w) is below the bubblepoint pressure (Fig. 12). Thus,

$$q_o = PI \times (\overline{p}_r - p_{wf})$$
 for $p_{wf} \ge p_b$

and

$$\begin{split} q_o &= q_b + \left(\frac{PI \times p_b}{1.8}\right) \\ &\left[1.0 - 0.2 \left(\frac{p_{wf}}{p_b}\right) - 0.8 \left(\frac{p_{wf}}{p_b}\right)^2\right], \ p_{wf} < p_b \end{split}$$

where,

$$q_b = PI \times (\overline{p}_r - p_b)$$

= flow rate at $(p_{wf} = p_b)$.

MATRIX ENGINEERING MANUAL

Well Performance

Section 200	
July 1998	
Page 31 of 168	

Note that Vogel's IPR is independent of the skin factor and thus, applicable to undamaged wells only. Standing extended Vogel's IPR curves to damaged or stimulated wells.

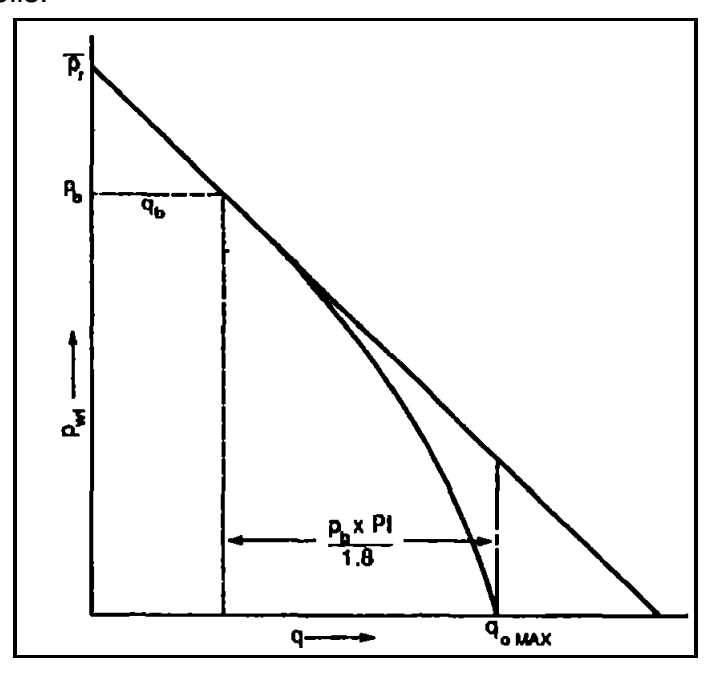


Fig. 12. Vogel's composite IPR.

2.12 Standing's Extension of Vogel's IPR

Standing extended the effect of skin on Vogel's IPR equation and came up with the concept of a flow efficiency factor or FE. If p_{wf} (Fig. 6) is defined as the bottomhole flowing pressure for an undamaged well and p_{wfl} and p_{wfl} are the bottomhole flowing pressures for damaged and stimulated wells, then,

$$FE = \frac{\overline{p}_r - p'_{wf}}{\overline{p}_r - p_{wf1}} \qquad Damaged Well$$

$$= 1 \qquad \qquad Undamaged Well$$

$$= \frac{\overline{p}_r - p'_{wf}}{\overline{p}_r - p_{wf2}} \qquad Simulated Well$$

Thus FE can be calculated using well testing methods. Vogel's IPR curves for different values of FE are provided in Fig. 13.

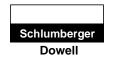
$$FE = \frac{pD_{(s=0)}}{pD_{(s)}} = \frac{ln(t_D) - 0.80907}{ln(t_D) - 0.80907 + 2s}$$

Section 200 July 1998

Page 32 of 168

MATRIX ENGINEERING MANUAL

Well Performance



where,

$$p_D = \frac{kh(p_i - p_{wf})}{141.2q\mu B}$$

$$t_D = \frac{0.000264 \ kt}{\phi \ \mu \ C_t \ r_w^2}$$

These p_D 's and t_D 's are obtained from appropriate type curves or well test information such as $\frac{kh}{\mu}$ and s, and other available well reservoir parameters.

From the definition of flow efficiency,

$$p'_{wf} \cdot = \overline{p}_r - FE(\overline{p}_r - p_{wfi})$$

So, Vogel's IPR can be written as (Eq. 8):

$$\frac{q_o}{q_{omax}} = 1.0 - 0.2 \left(\frac{p'_{wf}}{\overline{p}_r}\right) - 0.8 \left(\frac{p'_{wf}}{\overline{p}_r}\right)^2$$
 (8)

For a large negative skin or high FE (FE greater than one) and low pressures, these IPRs predict a lower rate with lower bottomhole pressure, contrary to reality. Clearly, this method cannot be recommended for these cases. Thus, in the case of stimulated wells, alternative methods to calculate an inflow performance relationship must be used.

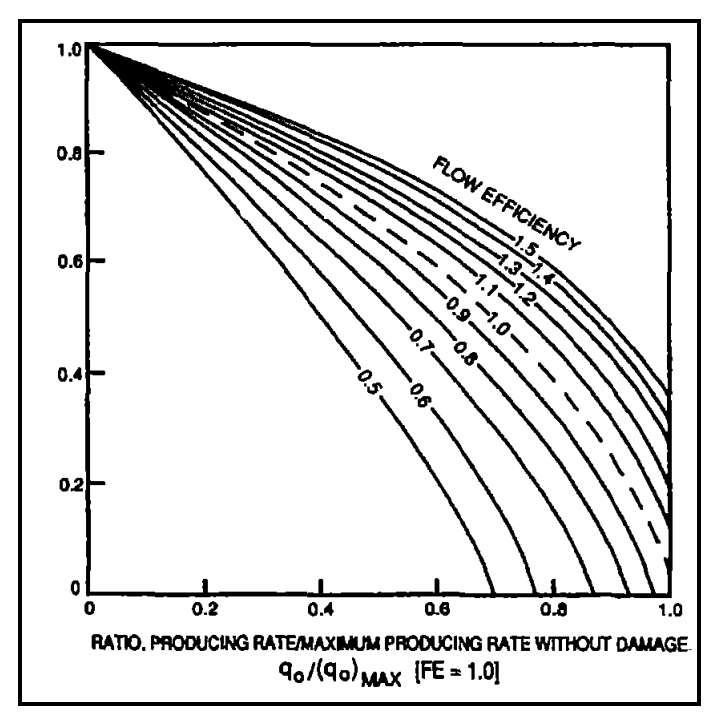
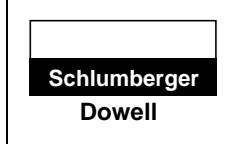


Fig. 13. Standing's correlation for wells with FE values not equal to 1.



Well Performance

Section 200
July 1998
Page 33 of 168

2.13 Fetkovich Method

Multipoint backpressure testing of gas wells is a common procedure to establish the performance curve of gas wells or deliverability. Fetkovich applied these tests on oil wells with reservoir pressures above and below the bubblepoint pressure. The general conclusion from these backpressure tests is that as in gas wells, the rate pressure relationship in oil wells or the oil well IPR is of the form (Eq. 9):

$$q_o = C(\overline{p}_r^2 - p_{wf}^2)^n \tag{9}$$

This equation is also referred to as the oil and gas deliverability equation. The exponent "n" was found to be between 0.5 and 1.000 for both oil and gas wells. An "n" less than 1.0 is often due to nondarcy flow effects. In these cases, a nondarcy flow term can be used. The coefficient "C" represents the Productivity Index of the reservoir. Consequently, this coefficient increases as k and h increase and decreases as the skin increases.

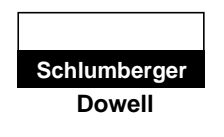
The Fetkovich IPR is a customized IPR for the well, and is obtained by multipoint backpressure testing, for example, flow after flow or isochronal testing.

2.14 Multipoint or Backpressure Testing

Multipoint and backpressure tests are performed on a shut-in well which has achieved a stabilized shut-in pressure throughout the drainage area. These tests are also called deliverability tests because they are used to predict the deliverability of a well or flow rate against any backpressure (p_{wf}) imposed on the reservoir. Typically, these backpressure tests consist of a series of at least three stabilized flow rates and the measurement of bottomhole flowing pressures as a function of time during these flow intervals. The results of backpressure tests are plotted on log-log graph papers as $\log (\overline{p}_r^2 - p_{wf}^2)$ versus $\log q$. Typical flow-after-flow test sequences are shown in Fig. 14 and Fig. 15

Section 200				
July 1998				
Page 34 of 168				

Well Performance



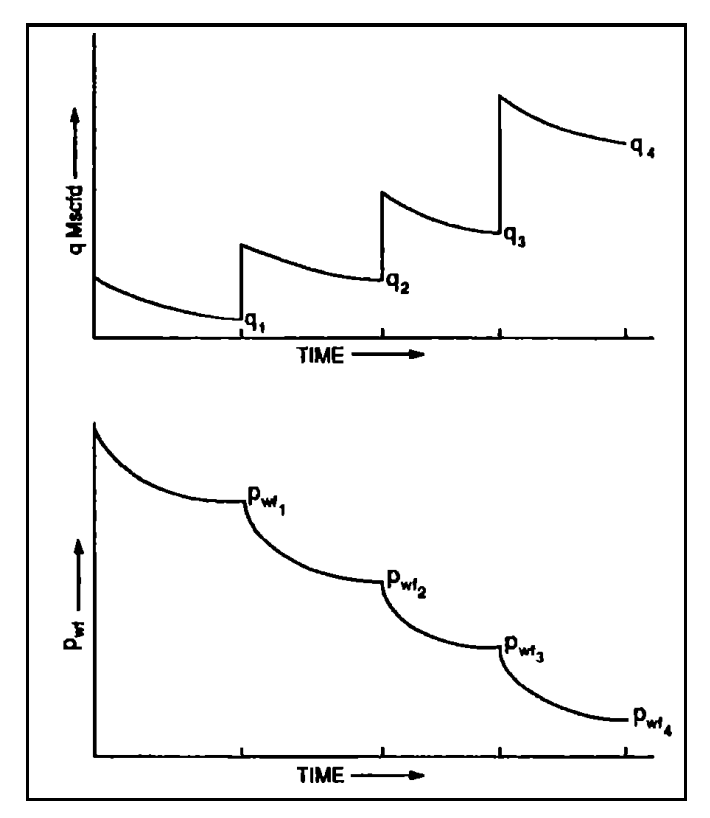


Fig. 14. Flow after flow, normal sequence (after Fetkovich).

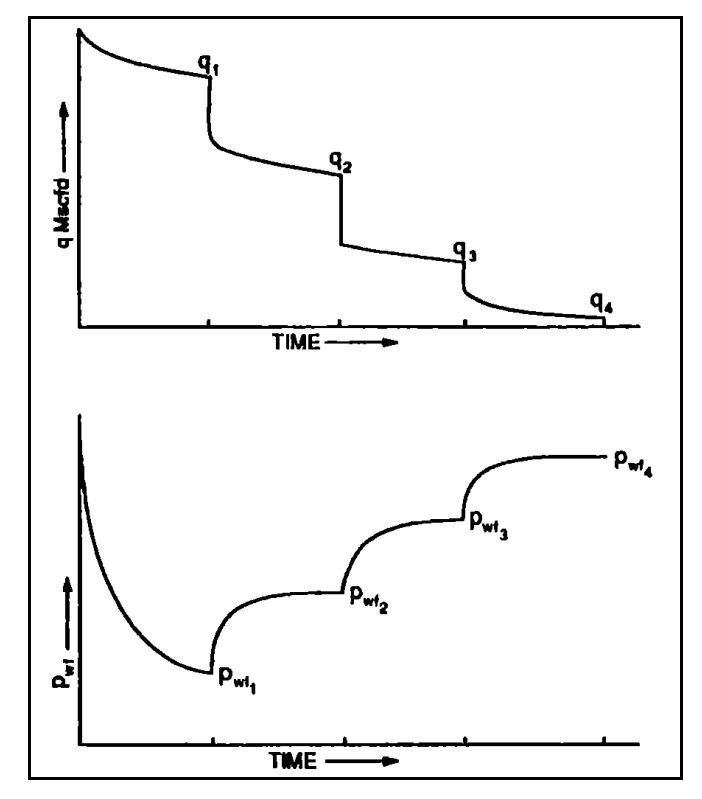
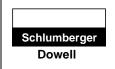


Fig. 15. Flow after flow, reverse sequence (after Fetkovich).



Well Performance

Section 200
July 1998
Page 35 of 168

EXAMPLE

The purpose of this exercise is to calculate C, n, and AOF using the conventional equations.

Given

$$\overline{p}_r = 201 \text{ psia}$$

Duration (hr)	p _{wf} (psia)	m (p) (MMpsia²/cp)	Flow Rate (MMcf/D)
0	201	3.56	0.00
3	196	3.38	2.73
2	195	3.35	3.97
2	193	3.28	4.44
4	190	3.18	5.50

After the deliverability test is conducted, the coefficients of the deliverability equation such as C and n are computed from the log-log plot of $(\overline{p}_r^2 - p_{s\!f}^2)$ versus q. After these points are plotted, the best fit straight line is drawn through them. The straight line then obtained is called the deliverability curve.

where,

$$n = \frac{\log(q_2) - \log(q_1)}{\log (\overline{p}_r^2 - p_{wf2}^2) - \log (\overline{p}_r^2 - p_{wf1}^2)}$$

and

$$C = \frac{q}{(\overline{p}_r^2 - p_{wf}^2)^n}$$

calculated for any q and the corresponding p_{wf} obtained from the deliverability curve.

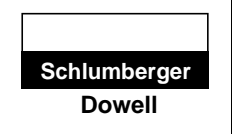
2.15 Isochronal Tests

Isochronal tests are performed in low-permeability reservoirs where it takes a prohibitive amount of time to yield stabilized backpressure. This happens in low-permeability oil or gas reservoirs that normally need stimulation. Typical isochronal tests involve flowing the well at several rates with shut-in periods in between. The durations of the flow periods are the same and the shut-in times are maintained long enough for the pressure in the drainage to stabilize to the average reservoir pressure. These tests are ended with an extended drawdown (Fig. 16).

To analyze these tests, $\log (\overline{p}_r^2 - p_{wfs}^2)$ versus $\log q$ are plotted as shown in Fig. 17 for each of the flow periods. The best straight lines are drawn through these points, one for each of the flow periods. The slopes of these straight lines should be the same, and these lines should be parallel. These lines should get closer with

Section 200				
July 1998				
Page 36 of 168				

Well Performance



increasing time. The slope n is calculated for any of these straight lines by the equation used for the flow-after-flow test. The coefficient C is calculated from the straight line with slope n plotted through the point corresponding to the last stabilized rate in the extended drawdown test period.

A more accurate method of determining C is shown in Fig. 18 which is a plot of log C versus log t. A smooth curve is drawn through these points. The value of C where this curve becomes asymptotic to the time axis is considered the actual value of C. Frequently, this curve may need extrapolation to determine the actual value of C.

In low-permeability formations, the duration of shut-in periods in isochronal tests to achieve pressure stabilization becomes too high. In these cases, a modified isochronal test as shown in Fig. 19 and Fig. 20 is performed. In a modified isochronal test the shut-in periods are of the same duration as the flow periods. In this case, the difference of the squares of the initial and final pressures are plotted on a log-log scale for each flow period. A straight line with the best fit is drawn through these points. $(\overline{p}_r^2 - p_{wfs}^2)$ is plotted against the final extended flow rate and a straight line parallel to the previous line is drawn through this point. Absolute Open Flow Potential (AOFP) is calculated from this straight line assuming zero bottomhole flowing pressure. (For further details, refer to *Theory and Practice of the Testing of Gas Wells*, Chapter 3, Energy Resources Conservation Board, Calgary, Canada, 1975).

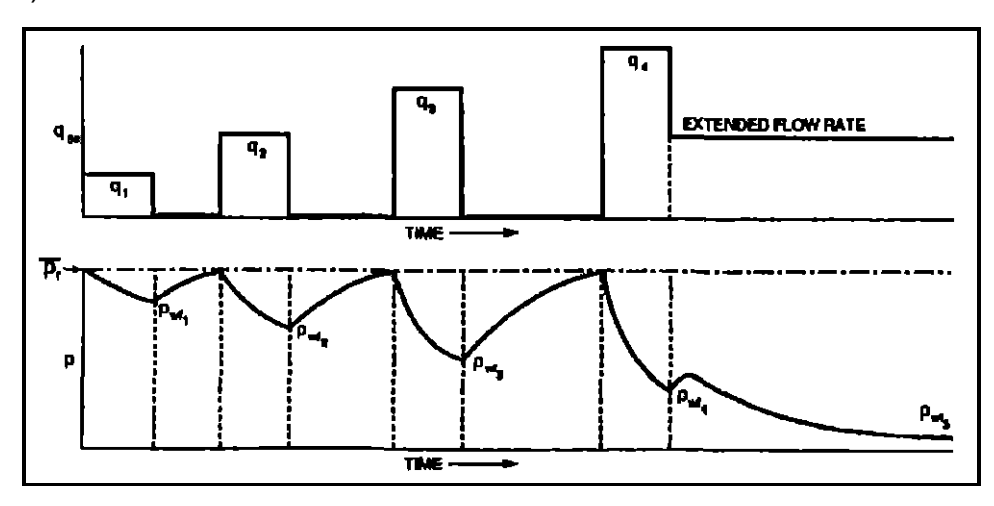


Fig. 16. Isochronal test, flow rate and pressure diagrams.

MATRIX ENGINEERING MANUAL

Well Performance

Section 200
July 1998
Page 37 of 168

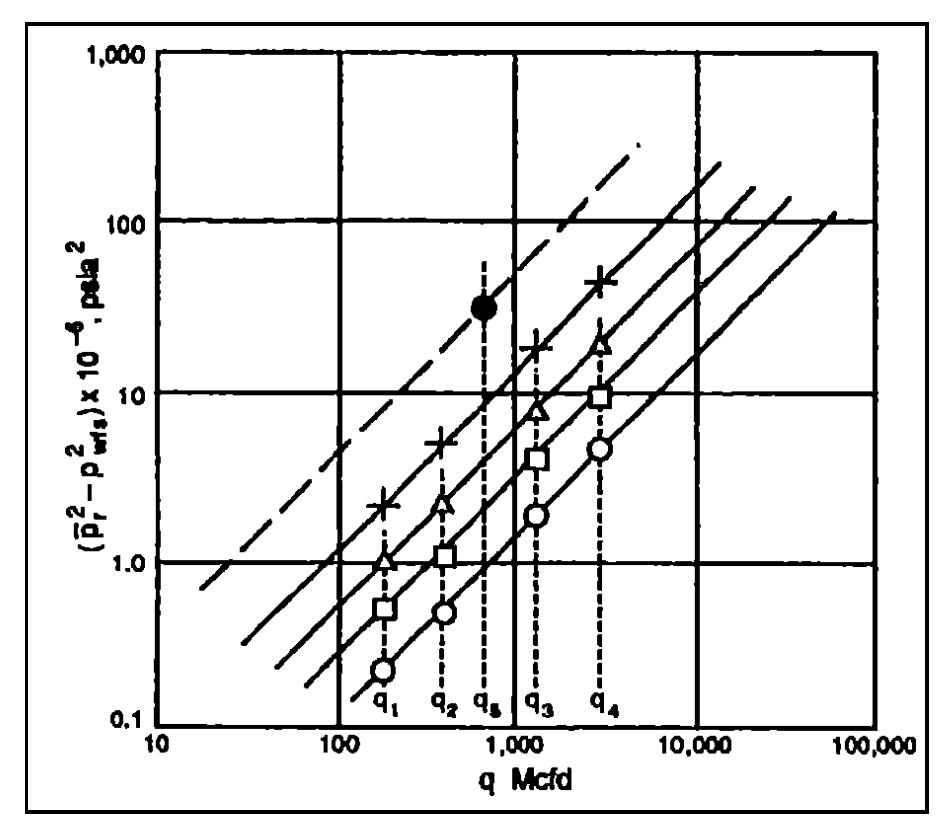


Fig. 17. $(\overline{p}_r^2 - p_{wfs}^2)$ versus q for isochronal test.

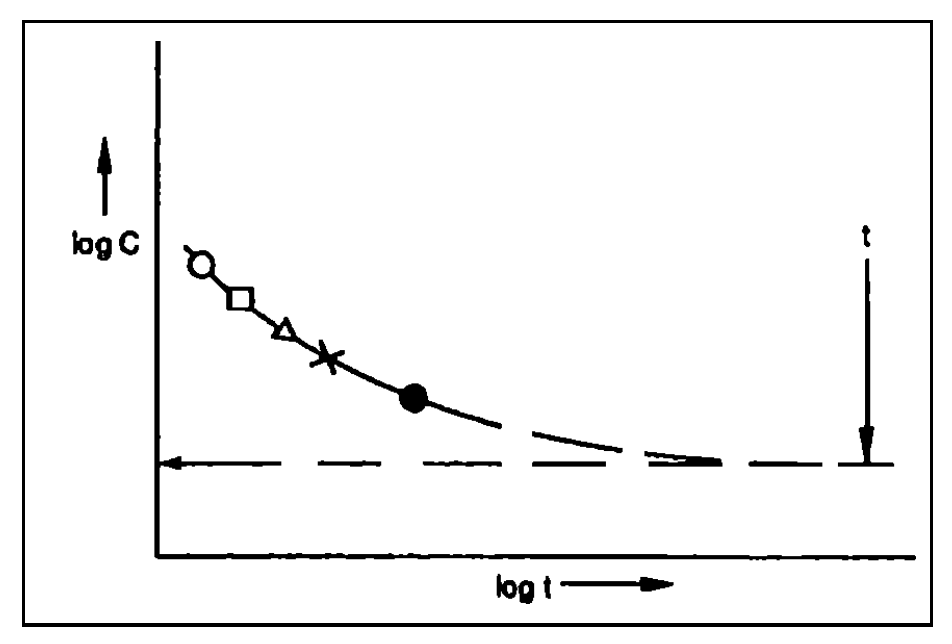
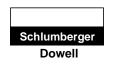


Fig. 18. Graph of $\log C$ versus $\log t$ for isochronal test.

Section 200					
July 1998					
Page 38 of 168					

Well Performance



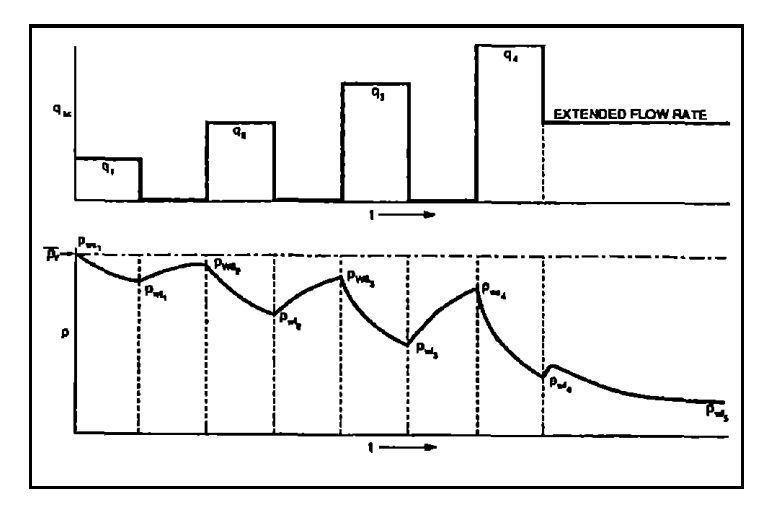


Fig. 19. Modified isochronal test, flow rate and pressure diagrams.

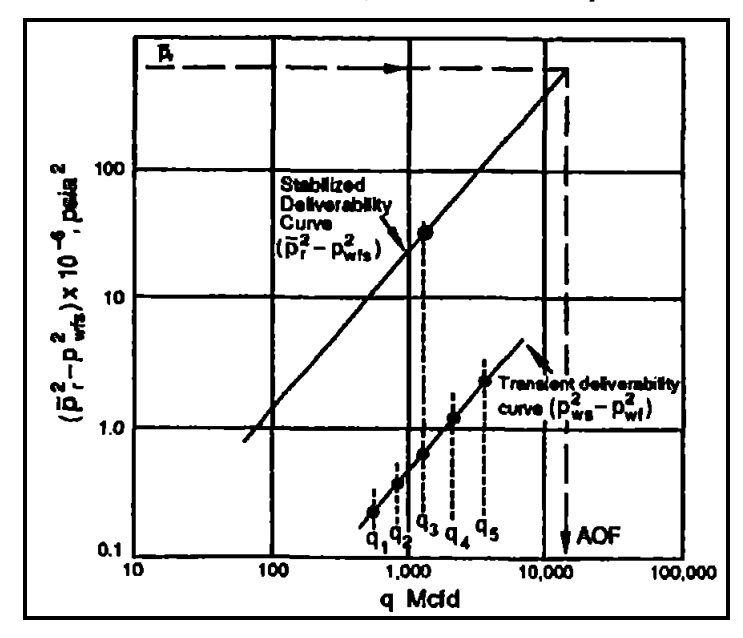


Fig. 20. $(\overline{p}_r^2 - p_{wf}^2)$ versus q for isochronal test.

2.16 Horizontal Wells

Darcy's law suggests that the net thickness or the productive length of vertical wells is directly proportional to the productivity of a well. The productive length of a horizontal well can be considerably greater. In horizontal wells, the productivity does not directly increase with its length. The productivity increase in horizontal wells with the length of the well is much slower. However, horizontal wells can be very long unless economically limited. In heterogeneous reservoirs or naturally fractured reservoirs, these wells can be drilled perpendicular to the natural fracture planes to substantially improve productivity. In the Rospo Mare field in Italy, a horizontal well is reported to produce ten times more than its vertical neighbors. In thin, low-permeability reservoirs, large increases are also possible.

MATRIX ENGINEERING MANUAL

Well Performance

Section 200					
July 1998					
Page 39 of 168					

The inflow performance relationship for a horizontal well at the mid-thickness of a reservoir (Fig. 21) is:

$$Q_o = \frac{7.08 \times 10^{-3} \ k_h \ h(\overline{p}_r - p_{wf})}{\mu_o B_o \left\{ ln \left[\frac{a + \sqrt{a^2 - \left(\frac{L}{2}\right)^2}}{\left(\frac{L}{2}\right)} \right] + \frac{\beta h}{L} \ ln \left(\frac{\beta h}{(\beta + I)r_w}\right) \right\}}$$

where:

a =one-half the major axis of a drainage ellipse in a horizontal plane (Fig. 21).

$$= \frac{L}{2} \left[0.5 + \sqrt{0.25 + \left(\frac{2r_{eh}}{L}\right)^4} \right]^{0.5}$$

$$\beta = \sqrt{\frac{k_h}{k_v}}$$

$$k = \sqrt{(k_h k_v)}$$

where subscripts h and v refer to horizontal and vertical. This equation has all the variables in oilfield units and can be easily converted for a gas well IPR as in Darcy's law for gas.

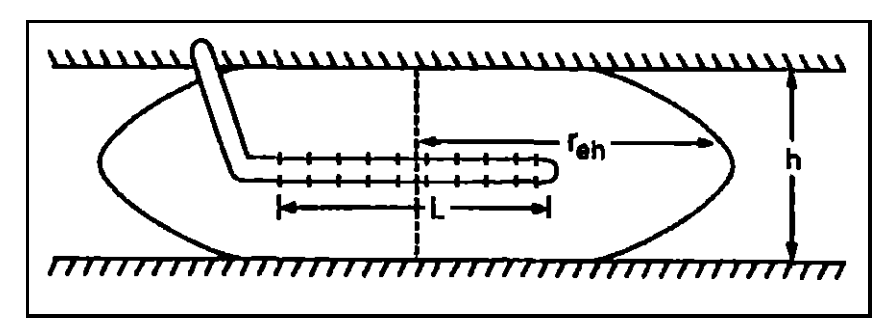


Fig. 21. Horizontal well drainage model.

EXAMPLE

Gas Well: Calculate flow rate through this horizontal well.

Spacing	160 acres
Horizontal permeability, k_h	0.06 md
Vertical permeability, k_{ν}	0.06 md
Average reservoir pressure, \overline{p}_r	800 psia

July 1998

Page 40 of 168

MATRIX ENGINEERING MANUAL

Well Performance



Bottomhole flowing pressure, p_{wf} 400 psia

Wellbore radius, r_w 5 in.

Reservoir temperature, T_r 80°F

Specific gravity of gas, γ_{ϵ} 0.65

Net pay thickness, *h* 1600 ft

Horizontal well length, L 2770 ft

Calculations

z = 0.9 (from Standing's correlation)

 $\mu_{\rm g} = 0.0123$ cp (from Carr et al.)

$$q_{sc} = \frac{703 \times 10^{-6} \, k_h \, h(\overline{p}_r^2 - p_{wf}^2)}{T \overline{\mu}_g \, \overline{z} \left\{ ln \, \left[\frac{a + \sqrt{a^2 - \left(\frac{L}{2}\right)^2}}{\left(\frac{L}{2}\right)} \right] + \frac{\beta h}{L} \, ln \left(\frac{\beta h}{(\beta + 1) r_w}\right) \right\}}$$

$$x = \frac{703 \times 10^{-6} \, h}{T\overline{\mu}_g \, \overline{z}} = \frac{703 \times 10^{-6} \times 1600}{540 \times 0.0123 \times 0.9} = 0.19$$

$$x' = x(\overline{p}_r^2 - p_{wf}^2 = 0.19(800^2 - 400^2) = 91,200$$

$$q_{sc} = \frac{91,200k}{0.79 + 0.58\beta \ln{(1920\beta)}} \left(\frac{Mscf}{D}\right) = 1057 \frac{Mscf}{D}$$

2.17 Tight Formations

It is difficult to design a meaningful well test in a low-permeability (less than 0.1 md) reservoir. The main problem in these cases is the time required to reach infinite-acting radial flow which is large, making these tests impractical. Consequently, it becomes difficult to obtain the reservoir parameters such as (kh/μ) , s and \bar{p}_r , to establish the Productivity Index in these cases. Multipoint tests to determine the IPR also become quite difficult due to the long time taken by these wells to stabilize at any flow rate if these wells flow. Unfortunately, these low permeability wells are normally fractured and once they are fractured their effective wellbore radii increases substantially. In these cases, it becomes even more difficult to obtain radial flow permitting a Horner-type analysis from a postfracture well test. These post-fracture tests in these cases only yield the fracture properties like fracture conductivity and fracture half-length. Often, where conventional analysis (for example, Horner/semilog analysis) fails to interpret well test data, a type-curve matching technique is used to determine the required reservoir data such as (k_h/μ) and s.

MATRIX ENGINEERING MANUAL

Well Performance

Section 200					
July 1998					
Page 41 of 168					

Once the reservoir parameters are determined, type curves can also be used to generate the transient inflow performance relationships. The tight formations normally remain transient for a long time after the production resumes. During this transient time, type curves can be used to generate the transient IPR. Transient IPRs allow the calculation of cumulative production during the transient time, in addition to the flow rates normally obtained using a steady-state IPR.

2.18 Type Curves

Type curves are graphical representations of the solution of the diffusivity equation for constant-rate drawdown under different boundary conditions. The diffusivity equation is a mathematical description of the fluid flow phenomena through the reservoir into the wellbore. Each type curve assumes the following reservoir and well types.

- homogeneous reservoir with or without wellbore storage and skin
- homogeneous reservoir with or without induced fractures in the wellbore
- dual porosity or naturally fractured reservoirs
- layered reservoir.

The three variables in x, y, and z dimensions in the type curve are dimensionless pressure, dimensionless time, and a variable representing the near wellbore condition or the boundary shape. Depending on the wellbore (completion) condition, the z variable may be

- wellbore storage (c) and skin (s) in the case of homogeneous reservoirs
- Fracture conductivity $(C_{\mathcal{D}})$ in the case of wells with an induced fracture.

All type curves are plotted on log-log graph paper, so the shape of the curves strictly depends on the pressure and time data obtained from transient well tests. The effects of other parameters such as k_h , μ , q, and ϕ are strictly translational. This can be explained with a real type curve for a homogeneous reservoir with wellbore storage and skin.

2.19 Homogeneous Reservoir Type Curve

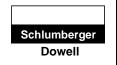
The type curve for a homogeneous reservoir with wellbore storage and skin presents p_D as a function of t_D/C_De^2 for different C_D in Fig. 22 (Gringarten et al Flopetrol Johnston Schlumberger). This typecurve is commonly known as a Flopetrol Johnston type curve. The wellbore storage dominated periods for all values of C_De^2 fit on one unit slope line. The end of a unit slope line for different values of C_De^2 is marked on the type curve. The start of the infinite-acting radial flow is also clearly marked. This curve does not show the effect of boundaries to make it applicable strictly to an infinite reservoir. In reality, as the well sees the effect of a boundary, these type curves bend upward. The dimensionless time when these boundary

July 1998

Page 42 of 168

MATRIX ENGINEERING MANUAL

Well Performance



effects are seen depends on how far the boundary is from the wellbore. A typical type curve for a fractured well with no flow boundary is provided in Fig. 23.

The advantage of the Flopetrol Johnston type curve is the ease of matching and clear definition of the flow regimes, such as end of wellbore storage and beginning of infinite-acting radial flow. In this type curve, the dimensionless variables are defined as follows:

 p_D = dimensionless pressure

$$= \frac{kh}{141.2 \ qB_o U} \Delta p$$

$$tD/CD = 0.000295 \frac{kh}{\mu} \frac{\Delta t}{C}$$

$$CD = \frac{0.8936 \ C}{\phi \ h \ C_t \ r_c^2}$$

These dimensionless groups represent universal pressure and time scales. The type curves actually represent a global description of the pressure response with time for different production or injection rates. The presentation of these dimensionless variables in log-log coordinates makes possible a match of the pressure versus time data obtained from a well test. The rationale for that is:

$$log p_D = log\Delta p + log \frac{kh}{141.2 \ qB\mu}$$
$$= log \Delta p + log y$$

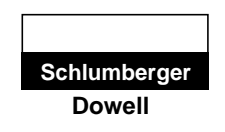
where y = constant for a particular reservoir.

Similarly,

$$log(t_D/C_D) = log\Delta p + log\left(0.000295 \frac{kh}{\mu C}\right)$$
$$= log\Delta t + log x$$

where $x = f(k, h, \mu, C)$ = constant for the well reservoir system.

Consequently, $\log p_D$ and $\log t_D$ are actually $\log \Delta p$ and $\log \Delta t$, translated by some constants defined by reservoir parameters. Therefore, if the proper type curve representing the reservoir model is used, real and theoretical pressure-versus-time curves are identical in shape but are translated in scale when plotted on the same $\log \log p$



Well Performance

Section 200
July 1998
Page 43 of 168

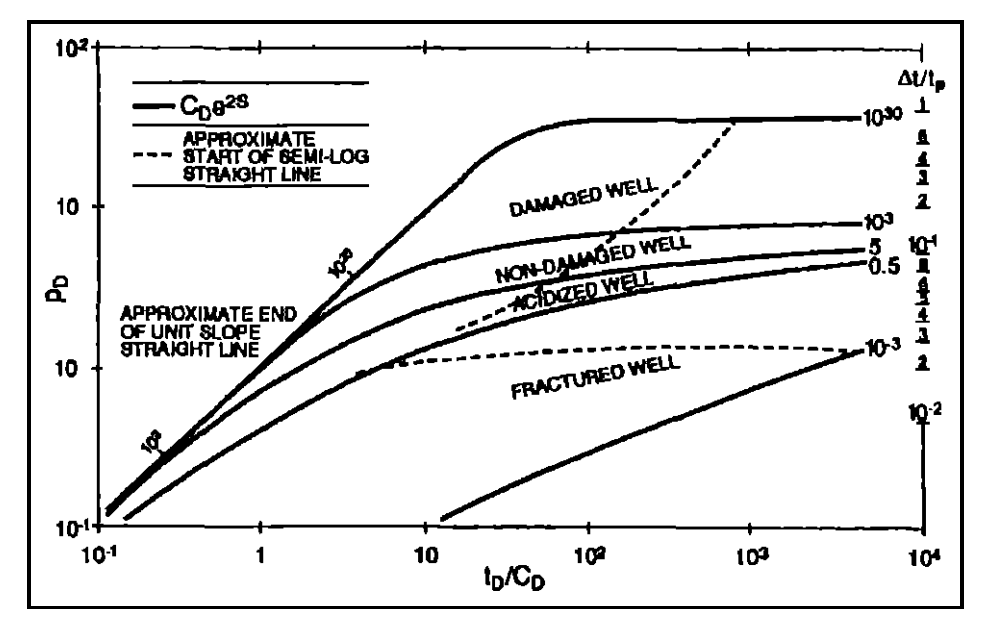


Fig. 22. Homogeneous reservoir type curve.

2.20 Transient IPR

2.20.1 Infinite Homogeneous Reservoir

Transient IPR curves for homogeneous reservoirs can be generated using the Flopetrol Johnston type curves as follows.

EXAMPLE

Given

k = 1 md

 $\phi = 0.2$

h = 20 ft

 $c_t = 10^{-5} \text{ psi}^{-1}$

 $\mu_o = 1 \text{ cp}$

C = 0.001 bbl/psi

 $B_a = 1.0 \text{ res bbl/STB}$

time = 0.1, 1, 10, 100 hr

 \overline{p}_r = 2000 psia

s = 1.21

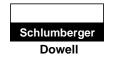
 $r_w = 0.5 \text{ ft}$

July 1998

Page 44 of 168

MATRIX ENGINEERING MANUAL

Well Performance



Calculation

$$\frac{t_D}{C_D} = 0.000295 \frac{kh}{\mu} \frac{\Delta t}{C} = 5.9 \Delta t$$

$$C_D = \frac{0.8936C}{\phi h C_t r_w^2} = 89.36$$

$$C_D e^{2s} = 89.36 \times e^{2.42} = 1000$$

In the type curve for Fig. 22, for $C_D e^{2s} = 1000$, $p_D s$ are obtained for different values of t_D/C_D as a function of time. Then, the absolute open flow potential is:

$$q = \frac{kh}{141.2B_o \,\mu_o} \, \frac{\overline{p}_r}{p_D}$$

∆t (hr)	t_D/C_D	p _D (from TC)	Absolute Open Flow Potential (bbl/day)
0.1	0.59	0.56	506
1	5.9	3.15	90
0	59	5.9	48
100	590	7.2	39

For homogeneous reservoirs, the well-known infinite-acting semilog approximation for a well with a skin s, producing at a constant rate q after the wellbore storage effects subside is given by:

$$p_D = 1/2 (ln \ t_D + 0.80907 + 2s).$$

This equation represents the homogeneous reservoir type curve until the pressure transients start seeing the boundary. This time depends on the boundary radius and can be calculated based on some of the reservoir properties as follows.

$$t_{(hours)} = 948 \left(\frac{\phi \,\mu \,C_t \, r_e^2}{k} \right)$$

The equation for p_D can be simplified as:

$$q_{o} = \frac{kh (\overline{p}_{r} - p_{wf})}{162.6 \ \mu_{o} B_{o} \left[\left\{ log \left(\frac{k}{\phi \mu \ C_{t} \ r_{w}^{2}} \right) - 3.23 + 0.87s \right\} + log(t) \right]}$$

The transient IPR equation for gas reservoirs is provided in Section 6.4.

EXAMPLE

Same as previous problem. $r_e = 2000 \text{ ft}$

MATRIX ENGINEERING MANUAL

Well Performance

Section 200	
July 1998	

Page 45 of 168

time to end of infinite-acting radial flow, t (hr)

$$= 948 \frac{0.2 \times 10^{-5} \times 2000^{2}}{1} = 7584 \text{ hr}$$

$$q_{O/AOFP} = \frac{20 \times 2000}{162.6 \left[\left\{ log \left(\frac{1}{0.2 \times 10^{-5} \times 0.5^{2}} \right) - 3.23 + 0.87s \right\} + log(t) \right]}$$

$$= \frac{246}{log t + 4.3}$$

t (hr)	$q_{\scriptscriptstyle o}$ (Absolute Open Flow Potential)
0.1	74.55
10	46.42
100	39.05
1000	33.70
7584	30.07

Note the discrepancy in the absolute open-flow potentials at early times less than 100 hr. This is due to the wellbore storage effects not considered in the semilog approximation.

2.20.2 Homogeneous Reservoir With Induced Vertical Fracture

Meng and Brown provided type curves for wells with an induced vertical fracture at the center of the reservoir for different closed rectangular drainage areas. The fluid is considered slightly compressible with constant viscosity μ . For gas flow, the real gas pseudopressure function (Al-Hussainy et al., 1966) is used where gas properties are evaluated at the initial reservoir pressure. The dimensionless variables used in these type curves are defined as follows.

 p_D = dimensionless wellbore pressure drop

$$= \frac{kh [p_i - p_{wf}^{(t)}]}{141.2 q \mu B} \text{ (oil)}$$

$$p_{D} = \frac{kh \{ m (p_{i}) - m[p_{wf}^{(t)}] \}}{1424 \ qT}$$
 (gas)

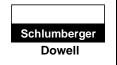
 t_{Dxf} = dimensionless time

$$\frac{0.000264 \text{ } kt}{\phi \mu C_t x_f^2}$$
 (oil)

Page 46 of 168

MATRIX ENGINEERING MANUAL

Well Performance



$$t_{Dxf} = \frac{0.000264 \ kt}{\phi \ (\mu \ C_t)_i x_f^2}$$
 (gas)

 C_{D} = dimensionless fracture conductivity

$$= \frac{k_f w}{k x_f}$$

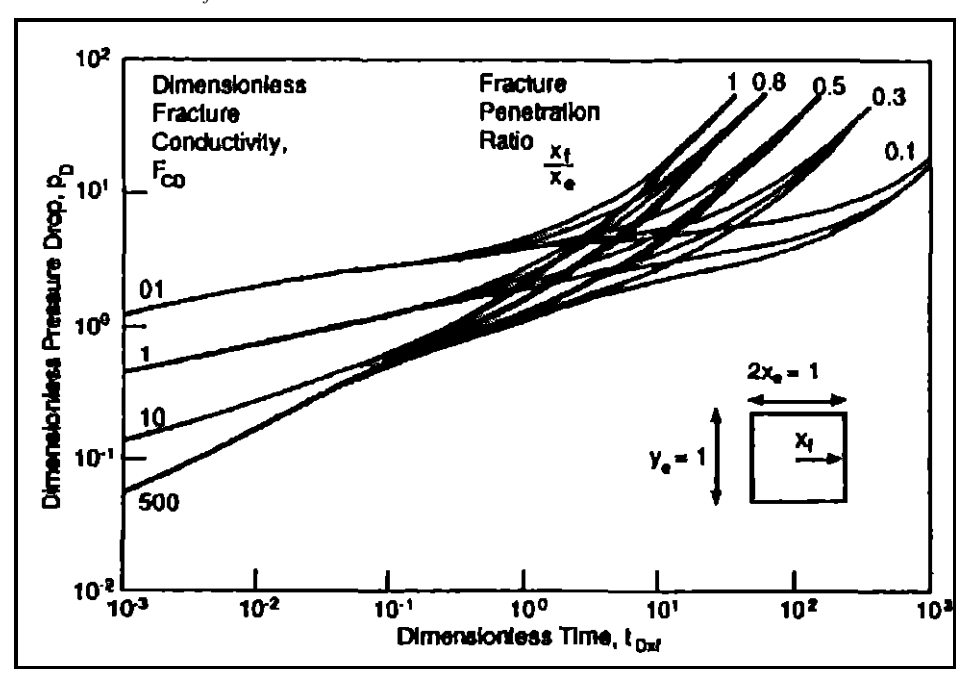


Fig. 23. Constant rate type curve for finite-conductivity fracture-closed square system ($x_e/y_e = 1$).

A few of these type curves are provided in Fig. 23. It is important to note that the early time pressure behavior depends on the C_D ; whereas the late time or after depletion starts, the pressure response is influenced by the shape and the size of drainage.

As in the homogeneous reservoir case, transient IPR curves can be generated for fractured reservoirs using appropriate type curves provided in Fig. 23. These type curves can be used for both single-phase oil or single-phase gas. In the case of gas, m(p) is used instead of pressure. For oil wells below the bubblepoint pressure, Vogel's IPR is used. A step-by-step procedure to calculate transient IPR follows.

- 1. Calculate the dimensionless fracture conductivity defined earlier.
- 2. A drainage geometry x_e/y_e is assumed for a closed reservoir; calculate the fracture penetration ratio x_f/x_e .
- 3. Calculate dimensionless time t_{Dxf} for any assumed time and for known parameters such as k, ϕ , C_t and x_f .
- 4. From the type curves, determine the dimensionless pressure p_D (t_{Dxf} , C_{fD} , x_f/x_e , x_e/y_e).

MATRIX ENGINEERING MANUAL

Well Performance

Section 200 July 1998

Page 47 of 168

5. Calculate q_b and PI at the bubblepoint pressure using the following:

$$q_{b} = \frac{kh (p_{i} - p_{b})}{141.2B_{o}\mu p_{D} \left(t_{Dxf}, C_{fD}, \frac{w_{f}}{x_{e}}, \frac{x_{e}}{y_{e}}\right)}$$

and

$$PI = \frac{q_b}{p_i - p_b}$$

where p_b is the bubblepoint pressure and qb is the rate at the bubblepoint pressure.

6. Calculate q_{Vogel} , where,

$$q_{Vogel} = \frac{p_b \times PI}{1.8}$$

7. Calculate p_{wf} versus q below the bubblepoint pressure using Vogel's equation:

$$q = q_b + q_{Vogel} \left[1 - 0.2 \left(\frac{p_{wf}}{p_b} \right) - 0.8 \left(\frac{p_{wf}}{p_b} \right)^2 \right]$$

For gas wells, Steps 1 to 5 are followed to generate IPR curves.

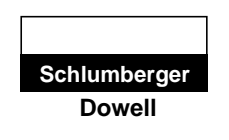
3 Completion System

Most oil and gas wells are completed with casing. The annulus behind the casing is normally cemented. Once the casing is cemented, it is hermetically insulated from the formation. To produce any fluid from the formation, the casing is perforated using perforation guns. Perforated completions provide a high degree of control over the pay zone, because selected intervals can be perforated, stimulated and tested as desired. It is also believed that hydraulic fracturing and sand control operations are more successful in perforated completions. However, the perforations impose restrictions to flow from the formation to the wellbore in the form of additional pressure losses. Consequently, if not adequately designed and understood, perforations may substantially reduce the flow rates from a well.

Shaped-charge perforating is the most common and popular method of perforating. A typical cross section of a shaped charge is shown in Fig. 24. As the shaped charge is detonated, the various stages in the jet development are shown in Fig. 25a and Fig. 25b. The velocity of the jet tip is in excess of 30,000 ft/sec, which causes the jet to exert an impact of some four million psi on the target. Every shaped-charge manufacturer provides a specification sheet for charges regarding the length of penetration and diameter of the entrance hole in addition to other API required specifications.

Section 200					
July 1998					
Page 48 of 168					

Well Performance



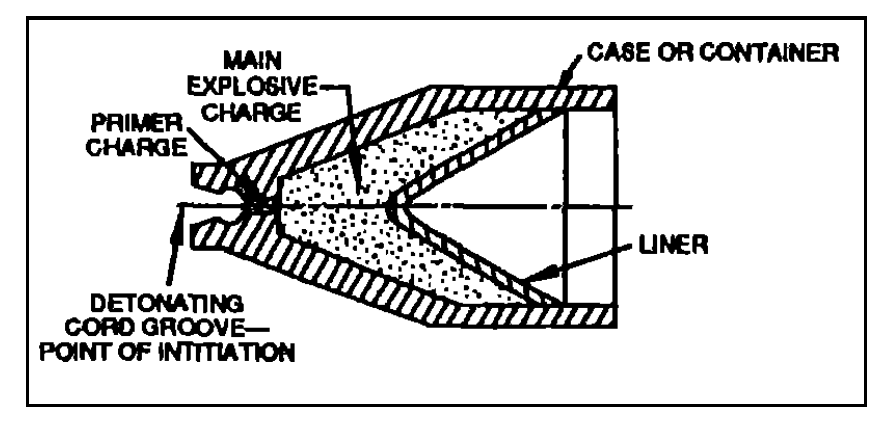


Fig. 24. Typical shaped charge.

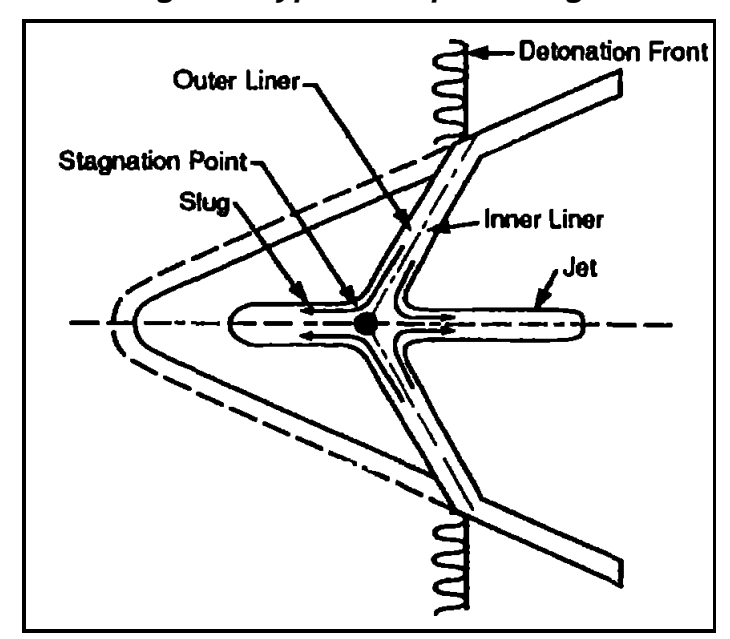


Fig. 25a. Jet/slug formation.

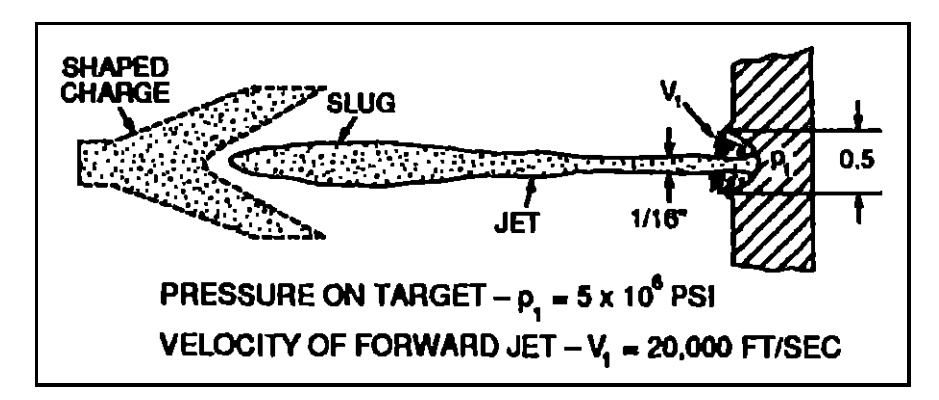


Fig. 25b. Approximate jet velocities and pressures.



Well Performance

Section 200					
July 1998					
Page 49 of 168					

3.1 Pressure Loss in Perforations

The effect of perforations on the productivity of wells can be quite substantial. Therefore, much work is needed to calculate the pressure loss through perforation tunnels. A brief review of the background work in the area was presented by Karakas and Tariq (1988). Most of the calculations on perforation pressure losses are based on single-phase gas or liquid flow. It is generally believed that if the reservoir pressure is below the bubblepoint, causing two-phase flow through the perforations, the pressure loss may be an order of magnitude higher than that for single-phase flow. Perez and Kelkar (1988) presented a new method for calculating two-phase pressure loss across perforations. Two methods of calculating the pressure loss in perforations are provided here with appropriate examples. These methods were proposed by McLeod (1983) and Karakas and Tariq (1988).

3.1.1 McLeod Method

Pressure loss in a perforation is calculated using the modified Jones, Blount, and Glaze equations proposed by McLeod. McLeod treated an individual perforation tunnel as a miniature well with a compacted zone of reduced permeability around the tunnel. It is believed that the compacted zone is created due to the impact of the shaped charge jet on the rock. However, there is no physical means to actually calculate the permeability of the compacted zone. McLeod suggested from his experience that the permeability of the compacted zone is:

- 10% of the formation permeability, if perforated overbalanced
- 40% of the formation permeability, if perforated underbalanced.

These numbers may be different in different areas.

The thickness of the crushed zone is assumed to be 0.5 in. The massive reservoir rock surrounding a well perforation tunnel renders it feasible to assume a model of an infinite reservoir surrounding the well of the perforation tunnel. Thus, in the application of Darcy's law, -0.75 in the denominator can be neglected. A cross section of McLeod's perforation flow model is provided in Fig. 26. The pressure loss equations through perforations are:

Oil Well

$$p_{wfs} - p_{wf} = aq_o^2 + bq_o (10)$$

where the constants a and b are defined in Section 6. Note that the flow q_o in this equation is not the well production rate but the flow rate through an individual perforation.

Gas Well

$$p_{wfs}^2 - p_{wf}^2 = aq_g^2 + bq_g (11)$$

The constants a and b are adequately defined in Section 6. Again, the gas flow rate (q_s) is the flow rate through an individual perforation.

Section 200				
July 1998				
Page 50 of 168				

Well Performance



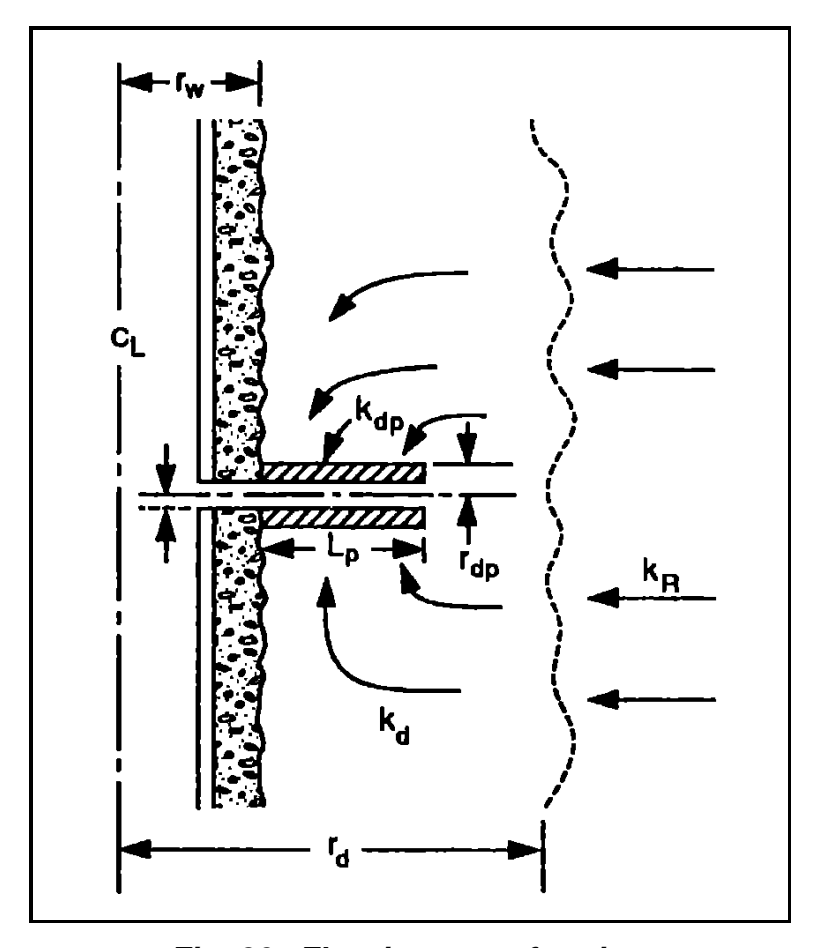


Fig. 26. Flow into a perforation.

EXAMPLE

Oil Well

Make a completion sensitivity study for the following well:

k = 20 md

 \overline{p}_r = 3000 psia

 $r_e = 2000 \text{ ft}$

h = 25 ft

 $h_p = 20 \text{ ft}$

 $r_p = 0.021 \text{ ft}$

 $L_p = 0.883 \text{ ft}$

 $k_p = 0.4 \text{ x } k \text{ md}$

 $r_c = 0.063 \text{ ft}$

 $r_w = 0.365 \text{ ft}$

MATRIX ENGINEERING MANUAL

Well Performance

Section 200 July 1998

Page 51 of 168

$$API = 35^{\circ}$$

$$\gamma_g = 0.65$$

$$B_o = 1.2 \text{ (res bbl/STB)}$$

$$\mu_o = 1 \text{ cp}$$

- Calculate the pressure loss through perforations for 2, 4, 8, 12, 20, and 24 spf in the flow rate range from 100 to 1200 STB/D.
- Plot completion sensitivities q versus Δp .

Solution

Pressure loss through individual perforation,

$$p_{wfs} - p_{wf} = aq_o^2 + bq_o$$

where:

$$a = \frac{2.30 \times 10^{-14} \, B_o^2 \; \beta_o \; \rho \left(\frac{1}{r_p} - \frac{1}{r_c}\right)}{L_p^2}$$

$$b = \frac{\mu_o B_o \left(ln \frac{r_c}{r_p} \right)}{7.08 \times 10^{-3} L_p k_p}$$

Calculations:

$$B_o = \frac{2.33 \times 10^{10}}{k_p^{1.201}} = \frac{2.33 \times 10^{10}}{(0.4 \times 20)^{1.201}} = 1.9175~E9$$

$$a = \frac{2.30 \times 10^{-14} \times 1.2^2 \times \beta_o \times 53.03 \times 31.75}{0.883^2}$$

$$b = \frac{1.2 \left(\ln \frac{0.063}{0.021} \right)}{7.08 \times 10^{-3} \times 0.883 \times 8} = 26.3598$$

Therefore,

$$\Delta p = 0.1371 \ q_o^2 + 26.3598 \ q_o$$

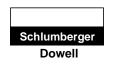
where,

$$q_o = oil \ flow \ rate \ per \ perforation, \ BPD$$

$$= \frac{well \ flow \ rate}{(shot \ per \ foot) \times (perforated \ well)}$$

Section 200					
July 1998					
Page 52 of 168					

Well Performance



Well Flow Rate (bbl/day)										
Shot Density (SPF)	100		200		400		800		1200	
	q _。 (B/D/perf)	∆ <i>p</i> (psi)								
2	2.5	67	5	135	10	277	20	582	30	914
4	1.25	33	2.5	67	5	135	10	277	15	426
8	0.625	16.5	1.25	33	2.5	67	5	135	7.5	205
12	0.4167	11.0	0.833	2	1.667	44	3.33	89	5	135
20	0.25	6.6	0.5	13	1	27	2.0	53	3	80
24	0.208	5.5	0.4167	11	0.833	22	1.67	44	2.5	67

Gas Well

For gas wells,

$$p_{wfs}^2 - p_{wf}^2 = aq_g^2 + bq_g$$

The constants a and b are calculated exactly the same way as shown in the oil well example using the gas well equations provided in Section 6.5.2. To calculate the pressure loss through perforations, p_{wfs} is calculated from the IPR curve for the given well flow rate, then p_{wf} is calculated as :

$$p_{wf} = \sqrt{p_{wfs}^2 - (aq_g^2 + bq_g)}$$

$$\Delta p = p_{wfs} - p_{wf}$$

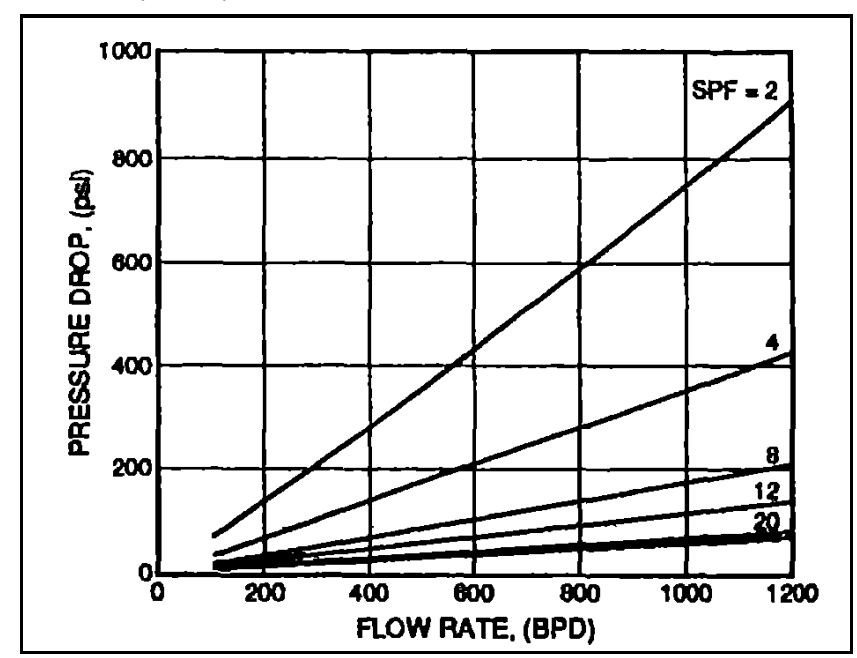
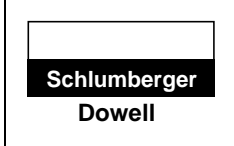


Fig. 27. Plot of flow rate versus pressure drop for varying shot densities.



Well Performance

Section 200
July 1998
Page 53 of 168

3.1.2 Karakas and Tariq Method

For practical purposes, McLeod's method gives fair estimates of pressure loss through perforations. However, this model is not sophisticated enough to consider the effects of the phasing and spiral distribution of the perforations around the wellbore. Karakas and Tariq (1988) presented a semianalytical solution to the complex problem of three-dimensional (3D) flow into a spiral system of perforations around the wellbore. These solutions are provided for two cases.

- A two-dimensional (2D) flow problem valid for small, dimensionless perforation spacings (large perforation penetration or high-shot density). The vertical component of flow into perforations is neglected.
- A 3D flow problem around the perforation tunnel, valid in low-shot density perforations.

Karakas and Tariq presented the perforation pressure losses in terms of pseudoskins, enabling the modification of the IPR curves to include the effect of perforations on the well performance as follows.

For steady-state flow into a perforated well:

$$q = \frac{2\pi k h (\overline{p}_r - p_w)}{\mu B \left(ln \frac{r_e}{r_w} + s_t \right)}$$

where:

s_t = total skin factor including pseudoskins due to perforation (obtained from well test),

k = formation permeability, and

h = net thickness of the formation.

For the total skin:

 $S_t = S_p + S_{dp},$

 s_p = perforation skin factor, and

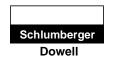
 s_{dp} = damage skin factor.

The damaged skin factor (s_{dp}) is the treatment skin component in a perforated completion. The perforation skin (s_p) is a function of the perforation phase angle θ , the perforation tunnel length (l_p) the perforation hole radius (r_p) the perforation shot density (n_s) and the wellbore radius (r_w) . The following dimensionless parameters are used to correlate the different components of the perforation skin (s_p) .

Dimensionless perforation height:

$$h_D = \frac{h}{l_p} \sqrt{\frac{k_v}{k_h}}$$

Well Performance



Page 54 of 168

Dimensionless perforation radius:

$$r_{pD} = \frac{r_p}{2h} \left(I + \sqrt{\frac{k_v}{k_h}} \right)$$

Dimensionless well radius:

$$r_{wD} = \frac{r_w}{(l_p + r_w)}$$

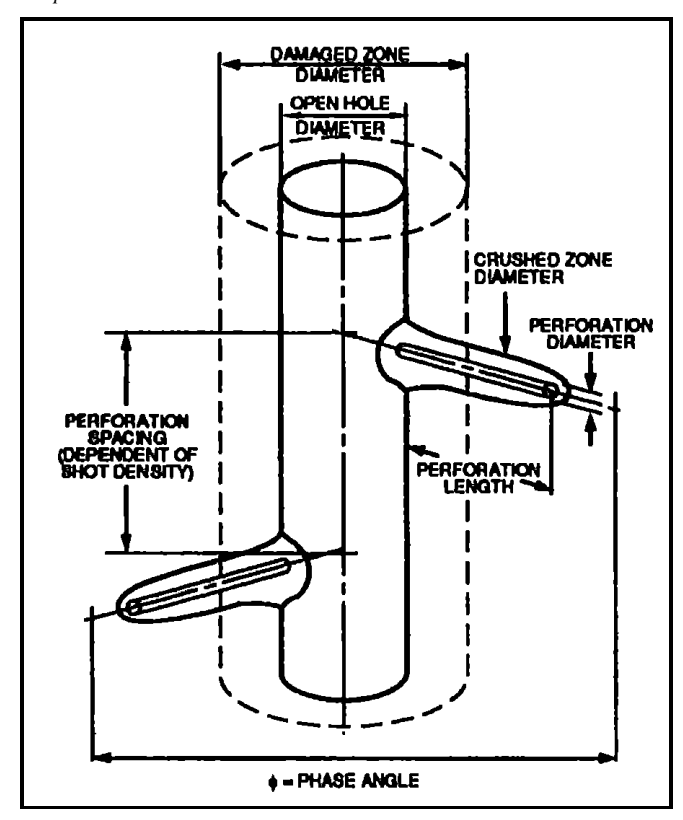


Fig. 28. Perforation geometry.

The calculation of perforation skin (s_p) is essential to estimate the damage skin (s_{dp}) from a prior knowledge of total skin (s_t) determined from well tests. Karakas and Tariq characterized the perforation skin as:

$$S_p = S_h + S_{wb} + S_v$$

where,

 s_h = pseudoskin due to phase (horizontal flow) effects,

 s_{wb} = pseudoskin due to wellbore effects (dominant in zero degree phasing),

 s_{ν} = pseudoskin due to vertical converging flow effects (negligible in the case of high-shot density; 3D effect),

MATRIX ENGINEERING MANUAL

Well Performance

Section 200
July 1998
Page 55 of 168

$$s_h = ln\left(\frac{r_w}{r_{we}(\theta)}\right)$$

where $r_{we}(\theta)$ is the effective wellbore radius as a function of the phasing angle, θ and perforation tunnel length.

$$r_{re}(\theta) = \begin{cases} 0.25 \, l_p & \text{if } \theta = 0^{\circ} \\ a_{\theta}(r_w + l_p) & \text{otherwise} \end{cases}$$

 α_{θ} is a correlating parameter used by Karakas and Tariq and is provided in Table 2.

Table 2. Dependence of σ_{θ} on Phasing		
Perforation Phasing	$\sigma_{ heta}$	
(360°) 0°	0.250	
180°	0.500	
120°	0.648	
90°	0.726	
60°	0.813	
45°	0.860	

The pseudoskin effect due to the wellbore (s_{wb}) can be calculated by using the following empirical relationship:

$$s_{wb}(\theta) = C_1(\theta) \exp [C_2(\theta) r_{wd}]$$

This component of perforation pseudoskin is significant in the case of 0° phasing. However, for r_{wd} less than 0.5, the wellbore effect can be considered negligible for phasing less than 120°. Table 3 provides the coefficients C_1 and C_2 as functions of phasing angle θ .

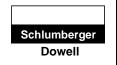
Table 3. Variables C₁ and C₂		
Perforating Phasing	C,	C ₂
(360°) 0°	1.6E-1	2.675
180°	2.6E-2	4.532
120°	6.6E-3	5.320
90°	1.9E-3	6.155
60°	3.0E-4	7.509
45°	4.6E-5	8.791

July 1998

Page 56 of 168

MATRIX ENGINEERING MANUAL

Well Performance



For high-shot density and unidirectional perforations, or where s_v is negligible, the perforation skin (s_n) is independent of the perforation hole diameter.

Karakas and Tariq suggested that for a low-shot density or high dimensionless perforation height (h_D) the pseudovertical skin (s_v) can be estimated using the following equation:

$$s_v = 10^a \ h_D^{b-1} \ r_{pD}^b$$

where the coefficients a and b are given by

$$a = a_1 \log r_{pD} + a_2$$

$$b = b_1 r_{pD} + b_2$$

The constants a_1 , a_2 , b_1 and b_2 are provided in Table 4, as functions of the phasing angle θ .

Table 4. Vertical Skin Correlation Coefficients				
Phasing	a,	$\mathbf{a}_{_{2}}$	b ₁	b_{2}
0°(360°)	-2.091	0.0453	5.313	1.8672
180°	-2.025	0.0943	3.0373	1.8115
120°	-2.018	0.0634	1.6136	1.7770
90°	-1.905	0.1038	1.5674	1.6935
60°	-1.898	0.1023	1.3654	1.6490
45°	-1.788	0.2398	1.1915	1.6392

EXAMPLE

Given

$$r_w = 0.5 \text{ ft}$$

$$l_p = 1.25 \text{ ft}$$

$$n_s = 16$$

(a) Calculate the perforation pseudoskin, s_p for 0° phasing.

Solution

$$s_p = s_h + s_{wb}$$
 (s_v is negligible for 16 spf)

$$s_h = 0.25 \times 1.25 = 0.31$$

$$r_{wD} = \frac{r_w}{r_w + l_p} + \frac{0.5}{0.5 + 1.25} = \frac{0.5}{1.75} = 0.29$$

From Table 3, $C_1 = 0.16$ and $C_2 = 2.675$.

$$s_{wb} = 0.16 \exp(2.675 \times 0.29) = 0.34$$

MATRIX ENGINEERING MANUAL

Well Performance

Section 200
July 1998
Page 57 of 168

$$s_p = s_h + s_{wb} = 0.65$$

(b) If this well is tested and the total skin calculated from buildup is 4, what is the treatable skin?

$$s_t = 4 = s_p + s_{dp}$$

 $s_{dp} = 4 - s_p = 4 - 0.65 = 3.35.$

This is just an estimate and is more accurately characterized later.

3.1.3 Crushed-Zone Effect

For conditions of linear flow into perforations, the effect of a crushed or compacted zone may be neglected. In the case of 3D flow, an additional skin due to the crushed zone can be calculated as follows:

$$s_c = \frac{h}{l_p} \left(\frac{k}{k_c} - I \right) ln \left(\frac{r_c}{r_p} \right)$$

where the crushed zone permeability and radius (k_c and r_c) can be calculated using the McLeod method.

3.1.4 Anisotropy Effects

The formation anisotropy affects the pseudovertical skin, s_v . The flow into perforations in the vertical plane is elliptical (otherwise radial) in anisotropic formations. The effective equivalent perforation radius in this case is given by:

$$r_{pe} = \frac{r_p}{2} \left(I + \sqrt{\frac{k_h}{k_v}} \right)$$

3.1.5 Damaged-Zone Effects

In a perforated completion, the contribution of a damaged zone to the total skin largely depends on the relative position of the perforations with respect to the damaged-zone radius. Karakas and Tariq showed that the skin damage for perforations terminating inside the damaged zone can be approximated by:

$$s_{dp} = \left(\frac{k}{k_d} - I\right) \left\{ ln\left(\frac{r_d}{r_w}\right) + sp \right\} + \frac{k}{k_d} s_x, \text{ for } l_p \leq l_d$$

where s_x is a pseudoskin to take into account the boundary effects for perforations terminating close to the damaged zone boundary. s_x is negligible for r_d greater than 1.5 $(r_w + l_p)$.

 k_d = permeability of damaged zone

 l_d = length of damaged zone

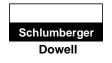
 r_d = radius of damaged zone

July 1998

Page 58 of 168

MATRIX ENGINEERING MANUAL

Well Performance



$$s_x = \ln \left\{ 1 - \left(\frac{1}{r_d^2}\right) \left(r_w + \frac{l_p}{2}\right)^2 \right\}$$

Table 5 provides values of s_x for 180° phasing.

Table 5. Skin Due to Boundary Effect, 180° Phasing		
$\frac{r_e}{(r_w + l_p)}$	S_{x}	
18.0	0.000	
10.0	-0.001	
2.0	-0.002	
1.5	-0.024	
1.2	-0.085	

For perforations extending beyond the damaged zone ($k_d = 0$), Karakas and Tariq contended the total skin (s_t) equals the pseudoskin due to perforations (s_p). That is:

$$s_t = s_p$$
, for $l_p > l_d$

The pseudoskin due to perforation (s_p) is calculated using modified l_p and modified r_w as:

$$l_p' = l_p - \left(1 - \frac{k_d}{k}\right) l_d$$

$$r_w' = r_w + \left(1 - \frac{k_d}{k}\right) l_d$$

EXAMPLE

Given

For the previous example, calculate the perforation skin (s_p) if the perforation tunnel extends beyond the damaged zone where:

$$l_d = 2 \text{ ft}$$

$$k = 2 \text{ md}$$

$$k_d = 1.0 \text{ md}$$

MATRIX ENGINEERING MANUAL

Well Performance

Section 200	
July 1998	

Page 59 of 168

Solution

$$l'_{p} = l_{p} - \left(1 - \frac{1}{2}\right)2 = 1.25 - \frac{1}{2} \times 2 \text{ ft}$$

$$= 0.25$$

$$r'_{w} - r_{w} - \left(1 - \frac{1}{2}\right) \times 2 = 0.5 + 1 = 1.5 \text{ ft}$$

$$s_{h} = 0.25 \times l'_{p} = 0.25 \times 0.25 = 0.0625$$

$$r_{wD} = \frac{1.5}{1.5 + 0.25} = \frac{1.5}{1.75} = 0.86$$

$$s_{wb} - 0.16 \text{ exp } (2.675 \times 0.86) = 1.60$$

$$s_{p} = s_{h} + s_{wb} = 0.06 + 1.60 = 1.66$$

Remember, this perforation skin (s_p) is also the total skin (s_p) and it includes the effect of damage.

3.2 Pressure Loss in Gravel Packs

Gravel pack operations are performed to control sand production from oil and gas wells. Sand production can cause a reduction in hydrocarbon production, eroding surface and downhole equipment, and can lead to casing collapse. Although the dynamics of gravel packing is not in the scope of this manual, a typical cross section of a gravel-packed well is shown in Fig. 29a and Fig. 29b. The figures show the flow path the reservoir fluid has to follow to produce into the wellbore. Evaluation of well performance in a gravel-packed well thus requires an accounting of the pressure losses caused by the flow through the gravel packs. Jones, Blount, and Glaze equations are adapted with minor modifications to account for the turbulence effects for the calculation of the pressure loss through the gravel packs. These modified equations for oil and gas cases are:

Oil Wells

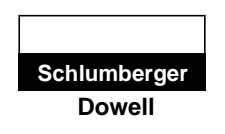
$$\begin{split} p_{wfs} - p_{wf} &= \Delta p = aq^2 + bq \\ \Delta p &= \frac{9.08 \times 10^{-13} \, \beta \, B_o^2 \rho \, L}{A^2} (q^2) \\ &+ \frac{\mu \, B_o L}{1.127 \times 10^{-3} \, k_o A} (q) \end{split}$$

where:

$$q = \text{flow rate (BPD)},$$

Section 200
July 1998
Page 60 of 168

Well Performance



 p_{wf} = pressure, well flowing (wellbore) (psi),

 p_{wfs} = flowing bottomhole pressure at the sandface,

 β = turbulence coefficient (ft⁻¹).

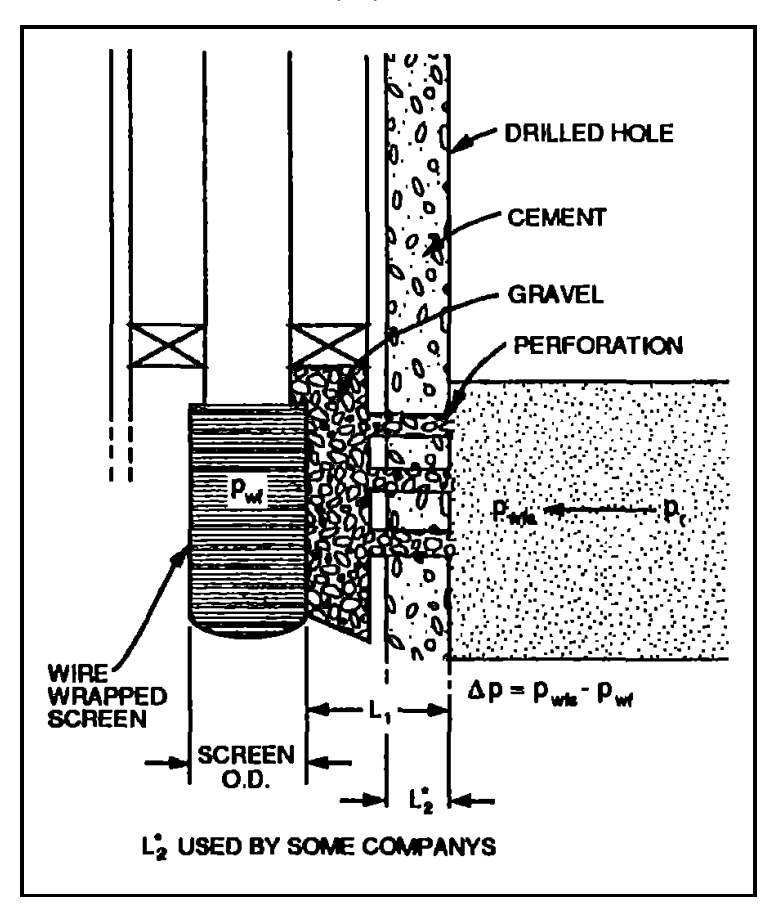


Fig. 29a. Gravel pack schematic.

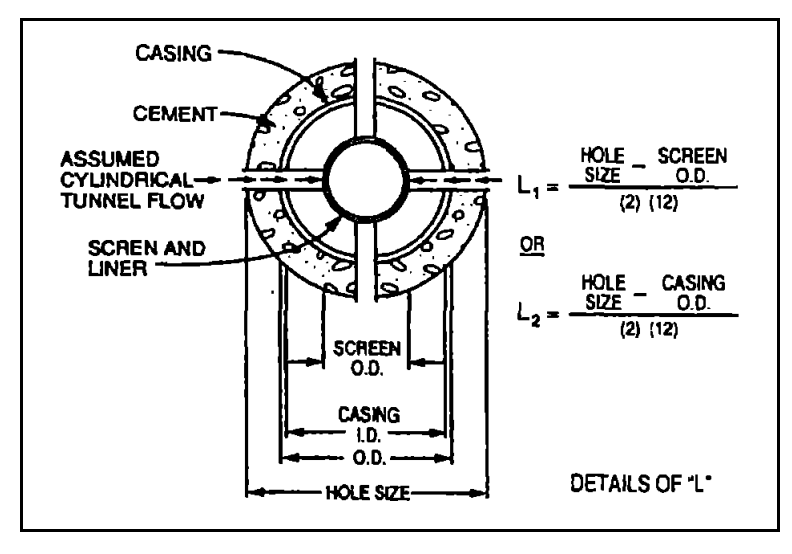


Fig. 29b. Cross section of gravel pack across a perforation tunnel.

MATRIX ENGINEERING MANUAL

Well Performance

Section 200 July 1998

Page 61 of 168

For gravel, the equation for β is:

$$\beta = \frac{1.47 \times 10^7}{k_g^{0.55}}$$

where:

 B_o = formation volume factor (rb/stb),

 ρ = fluid density (lb/ft³),

L = length of linear flow path (ft),

a = total area open to flow (ft²) (A = area of one perforation x shot density x perforated interval),

 k_s = permeability of gravel (md).

Gas Wells

$$\begin{split} p_{wfs}^2 - p_{wf}^2 &= aq^2 + bq \\ p_{wfs}^2 - p_{wf}^2 &= \\ \frac{1.247 \times 10^{-10} \, \beta \gamma_g \, TZL}{A^2} \, q^2 + \frac{8.93 \times 10^3 \, \mu \, TZL}{k_g A} \, q, \end{split}$$

where:

$$a = \frac{1.247 \times 10^{-10} \, \beta \gamma_g TZL}{A^2}$$

$$b = \frac{8.93 \times 10^3 \,\mu\,TZL}{k_o A}$$

q = flow rate (Mcf/D),

 p_{wfs} = flowing bottomhole pressure at the sandface (psia),

 p_{wf} = flowing bottomhole pressure in the wellbore (psia),

 β = turbulence factor (ft⁻¹),

$$= \frac{1.47 \times 10^7}{k_g^{0.55}}$$

 $\gamma_{\rm s}$ = gas specific gravity (dimensionless),

T = temperature, °R (°F + 460),

Z = supercompressibility (dimensionless),

L = linear flow path,

A =total area open to flow

A = area of one perforation x shot density x perforated interval),

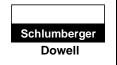
 μ = viscosity (cp).

July 1998

Page 62 of 168

MATRIX ENGINEERING MANUAL

Well Performance



4 Flow Through Tubing and Flowlines

Fluid flow through the reservoir and completion are discussed in the previous sections. However, the performance evaluation of a well is not complete until the effects of the tubing and flowline are also considered. This section discusses the flow through the plumbing system in the well. The objective here is to calculate the pressure loss in the tubing or in the flowline as a function of flow rates of different flowing phases. In most oil and gas wells, two- or three-phase (oil, gas and water) flow occurs in the plumbing system. Consequently, a brief discussion on the theory of multiphase flow in pipes is provided. This theory is an extension of the theory of single-phase flow.

The pressure gradient equation under a steady-state flow condition for any singlephase incompressible fluid can be written as (Eq. 12):

$$-144\frac{dp}{dL} = \left(\frac{g}{g_c}\right)\rho\sin\theta + \frac{\rho v^2}{2g_c d} + \rho\frac{v dv}{g_c a(dL)}$$
 (12)

where:

 $\frac{dp}{dL}$ = pressure drop per unit length of pipe (psi/ft),

 ρ = density of fluid (lbm/ft³),

 θ = angle of inclination of pipe,

v =fluid velocity (ft/sec),

f = friction factor,

d = internal diameter of the pipe (ft),

 α = correction factor to compensate for the velocity variation over the pipe cross section. It varies from 0.5 for laminar flow to 1.0 for fully developed turbulent flow.

This equation applies to any fluid in a steady-state flow condition. Important to note in this equation is that the total pressure gradient is the sum of three principal components.

- hydrostatic gradient ($\rho \sin \theta$)
- friction gradient $\left(\frac{fv^2\rho}{2g_c d}\right)$
- acceleration gradient $\left(\frac{\rho v \, dv}{g_c \, dL}\right)$

The friction factor, f for laminar, single-phase flow is calculated using an analytical expression such as:

$$f = \frac{64}{N_{Re}}$$

MATRIX ENGINEERING MANUAL

Well Performance

Section 200
July 1998
Page 63 of 168

where N_{Re} is the Reynolds Number and is defined as:

$$N_{Re} = \frac{dv \, \rho}{\mu}$$

where:

 μ = viscosity of the flowing fluid.

For turbulent flow (when the Reynolds Number exceeds 2000), the relationship between the friction factor and Reynolds Number is empirical in nature. This relationship is sensitive to the characteristics of the pipe wall and is a function of relative roughness, ϵ/d , where ϵ is defined as the absolute roughness of the pipe. The most widely used method to calculate the friction factor in turbulent flow is the equation of Colebrook (1938):

$$\frac{1}{\sqrt{f}} = 1.74 - 2\log\left(\frac{2\varepsilon}{d} + \frac{18.7}{N_{Re} f^{0.5}}\right)$$

Note that the friction factor, f occurs on both sides of this equation requiring a trial and error solution procedure. For this reason, the solution of these equations presented by Moody (1944) in graphical form (Moody diagram) is widely used for the calculation of the friction factor. A Moody diagram is provided in Fig. 30. A simple equation proposed by Jain (1976) reproduces the Colebrook equations over essentially the entire range of Reynolds Number and relative roughness of interest, and is (Eq. 13):

$$\frac{1}{\sqrt{f}} = 1.14 - 2\log\left(\frac{\varepsilon}{d} + \frac{21.25}{N_{Re}^{0.9}}\right)$$
 (13)

Selecting the absolute pipe roughness is often a difficult task because roughness can depend upon the pipe material, manufacturing process, age, and type of fluids flowing through the pipe. Glass pipe and many types of plastic pipe can often be considered as smooth pipe. It is common to use a roughness of 0.00005 ft for well tubing. Commonly used values for line pipe range from 0.00015 ft for clean, new pipe to 0.00075 ft for dirty pipe. An acceptable procedure used by many investigators is to adjust the absolute roughness to permit matching measured pressure gradients.

4.1 Single-Phase Gas Flow in Pipes

For gas flow or compressible flow, the density of fluid is a function of pressure and temperature. The energy balance (Eq. 12) can be modified to account for pressure and temperature-dependent density. The energy balance equation for steady-state flow can be written as (Eq. 14):

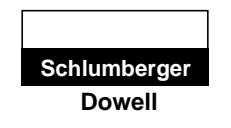
$$\frac{144}{\rho}dp + \frac{g}{g_c}\sin\theta \, dL + \frac{fv^2}{2g_c d}dL = \frac{vdv}{g_c} = 0 \tag{14}$$

July 1998

Page 64 of 168

MATRIX ENGINEERING MANUAL

Well Performance



The energy loss term due to friction uses the Moody friction factor (f). The kinetic energy term, $(vdv)/g_c$, is negligible for all cases of gas flow as shown by Aziz (1963). Applying real gas law, the density of gas (ρ) becomes (Eq. 15):

$$\rho \left(\frac{lbm}{ft^3}\right) = 2.7047 \frac{p\gamma_g}{zT} \tag{15}$$

Eq. 14 can be rewritten as (Eq. 16):

$$\frac{53.24TZ}{\gamma_g} \frac{dp}{p} + \sin\theta \, dL + \frac{fv^2 dL}{2g_c \, d} = 0 \tag{16}$$

The velocity of gas at in-situ pressure and temperature conditions is:

$$v = 0.4152 \frac{Tz \ q}{pd^2}$$

where:

q = gas production rate (MMscf/D) (14.65 psia, 60°F),

v = gas velocity in pipe (ft/sec),

d = pipe diameter (ft),

 γ_s = gas gravity (air = 1).

Substituting the velocity term in gives (Eq. 17):

$$\frac{53.24 \text{ TZ}}{\gamma_g} \frac{dp}{p} + \sin \theta \, dL + 0.002679 \frac{f}{d^5} \left(\frac{Tz}{p}\right)^2 q^2 \, dL = 0 \tag{17}$$

This is the most practical form of an energy balance equation used for gas flow calculations. The friction factor is calculated using the Moody diagram (Fig. 30) or using any of the friction-factor equations provided in the previous section as functions of the Reynolds Number and relative roughness factor. For steady-state gas flow, the Reynolds Number is defined as:

$$N_{Re} = 1671 \frac{q \gamma_g}{\mu d}$$

where the viscosity of gas (μ) is in centipoise. For diameter (d) in inches:

$$N_{Re} = 20,050 \frac{q \gamma_g}{\mu d}$$

MATRIX ENGINEERING MANUAL

Well Performance

Section 200 July 1998

Page 65 of 168

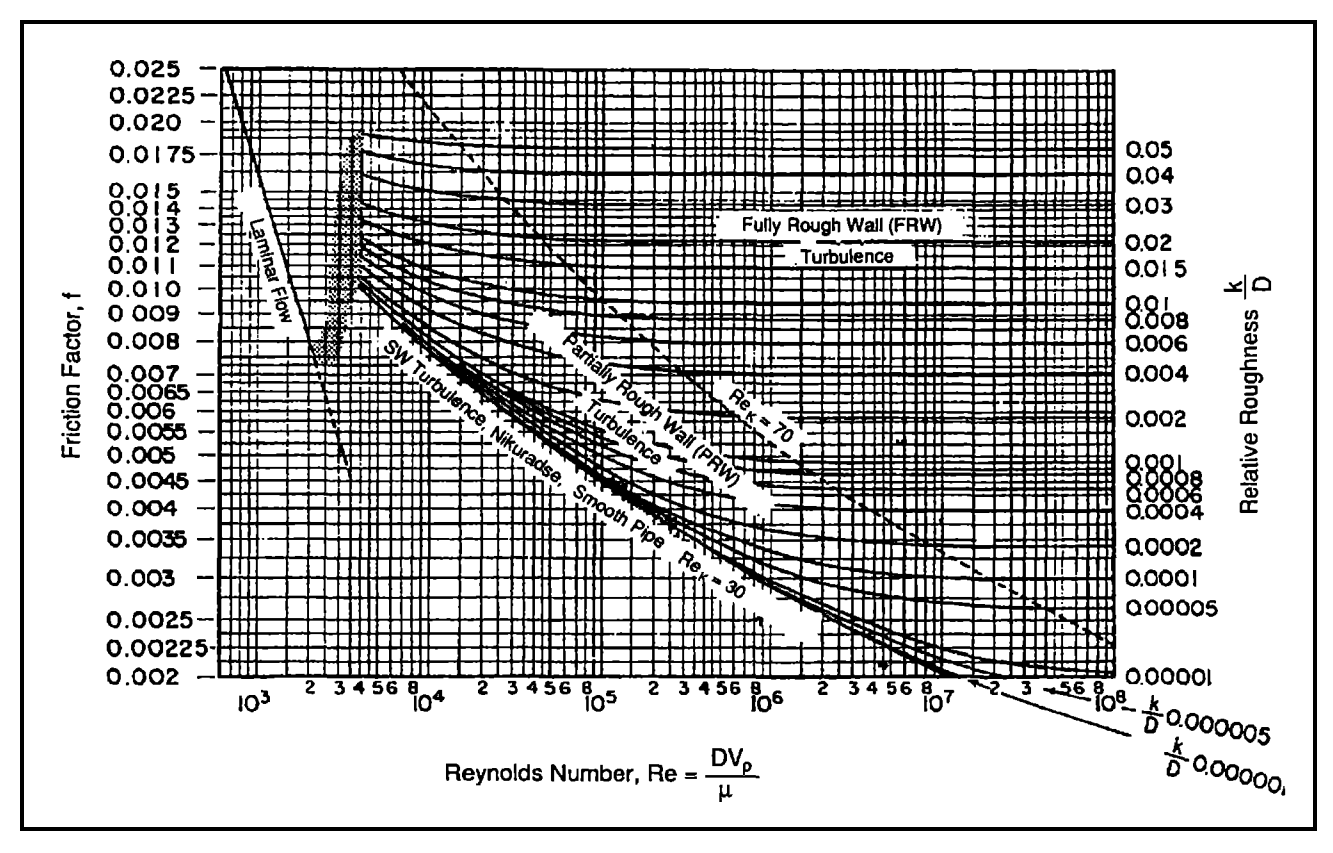


Fig. 30. Pipe friction factors for turbulent flow (modified after Moody, L.F., Trans. ASME, 66, 671, 1944).

4.2 Estimation of Static Bottomhole Pressure

Ignoring the friction loss term and appropriately integrating over the pressure and length:

$$\int_{p_{wh}}^{p_{bh}} \frac{dp}{p} = + \int_{0}^{L} \frac{\gamma_g \sin \theta}{53.2 \, \overline{Tz}} dL$$

$$\ln \frac{p_{bh}}{p_{wh}} = \frac{\gamma_g \sin \theta}{53.2 \, \overline{Tz}} L$$
(18)

Therefore,

$$p_{bh} = p_{wh} \ e \left(\frac{\gamma_g \sin \theta}{53.2 \ \overline{Tz}} L \right)$$

where:

 p_{bh} = static bottomhole pressure (psia),

 p_{wh} = static wellhead pressure (psia),

 \overline{T} = average temperature between bottomhole and surface,

 \overline{z} = compressibility factor at average pressure and average temperature.

July 1998

Page 66 of 168

MATRIX ENGINEERING MANUAL

Well Performance



Eq. 18 is used extensively to calculate the weight of the gas column. The solution of this equation is iterative in pressure as \bar{z} is a function of pressure. To calculate the bottomhole pressure from known surface pressure and temperature, a value of bottomhole pressure has to be assumed. Then the average pressure and average temperature knowing the geothermal gradient should be calculated and the average z-factor determined. Then, using Eq. 18, a new bottomhole flowing pressure is calculated. If this calculated p_{bh} does not compare with the assumed bottomhole pressure, the iterative procedure should continue until convergence of the assumed and calculated bottomhole pressures occurs.

4.3 Estimation of Flowing Bottomhole Pressure

Cullender and Smith (1956) proposed a simple method of calculating the flowing bottomhole pressure based on Eq. 17. Cullender and Smith rearranged Eq. 17 and integrated the pressures over the whole length of the pipe. Thus:

$$\frac{\gamma_g L}{53.24} = \int_{p_{wh}}^{p_{bh}} \frac{\left(\frac{p}{Tz}\right) dp}{\left\{0.002679 \frac{fq^2}{d^5} + \left(\frac{p}{Tz}\right)^2 \sin\theta\right\}}$$
(19)

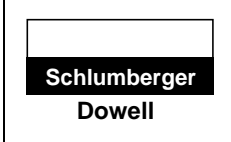
Eq. 19 can be solved by any standard numerical integration schemes (for example, Simpson's rule). Eq. 19 uses the Moody friction factor and the diameter, d is in feet. A brief derivation of Eq. 19 is provided in Section 9.

4.4 Multiphase Flow

The energy balance equation for multiphase flow is similar to that of the single-phase flow. In this case, the velocities and fluid properties of the total fluid mixture are used instead of the single-phase fluid properties. However, the definition of a fluid mixture becomes complicated in this case. The quality of a fluid mixture changes with the pipe diameter, pipe inclination, temperature and pressure, mainly due to slippage between the phases. In the absence of slippage, the mixture properties should be the input volumetric fraction weighted average of all the phases constituting the mixture. For example, if the mixture contains 50% oil and 50% gas at the pipe entry, then the average mixture density should be

$$\rho_m = \rho_o \times 0.5 + \rho_g \times 0.5$$

However, averaging is not practically valid in the case of multiphase flow in pipes. When gas and liquid phases flow in pipes, due to buoyancy or density contrast between the phases, the gas phase tends to gain an upward velocity with respect to the liquid phase. Thus, in the case of upward two-phase flow (production), the gas gains velocity in the direction of flow as liquid slips down or loses velocity. To satisfy the conservation of mass, the cross section of pipe occupied by a liquid or gas phase changes continuously. The fraction of pipe cross section occupied by liquid at any point in the multiphase flow string is called the liquid holdup (H_L). The



Well Performance

Section 200
July 1998
Page 67 of 168

complementary fraction of pipe cross section occupied by gas is called the gas void fraction. The actual mixture property in a multiphase flow should be the holdup weighted sum of the single phase fluid property. Since the liquid holdup continuously changes in the pipe, the phase velocities also change. This section discusses some of the important flow properties (for example, holdup) and different velocities used in multiphase flow calculations.

4.5 Liquid Holdup

In gas/liquid two-phase flow, due to the contrast in phase densities, the gas phase tends to move up while the liquid phase tends to move down with respect to the gas phase, creating a slippage between the phases. As a result in upflow, a liquid loses velocity requiring increased pipe cross section to flow with the same volumetric flow rate. This phenomenon of slippage causes the flowing liquid content in a pipe to be different from the input liquid content. The flowing liquid content is called the liquid holdup. Liquid holdup is also defined as the ratio of the volume of a pipe segment occupied to the total volume of that pipe segment. That is:

$$H_L = \frac{volume \ of \ liquid \ in \ pipe \ segment}{volume \ of \ pipe \ segment}$$

Liquid holdup is a fraction that varies from zero for single-phase gas flow to one for single-phase liquid flow. The most common method of measuring liquid holdup is to isolate a segment of the flow stream between quick-closing valves and to physically measure the liquid trapped. There are different mechanistic and empirical models for the prediction of liquid holdup. The remainder of the pipe segment is occupied by gas, which is referred to as gas holdup or void fraction. That is:

$$H_g = 1 - H_L$$
.

4.6 No-Slip Liquid Holdup

No-slip holdup, sometimes called input liquid content, is defined as the ratio of the volume of liquid in a pipe segment divided by the volume of the pipe segment that would exist if the gas and liquid traveled at the input or entrance velocity (no slippage). It can be calculated directly from the known gas and liquid flow rates from:

$$\lambda_L = \frac{q_L}{q_L + q_g}$$

where q_L and q_s are the in-situ liquid and gas flow rates. The no-slip gas holdup or void fraction is defined as:

$$\lambda_g = 1 - \lambda_L = \frac{q_g}{q_L + q_g}$$

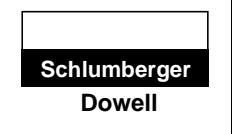
It is obvious that the difference between the liquid holdup and the no-slip holdup is a measure of the degree of slippage between the gas and liquid phases. Since no-slip

July 1998

Page 68 of 168

MATRIX ENGINEERING MANUAL

Well Performance



holdup is an analytically-determined parameter, it is often used as an independent variable to determine important two-phase flow parameters, for example, the liquid holdup.

4.7 Superficial Velocity

Many two-phase flow correlations are based on a variable called superficial velocity. The superficial velocity of a fluid phase is defined as the velocity that the fluid phase would exhibit if it flowed through the complete cross section of the pipe.

The superficial liquid velocity is:

$$V_{SL} = \frac{q_L}{A}$$

The superficial gas velocity is:

$$V_{sg} = \frac{q_g}{A}$$

where, q_L and q_s are liquid and gas flow rates and A is the cross-sectional area of the pipe.

The actual phase velocities are defined as:

$$V_L = \frac{V_{SL}}{H_I}$$

and

$$v_g = \frac{V_{sg}}{H_g}$$

where v_L and v_g are liquid and gas velocities as they flow in the pipe.

4.8 Mixture Velocity

The mixture velocity (v_m) used in two-phase flow calculations is:

$$v_m = v_{SL} + v_{sg}$$

It is an important correlating parameter in two-phase flow calculations.

4.9 Slip Velocity

The slip velocity is defined as the difference in the actual gas and liquid velocities:

$$v_s = v_g - v_L$$

4.10 Liquid Density

The total liquid density may be calculated from the oil and water densities and flow rates if no slippage between the oil and water phases is assumed:

$$\rho_L = \rho_o f_o + \rho_w f_w$$

MATRIX ENGINEERING MANUAL

Well Performance

Section 200	
July 1998	

Page 69 of 168

where:

$$f_{o} = \frac{q_{o}}{q_{o} + q_{w}} = \frac{q'_{o}B_{o}}{q'_{o}B_{o} + q'_{w}B_{w}}$$

$$= \frac{1}{1 + WOR\left(\frac{B_{w}}{B_{o}}\right)}$$

$$f_{w} = 1 - f_{o}$$

$$WOR = water / oil \ ratio = \frac{q'_{w}}{q'_{o}}$$

$$q'_{(o,w)} = oil \ or \ water \ flow \ rate \ (stb / D)$$

4.11 Two-Phase Density

The calculation of two-phase density requires knowledge of the liquid holdup. Three equations for two-phase density are used in two-phase flow.

$$\rho_s = \rho_L H_L + \rho_g H_g$$

$$\rho_n = \rho_L \lambda_L + \rho_g \lambda_g$$

$$\rho_k = \frac{\rho_L \lambda_L^2}{H_L} + \frac{\rho_g \lambda_g^2}{H_g}$$

The density of the gas/liquid mixture (ρ_s) is used (by most) to determine the pressure gradient due to the elevation change. Some correlations are based on the assumption of no-slippage and, therefore, use ρ_n for two-phase density. ρ_k is used (by some) to define the mixture density used in the friction loss term and the Reynolds Number.

4.12 Viscosity

The viscosity of an oil/water mixture is usually calculated using the water/oil ratio as a weighting factor. The equation is:

$$\mu_L = \mu_o f_o + \mu_w f_w$$

4.13 Two-Phase Viscosity

The following equations have been used to calculate a two-phase viscosity.

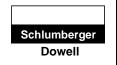
$$\mu_n = \mu_L \lambda_L + \mu_g \lambda_g$$
, no slip mixture viscosity $\mu_s = \mu_L H_L + \mu_g H_g$, slip mixture viscosity

July 1998

Page 70 of 168

MATRIX ENGINEERING MANUAL

Well Performance



4.14 Surface Tension

Correlations for the interfacial tension between water and natural gas at various pressures and temperature are obtained from measured data or PVT correlation. The interfacial tension between natural gas and crude oil depends on oil gravity, temperature dissolved gas and other variables.

When the liquid phase contains water and oil, the same weighting factors as used for calculating density and viscosity are used. That is:

$$\sigma_L = \sigma_o f_o + \sigma_w f_w$$

where:

 σ_o = surface tension of oil

 σ_{w} = surface tension of water

and f_o , f_w are oil and water fractions.

4.15 Multiphase-Flow Pressure Gradient Equations

The pressure gradient equation for single-phase flow can now be extended for multiphase flow by replacing the flow and fluid properties by the mixture properties. Thus:

$$\frac{dp}{dL} = \left(\frac{g}{g_c}\right) \rho_m \sin\theta + \frac{f\rho_m v_m^2}{2g_c d} + \frac{\rho_m v_m (dv_m)}{g_c (dL)}$$
(20)

where:

 ρ = density,

v = velocity,

d = pipe diameter (ID),

g = acceleration due to gravity,

 g_c = gravity conversion factor,

f = friction factor,

 $\frac{dp}{dI}$ = pressure gradient,

m = mixture properties,

 θ = angle of inclination from horizontal.

The equation is usually adapted for two-phase flow by assuming that the gas/liquid mixture can be considered to be homogeneous over a finite volume of the pipe. For two-phase flow, the hydrostatic gradient is:

$$\frac{g}{g_c}\rho_s\sin\theta$$

MATRIX ENGINEERING MANUAL

Well Performance

Section 200
July 1998
Page 71 of 168

where ρ_s is the density of the gas/liquid mixture in the pipe element.

Considering a pipe element that contains liquid and gas, the density of the mixture can be calculated from

$$\rho_s = \rho_L H_L + \rho_g H_g$$

The friction loss component becomes:

$$\frac{f_{tp} \, \rho_f v_m^2}{2g_c \, d}$$

where f_{tp} and ρ_f are defined differently by several investigators (Duns and Ros [1963] and Hagedorn and Brown [1965]).

4.16 Two-Phase Friction

Previously, it was shown that the term $(dp/dL)_f$ represents the pressure losses due to friction when gas and liquid flow simultaneously in pipes. This term is not analytically predictable except for the case of laminar single-phase flow. Therefore, it must be determined by experimental means or by analogies to single-phase flow. The method that has received by far the most attention is the one resulting in two-phase friction factors. The different expressions for the calculation of two-phase friction gradient are the following:

$$\left(\frac{dp}{dL}\right)_{FRICTION} = \frac{f_L \, \rho_L \, v_{SL}^2}{2g_c \, d} \quad (used in bubble flow)$$

$$\left(\frac{dp}{dL}\right)_{FRICTION} = \frac{f_g \, \rho_g v^2 s_g}{2g_c \, d} \quad (used in annular flow regime)$$

$$\left(\frac{dp}{dL}\right)_{FRICTION} = \frac{f_{tp} \, \rho_f \, v_m^2}{2g_c \, d}$$

In general, the two-phase friction factor methods differ only in the way the friction factor is determined, and to a large extent, on the flow pattern. For example, in a mist-flow pattern, the equation based on gas is normally used; whereas, in a bubble-flow regime, the equation based on liquid is frequently used. The definition of ρ_{r} can differ widely depending on the investigator.

Most correlations attempt to correlate friction factors with some form of a Reynolds Number. Recall that the single-phase Reynolds Number is defined as:

$$N_{Re} = \frac{\rho v d}{\mu}$$

One consistent set of units frequently used for calculating N_{Re} is:

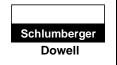
$$\rho$$
 = density (lbm/ft³),

July 1998

Page 72 of 168

MATRIX ENGINEERING MANUAL

Well Performance



v = velocity (ft/sec),

d = pipe diameter (ft)

 μ = viscosity (lbm/ft-sec).

Since viscosity is more commonly used in centipoise, the Reynolds Number with μ in cp is:

$$N_{Re} = 1488 \frac{\rho \, v \, d}{\mu}$$

4.17 Hydrostatic Component

From the pressure gradient equation in single and multiphase flow, it becomes evident that the elevation component drops out in horizontal flow. However, the elevation or the hydrostatic gradient component is by far the most important of all the three components in vertical and inclined flow. It is the principal component that causes wells to load up and die. Gas well loading is a typical example where the hydrostatic component builds up in the well due to liquid slippage and overcomes reservoir pressure, reducing the gas intake.

4.18 Friction Component

This component is always more dominant in horizontal flow. Also, in vertical or inclined gas, gas condensate, or high gas/liquid ratio multiphase flow, the friction loss can be dominant. In gas-lift wells, injection above an optimum gas/liquid ratio causes a reversal of the tubing gradient due to high friction losses compared to hydrostatic losses. In fact, by injecting more gas, oil production can be lost in a gas-lift well.

4.19 Acceleration Component

The acceleration component, which sometimes is referred to as the kinetic energy term, constitutes a velocity-squared term (Eq. 20) and is based on a changing velocity that must occur between various positions in the pipe. In about 98% of the actual field cases, this term approaches zero but can be significant in some instances, showing up to 10% of the total pressure loss. In those cases of low pressure and hence low densities and high gas volumes or high gas/oil ratios, a rapid change in velocity occurs and the acceleration component may become significant. It should always be included in any computer calculations.

The acceleration component is completely ignored by some investigators and ignored in some flow regimes by others. When it is considered, various assumptions are made regarding the relative magnitudes of parameters involved to arrive at some simplified procedure to determine the pressure drop due to the kinetic energy change. This pressure gradient component is important near the surface in high gas/liquid ratio wells.

MATRIX ENGINEERING MANUAL

Well Performance

Section 200			
July 1998			
Page 73 of 168			

From the discussion of the various components contributing to the total pressure gradient, it is essential that methods to predict the liquid holdup and two-phase friction factor be developed. This is the approach followed by most researchers in the study of two-phase flowing pressure gradients.

4.20 Flow Patterns

Whenever two fluids with different physical properties flow simultaneously in a pipe, there is a wide range of possible flow patterns. The flow pattern indicates the geometric distribution of each phase in the pipe relative to the other phase. Many investigators such as Mukherjee and Brill (1985) have attempted to predict the flow pattern that will exist for various flow conditions. This is particularly important as the liquid holdup is found to be dependent on the flow pattern. In recent studies, it was confirmed that the flow pattern is also dependent on the angle of inclination of the pipe and direction of flow (for example, production or injection). Consequently, some of the more reliable pressure loss correlations are dependent on the accurate prediction of a flow pattern.

(can be present in both upflow or downflow)

There are four important flow patterns.

Annular/mist flow:

Bubble flow: (can be present in both upflow or downflow)
 Slug flow: (can be present in both upflow or downflow)

Stratified flow: (only possible in downflow)

Bubble flow in gas/liquid two-phase flow is defined as the flow regime where both the phases are almost homogeneously mixed or the gas phase travels as small bubbles in a continuous liquid medium. Slug flow on the other hand is defined as the flow condition where gas bubbles are longer than one pipe diameter and flow through the pipe as discrete slugs of gas followed by slugs of liquids. Due to continuous segregation of phases in the direction of flow, slug flow results in substantial pressure fluctuations in the pipe. This creates production problems, for example, separator flooding and improper functioning of gas-lift valves. Annular flow is defined as the flow pattern where the gas phase flows as a core with the liquid flowing as an annular film adjacent to the pipe wall. This happens at a high gas velocity. The stratified flow only occurs in two phase downflow. This flow pattern is characterized by fluid stratification along the cross section of the flow conduit or pipe. The heavier fluid flows through the bottom of the pipe, whereas the lighter fluid/gas occupies the upper cross section of the pipe. Fig. 31a shows a geometric configuration of gas/liquid control volume in different flow patterns. In two-phase gas/liquid flow, the momentum balance equation (Eq. 20) depends on the flow pattern. The prediction of flow patterns is possible using the Mukherjee and Brill (1979) or Barnea et al. (1982) and Taitel et al. (1980) methods. Fig. 32, Fig. 33 and Fig. 34 show some of the flow pattern maps for vertical upflow to horizontal flow. The flow pattern maps are presented with liquid and gas velocity numbers as the independent variables. These are defined as follows.

O	
Section	n 200

July 1998

Page 74 of 168

MATRIX ENGINEERING MANUAL

Well Performance



$$\begin{aligned} & \textit{Liquid Velocity Number} = N_{LV} = 1.938 \ V_{sL} \sqrt[4]{\frac{\rho_L}{\sigma_L}} \\ & \textit{Gas Velocity Number} = N_{gV} = 1.938 \ V_{sg} \sqrt[4]{\frac{\rho_L}{\sigma_L}} \end{aligned}$$

where:

 V_{sL} = superficial liquid velocity (ft/sec),

 V_{sg} = superficial gas velocity (ft/sec),

 $\rho_L = lbm/ft^3$,

 σ_L = surface tension of liquid (dynes/cm).

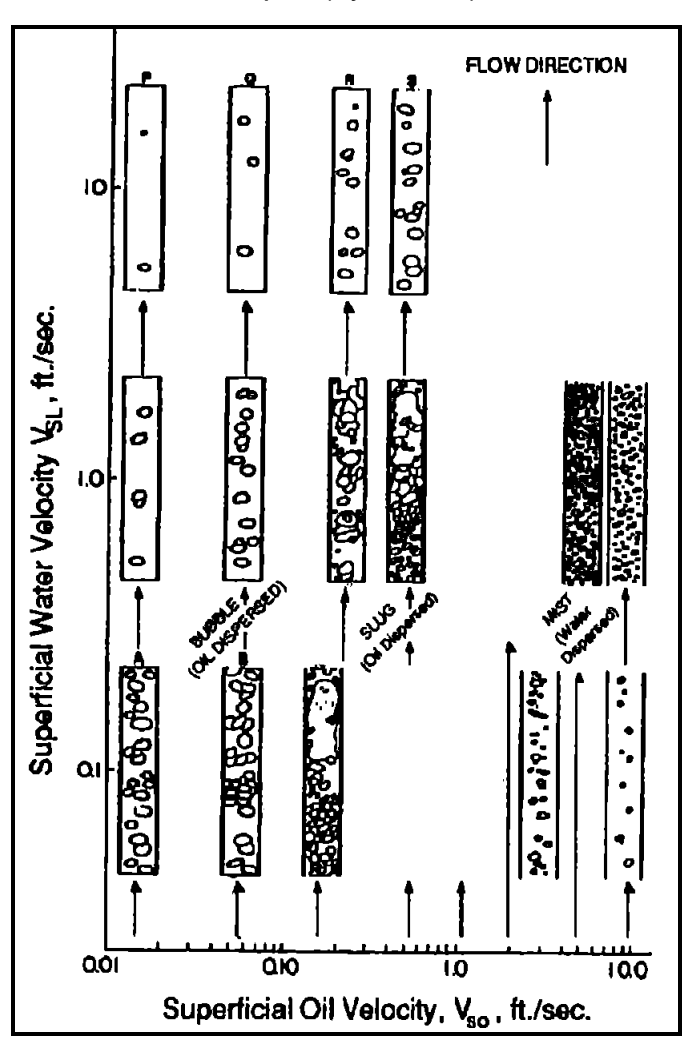


Fig. 31a. Flow patterns for 20.09-cp viscosity, 0.851-specific gravity oil, and water mixtures in a 1.04-in. pipe based on observations of Govier, Sullivan and Wood, 1961.

MATRIX ENGINEERING MANUAL

Well Performance

Section 200

July 1998

Page 75 of 168

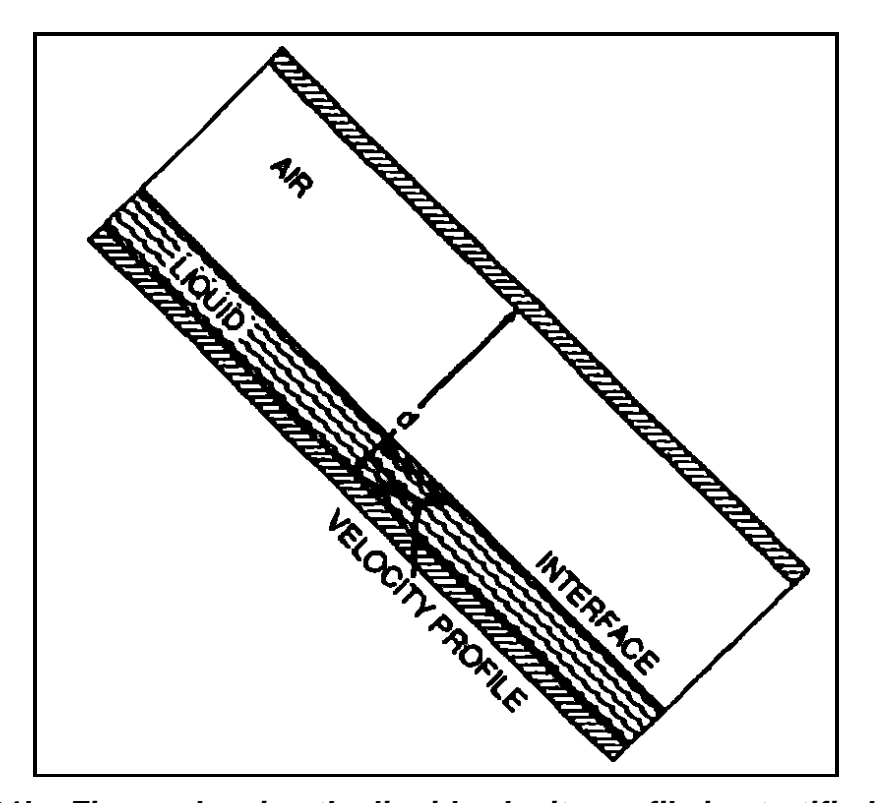


Fig. 31b. Figure showing the liquid velocity profile in stratified flow.

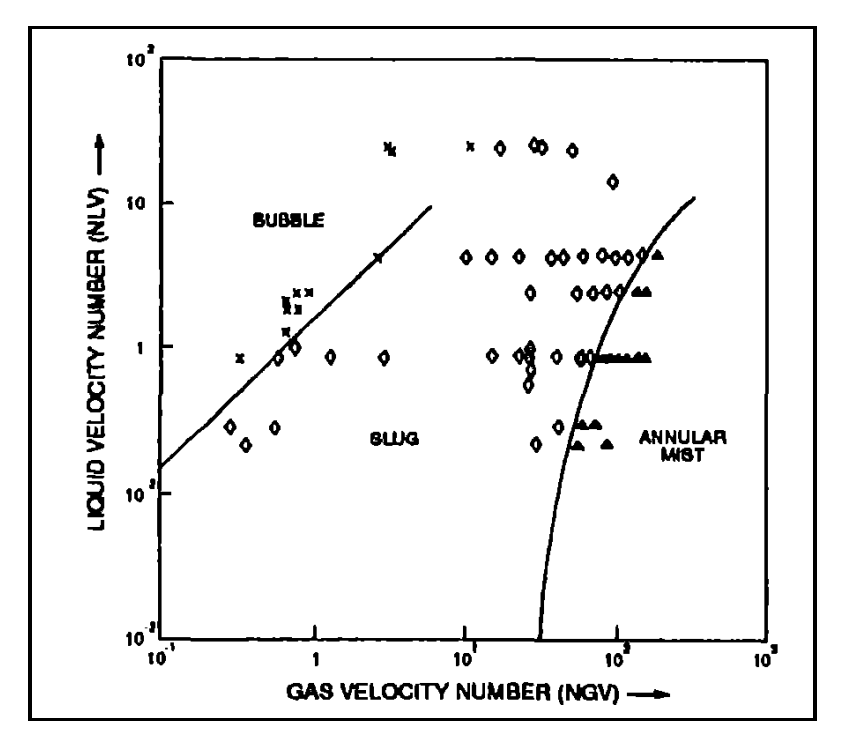
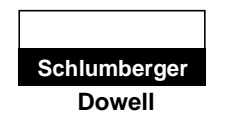


Fig. 32. Predicted flow pattern transition lines superimposed on the observed flow pattern map for kerosene in vertical uphill flow.

Section 200				
July 1998				
Page 76 of 168				



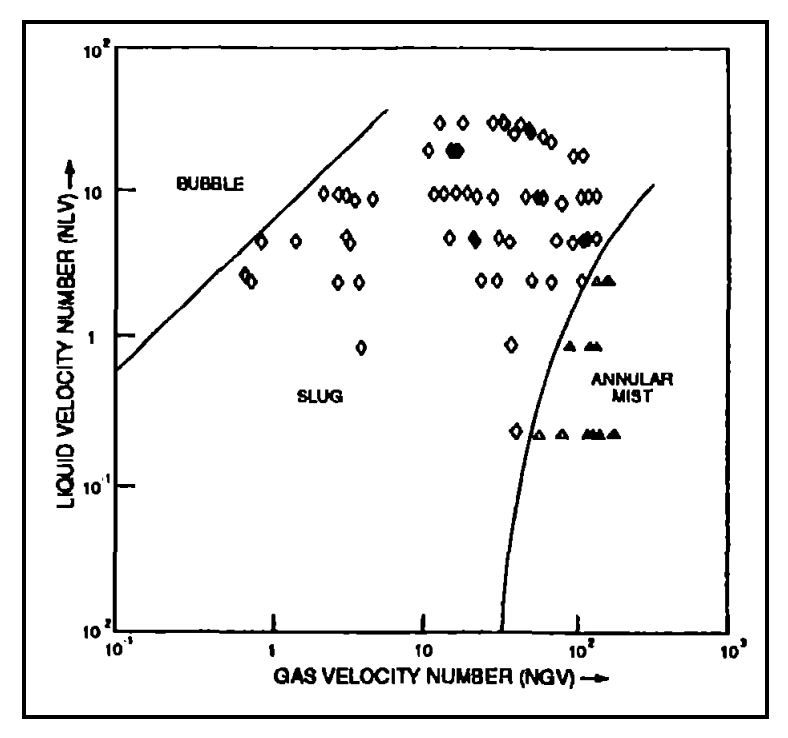


Fig. 33. Predicted flow pattern transition lines superimposed on the observed flow pattern map for kerosene in uphill 30° flow.

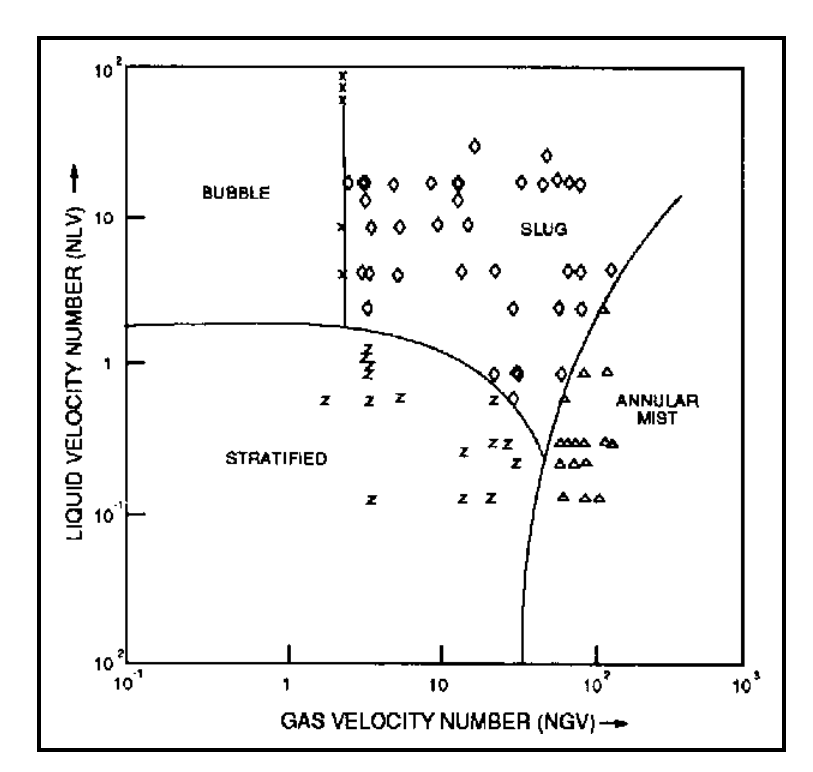


Fig. 34. Predicted flow pattern transition lines superimposed on the observed flow pattern map for kerosene in horizontal flow.

MATRIX ENGINEERING MANUAL

Well Performance

Section 200

July 1998 Page 77 of 168

EXAMPLE

Given

Tubing ID = 2.441 in., (2-7/8-in. tubing)

Surface tension of oil = 26 dynes/cm Oil rate = 250 STB/D

API gravity = 30°

GOR = $56 \frac{scf}{STB}$

Determine the flow pattern for this vertical producing well.

Solution

Specific gravity of oil =
$$\frac{141.5}{131.5 + API} = \frac{141.5}{131.5 + 30} = 0.88$$

Tubing cross – section =
$$\frac{\pi d^2}{4} = \frac{\pi}{4} \left(\frac{2.441}{12} \right)^2 = 0.0325 \text{ ft}^2$$

Superficial oil velocity,
$$V_{SL} = \frac{250 \times 5.615}{86,400 \times 0.0325}$$
 ft/sec

$$= 0.5 ft/sec$$

Liquid velocity number,
$$N_{Lv} = 1.938 \times 0.5 \sqrt{\frac{0.88 \times 62.4}{26}}$$

$$= 1.938 \times 0.5 \times 1.2055$$

Superficial gas velocity,
$$V_{sg} = \frac{250 \times 56}{86,400 \times 0.0325}$$
 ft/sec

$$= 5 ft/sec$$

Gas velocity number = 1.938×1.2055

$$= 11.7$$

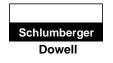
From Fig. 32 for N_{LV} = 1.2 and N_{gV} = 11.7, the predicted flow pattern is slug flow.

4.21 Calculation of Pressure Traverses

A number of methods have been proposed to calculate the pressure loss when gas and liquid simultaneously flow through a pipeline. These methods provide means to predict flow patterns for given flow and fluid parameters, for example, the individual phase flow rates, fluid properties, pumping system dimensions and one of the Section 200 July 1998

MATRIX ENGINEERING MANUAL

Well Performance



Page 78 of 168

terminal pressures (wellhead/separator pressure). For the predicted flow patterns, liquid holdup and friction factors are calculated to determine the hydrostatic gradient and friction gradient. A detailed discussion on some of these methods is presented by Brown and Beggs (1977).

The NODAL software, SAM+ software and STAR* software contain the following pressure loss correlations.

- Duns and Ros (1963)
- Orkiszewski (1967)
- Hagedorn and Brown (1965)
- Beggs and Brill (1973)
- Mukherjee and Brill (1985)
- Dukler (1964).

The first three correlations are developed for vertical upflow or for production wells. Only the Beggs and Brill and Mukherjee and Brill correlations are developed for inclined multiphase flow, and are valid for both production and injection wells as well as for hilly-terrain pipelines. These are also valid for horizontal single or multiphase flow. The Dukler correlation is only valid for horizontal flow. All these correlation programs can also be used for single-phase gas or single-phase liquid flow. Only the Mukherjee and Brill correlation predicts the flow pattern transitions in inclined two-phase flow.

4.22 Gradient Curves

Gradient curves are graphical presentations of pressure versus length or depth of flowline or tubing for a set of fixed flow and fluid parameters. Fig. 35 is a typical gradient curve for 2-7/8-in. tubing with 1000 B/D liquid production at 50% oil. The fixed fluid properties, for example, specific gravity of gas are provided on the top right corner of the plot. On each gradient curve, a family of curves is provided for a number of gas/liquid ratios. These curves are computer generated and are used for design calculations in the absence of a computer program. Gradient curves are used to calculate one of the terminal pressures when the other terminal pressure and the appropriate flow and fluid properties are known.

Brown et al. (1980) presented a number of gradient curves for a wide range of tubing size and flow rates using the Hagedorn and Brown (1965) correlation. A few of these are appended for the solution of some of the problems. Fig. 35, Fig. 36, Fig. 37 and Fig. 38 are a set of sample gradient curves (Brown). The gradient curves for the horizontal flow (Fig. 37) and vertical flow in tubing (Fig. 35 and Fig. 36) start at atmospheric pressure at zero length or depth. To use these gradient curves for a nonatmospheric separator or wellhead pressures, a concept of equivalent length is used. The use of these gradient curves is shown in the following example.

.

⁺ Mark of Tenneco Oil Company

Mark of Schlumberger

18

20

MATRIX ENGINEERING MANUAL

Well Performance

Section 200 July 1998

300

400

800

800

\$

Page 79 of 168

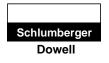
160 PSI PRESSURE, 100 PSI 3,360 PSI 16 32 40 48 56 1,400 FT **VERTICAL FLOWING PRESSURE GRADIENTS** (OIL PERCENT = 50)
TUBING SIZE = 2.441-IN. ID
PRODUCTION RATE = 1,000 BL/D
GAS SPECIFIC GRAVITY = 0.65 AVERAGE FLOWING TEMPERATURE = 150°F OIL API GRAVITY = 35.0 API WATER SPECIFIC GRAVITY = 1.07 DEPTH, 1,000 FT 12 CASTIQUID PATIO, SCHIBBI 0 14 50 100 16 200

Fig. 35. Vertical multiphase flow: How to find the flowing bottomhole pressure.

³,00,00

Section 200
July 1998
Page 80 of 168

MATRIX ENGINEERING MANUAL



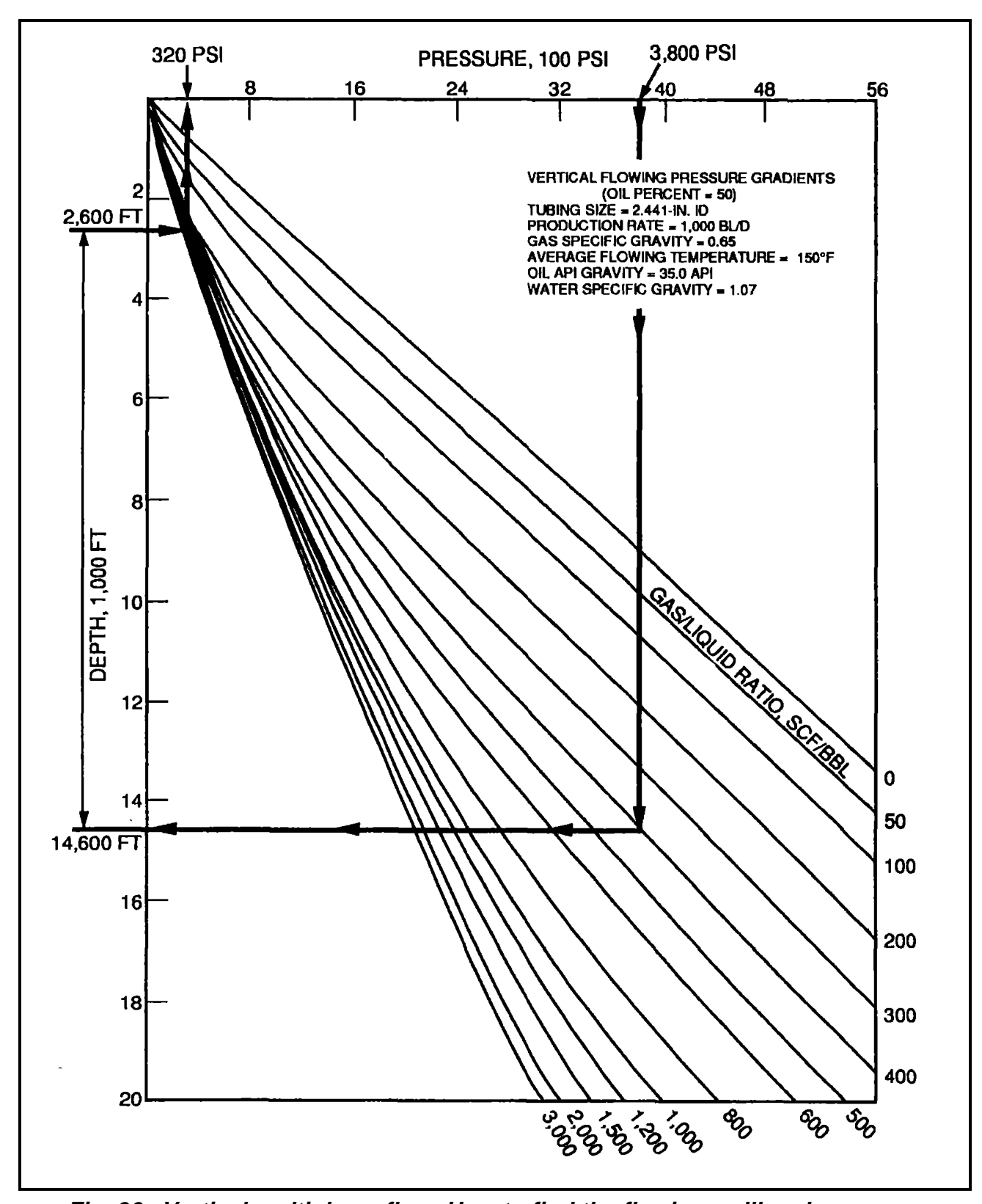


Fig. 36. Vertical multiphase flow: How to find the flowing wellhead pressure.

MATRIX ENGINEERING MANUAL

Well Performance

Section 200
July 1998
Page 81 of 168

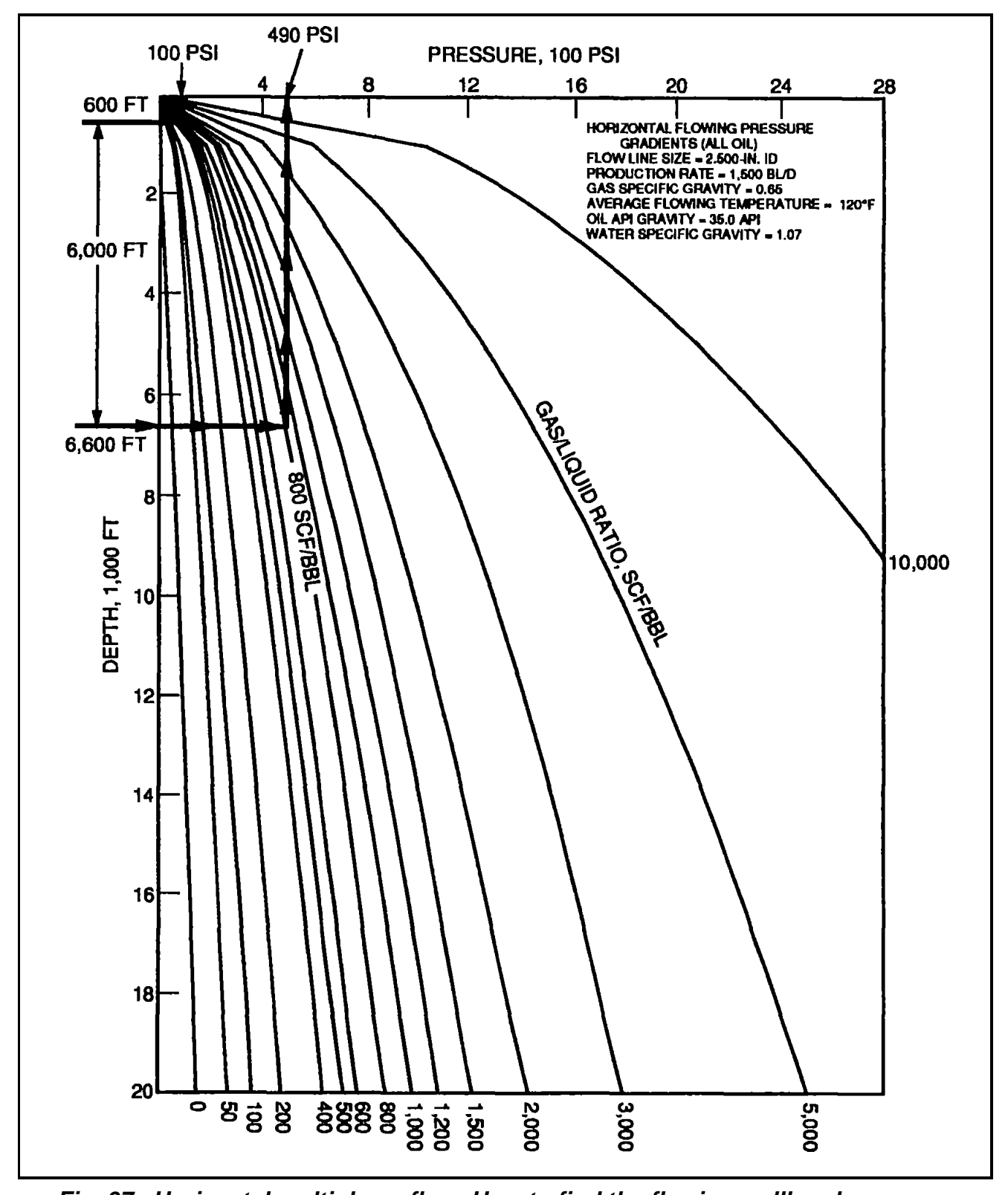
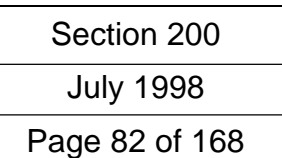
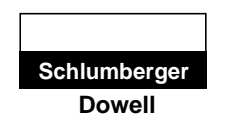


Fig. 37. Horizontal multiphase flow: How to find the flowing wellhead pressure.





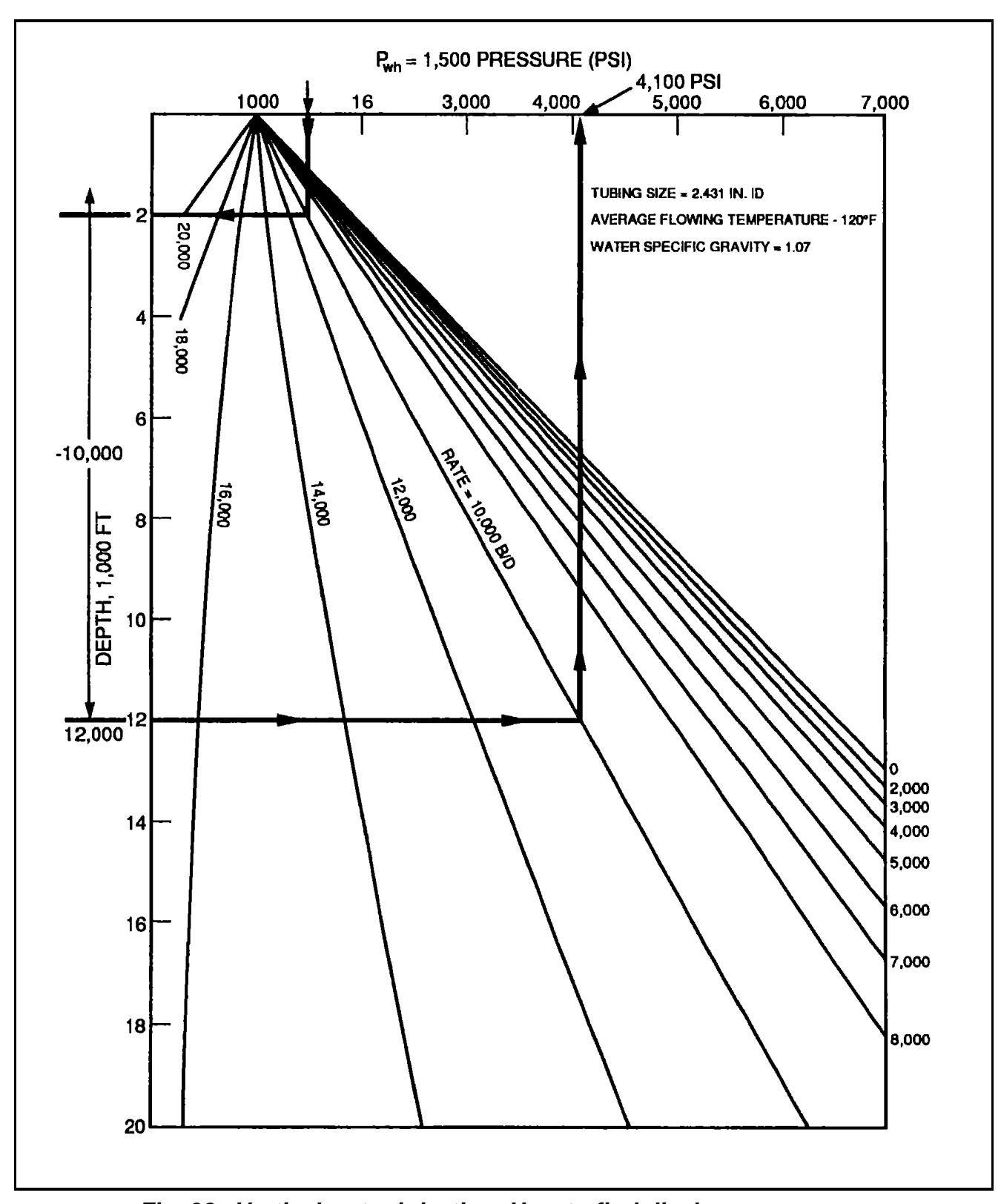


Fig. 38. Vertical water injection: How to find discharge pressure.

MATRIX ENGINEERING MANUAL

Well Performance

Section 200			
July 1998			
Page 83 of 168			

EXAMPLE

Given

 p_{wh} = 100 psig GLR = 400 scf/bbl

 γ_s = 0.65 Tubing ID = 2 in. Wellhead temperature = 70°F T_{res} = 140°F

Depth = 5000 ft (mid-perforation)

API Gravity = 35° API

Calculate and plot the tubing intake curve.

Solution

A plot of the bottomhole flowing pressure versus flow rate is obtained based on pressure gradients in the piping.

Using the vertical multiphase flow correlations in Fig. 39, Fig. 40, Fig. 41, and Fig. 42, assume various flow rates and determine the tubing intake pressure, p_{wf} . Construct a table as follows.

Assumed q (B/D)	$P_{\scriptscriptstyle wf}$ (psig)
200	730
400	800
600	910
800	1080

Sample Calculation

Using Fig. 39, start at the top of the gradient curve at a pressure of 100 psig. Proceed vertically downward to a gas liquid ratio of 400 scf/bbl. Proceed horizontally from this point and read an equivalent depth of 1600 ft. Add the equivalent depth to the depth of the well at mid-perforation. Calculate a depth of 6600 ft on the vertical axis, and proceed horizontally to the 400 scf/bbl gas/liquid ratio curve. From this point, proceed vertically upward and read a tubing intake pressure for 200 BPD of 730 psig.

Repeat this procedure for flow rates of 400, 600 and 800 BPD using Fig. 40, Fig. 41, and Fig. 42.

Plot the p_{wf} versus q values tabulated above as shown in Fig. 43 to complete the desired tubing intake curve.

Section 200
July 1998
Page 84 of 168

MATRIX ENGINEERING MANUAL



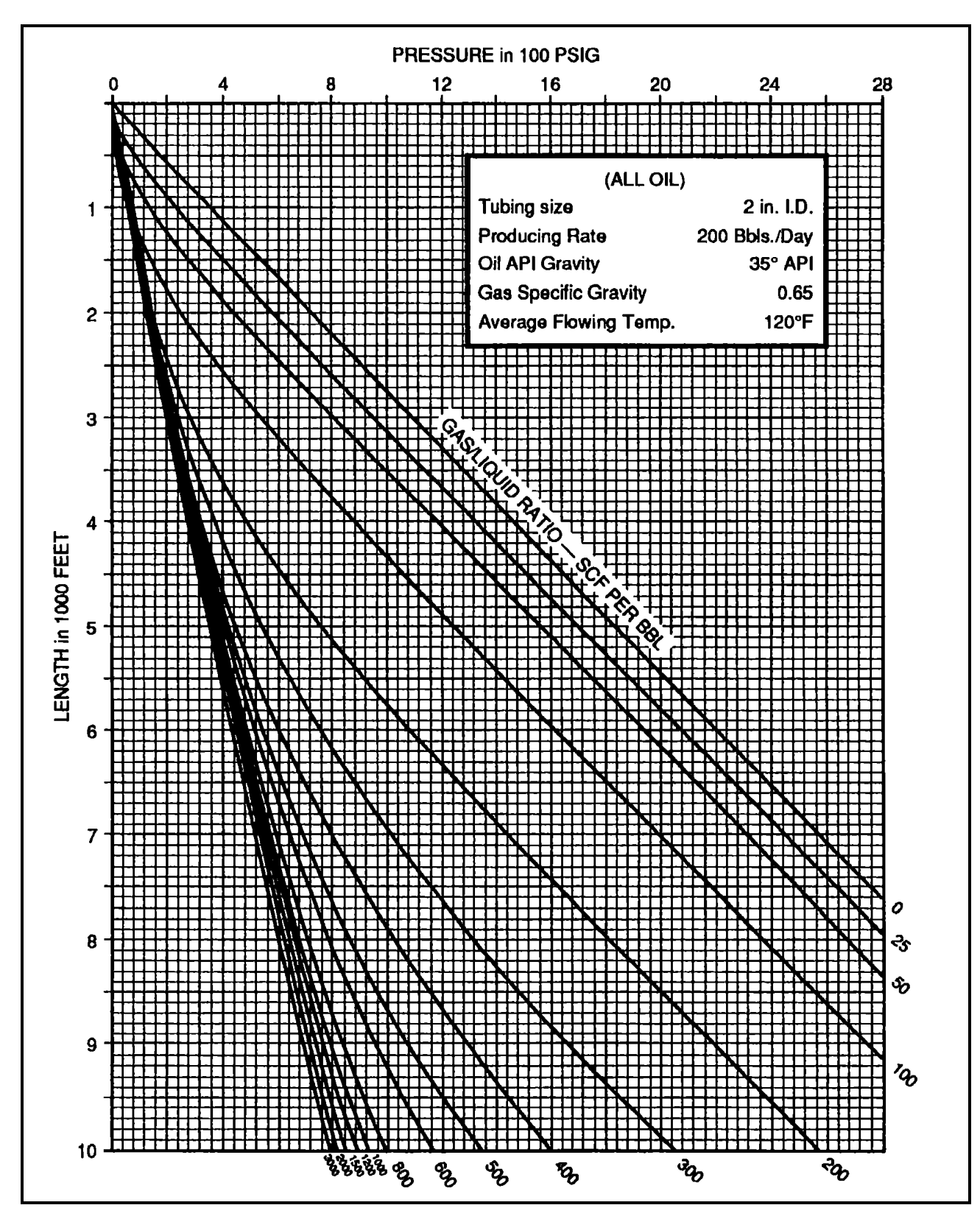


Fig. 39. Vertical flowing pressure gradients.

MATRIX ENGINEERING MANUAL

Well Performance

Section 200 July 1998

Page 85 of 168

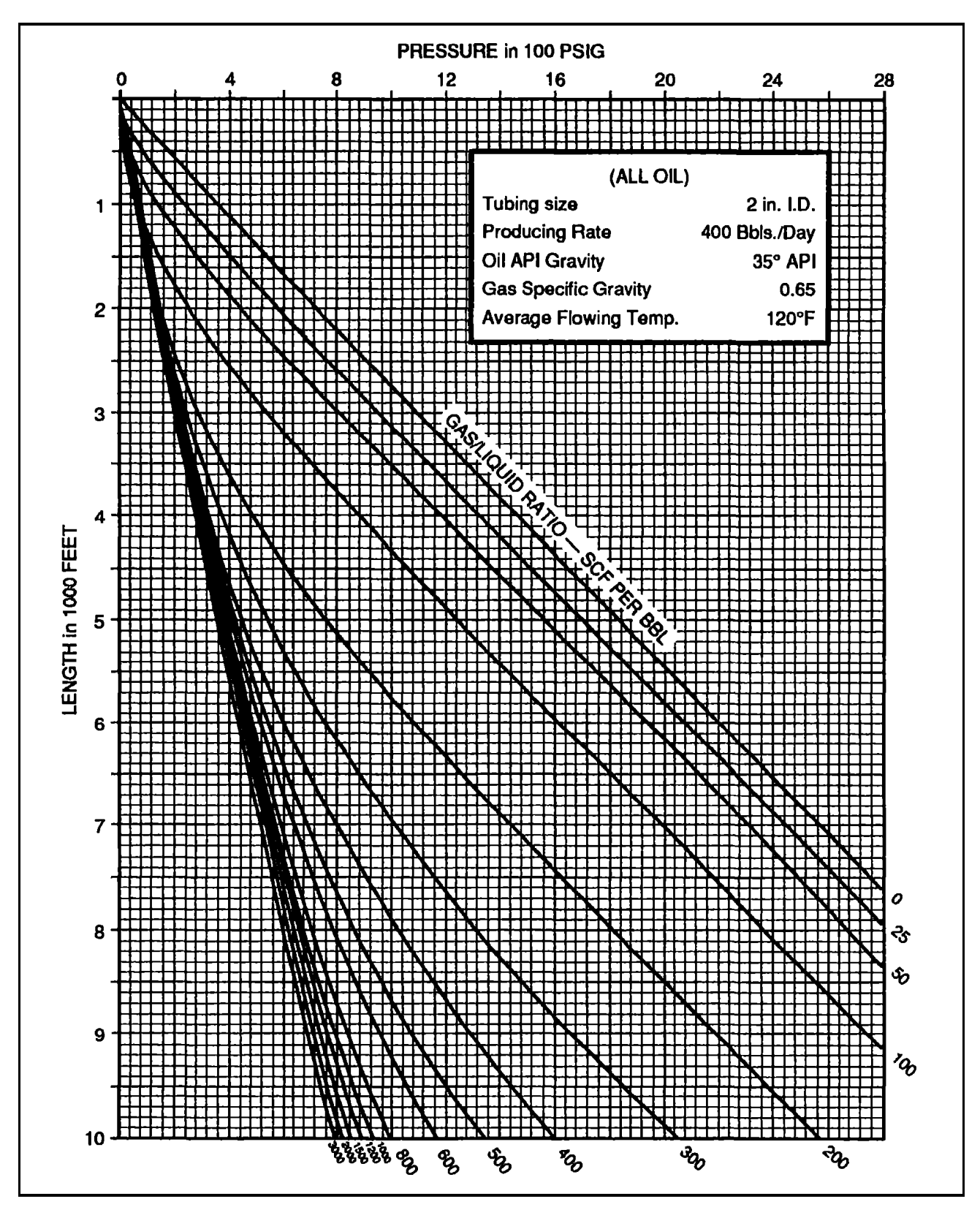


Fig. 40. This figure was used to determine p_{wf} = 800 psig for a rate of 400 BPD through 2-in. ID tubing.

Section 200
July 1998
Page 86 of 168

MATRIX ENGINEERING MANUAL



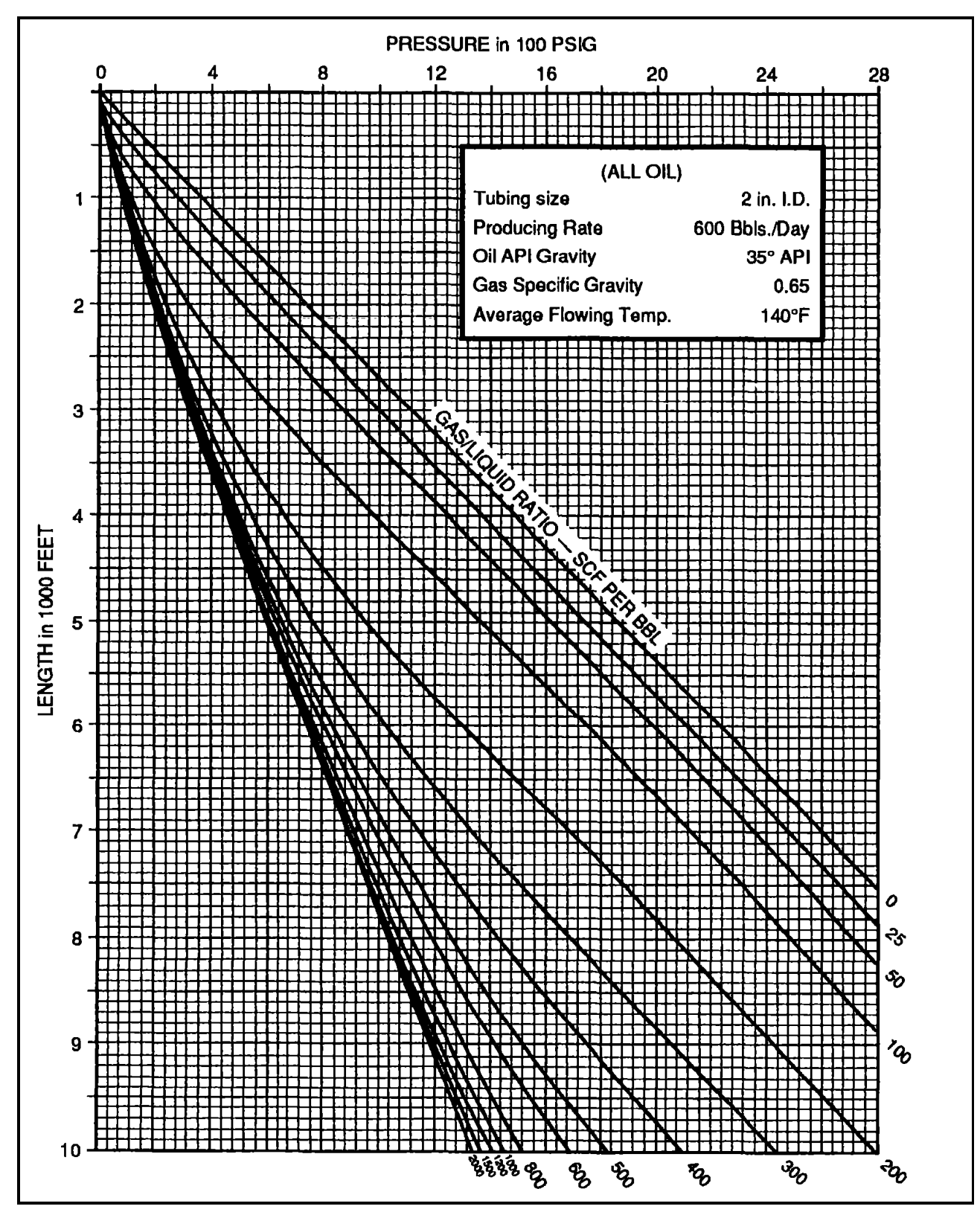


Fig. 41. This figure was used to determine p_{wf} = 910 psig for a rate of 600 BPD through 2-in. tubing.

MATRIX ENGINEERING MANUAL

Well Performance

Section 200 July 1998

Page 87 of 168

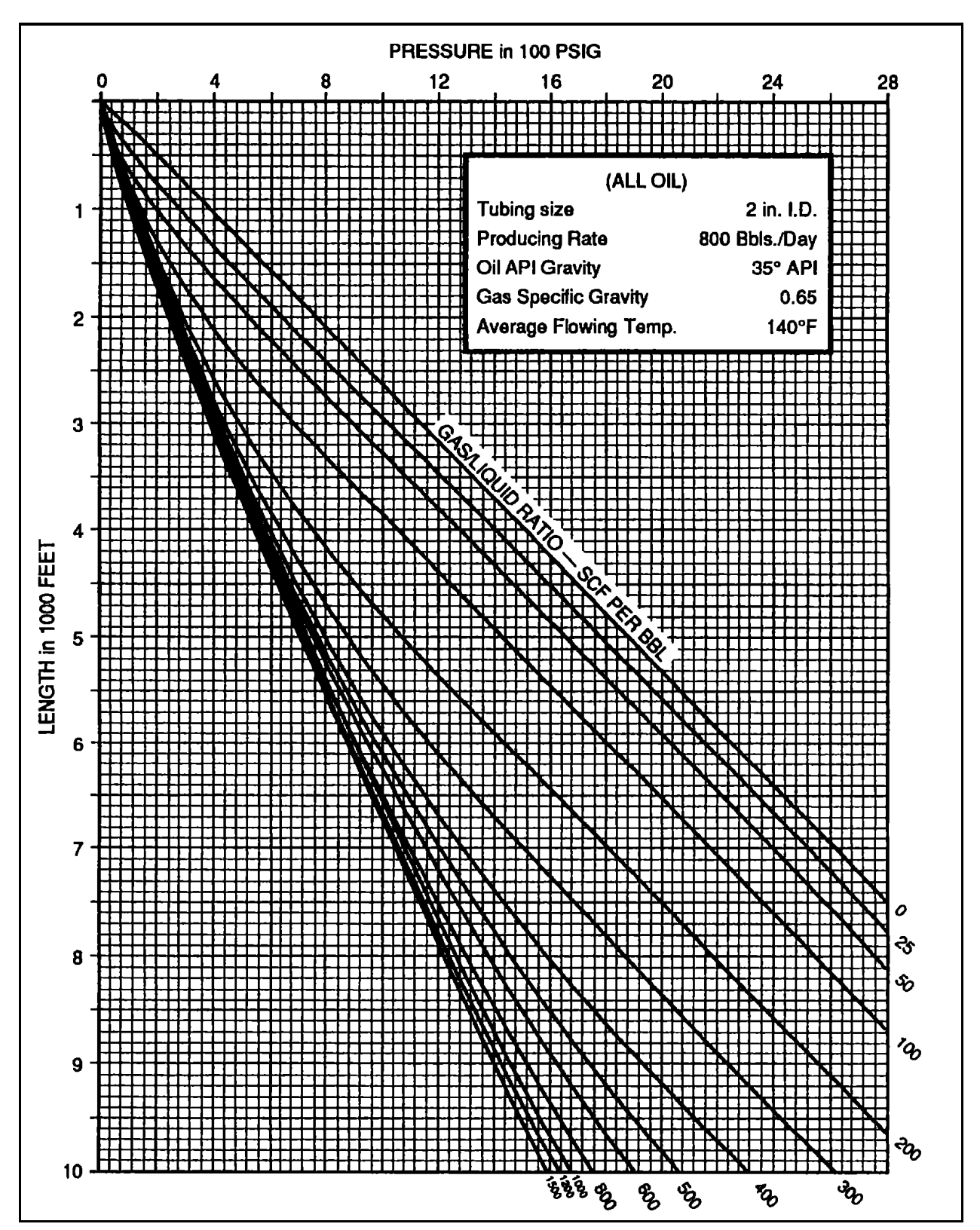
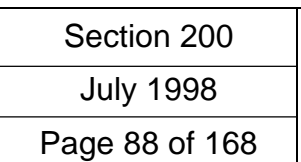
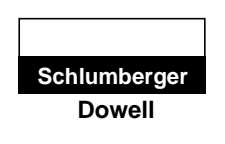


Fig. 42. This figure was used to determine P_{wfs} = 1080 psig for a rate of 800 BPD through 2-in. ID tubing.



Well Performance



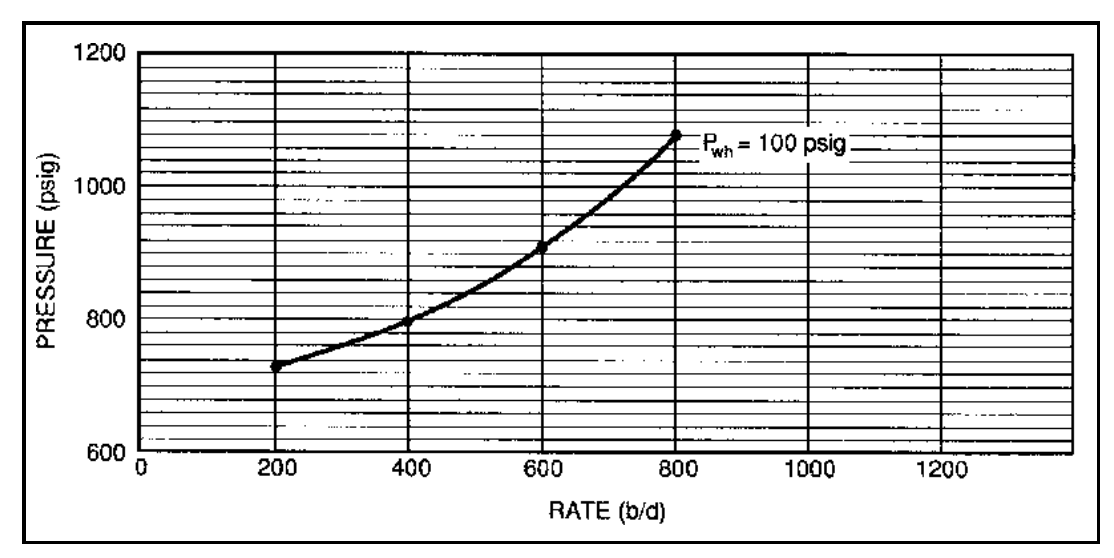


Fig. 43. This figure shows a tubing intake or outflow performance curve for a wellhead pressure of 100 psig.

5 Well Performance Evaluation Of Stimulated Wells

An effective way to evaluate stimulation or to compare different stimulation designs is by comparing net payout due to stimulation over time. If a particular stimulation design pays out the cost of stimulation and yields a net revenue of x dollars in five months (whereas an alternative design does it in 10 months), the first design undoubtedly is the most acceptable or sellable design. Fig. 44 is an example plot of net payout versus time.

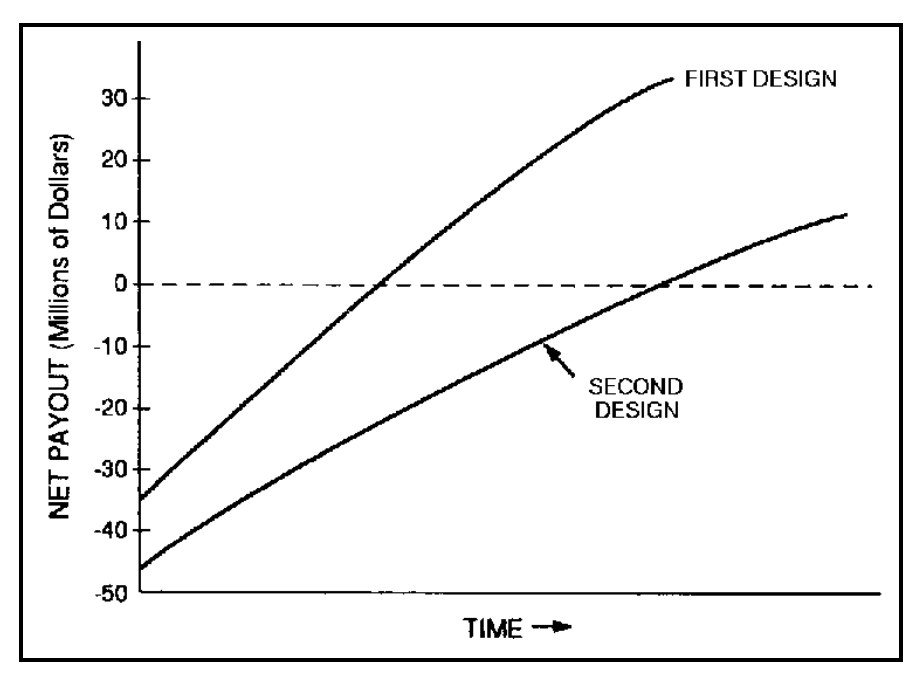
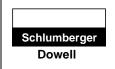


Fig. 44. Net payout at any time = Extra revenue from oil or gas production due to stimulation at any time, t - cost of stimulation.



Well Performance

Section 200				
July 1998				
Page 89 of 168				

5.1 Artificial Lift

Artificial lift methods are used in oil wells that have adequate productivity but inadequate pressure to lift the oil to the surface. There are two methods of artificial lift, pumping and gas lift.

5.1.1 Pumping Wells

Downhole pumps add pressure to the flowing system. As shown in Fig. 45, the dead oil column is stagnant and the hydrostatic pressure of the column overcomes the reservoir pressure stopping inflow into the wellbore. Installation of a pump modifies the pressure profile by adding a fixed pressure gain between the suction and discharge sides of the pump. When properly designed, this pressure gain allows the fluid to flow to the surface at a fixed wellhead pressure. Pumps always operate with a positive suction pressure provided by a fluid column in the annulus above the pump level. This fluid level in the annulus can be monitored by an echometer. Before stimulating a pumping well, the fluid level in the annulus should be monitored to make the post-stimulation troubleshooting possible.

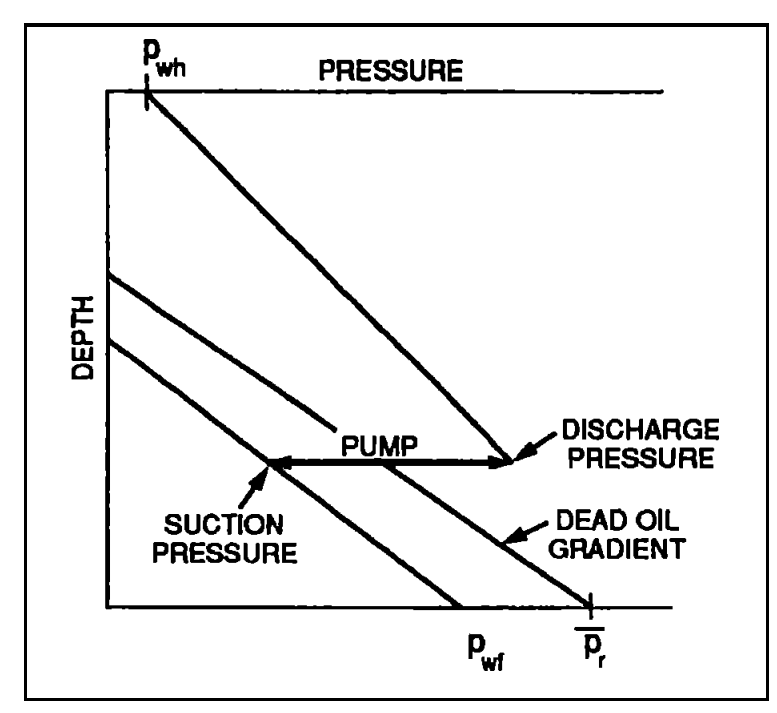


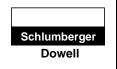
Fig. 45. Effect of subsurface pumps of well pressure profile.

Diagnosis of Potential Stimulation Needs in Pumping Oil Wells

Typically, if the fluid level rises and the pump discharge rate falls, the problem is in the pump, (Case 1, Fig. 46). It is not uncommon to encounter these types of problems after stimulation of a pumping well. In most cases, the old pump needs to be replaced or repaired.

Section 200				
July 1998				
Page 90 of 168				

Well Performance



The other common problem is when the flow rate falls and the fluid level stays the same or recedes. This is commonly due to a reservoir problem, for example, depletion or skin buildup (Case 2, Fig. 46).

Note also that in a pumping well after a successful stimulation, the pumps may need to be redesigned for optimum flow. It is possible that after a successful stimulation in a pumping well, the post-stimulation production did not increase substantially due to existing pump limitations.

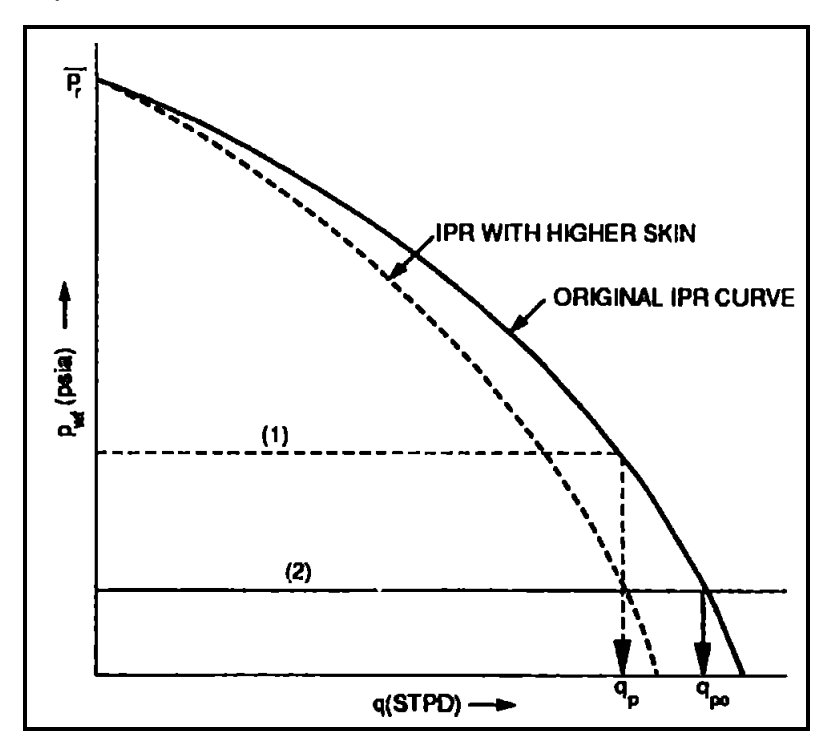


Fig. 46. Showing potential problems in a pumping well through IPR curves.

5.1.2 Gas-Lift Wells

Gas lift is an artificial lift method where gas is injected into the liquid production string, normally through the tubing-casing annulus to aerate the liquid column, reducing the hydrostatic head of the liquid column. This reduces the bottomhole flowing pressure, increasing production. The deeper the injection point, the longer the column of tubing fluid aerated and the lower the bottomhole pressure. Thus, the objective of gas lift is to inject the optimum gas volume at the deepest possible point in the tubing. An optimum gas volume injection is important because any higher volume leads to excessive friction pressure loss in the tubing, overcoming the hydrostatic pressure gain. This situation results in an increase in the bottomhole flowing pressure, reducing production.

Fig. 47 shows a typical gas injection sequence used to unload or kick off a gas-lift well. Gas-lift valves are used to close and open at fixed casing or tubing pressures. The objective of unloading is to start aerating a fluid column in smaller lengths

MATRIX ENGINEERING MANUAL

Well Performance

Section 200			
July 1998			
Page 91 of 168			

beginning at the top and then close the top valve to aerate through the second valve, and so on until the injection valve is reached. This valve is set so that it remains open all the time. This stepwise unloading is done to kick off a well with limited surface injection pressure.

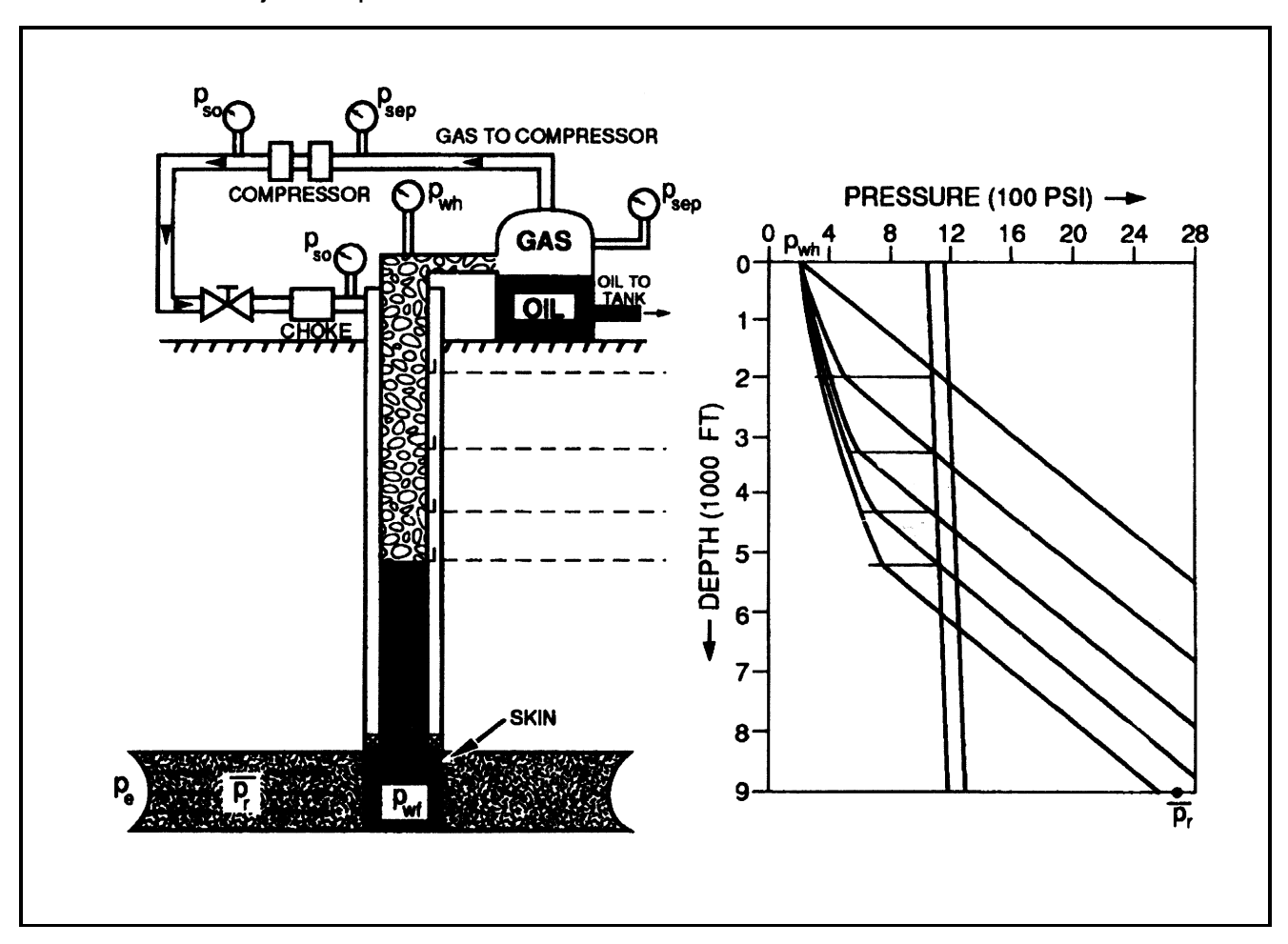


Fig. 47. Unloading wells with gas lift.

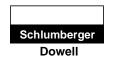
5.1.2.1 Effect of Stimulation of Gas Lift Wells

After stimulation, with the improved IPR curve, a redesign of the gas-lift system is normally required for optimized flow. This requires new setting of gas-lift valves. It is possible that after stimulation a gas-lift well loses production due to gas-lift design problems. This section is to caution engineers against gas-lift system failures in a successfully stimulated well.

Page 92 of 168

MATRIX ENGINEERING MANUAL

Well Performance



5.2 Example Problem — Clay Consolidation

(Effect of moving damage away from the wellbore)

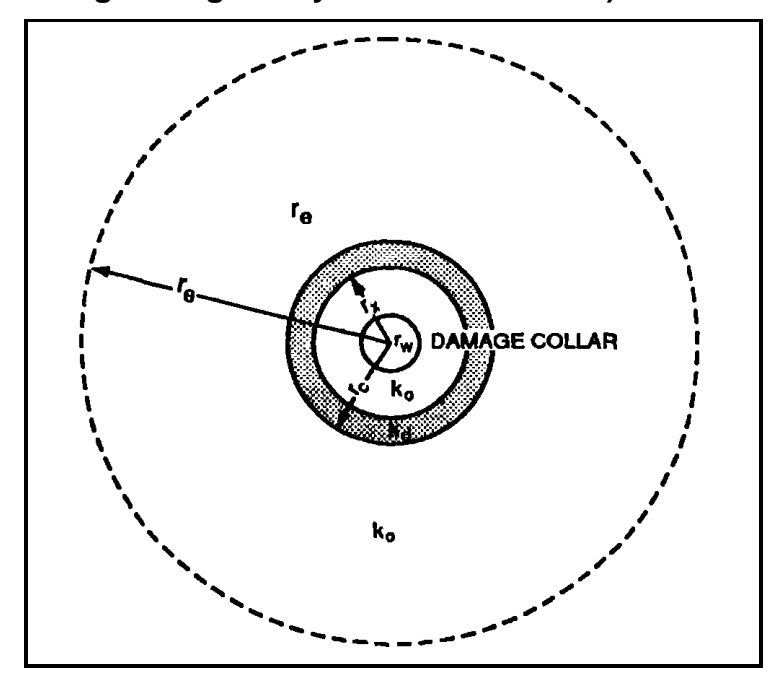


Fig. 48. Effect of moving damage away from the wellbore.

$$Average \ Permeability, \ \overline{k} = \frac{log\left(\frac{r_e}{r_w}\right)}{\frac{1}{k_o}log\frac{r_x}{r_w} + \frac{1}{k_d}log\frac{r_c}{r_x} + \frac{1}{k_o}log\frac{r_e}{r_c}}$$

Percentage of Original Permeability = $\frac{\overline{k}}{k_o} \times 100$

Given:

 $r_w = 0.365 \text{ ft}$

k = 100 md

Spacing = 160 acres

- (a) Calculate the percentage of original productivity due to 80% damage one foot deep around the wellbore.
- (b) Calculate the percentage of original productivity due to an 80% damage collar, one foot wide and four feet from the wellbore.

MATRIX ENGINEERING MANUAL

Well Performance

Section 200 July 1998

Page 93 of 168

Solution

(a)
$$k_{80\%} = \frac{log\left(\frac{1489}{0.365}\right)}{\frac{1}{20}log\frac{1.365}{0.365} + \frac{1}{100}log\frac{1489}{1.365}}$$
$$= \frac{3.6106}{0.0286 + 0.0304}$$
$$= 61.2md$$

∴ Percentage of original productivity = 61%

(b)
$$k_{80\%} = \frac{\log\left(\frac{1489}{0.365}\right)}{\frac{1}{100}\log\frac{4.365}{0.365} + \frac{1}{20}\log\frac{5.365}{4.365} + \frac{1}{100}\log\frac{1.489}{5.365}}$$
$$= \frac{3.6106}{0.01078 + 0.00448 + 0.02443}$$
$$= 91md$$

∴ Percentage of original productivity = 91%

5.3 Example Problem — Pre- and Post-Acid Evaluation

Summary

An offshore Louisiana well was tested following its completion in the Pliocene formation. It produced 1200 B/D at a wellhead pressure of 1632 psig from a 71 ft gravel-packed unconsolidated sandstone reservoir.

Analysis of the test data identified severe wellbore damage which was restricting production (Skin = 210). It also showed that the production rate could be increased to 6850 B/D at the same wellhead pressure should that damage be removed.

To treat the damage effectively, a clear understanding of its origin is required. The analysis of the test data indicated inadequate perforations and a high probability of formation damage. This was confirmed by core analysis and production logs run after the test. An acid treatment was formulated and the post-acid test indicated a significant improvement in skin (Skin = 15). The production rate increased to 4400 B/D at a wellhead pressure of 2060 psig.¹

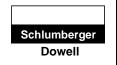
¹ Form more details refer to SPE 14820 presented at the 1986 SPE Symposium on Formation Damage Control, Lafayette, LA, February 26-27, 1986.

Section 200 July 1998

Page 94 of 168

MATRIX ENGINEERING MANUAL

Well Performance



Pre-Acid Test Results

The main results are summarized on page 1 of the referenced paper.¹ The test procedure and analysis plots are provided on page 2, page 3, page 4 and page 5. The Model Verified Interpretation (page 3) indicates a high-permeability homogeneous reservoir with wellbore storage and severe skin effect. The NODAL analysis (page 4) shows that the production rate is significantly restricted by the skin effect, and projects a rate increase of 5650 B/D if the wellbore damage is removed. Finally, the shot density sensitivity plot (page 5) suggests adequate perforations and the likelihood of formation damage. The interpretation charts and computation sheets are presented.

Production Logs Results

The production logging data indicate that all of the 40 ft perforated zone is contributing to the flow rate except the bottom 5 to 6 feet. Since the permeability variation in the perforated interval is minimal and the flow profile appears nonuniform, it is assumed that formation damage has affected the producing zone unevenly.

Post-Acid Test Results

Significant improvement in the wellbore condition is noticed. The resulting increase in production rate matches the prediction of the NODAL analysis. The charts and computation sheets are presented in this section.

¹ Form more details refer to SPE 14820 presented at the 1986 SPE Symposium on Formation Damage Control, Lafayette, LA, February 26-27, 1986.

MATRIX ENGINEERING MANUAL

Well Performance

Section 200 July 1998

Page 95 of 168

Pre-Acid Analysis Nodal Analysis				
Test Identification	Test String Configuration			
Test Type SPRO	Tubing Vertical Multiphase Flow Hagedorn-Brown			
Test No1	Tubing Length (ft)/ID (in.) 11,830/2.992			
Formation E-3 SAND	Packer Depth (ft) 11,826			
Test Interval (ft) 11,942-11,982	Gauge Depth (ft)/Type11,920/DPTT			
Completion Configuration Tubing Absolute Roughness (ft)5.0E-0				
Total Depth (MD/TVD) (ft)11,920/10,800	Rock/Fluid/Wellbore Properties			
Casing/Liner ID (in.)6.094	Oil Density (° API)29.5			
Hole Size (in.)8.5	Gas Gravity 0.600			
Perforated Interval (ft)40	GOR (scf/STB)			
Shot Density (spf)12	Water Cut (%) 0			
Perforation Diameter (in.)0.610	Viscosity (cp) 0.70			
Net pay (ft)71	Total Compressibility (1/psi)9.00E-06			
Interpretation Results	Porosity (%)			
Model of Behavior Homogeneous	Reservoir Temperature (°F)			
Fluid Type Used for AnalysisLiquid	Form. Vol. Factor (bbl/STB) 1.37			
Reservoir Pressure (psi)5,585	Bubblepoint Pressure (psi) 5,120			
Transmissibility (md-ft/cp)53,390	Wellhead Pressure (psig) 1,632			
Effective Permeability (md)526.0	Wellhead Temperature (°F) 100.0			
Skin Factor210.0	Production Time (days)3.0			
Maximum Production Rate During Test: 1200 BPD				

Test Objectives

The objectives of this test were to evaluate the completion efficiency and estimate the production potential of the well.

Comments

The test procedure and measurements are summarized on the following pages. The system behaved as a well in a homogeneous reservoir with wellbore storage and skin. The well and reservoir parameters listed above reveal a high-permeability formation and a severely damaged wellbore. Removing this damage would result in increasing the production rate to 6850 B/D at the same wellhead pressure of

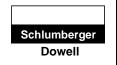
Section 200

July 1998

Page 96 of 168

MATRIX ENGINEERING MANUAL

Well Performance



1632 psig, without jeopardizing the integrity of the gravel pack. The shot density sensitivity plot suggests adequate perforations and high formation damage. This could be confirmed by production logs and core analysis. Acid treatment is recommended for removing the wellbore damage and increasing the production. Note that the skin due to partial penetration cannot be eliminated by acidizing, consequently the ideal production rate may not be achieved.

Pre-Acid Test Computations

- 1. Log-Log Analysis
 - 1.1 Match Parameters

Model: Homogeneous, WBS & S

 $C_D e^{2s}$ = 1.0E185

Pressure Match: $P_D/\Delta P$ = 0.23

Time Match: $(T_D/C_D)/\Delta t = 1700$

1.2 Reservoir Parameter Calculations

$$kh = 141.2 \ Q_o \beta_o \mu_o \left(\frac{P_D}{\Delta P}\right)_{match} = 37373.4 \ md - ft$$

$$C = \left(\frac{kh}{3389 \ \mu_o}\right) \left[\frac{\Delta t}{\left(\frac{T_D}{C_D}\right)}\right]_{match} = 0.0093 \ bbl \ / \ psi$$

$$C_D = \frac{0.8936 \ C}{\phi \ C_t \ h \ r_w^2} = 370.7$$

$$s = \frac{1}{2} ln \left(\frac{C_D e^{2s}}{C_D} \right) = 210$$

- 2. Generalized Horner Analysis
 - 2.1 Straight Line Parameters

Superposition slope: m' = 4.1112 E-03

P (intercept): $P^* = 5585 \text{ psia}$

Pressure at one hour: P (1 hr) = 5575 psia

Pressure at time zero: P(0) = 4622 psia

MATRIX ENGINEERING MANUAL

Well Performance

Section 200

July 1998

Page 97 of 168

2.2 Reservoir Parameter Calculations

$$kh = \frac{162.6 \ B_o \mu_o}{m'} = 37,929 \ md - ft$$

$$s = 1.151 \left\{ \left(\frac{P(1 \, hr) - P(O)}{m' Q_o} \right) - log \left(\frac{k}{\phi \, \mu_o C_t r_w^2} \right) + 3.23 \right\} = 210$$

Nomenclature

k = permeability (md)

h = formation height (ft)

c = wellbore storage constant (bbl/psi)

e = scientific notation

 q_o = oil flow rate B/D

 P_D = dimensionless pressure

 ΔP = pressure change (psi)

 T_D = dimensionless time

 C_D = dimensionless wellbore storage constant

 Δt = time change (hr)

 B_o = oil formation volume factor (bbl/STB)

 μ_o = oil viscosity (cp)

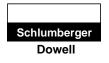
 ϕ = formation porosity

Section 200

July 1998

Page 98 of 168

MATRIX ENGINEERING MANUAL



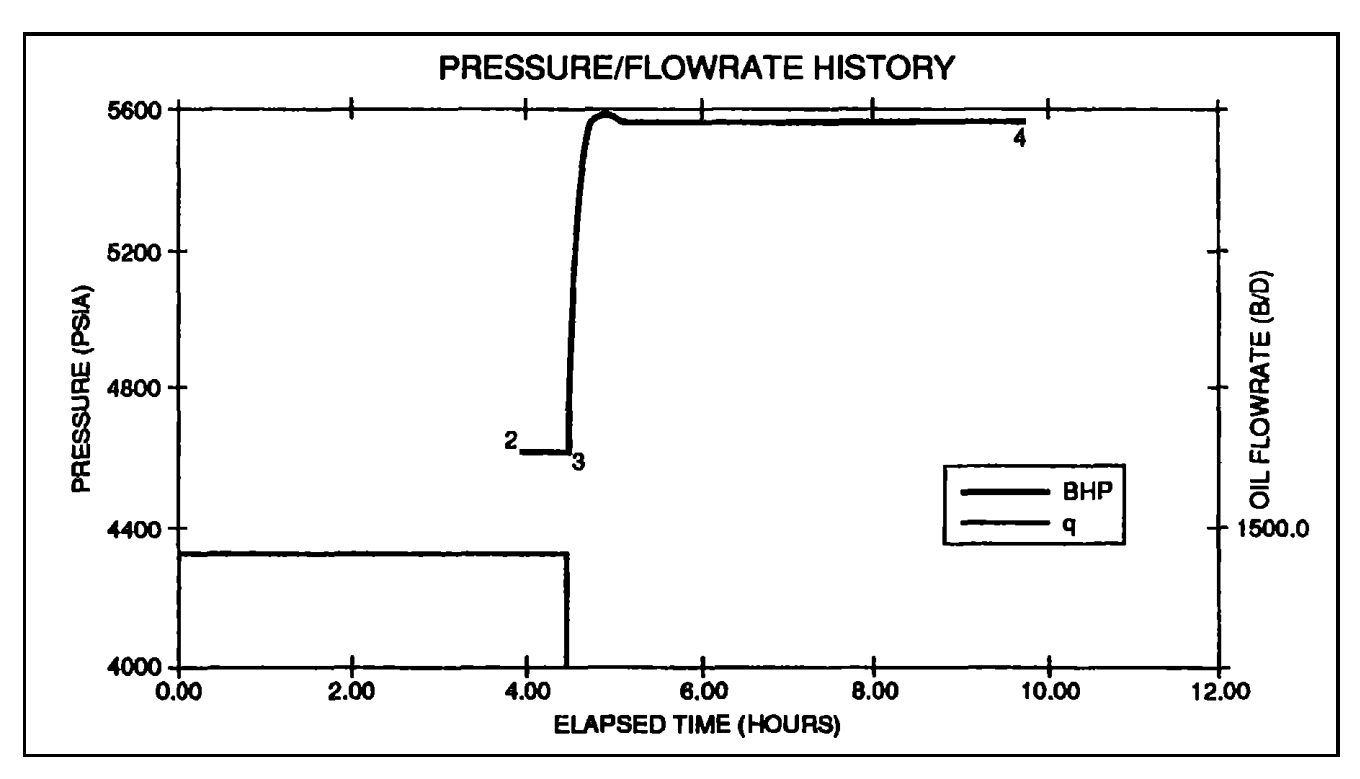
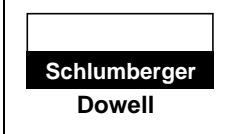


Fig. 49. Pressure/flowrate history.

Sequence of Events						
Event No.	Date	Time (hr:min)	Description	Elapsed Time (hr:min)	BHP (psia)	WHP (psia)
1	23-APR	12:28	Run in Hole Flowing	0:48	1613.0	1636.0
2	23-APR	15:40	Start Monitoring Flow	4:00	4621.0	1649.0
3	23-APR	16:08	End Flow and Start Shut-In	4:28	4623.0	1648.0
4	23-APR	21:25	End Shut-In, POOH	9:45	5579.0	2434.0



Section 200				
July 1998				
Page 99 of 168				

Summary of Flow Periods						
Period	Duration (hr:min)	Pressure (psia)		ressure (psia) Flowrate		Choke Size (in.)
		Start	Stop	Oil (B/D)	Gas (MMSCF/D)	
#1, DD	3:40	1613.0	4623.0	1200.0	0.754	0/64
#2, BU	5:17	4623.0	5579.0	0	0	

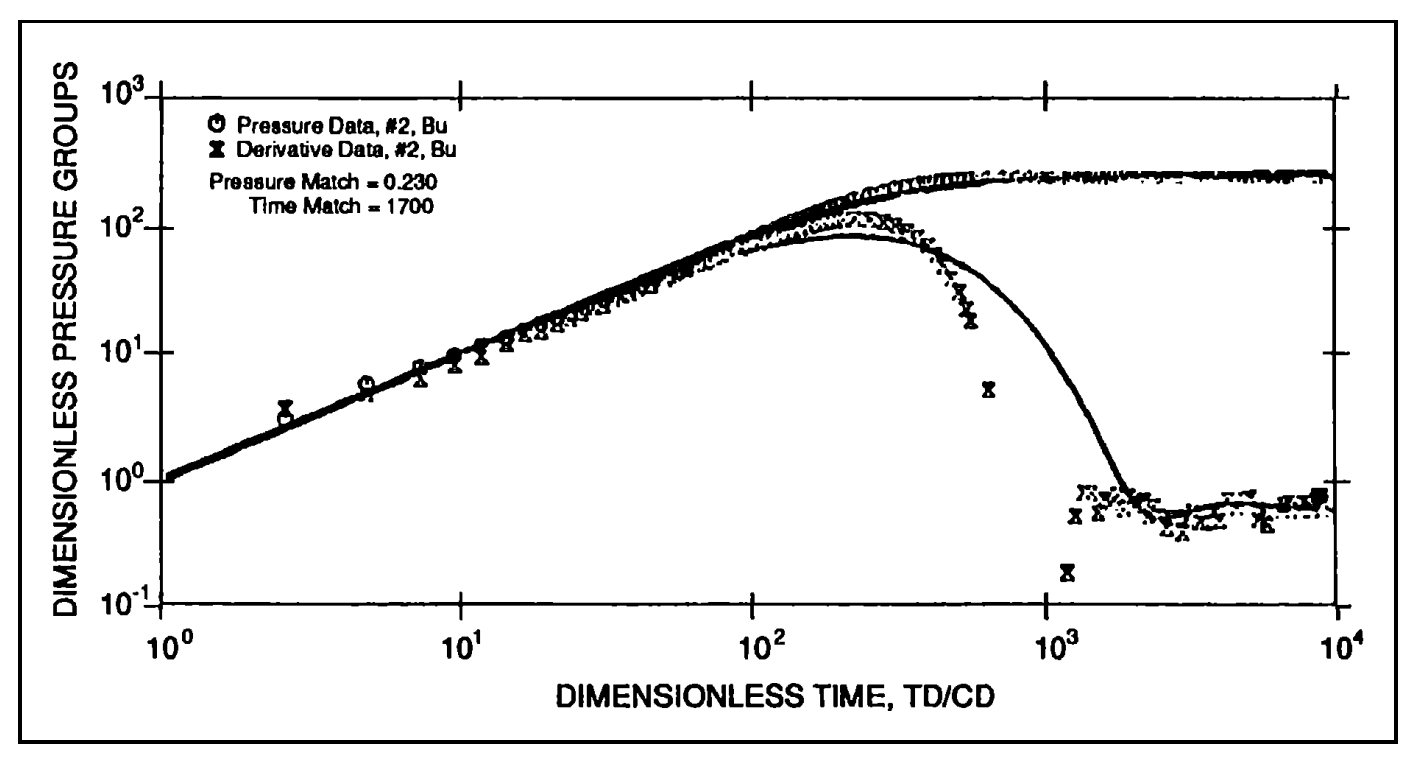


Fig. 50. Diagnostic plot.



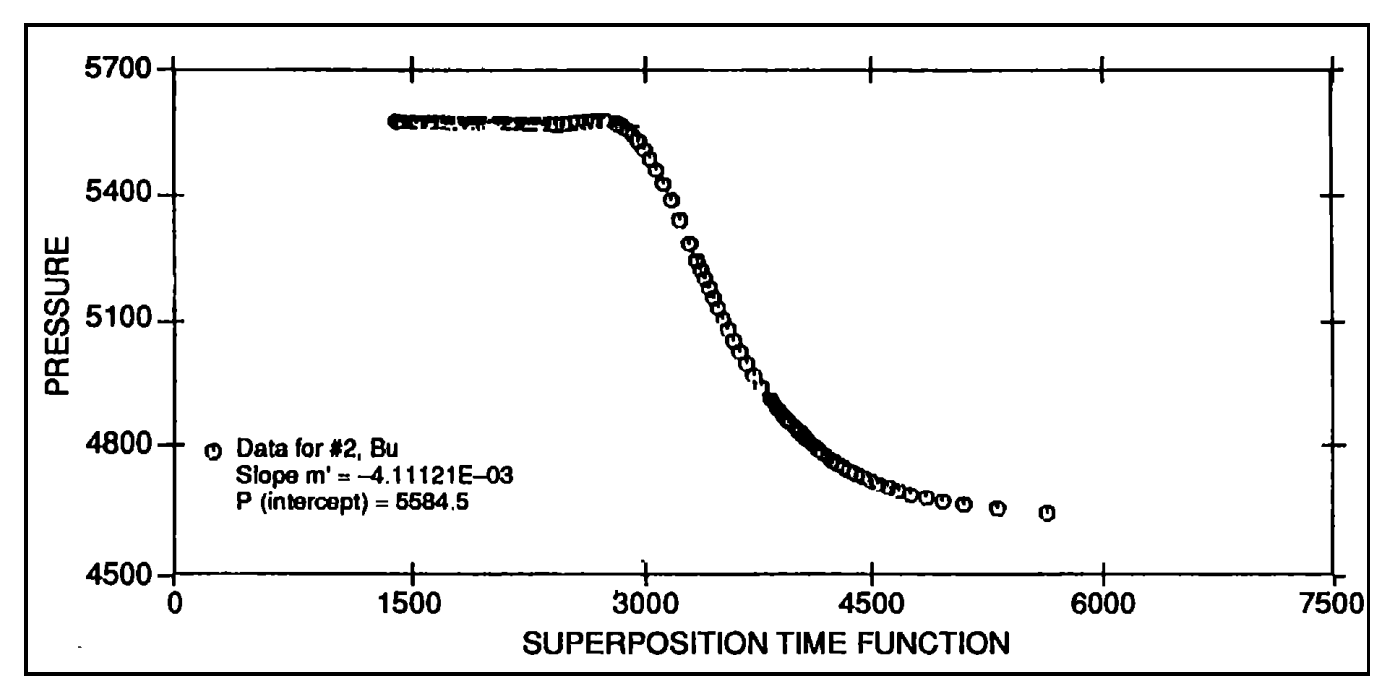


Fig. 51. Dimensionless superposition.

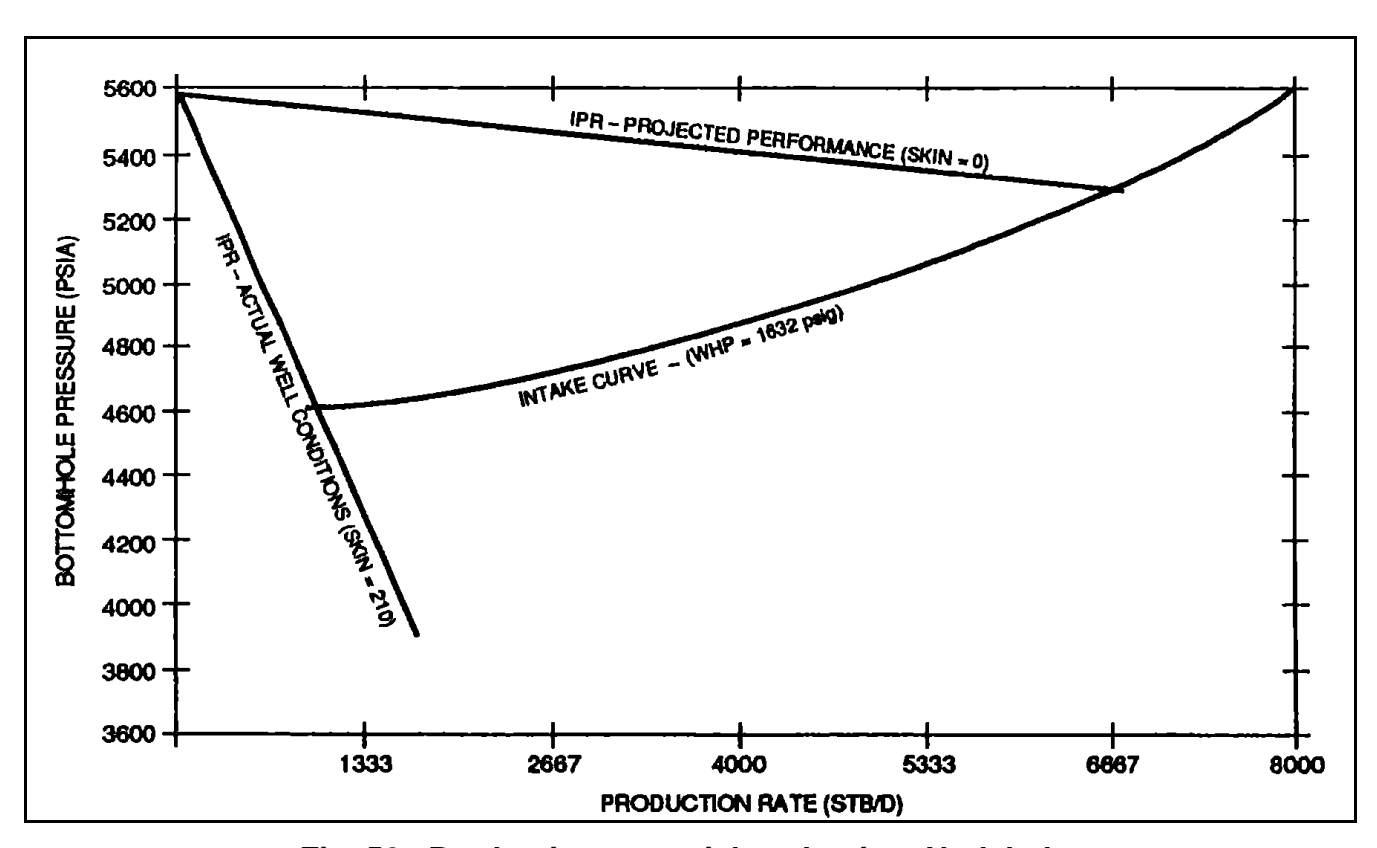


Fig. 52. Production potential evaluation, Nodal plot.



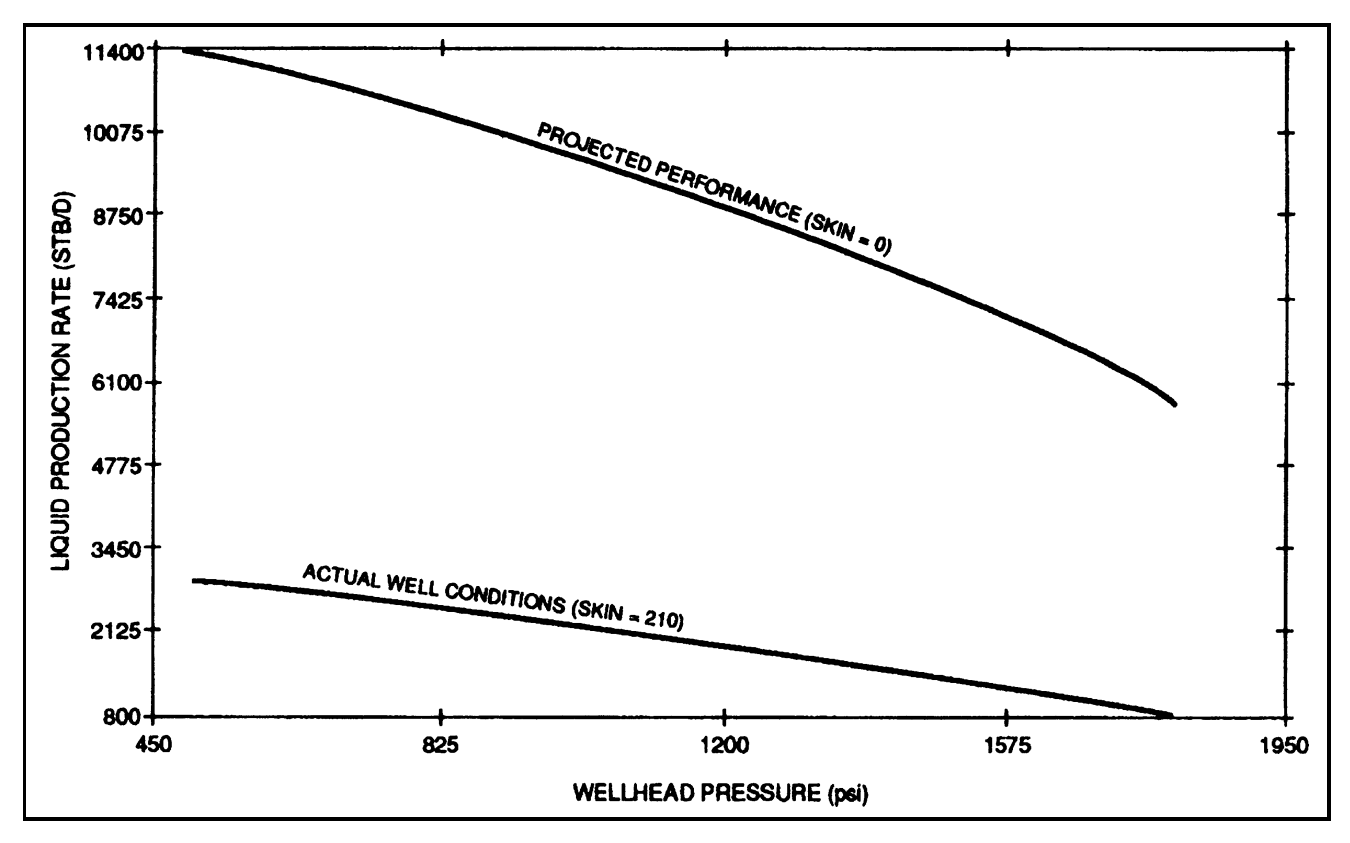


Fig. 53. Production potential evaluation, rate versus wellhead pressure.

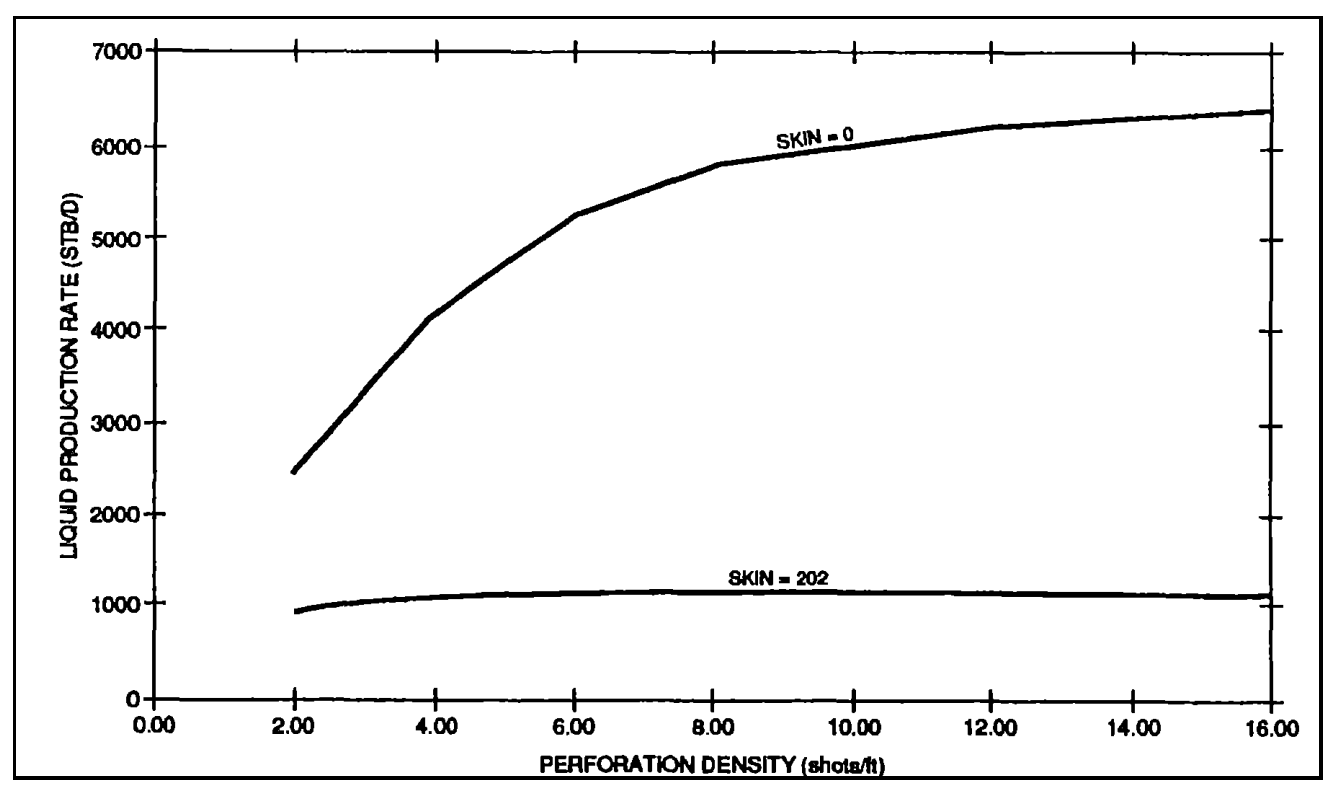


Fig. 54. Production potential evaluation, well performance rate versus shot density.

Section 200

July 1998

Page 102 of 168

MATRIX ENGINEERING MANUAL



Pre-Acid Test Buildup Data								
	Delta Time (hr)	Bottom hole Pressure (psia)		Delta Time (hr)	Bottom hole Pressure (psia)		Delta Time (hr)	Bottom hole Pressure (psia)
1	0.00000E+00	4622.6	45	9.45000E-02	5127.6	89	1.6445	5576.2
2	1.50000E-03	4624.3	46	0.10000	5152.0	90	1.6945	5576.2
3	2.83333E-03	4635.5	47	0.10567	5175.7	91	1.7445	5576.2
4	4.16667E-03	4647.4	48	0.11117	5198.6	92	1.7945	5576.4
5	5.66667E-03	4656.5	49	0.11667	5220.8	93	1.8445	5576.4
6	7.00000E-03	4664.6	50	0.12233	5242.4	94	1.8945	5576.5
7	8.33333E-03	4672.7	51	0.13333	5283.0	95	1.9445	5576.4
8	9.83333E-03	4681.0	52	0.15000	5338.3	96	1.9945	5576.5
9	1.11667E-02	4689.4	53	0.16667	5386.6	97	2.0445	5576.6
10	1.25000E-02	4697.6	54	0.18333	5427.9	98	2.0945	5576.7
11	1.40000E-02	4705.9	55	0.20000	5462.8	99	2.2612	5576.8
12	1.53333E-02	4714.0	56	0.21667	5491.8	100	2.3445	5576.9
13	1.66667E-02	4722.1	57	0.23333	5515.2	101	2.5112	5577.0
14	1.81667E-02	4730.3	58	0.25000	5534.0	102	2.6778	5577.2
15	1.95000E-02	4738.4	59	0.26667	5548.4	103	2.8445	5577.4
16	2.08333E-02	4746.4	60	0.28333	5559.5	104	3.0112	5577.5
17	2.23333E-02	4754.5	61	0.30000	5567.5	105	3.1778	5577.7
18	2.36667E-02	4762.6	62	0.31667	5573.1	106	3.3445	5577.8
19	2.50000E-02	4770.6	63	0.32783	5576.0	107	3.4278	5577.9
20	2.65000E-02	4778.7	64	0.37783	5581.7	108	3.8612	5577.9
21	2.78333E-02	4786.6	65	0.42783	5582.3	109	3.8945	5578.0
22	2.91667E-02	4794.4	66	0.47783	5580.8	110	3.9278	5578.2
23	3.06667E-02	4802.4	67	0.52783	5578.2	111	4.0945	5578.3
24	3.20000E-02	4810.1	68	0.57783	5576.1	112	4.2612	5578.5
25	3.33333E-02	4817.9	69	0.62783	5574.0	113	4.4278	5578.5
26	3.48333E-02	4825.7	70	0.69450	5573.8	114	4.5945	5578.6
27	3.61667E-02	4833.4	71	0.74450	5574.1	115	4.7612	5578.7
28	3.75000E-02	4841.2	72	0.79450	5574.4	116	4.9278	5578.7
29	3.90000E-02	4848.9	73	0.84450	5574.5	117	5.0945	5578.9
30	4.03333E-02	4856.5	74	0.89450	5574.6	118	5.1333	5578.9
31	4.16667E-02	4864.1	75	0.94450	5574.9	119	5.1362	5578.9
32	4.31667E-02	4871.6	76	0.99450	5574.9	120	5.1390	5578.9
33	4.45000E-02	4879.3	77	1.0445	5575.1	121	5.1417	5579.0
34	4.58333E-02	4886.8	78	1.0945	5575.2	122	5.1473	5578.9
35	4.73333E-02	4894.3	79	1.1445	5575.3	123	5.1500	5579.0
36	4.86667E-02	4901.8	80	1.1945	5575.5	124	5.1528	5579.0
37	5.00000E-02	4909.1	81	1.2445	5575.5	125	5.1557	5579.0
38	5.56667E-02	4938.5	82	1.2945	5575.7	126	5.1583	5579.0
39	6.11667E-02	4967.3	83	1.3445	5575.7	127	5.1612	5579.0
40	6.66667E-02	4995.6	84	1.3945	5575.9	128	5.1945	5578.9
41	7.23334E-02	5023.2	85	1.4445	5575.9	129	5.2278	5578.9
42	7.78333E-02	5050.2	86	1.4945	5576.0	130	5.2612	5579.0
43	8.33334E-02	5076.6	87	1.5445	5576.1	131	5.2778	5579.0
44	8.90000E-02	5102.4	88	1.5945	5576.1	'''	0.2110	0070.0

MATRIX ENGINEERING MANUAL

Well Performance

Section 200

July 1998

Page 103 of 168

Post-Acid Analysis Nodal Analysis					
Test Identification	Test String Configuration				
Test TypeSPRO	Tubing Length (ft)/ID (in.)11,830/2.992				
Test No 2	Packer Depth (ft)11,826				
FormationE-3 SAND	Gauge Depth (ft)/Type11,920/DPTT				
Test Interval (ft)11,942-11,982	Downhole Valve (Y/N)/TypeN				
Completion Configuration	Test Condition				
Total Depth (MD/TVD) (ft) 11,920/10,800	Tubing/Wellhead Pressure (psi) 2,060				
Casing/Liner ID (in.) 6.094	Separator Pressure (psi)150				
Hole Size (in.) 8.5	Wellhead Temperature (°F)100.0				
Perforated Interval (ft)40	Rock/Fluid/Wellbore Properties				
Shot Density (spf)12	Oil Density (° API) 29.5				
Perforation Diameter (in.) 0.610	Gas Gravity 0.600				
Net pay (ft)71	GOR (scf/STB) 1,013				
Interpretation Results	Water Cut (%)				
Model of BehaviorHomogeneous	Viscosity (cp) 0.70				
Fluid Type Used for AnalysisLiquid	Total Compressibility (1/psi) 9.00E-06				
Reservoir Pressure (psi) 5,431	Porosity (%) 28				
Transmissibility (md-ft/cp) 53,751	Reservoir Temperature (°F) 218				
Effective Permeability (md) 530	Form. Vol. Factor (bbl/STB) 1.37				
Skin Factor15	Production Time (days) 2.5				
Maximum Production Rate During Test: 4398 BPD					

Test Objectives

The objective of the test was to evaluate the effectiveness of the acid stimulation treatment.

Comment

The test procedure and measurements are summarized. The acid treatment was effective in removing the formation damage. Analysis of the data revealed a significant improvement in the wellbore condition resulting in over a 3000 B/D increase in production at 428 psi higher wellhead pressure.

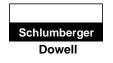
Section 200

July 1998

Page 104 of 168

MATRIX ENGINEERING MANUAL

Well Performance



Post-Acid Test Computations

- 1. Log-Log Analysis
 - 1.1 Match Parameters Model: Homogeneous, WBS & S

 $C_D e^{2s} = 1.0E16$

Pressure Match: $P_D/\Delta P$ = 0.06318

Time Match: $(T_D/C_D)/\Delta t = 1300$

1.2 Reservoir Parameter Calculations

$$kh = 141.2 \ Q_o \beta_o \mu_o \left(\frac{P_D}{\Delta P}\right)_{match} = 37,626.4 \ md - ft$$

$$C = \left(\frac{kh}{3389\mu_o}\right) \left[\frac{\Delta t}{\left(\frac{T_D}{C_D}\right)}\right]_{match} = 0.122 \ bbl \ / \ psi$$

$$C_D = \frac{0.8936 \ C}{\phi C_t \ h \ r_w^2} = 486$$

$$s = \frac{1}{2} ln \left(\frac{C_D e^{2s}}{C_D} \right) = 15$$

- 2. Generalized Horner Analysis
 - 2.1 Straight Line Parameters

Superposition slope: m' = 4.14328 E-03

P (intercept): $P^* = 5430 \text{ psia}$

Pressure at one hour: P(1 hr) = 5401 psia

Pressure at time zero: P (0) = 5041 psia

2.2 Reservoir Parameter Calculations

$$kh = \frac{162.6 \ B_o \mu_o}{m'} = 37,635 \ md - ft$$

$$s = 1.151 \left\{ \left(\frac{P(1 hr) - P(O)}{m'Q_o} \right) - log\left(\frac{k}{\phi \mu_o C_t r_w^2} \right) + 3.23 \right\} = 15$$

MATRIX ENGINEERING MANUAL

Well Performance

Section 200

July 1998

Page 105 of 168

Nomenclature

k = permeability (md)

h = formation height (ft)

C = wellbore storage constant (bbl/psi)

e = scientific notation

 Q_o = oil flow rate B/D

 P_D = dimensionless pressure

 ΔP = pressure change (psi)

 T_D = dimensionless time

 C_D = dimensionless wellbore storage constant

 Δt = time change (hr)

 β_o = oil formation volume factor (bbl/STB)

 μ_o = oil viscosity (cp)

 ϕ = formation porosity

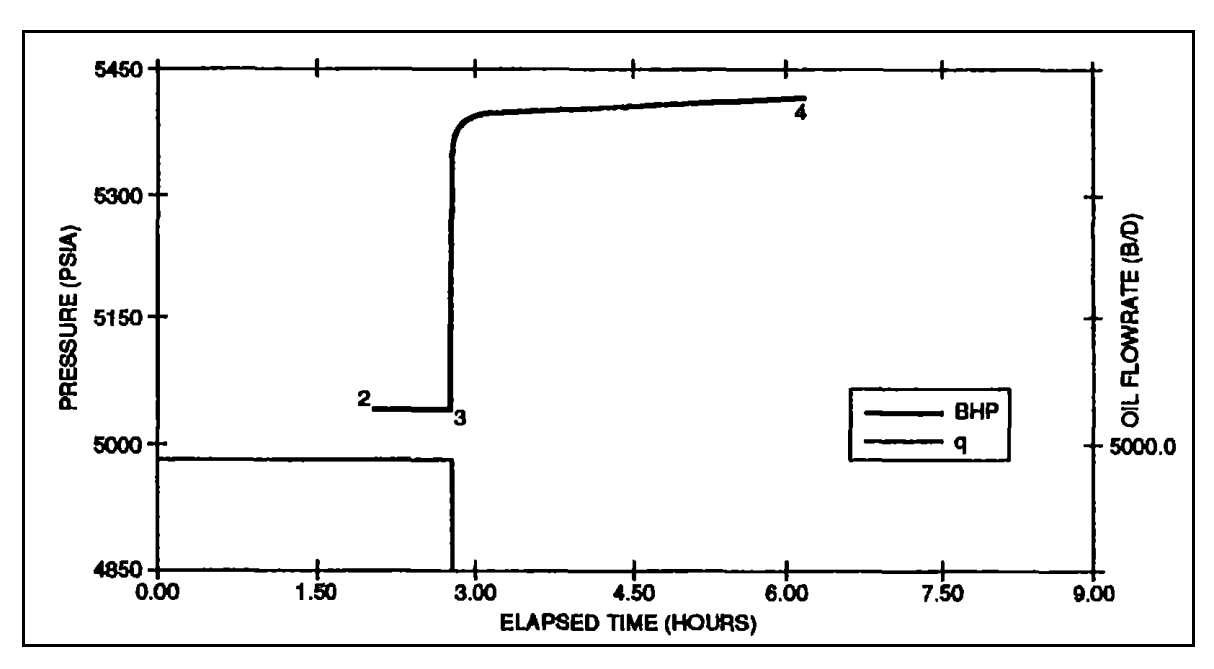


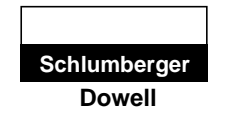
Fig. 55. Pressure/flowrate history.

Section 200

July 1998

Page 106 of 168

MATRIX ENGINEERING MANUAL



Sequence of Events							
Event No.	Date	Time (hr:min)	Description	Elapsed Time (hr:min)	BHP (psia)	WHP (psia)	
1	16-JUN	11:05	Start Flowing Well	-50:40	N/A	N/A	
2	17-JUN	11:05	Changed Choke	-26:40	N/A	N/A	
3	18-JUN	11:02	Changed Choke	-2:43	N/A	N/A	
4	18-JUN	13:45	Run in Hole Flowing	0:00	2083.0	2082.0	
5	18-JUN	15:48	Start Monitoring Flow	2:03	5040.0	2077.0	
6	18-JUN	16:30	End Flow & Start Shut-In	2:45	5041.0	2075.0	
7	18-JUN	19:58	End Shut-In, POOH	6:13	5411.0	2871.0	

Summary of Flow Periods								
Period	Duration (hr:min)	Pressure (psia)		Flowrate		Choke Size (in.)		
		Start	Stop	Oil (B/D)	Gas (MMSCF/D)			
#1, DD	24:00	N/A	N/A	3565.0	N/A	N/A		
#2, DD	23:57	N/A	N/A	4006.0	N/A	N/A		
#3, DD	5:28	N/A	5041.0	4398.0	4.45	N/A		
#4, BU	3:28	5041.0	5411.0	0	0			



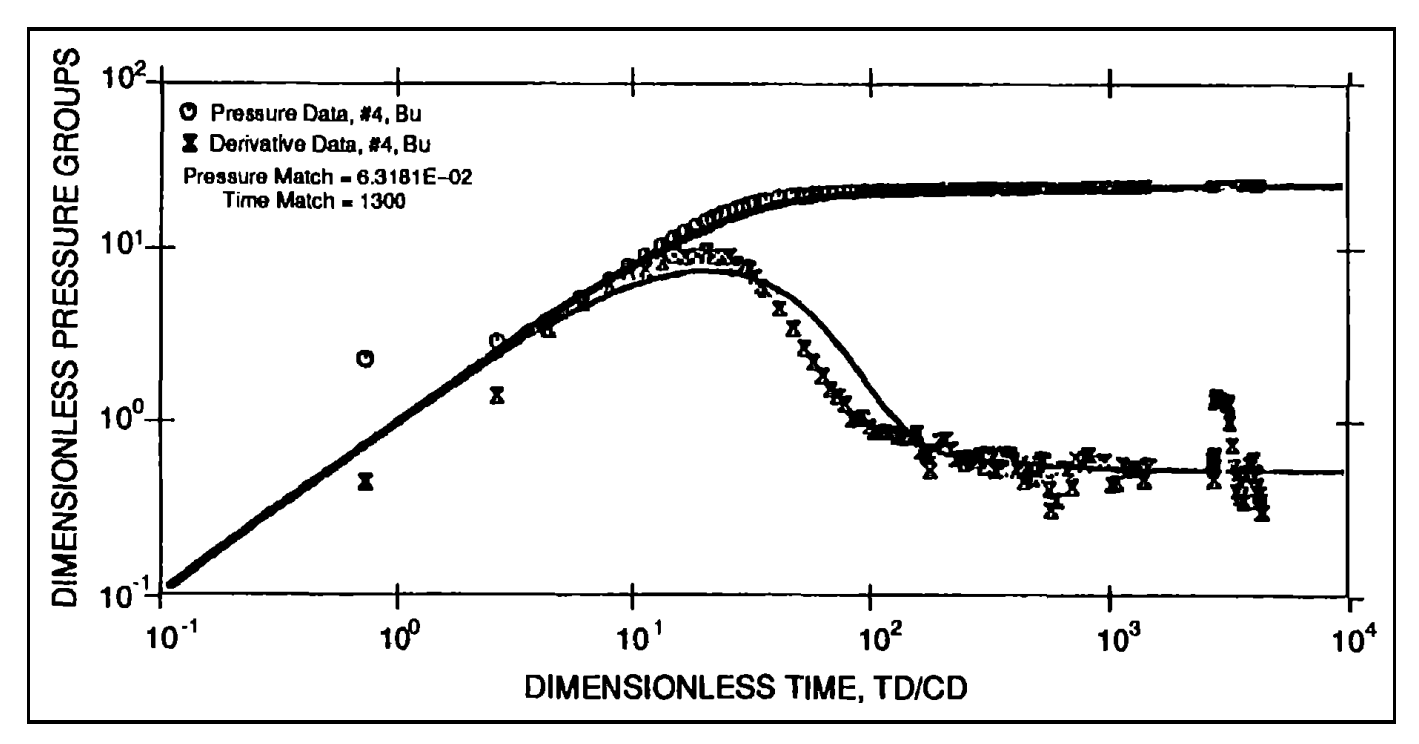


Fig. 56. Post-acid test validation, diagnostic plot.

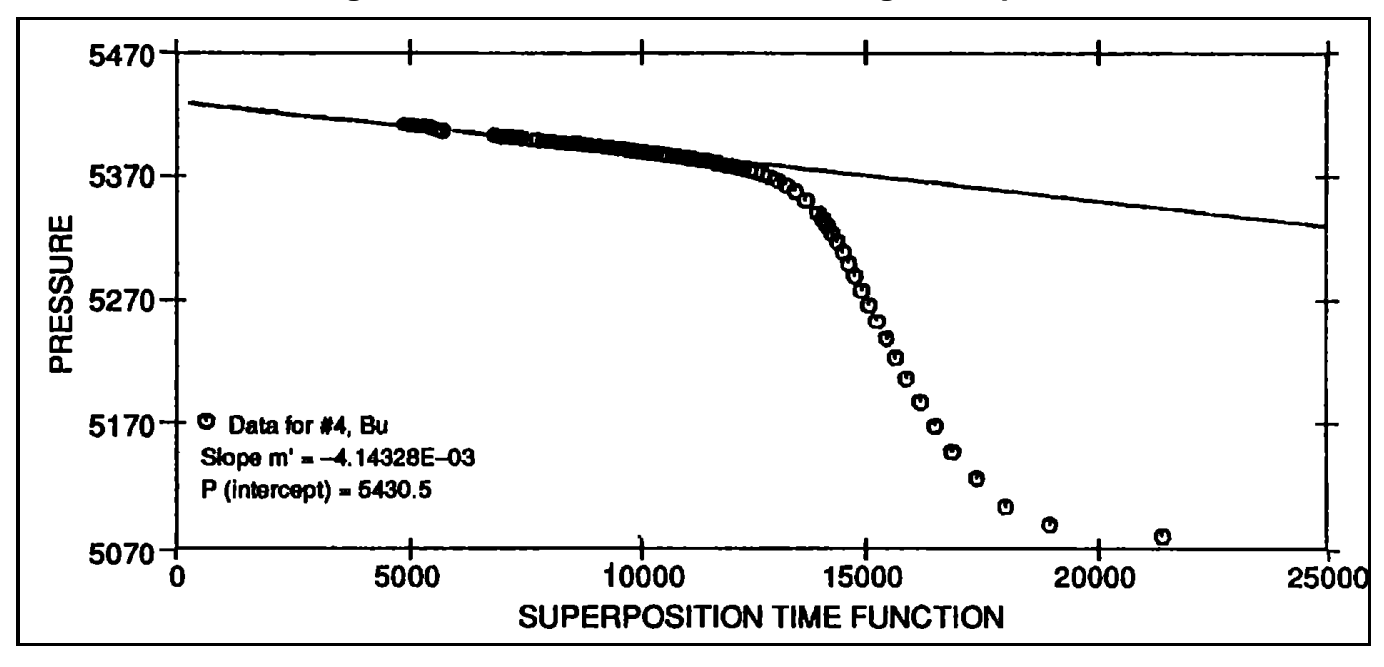
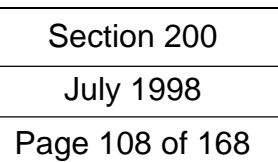
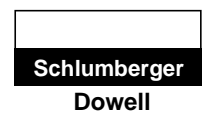


Fig. 57. Post-acid test validation, dimensionless superposition.





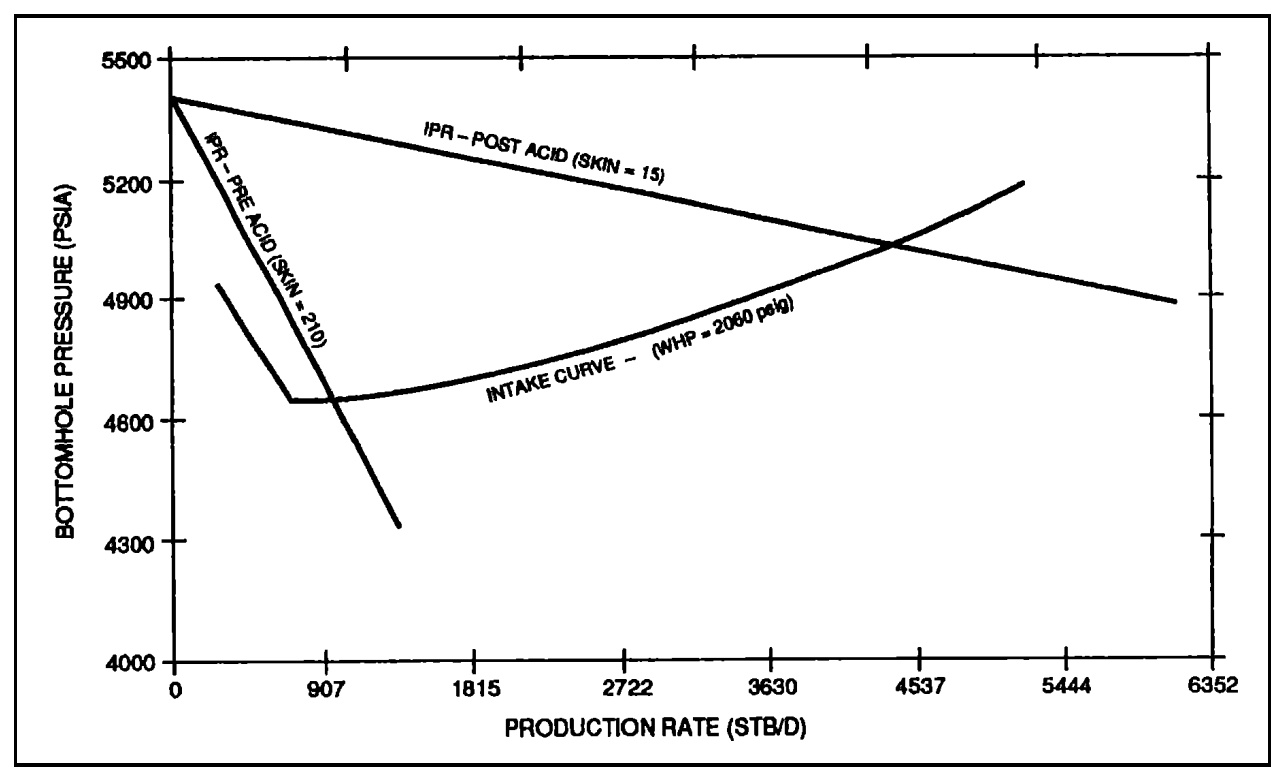


Fig. 58. Post-acid production evaluation, Nodal plot.

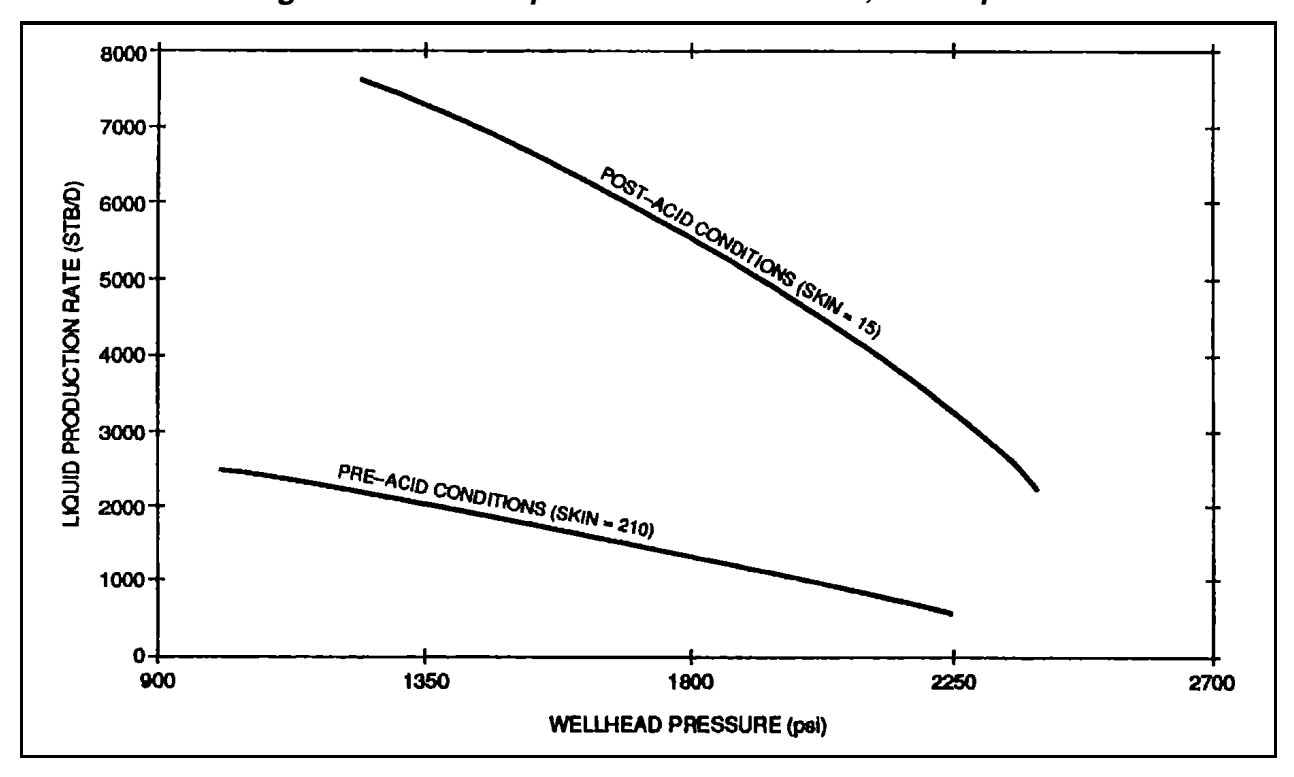
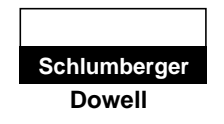


Fig. 59. Post-acid production evaluation, rate versus wellhead pressure.



Well Performance

Section 200

July 1998

Page 109 of 168

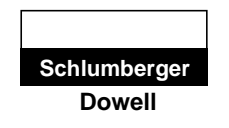
	Delta Time (hr)	Bottomhole		Delta Time (hr)	Bottomhole		Delta Time (hr)	Bottomhole
		Pressure (psia)		2010. 1 11110 (1117)	Pressure (psia)		,	Pressure (psia)
1	0.00000E+00	5040.6	49	0.11667	5380.6	97	0.50967	5395.4
2	1.33336E-03	5040.7	50	0.12083	5381.1	98	0.53467	5395.5
3	2.83330E-03	5040.7	51	0.12500	5381.5	99	0.55967	5395.9
4	4.16667E-03	5040.8	52	0.12917	5382.0	100	0.58467	5396.4
5	5.50003E-03	5040.8	53	0.13333	5382.5	101	0.60967	5396.5
6	6.99997E-03	5040.8	54	0.13750	5382.9	102	0.63467	5397.2
7	8.33333E-03	5041.9	55	0.14167	5383.3	103	0.65967	5397.4
8	9.66670E-03	5049.3	56	0.14583	5383.8	104	0.70967	5398.0
9	1.11666E-02	5058.2	57	0.15000	5383.9	105	0.75967	5398.7
10	1.25000E-02	5067.5	58	0.15417	5384.2	106	0.80967	5399.3
11	1.38334E-02	5076.5	59	0.15967	5384.6	107	0.85967	5399.5
12	1.53333E-02	5085.5	60	0.16800	5385.2	108	0.90967	5400.0
13	1.66667E-02	5099.5	61	0.17633	5385.9	109	0.95667	5400.5
14	1.80000E-02	5122.5	62	0.18467	5386.3	110	1.0097	5401.0
15	1.95000E-02	5144.3	63	0.19300	5386.9	111	1.0597	5401.2
16	2.08333E-02	5085.5	64	0.20133	5387.3	112	1.1097	5401.6
17	2.21667E-02	5184.7	65	0.20967	5387.6	113	1.1597	5402.0
18	2.36666E-02	5203.2	66	0.21800	5388.0	114	2.1638	5406.1
19	2.50000E-02	5220.2	67	0.22633	5388.4	115	2.1763	5406.3
20	2.63334E-02	5236.1	68	0.23467	5388.8	116	2.1888	5406.2
21	2.78333E-02	5250.8	69	0.24300	5389.0	117	2.2013	5406.3
22	2.91667E-02	5264.0	70	0.25133	5389.4	118	2.2138	5406.3
23	3.05000E-02	5276.3	71	0.25967	5389.8	119	5.1362	5578.9
24	3.20000E-02	5287.4	72	0.26800	5390.0	120	5.1390	5578.9
25	3.33333E-02	5297.4	73	0.27633	5390.4	121	5.1417	5579.0
26	3.46667E-02	5306.4	74	0.28467	5390.6	122	5.1473	5578.9
27	3.61666E-02	5314.4	75	0.29300	5390.8	123	5.1500	5579.0
28	3.75000E-02	5321.5	76	0.30133	5391.1	124	5.1528	5579.0
29	3.88334E-02	5327.7	77	0.30967	5391.4	125	5.1557	5579.0
30	4.03333E-02	5333.3	78	0.31800	5391.8	126	5.1583	5579.0
31	4.16667E-02	5338.1	79	0.32633	5391.9	127	5.1612	5579.0
32	4.58333E-02	5348.8	80	0.33467	5392.2	128	5.1945	5578.9
33	5.00000E-02	5356.2	81	0.34300	5392.4	129	5.2278	5578.9
34	5.41667E-02	5361.1	82	0.35133	5392.5	130	5.2612	5579.0
35	5.83333E-02	5364.7	83	0.35967	5392.8	131	5.2778	5579.0
36	6.25000E-02	5367.5	84	0.36800	5392.9	132	2.9138	5409.8
37	6.66667E-02	5369.7	85	0.37633	5393.2	133	2.9638	5410.2
38	7.08333E-02	5371.4	86	0.38467	5393.2	134	30.138	5410.0
39	7.50000E-02	5372.9	87	0.39300	5393.5	135	3.0638	5410.3
40	7.91667E-02	5374.1	88	0.40133	5393.6	136	3.1138	5410.2
41	8.33333E-02	5375.0	89	0.40967	5393.8	137	3.1638	5410.4
42	8.75000E-02	5376.0	90	0.41800	5393.9	138	3.2138	5410.8
43	9.16667E-02	5376.8	91	0.42633	5394.2	139	3.2638	5410.8
44	9.58333E-02	5165.2	92	0.43467	5394.2	140	3.3138	5410.9
45	0.10000	5378.2	93	0.44300	5394.5	141	3.3638	5410.9
46	0.10000	5378.8	94	0.45133	5394.8	142	3.4138	5411.1
47	0.10417	5379.5	95	0.45167	5394.8	143	3.4638	5411.0
48	0.10833	5380.1	96	0.48467	5394.9	170	0.4000	3-11.0

July 1998

Page 110 of 168

MATRIX ENGINEERING MANUAL

Well Performance



5.4 Example Problem — Producing Well

Using tubing data from the example provided in and reservoir parameters from the example provided in (s = -5), calculate the natural production of the well.

$$\begin{array}{ll} k & = 5 \text{ md} \\ h & = 20 \text{ ft} \\ \mu_o & = 1.1 \text{ cp} \\ \text{Spacing} & = 80 \text{ acres} \\ \overline{p}_r & = 2500 \text{ psig} \\ s & = -5 \\ B_o & = 1.2 \text{ res bbl/STB} \\ r_w & = 0.365 \text{ ft} \end{array}$$

Solution

$$Drainage \ radius, \ r_e = \sqrt{\frac{80 \times 43,560}{\pi}} = 1053 \ ft$$

$$AOFP = q = \frac{7.08 \times 10^{-3} \ kh \ \overline{p}_r}{\mu_o B_o \left[ln \left(\frac{r_e}{r_w} \right) - 0.75 + s \right]}$$

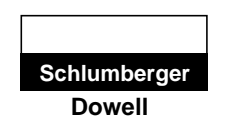
$$= \frac{7.08 \times 10^{-3} \times 5 \times 20 \times 2.500}{1.1 \times 1.2 \left[ln \left(\frac{1.053}{0.365} \right) - 0.75 - 5 \right]}$$

$$= 604 \ STB/D$$

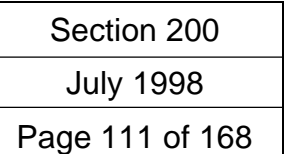
From the example provided in Section 4.2.2, the following tubing intake pressures are calculated for different flow rates.

q (BPD)	P_{w_f} (psig)
200	730
400	800
600	910
800	1080

These values are plotted in Fig. 60. The intersection of the tubing intake curve and the IPR curve gives the natural production of the well (410 STB/D).



Well Performance



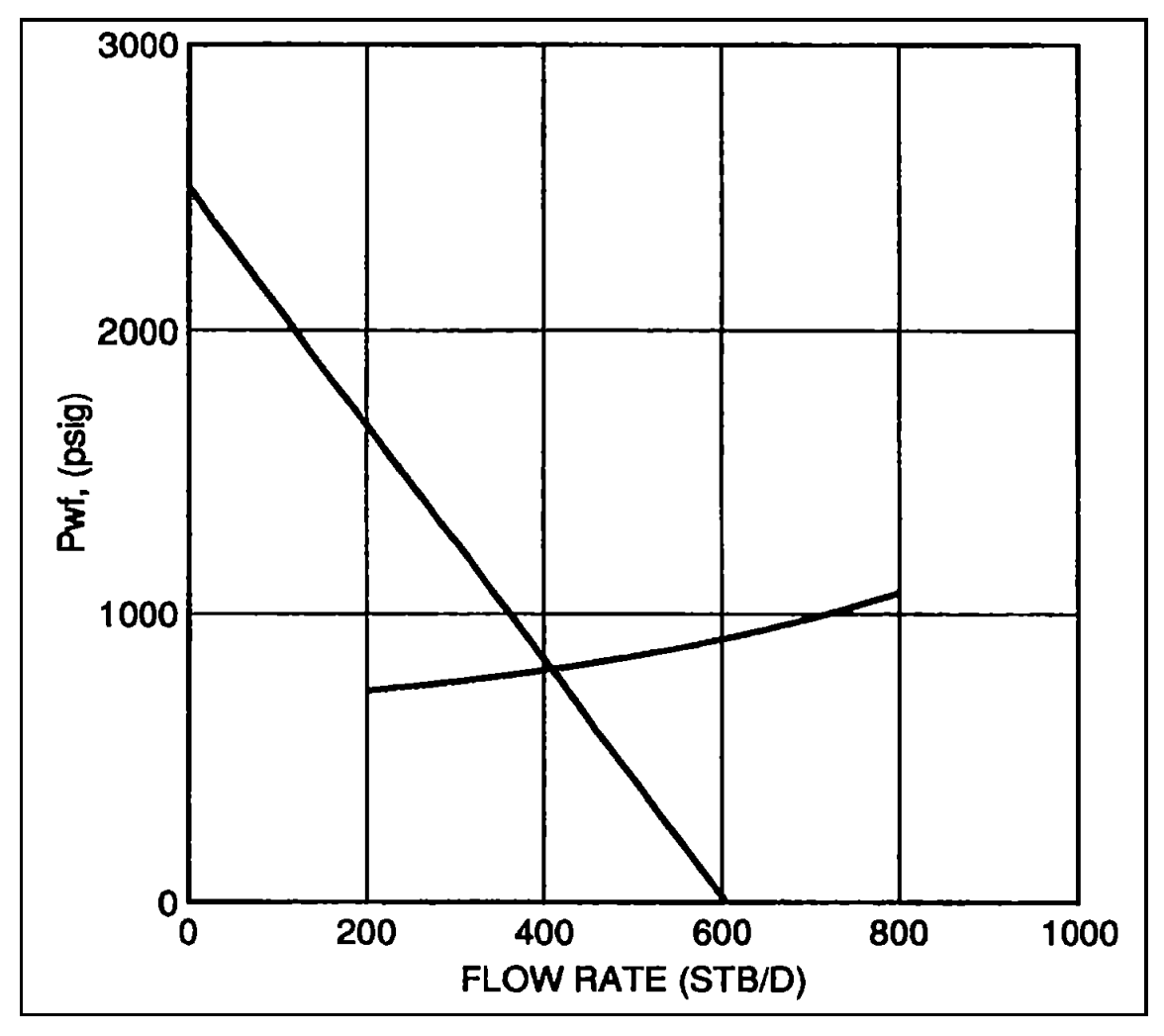


Fig. 60. Example 5.3 IPR and tubing intake curve.

5.5 Example Problem — Varying Wellbore Radius

Solve Example 5.3 for varying r_w , that is, $r_w = 100$ ft, 200 ft, 400 ft, and 800 ft. Make a plot of q versus r_w . (Use a skin factor of +2.)

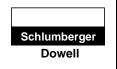
Solution

The tubing intake curve is plotted as shown in Example 5.3 with the following points.

q (BPD)	$P_{\it wf}$ (psig)
200	730
400	800
600	910
800	1080

Section 200		
July 1998		
Page 112 of 168		

Well Performance



Using data from Example 5.3, the value of production rate, q is calculated for different values of r_w and plotted.

(i)
$$r_w = 100 \text{ ft}$$

$$AOFP = q = \frac{7.08 \times 10^{-3} \text{ kh}\overline{p}_r}{\mu_o B_o \left[ln \left(\frac{r_e}{r_w} \right) - 0.75 + s \right]}$$

$$= \frac{7.08 \times 10^{-3} \times 5 \times 20 \times 2.500}{1.1 \times 1.2 \left[ln \left(\frac{1.053}{100} \right) - 0.75 + 2 \right]}$$

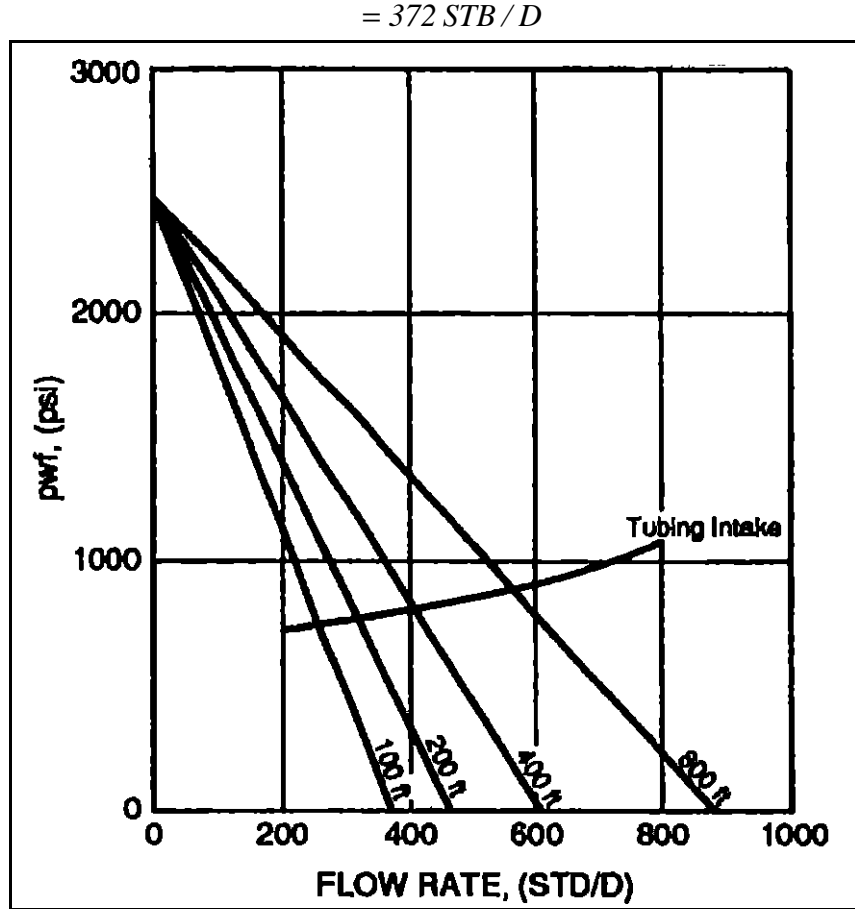


Fig. 61. Plot of tubing intake versus production rates for different r_w .



Well Performance

Section 200	
July 1998	
Page 113 of 168	

Similarly, the flow rates at other values of r_w are calculated and plotted:

r_w (ft)	q (STB/D)
100	372
200	461
400	605
800	879

From Fig. 61, production rate is read at the intersection of the tubing intake curves and the IPR curves for the different values of effective wellbore radius. These are tabulated and plotted.

r_w (ft)	q (STB/D)
100	265
200	320
400	410
800	565

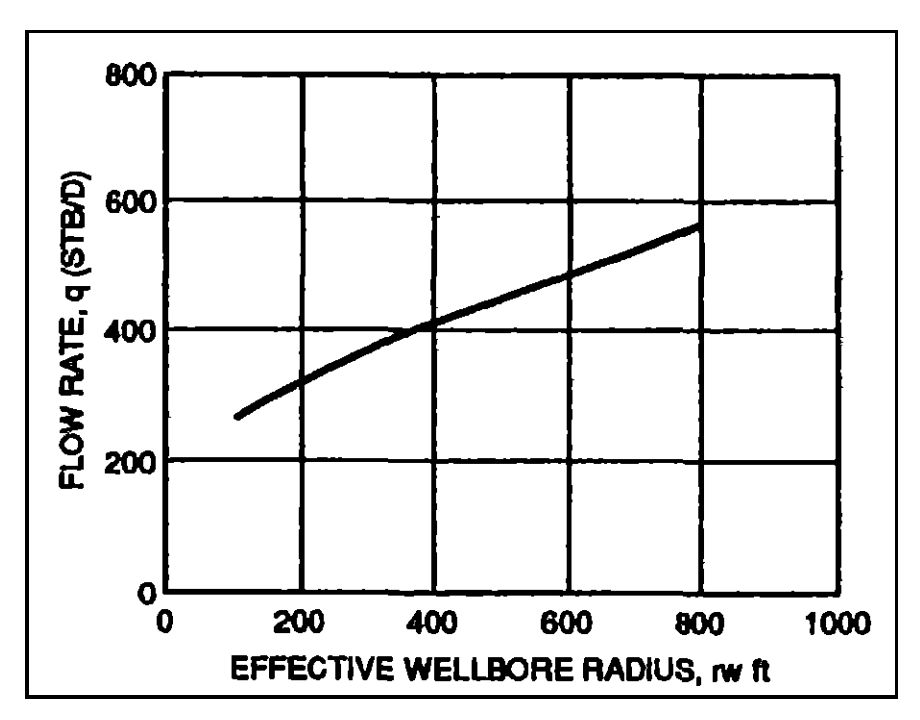
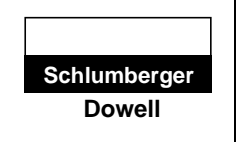


Fig. 62. Plot of flow rate versus effective wellbore radius.

Note: Hydraulically induced fractures increase the effective wellbore radius (Prats, 1961 – Section 11).

Section 200
July 1998
Page 114 of 168

Well Performance



5.6 Example Problem — Shot-Density Sensitivity Analysis

Using the data from Example 5.3 (tubing intake and IPR) and the example provided in Section 3.1.1 (Table 2), perform a shot density sensitivity analysis.

Solution

Calculate and plot the response curve from Fig. 60.

Response Curve Calculation		
q (STB/D)	Δ_p	
200	938	
250	713	
300	488	
350	244	
400	40	
410	0	

Using data from Table 2, plot the pressure drop versus flow rate for different shot densities on the same plot as the response curve.

The intersection of the response curve with the shot density curves gives the production rate for different shot densities.

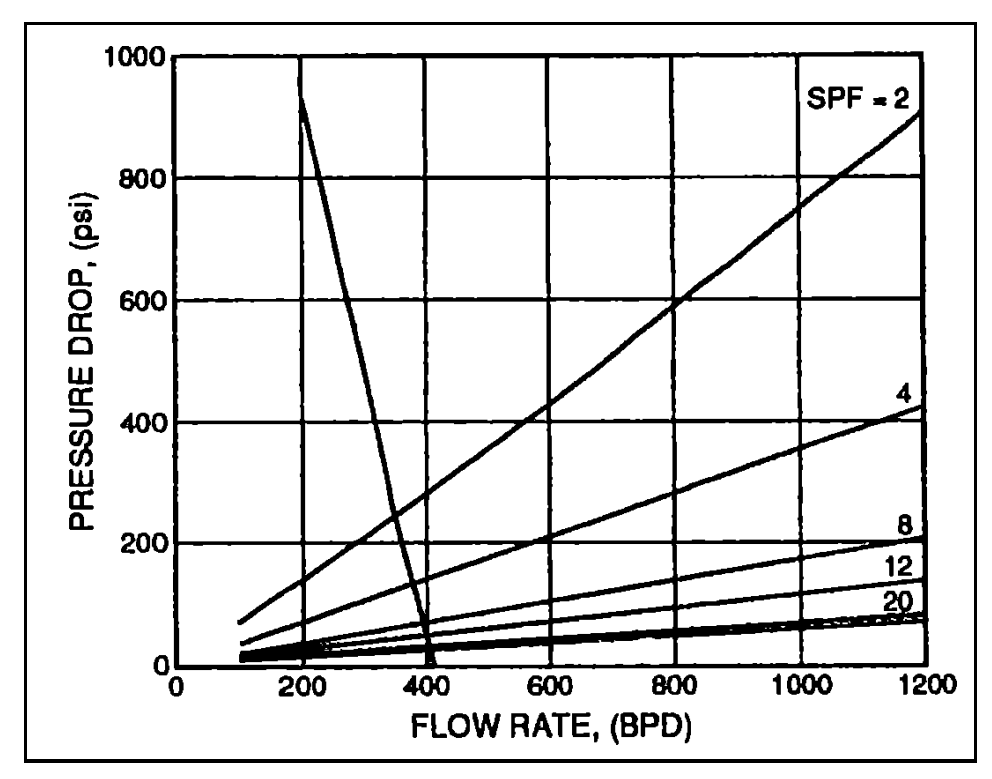
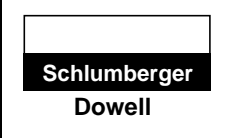


Fig. 63. Plot of flow rate versus pressure drop for varying shot densities.



Well Performance

Section 200	
July 1998	
Page 115 of 168	

These values are read and tabulated as:

Shot Density (SPF)	Flow Rate (BPD)
2	350
4	378
8	390
12	400
20	405
24	408

These values are then plotted as shown here.

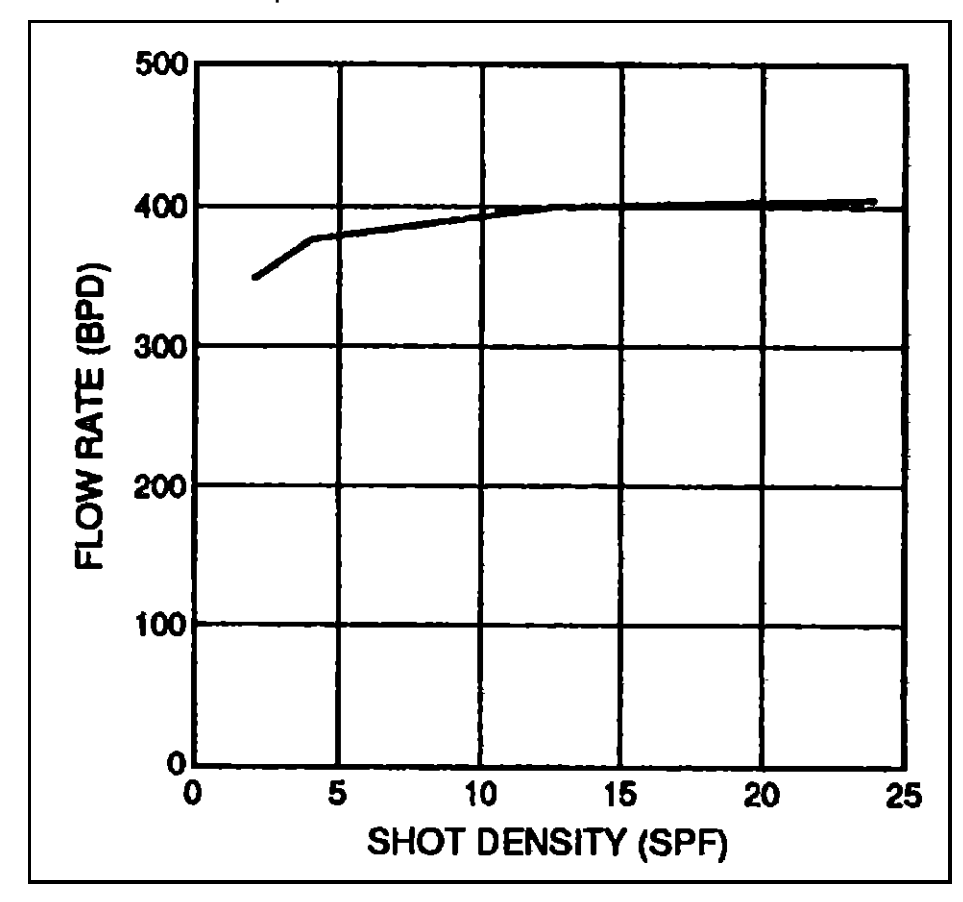


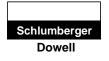
Fig. 64. Plot of shot density versus flow rate.

July 1998

Page 116 of 168

MATRIX ENGINEERING MANUAL

Well Performance



6 Pressure Loss Equations

6.1 Oil IPR Equations

6.1.1 Darcy's Law

$$q_o = \frac{7.08 \times 10^{-3} \, kh \left(\overline{p}_r - \overline{p}_{wfs}\right)}{\overline{\mu}_o B_o \left[ln \left(\frac{r_e}{r_w}\right) - \frac{3}{4} + s\right]}$$

$$PI = \frac{q}{\overline{p}_r - \overline{p}_{wfs}} = \frac{q}{\Delta p} = \frac{7.08 \times 10^{-3} \, kh}{\overline{\mu}_o B_o \left[ln \left(\frac{r_e}{r_w} \right) - \frac{3}{4} + s \right]}$$

$$AOF = (PI)(\overline{p}_r - 0)$$

where,

q = oil flow rate (B/D)

AOF = absolute open flow potential (B/D)

k = permeability (md)

h = net vertical formation thickness (ft)

 \bar{p}_r = average formation pressure (shut-in BHP) (psi)

 \overline{p}_{wfs} = average flowing bottomhole pressure at the sandface (psi)

 $\mu_{\scriptscriptstyle o}$ = average viscosity (cp)

 B_o = formation volume factor (res bbl/STB)

 r_e = drainage radius (ft)

 r_{w} = wellbore radius (ft)

S = skin factor (dimensionless)

PI = Productivity Index (B/D/psi)

6.1.2 Vogel Test Data $(\overline{P}_r \leq p_b)$

$$\frac{q_o}{q_{o max}} = 1 - 0.2 \frac{p_{wfs}}{\overline{p}_r} - 0.8 \left(\frac{p_{wfs}}{\overline{p}_r}\right)^2$$

MATRIX ENGINEERING MANUAL

Well Performance

Section 200 July 1998

Page 117 of 168

6.1.3 Combination Vogel = Darcy Test Data $(\overline{P}_r > p_b)$

1. For test when $p_{wftest} > p_b$.

$$PI = \frac{q}{\overline{p}_r - p_{wfs}}$$

$$q_b = PI(\overline{p}_r - p_b)$$

$$q_{o\,max} = q_b + \frac{PI \times p_b}{I.8}$$

Points on IPR curve

For
$$p_{wf} > p_b$$

$$q_o = PI\left(\overline{p}_r - p_{wf}\right)$$

For $p_{w_f} < p_b$

$$q_o = q_b + (q_{o max} - q_b) \times \left[1 - 0.2 \left(\frac{p_{wf}}{p_b} \right) - 0.8 \left(\frac{p_{wf}}{p_b} \right)^2 \right]$$

2. For test when $p_{wftest} < p_b$

$$PI = \frac{q}{\left(\overline{p}_r - p_b\right) + \frac{p_b}{1.8} \left[1 - 0.2 \left(\frac{p_{wf}}{p_b}\right) - 0.8 \left(\frac{p_{wf}}{p_b}\right)^2\right]}$$

$$q_b = PI\left(\overline{p}_r - p_b\right)$$

$$q_{o\,max} = q_b + \frac{PI \times p_b}{1.8}$$

Points on IPR curve

For
$$p_{wf} > p_b$$

$$q_o = (PI)(\overline{p}_r - p_{wf})$$

For
$$p_{wf} < p_b$$

$$(q_{o max} - q_b) \times \left[1 - 0.2 \left(\frac{p_{wf}}{p_b} \right) - 0.8 \left(\frac{p_{wf}}{p_b} \right)^2 \right]$$

where,

 $qo = flow \ rate \ (B/D)$

 q_b = flow rate at bubblepoint (BD)

 p_b = bubblepoint pressure (psi)

 q_{omax} = maximum flow rate (Vogel or combination) (B/D)

PI = Productivity Index (B/D/psi)

July 1998

Page 118 of 168

MATRIX ENGINEERING MANUAL

Well Performance



6.1.4 Jones IPR

$$p_r - p_{wfs} = aq^2 + b$$

$$p_{r} - p_{wfs} = \left(\frac{2.30 \times 10^{-14} \beta B_{o}^{2} \rho}{h_{p}^{2} r_{w}}\right) q^{2} + \left[\frac{\mu_{o} B_{o} \left[\ln \left\{0.472 \left(\frac{r_{e}}{r_{w}}\right)\right\} + s\right]}{7.08 \times 10^{-3} kh}\right] q$$

$$AOF = \frac{-b \pm \sqrt{b^2 + 4a(p_r - 0)}}{2a}$$

where,

$$a = \left(\frac{2.30 \times 10^{-14} \beta \ B_o^2 \rho}{h_p^2 \ r_w}\right) q^2 +$$

$$b = \left[\frac{\mu_o B_o \left[ln \left\{ 0.472 \left(\frac{r_e}{r_w} \right) \right\} + s \right]}{7.08 \times 10^{-3} \, kh} \right] q$$

q = flow rate (B/D)

 \overline{p}_r = average reservoir pressure (shut-in BHP) (psi)

 p_{wfs} = flowing BHP at sandface (psi)

 β = turbulence coefficient (ft⁻¹)

$$\beta = \frac{2.33 \times 10^{10}}{k^{1.201}} \quad (after Katz),$$

 B_o = formation volume factor (res bbl/STB)

 ρ = fluid density (lbm/ft³)

 h_p = perforated interval (ft)

 μ_o = viscosity (cp)

 r_e = drainage radius (ft)

 r_w = wellbore radius (ft)

S = skin factor (dimensionless)

k = permeability (md)

a = turbulence term

b = darcy flow term

MATRIX ENGINEERING MANUAL

Well Performance

Section 200 July 1998

Page 119 of 168

6.2 Gas IPR Equations

6.2.1 Darcy's Law (Gas)

$$q = \frac{703 \times 10^{-6} \, kh \left(\overline{p}_r^2 - p_{wfs}^2\right)}{\overline{\mu} \, \overline{T} \, \overline{Z} \left[ln \left(\frac{r_e}{r_w}\right) - \frac{3}{4} + s \right]}$$

where,

q = flow rate (Mcf/D)

k = permeability (md)

h = net vertical thickness (ft)

 \overline{p}_r = average formation pressure (shut-in BHP) (psia)

 p_{wfs} = sandface flowing BHP (psia)

 μ = viscosity (cp)

 $T = \text{temperature } (\circ R)$

Z = supercompressibility (dimensionless)

 r_e = drainage radius (ft)

 r_w = wellbore radius (ft)

S =skin factor (dimensionless)

6.2.2 Jones' Gas IPR (General Form)

$$\overline{p}_r^2 - \overline{p}_{wfs}^2 = aq^2 + bq$$

$$\overline{p}_{r}^{2} - \overline{p}_{wfs}^{2} = \frac{3.16 \times 10^{-12} \beta \gamma_{g} TZ}{h_{p}^{2} r_{w}} q^{2} + \frac{1.424 \times 10^{3} \mu TZ \left[ln \left(0.472 \frac{r_{e}}{r_{w}} \right) + s \right]}{kh} q$$

$$-b \pm \sqrt{b^{2} + 4a(\overline{p}_{r}^{2})}$$

$$AOFP = \frac{-b \pm \sqrt{b^2 + 4a(\overline{p}_r^2)}}{2a}$$

where,

$$a = \frac{3.16 \times 10^{-12} \ \beta \ \gamma_g TZ}{h_p^2 \ r_w}$$

$$b = \frac{1.424 \times 10^3 \ \mu \ TZ \left[ln \left(0.472 \frac{r_e}{r_w} \right) + s \right]}{kh}$$

q = flow rate (Mcf/D)

a = turbulence term

July 1998

Page 120 of 168

MATRIX ENGINEERING MANUAL

Well Performance



b = darcy Flow term

 \overline{p}_r = reservoir pressure (shut-in BHP) (psia)

 p_{wfs} = sandface flowing BHP (psia)

 β = turbulence coefficient (ft⁻¹)

$$\beta = \frac{2.33 \times 10^{10}}{k^{1.201}}$$

 γ_s = gas specific gravity (dimensionless)

T = reservoir temperature (${}^{\circ}$ R)

Z = supercompressibility (dimensionless)

 h_p = perforated interval (ft)

 μ = viscosity (cp)

 r_e = drainage radius (ft)

 r_w = wellbore radius (ft)

6.3 Backpressure Equation

$$q_g = c \left(\overline{p}_r^2 - \overline{p}_{wfs} \right)^n$$

where.

$$c = \frac{703 \times 10^{-6} \, kh}{\mu \, TZ \left[ln \left(\frac{r_e}{r_w} \right) - \frac{3}{4} + s \right]}$$

n = 0.5 < n < 1.0

 q_s = flow rate (Mcf/D)

k = permeability (md)

h = net vertical thickness (ft)

 \overline{p}_r = average formation pressure (shut-in BHP) (psia)

 p_{wfs} = sandface flowing BHP (psia)

 μ = viscosity (cp)

 $T = \text{temperature } (^{\circ}R)$

Z = supercompressibility (dimensionless)

 r_e = drainage radius (ft)

 r_w = wellbore radius (ft)

S =skin factor (dimensionless)



Well Performance

Section 200 July 1998

Page 121 of 168

6.4 Transient Period Equations

6.4.1 Time to Pseudosteady State

$$t_{stab} = 948 \left(\frac{\phi \, \mu \, c_t \, r_e^2}{k} \right)$$

where,

 ϕ = porosity (fraction)

 μ = viscosity (cp)

 c_t = total system compressibility (psi⁻¹)

 r_e = drainage radius (ft)

k = permeability (md)

 t_{stab} = time for pressure transient to reach r_e (hr)

6.4.2 Oil IPR (Transient)

$$q_{o} = \frac{kh(\bar{p}_{r} - p_{wfs})}{162.6 \ \mu_{o} \ B_{o} \left[log \left(\frac{kt}{\phi \ \mu \ c_{t} \ r_{w}^{2}} \right) - 3.23 + 0.87 \ S \right]}$$

where,

k = permeability (md)

h = net vertical thickness (ft)

 μ = viscosity (cp)

 B_o = formation volume factor (res bbl/STB)

 $t = time of interest; t_{stab} (hr)$

 ϕ = porosity (fraction)

 c_t = total system compressibility (psi⁻¹)

 r_w = wellbore radius (ft)

S = skin factor (dimensionless)

6.4.3 Gas IPR (Transient)

$$q_{g} = \frac{kh(\bar{p}_{r}^{2} - p_{wfs}^{2})}{1,638 \,\mu \, TZ \left[log \left(\frac{kt}{\phi \,\mu \, c_{t} \, r_{w}^{2}} \right) - 3.23 + 0.87 \, S \right]}$$

where,

 q_s = flow rate (Mcf/D)

k = permeability (md)

 \bar{p}_r = reservoir pressure (shut-in BHP) (psia)

July 1998

Page 122 of 168

MATRIX ENGINEERING MANUAL

Well Performance



 p_{wf} = flowing bottomhole pressure at sandface (psia)

 μ = viscosity (cp)

 $T = \text{temperature } (\circ R)$

Z = supercompressibility (dimensionless)

 $t = time of interest; t_{stab} (hr)$

f = porosity (fraction)

 c_t = total system compressibility (psi⁻¹)

 r_{w} = wellbore radius (ft)

S = skin factor (dimensionless)

6.5 Completion Pressure Drop Equations

6.5.1 Gravel-Packed Wells

1. Oil Wells (General)

$$p_{wfs} - p_{wf} = \Delta p = aq^2 + bq$$

$$\Delta p = \frac{9.08 \times 10^{-13} \ \beta \ B_o^2 \ \rho \ L}{A^2} \ q^2 \ + \frac{\mu \ B_o L}{1.127 \times 10^{-3} k_g A} \ q$$

where,

$$a = \frac{9.08 \times 10^{-13} \ \beta \ B_o^2 \ \rho \ L}{A^2}$$

$$b = \frac{\mu B_o L}{1.127 \times 10^{-3} k_g A}$$

q = flow rate (B/D)

 p_{wf} = pressure well flowing (wellbore) (psi)

 p_{wfs} = flowing BHP at sandface (psi)

b = turbulence coefficient (ft⁻¹)

For GP Wells:

$$\beta = \frac{1.47 \times 10^7}{k_g^{0.55}}$$

 B_o = formation volume factor (res bbl/STB)

 ρ = fluid density (lbm/ft³)

L = length of linear flow path (ft)

 $A = \text{total area open to flow (ft}^2)$

(A = area of one perforation x shot density x perforated interval),

 k_{g} = permeability of gravel (md)

MATRIX ENGINEERING MANUAL

Well Performance

Section 200

July 1998

Page 123 of 168

2. Gas Wells (General)

$$p_{wfs}^2 - p_{wf}^2 = aq^2 + bq$$

$$p_{wfs}^2 - p_{wf}^2 = \frac{1.247 \times 10^{-10} \ \beta \ \gamma_g \ TZL}{A^2} q^2 + \frac{8.93 \times 10^3 \ \mu \ TZL}{k_g \ A} q$$

where,

$$a = \frac{1.247 \times 10^{-10} \ \beta \ \gamma_g \ TZL}{A^2}$$

$$b = \frac{8.93 \times 10^3 \ \mu \ TZL}{k_g \ A}$$

q = flow rate (Mcf/D)

 p_{wfs} = flowing pressure at the sandface (psia)

 p_{wf} = flowing bottomhole pressure in wellbore (psia)

 β = turbulence factor (ft⁻¹)

$$\beta = \frac{1.47 \times 10^7}{k_g^{0.55}}$$

 γ_s = gas specific gravity (dimensionless)

 $T = \text{temperature } (^{\circ}R)$

Z = supercompressibility (dimensionless)

L = linear flow path (ft)

 $A = \text{total area open to flow (ft}^2)$

(A = area of one perforation x shot density x perforated interval),

 μ = viscosity (cp)

6.5.2 Open Perforation Pressure Drop

1. Oil Wells (General)

$$p_{wfs} - p_{wf} = aq^2 + bq = \Delta p$$

$$\Delta p = \left[\frac{2.30 \times 10^{-14} \ \beta \ B_o^2 \ \rho \left(\frac{1}{r_p} - \frac{1}{r_c} \right)}{L_p^2} \right] q^2 + \left[\frac{\mu \ B_o \left(ln \frac{r_c}{r_p} \right)}{7.08 \times 10^{-3} \ L_p k_p} \right] q$$

July 1998

Page 124 of 168

MATRIX ENGINEERING MANUAL

Well Performance



where,

$$a = \frac{2.30 \times 10^{-14} \; \beta \; B_o^2 \; \rho \left(\frac{1}{r_p} - \frac{1}{r_c}\right)}{L_p^2}$$

$$b = \frac{\mu B_o \left(ln \frac{r_c}{r_p} \right)}{7.08 \times 10^{-3} L_p k_p}$$

 q_o = flow rate/perforation (q/perforation) (B/D)

 β = turbulence factor (ft⁻¹)

$$\beta = \frac{2.33 \times 10^{10}}{k_p^{1.201}}$$

 B_o = formation volume factor (res bbl/STB)

 ρ = fluid density (lbm/ft³)

 L_p = perforation tunnel length (ft)

 μ = viscosity (cp)

 k_p = permeability of compacted zone (md)

 $k_p = 0.1$ k formation if shot overbalanced,

 $k_p = 0.4$ k formation if shot underbalanced,

 r_p = radius of perforation tunnel (ft)

 r_c = radius of compact zone (ft)

$$(r_c = r_p + 0.5 \text{ in.}).$$

2. Gas Wells (General)

$$p_{wfs}^2 - p_{wf}^2 = aq^2 + bq$$

$$= \left\lceil \frac{3.16 \times 10^{-12} \, \beta \, \gamma_g \, TZ \left(\frac{1}{r_p} - \frac{1}{r_c}\right)}{L_p^2} \right\rceil q^2 + \left\lceil \frac{1.424 \times 10^3 \, \mu \, TZ \left(\ln \frac{r_c}{r_p}\right)}{k_p L_p} \right\rceil q$$

MATRIX ENGINEERING MANUAL

Well Performance

Section 200 July 1998

Page 125 of 168

where,

$$a = \frac{3.16 \times 10^{-12} \beta \gamma_g TZ \left(\frac{1}{r_p} - \frac{1}{r_c}\right)}{L_p^2}$$

$$b = \frac{1.424 \times 10^3 \,\mu \, TZ \left(ln \frac{r_c}{r_p} \right)}{L_p \, k_p}$$

 q_o = flow rate/perforation (q/perforation) (B/D)

 β = turbulence factor (ft⁻¹)

$$\beta = \frac{2.33 \times 10^{10}}{k_p^{1.201}}$$

 γ_s = gas specific gravity (dimensionless)

 $T = \text{temperature } (\circ R)$

Z = supercompressibility factor (dimensionless)

 r_c = radius of compact zone (ft)

$$(r_c = r_p + 0.5 \text{ in.}),$$

 r_p = radius of perforation (ft)

 L_p = perforation tunnel length (ft)

 μ = viscosity (cp)

 k_p = permeability of compacted zone (md)

 $k_p = 0.1$ k formation if shot overbalanced,

 k_p = 0.4 k formation if shot underbalanced.

7 Fluid Physical Properties Correlations

7.1 Oil Properties

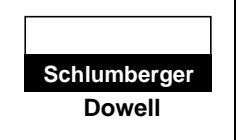
Oil in the absence of gas in solution is called dead oil. The physical properties of dead oil are a function of the API gravity of oil and pressure and temperature. The API gravity is defined as (Eq. 21):

API gravity =
$$\frac{141.5}{Sp Gr at 60^{\circ} F} - 131.5$$
 (21)

The API gravity of water is 10. With gas in solution, oil properties also depend on gas solubility in addition to the pressure, temperature, and API gravity of oil. Gas solubility is normally represented by R_s .

Section 200		
July 1998		
Page 126 of 168		

Well Performance



7.2 Gas Solubility

Gas solubility is defined as the volume of gas dissolved in one stock tank barrel of oil at a fixed pressure and temperature. Gas solubility in oil increases as the pressure increases up to the bubblepoint pressure of the oil. Above the bubblepoint pressure, gas solubility stays constant (Fig. 65).

There are different correlations to calculate the gas solubility, for example, the Standing correlation and the Lassater correlation. The Standing correlation states:

Gas solubility:

$$R_s \left(\frac{scf}{STB} \right) = \gamma_g \left[\frac{p}{18} \times \frac{10^{0.0125(API)}}{10^{0.0009I(T)}} \right]^{1.2}$$

where,

 γ_{s} = specific gravity of gas (air = 1.0),

p = pressure of oil (psia),

T = temperature of oil (°F),

API = API gravity of oil, $^{\circ}API$.

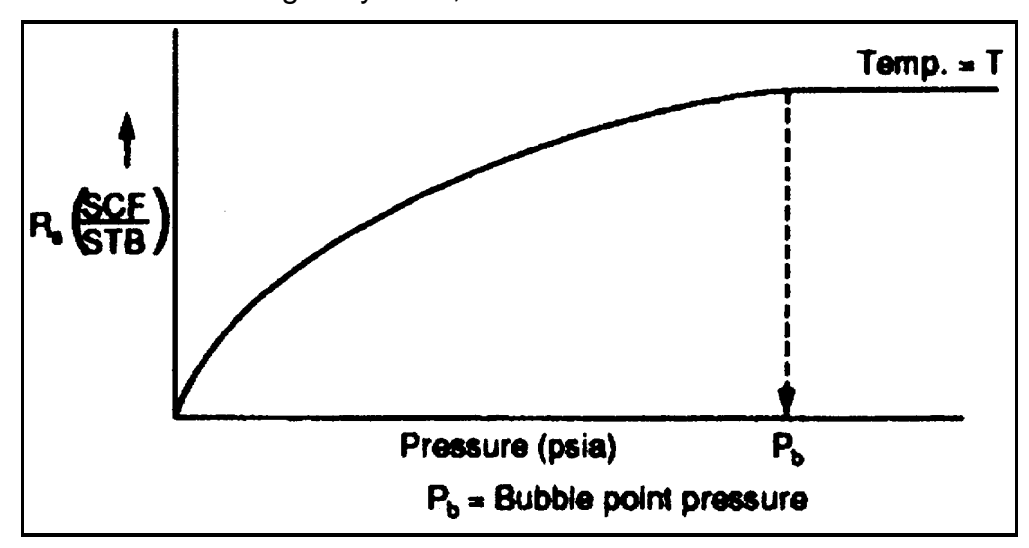


Fig. 65. Variation of gas solubility with pressure and temperature.

MATRIX ENGINEERING MANUAL

Well Performance

Section 200
July 1998
Page 127 of 168

7.3 Formation Volume Factor of Oil

The volume in barrels occupied by one stock tank barrel of oil with the dissolved gas at any elevated pressure and temperature is defined as the formation volume factor of oil. The B_o unit is reservoir barrels per stock tank barrel, which is dimensionless. It measures the volumetric shrinkage of oil from the reservoir to the surface conditions. The formation volume factor increases exponentially with pressure up to the bubblepoint pressure (Fig. 66). Since the oil stops dissolving more gas above the bubblepoint pressure, the formation volume factor decreases due to the compressibility of the liquid.

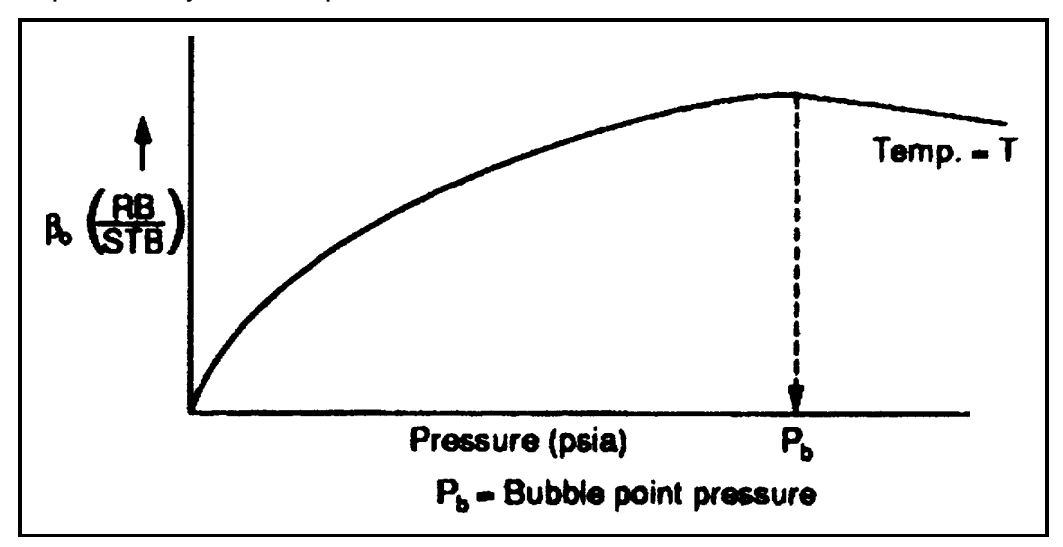


Fig. 66. Variation of formation volume factor with pressure and temperature.

There are different correlations for calculating the formation volume factor of oil. These correlations are empirical and based on data from different oil provinces in the United States. The Standing correlation developed from California crude is one of the oldest and is quite commonly used. The Standing correlation can be written as:

$$B_o = 0.972 + 0.000147 \times F^{1.175}$$

where,

$$F = R_s \left(\frac{\gamma_g}{\gamma_o}\right)^{0.5} + 1.25(T)$$

$$R_s = gas\ solubility\left(\frac{scf}{STB}\right),$$

T = temperature of oil (°F).

Standing also presented his correlation in graphical form (Fig. 67). For manual calculation of the formation volume factor this graphical method is convenient.

For the calculation of gas solubility, R_s and formation volume factor, B_o , a knowledge of the bubblepoint pressure, pb is necessary. Standing presented a nomograph

July 1998

Page 128 of 168

MATRIX ENGINEERING MANUAL

Well Performance

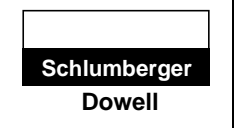


(Fig. 68) to determine the bubblepoint pressure. Gas solubility calculated at the bubblepoint pressure remains constant above the bubblepoint pressure. However, Standing's or any other correlation for formation volume factor cannot be used above the bubblepoint pressure. To calculate the formation volume factor of oil above bubblepoint pressure, the following equation is used:

$$B_o = B_{ob} \exp \left[-C_o (p - p_b)\right]$$

where B_{ob} is the formation volume factor at the bubblepoint pressure. The formation volume factor at the bubblepoint pressure can be calculated from Standing's correlation (Fig. 67) using $R_s = R_p$, R_p being the produced gas/oil ratio. The bubblepoint pressure can also be calculated using Standing's empirical equation representing the nomograph shown in Fig. 68 as follows:

$$p_b = 18.2 \left[\left(\frac{R_s}{\gamma_g} \right)^{0.83} 10^{(T/1100 - \circ API/80.0)} - 1.4 \right]$$

The parameter C_o is not a constant and can be calculated from the correlation presented by Trube as follows:

$$c_o = \frac{-1433 + 5 R_s + 17.2T - 1180 \gamma_g + 12.61 API}{p \times 10^5}$$

The formation volume factor, B_o is used to correct the volumetric flow rate of oil measured at the surface or stock tank to the volumetric flow rate at any other pressure or temperature conditions (for example, reservoir conditions).

MATRIX ENGINEERING MANUAL

Well Performance

Section 200 July 1998

Page 129 of 168

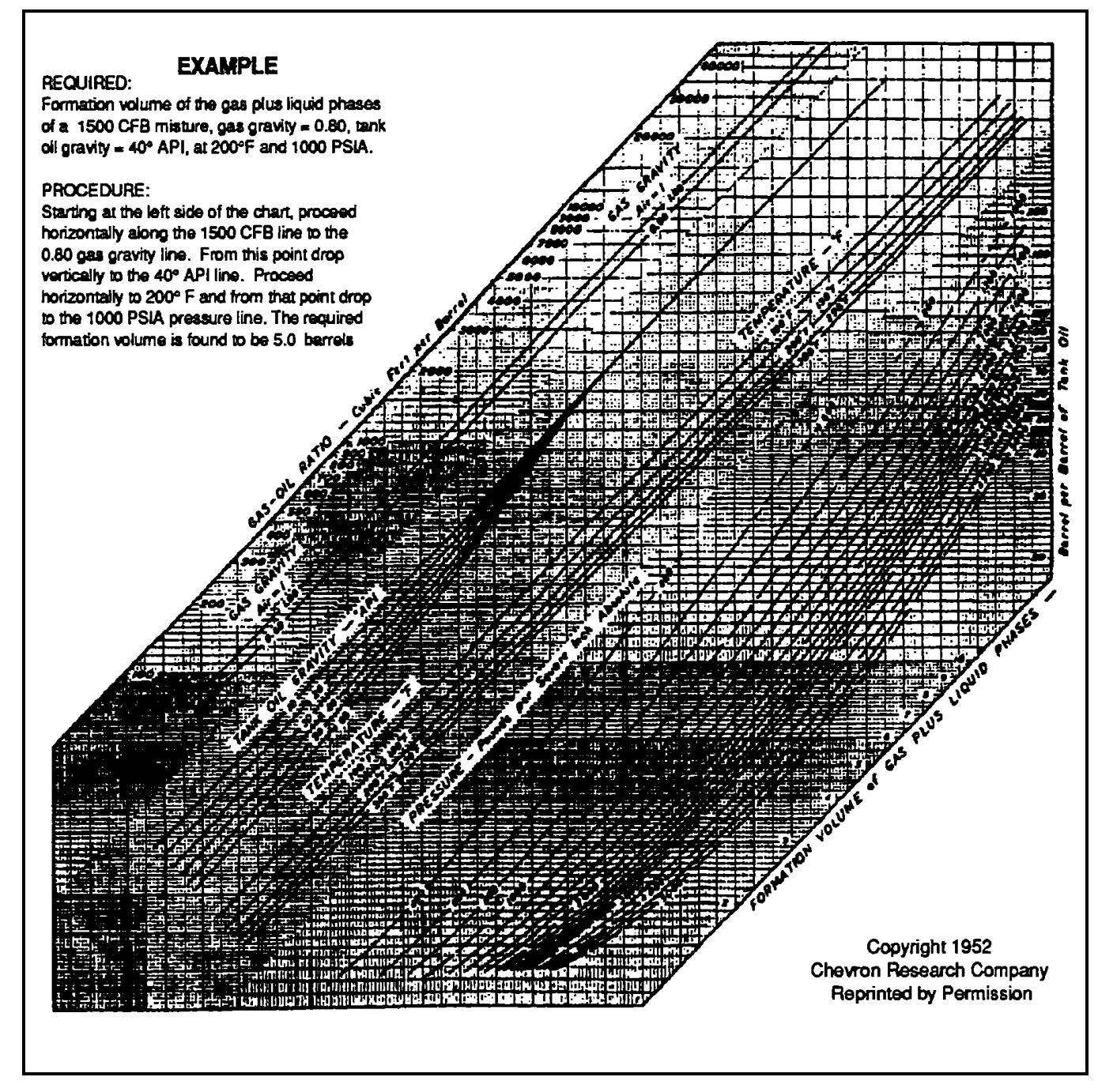


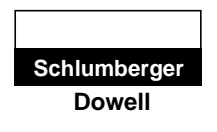
Fig. 67. Properties of natural mixtures of hydrocarbon gas and liquids, formation volume of gas plus liquid phase (after Standing).

Section 200 July 1998

Page 130 of 168

MATRIX ENGINEERING MANUAL

Well Performance



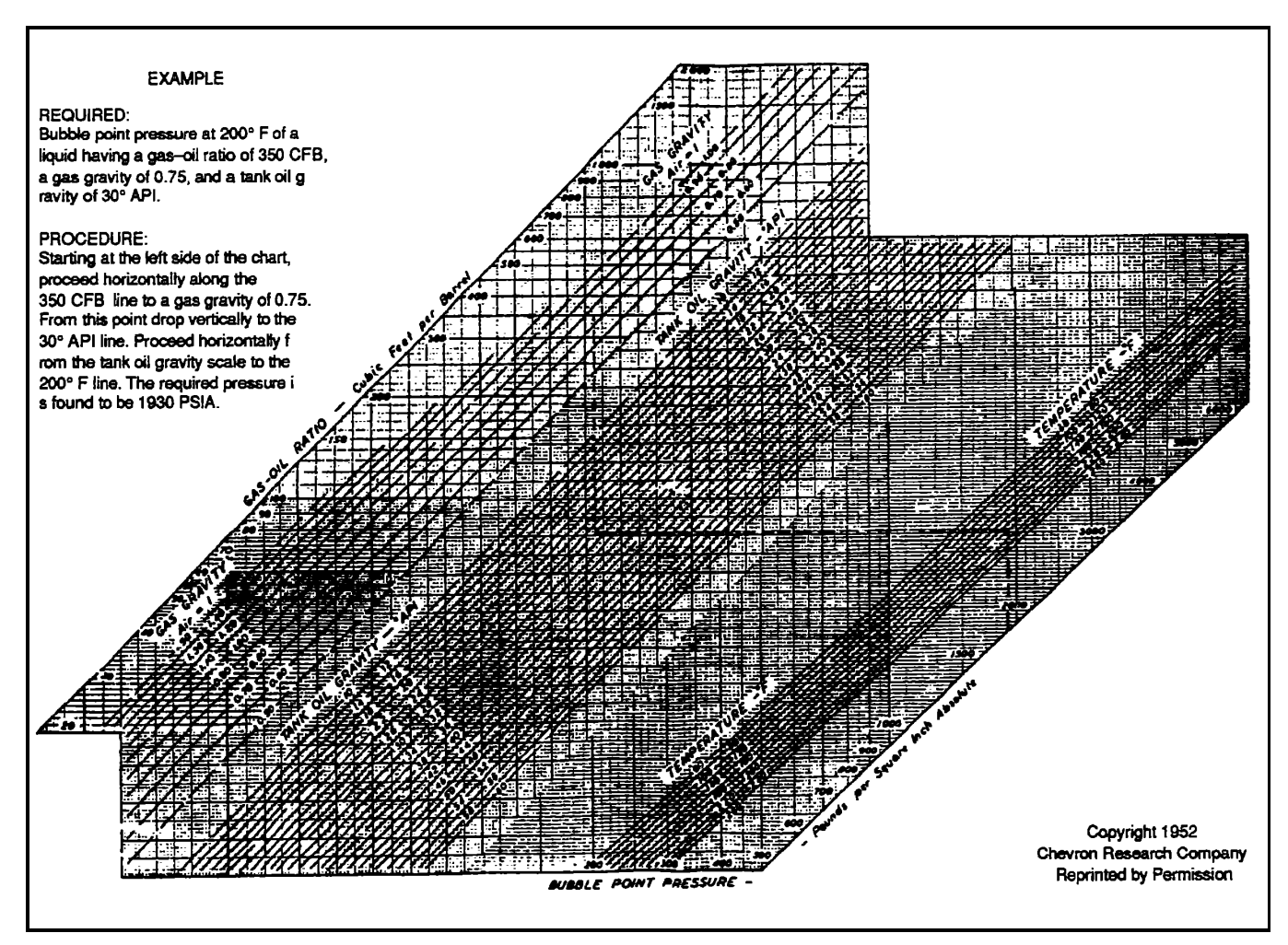


Fig. 68. Properties of natural mixtures of hydrocarbon gas and liquids, bubble-point pressure (after Standing).

7.4 Oil Viscosity

The oil viscosity of reservoir oil containing solution gas decreases with pressure up to the bubblepoint pressure. Above the bubblepoint pressure, the viscosity increases (Fig. 69). In the absence of laboratory determined data for the oil viscosity at any specified pressure and temperature, the Beal correlation is used. Beal correlated the absolute viscosity of gas-free oil with the API gravity of crude at atmospheric conditions for different temperatures (Fig. 70). The viscosity of gas saturated crude oil was correlated by Chew and Connally with the gas free crude oil viscosity and gas solubility (Fig. 71). Beal also presented a correlation to estimate the viscosity increase from the bubblepoint pressure (cp/1000 psi) to calculate the viscosity of oil above the bubblepoint pressure if the viscosity at the bubblepoint pressure is known (Fig. 72).

The laboratory-determined data for B_o , R_s and μ_o are recommended for use in any calculation whenever available.

MATRIX ENGINEERING MANUAL

Well Performance

Section 200

July 1998

Page 131 of 168

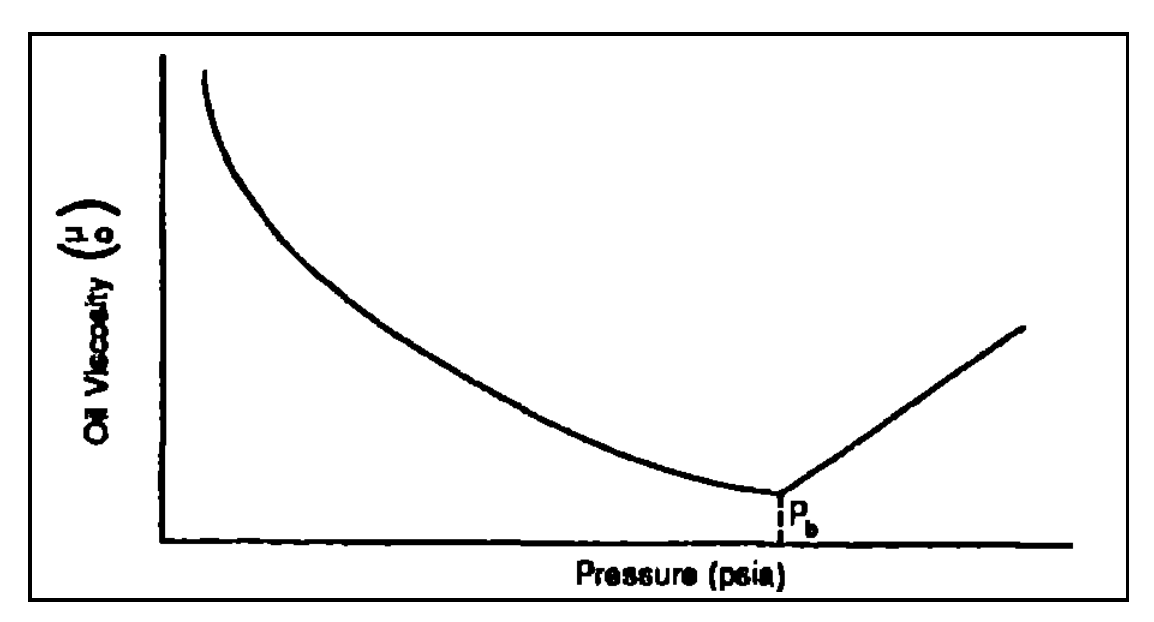
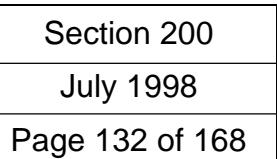
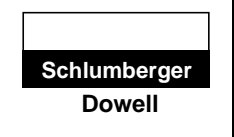


Fig. 69. Variation of oil viscosity with pressure.



Well Performance



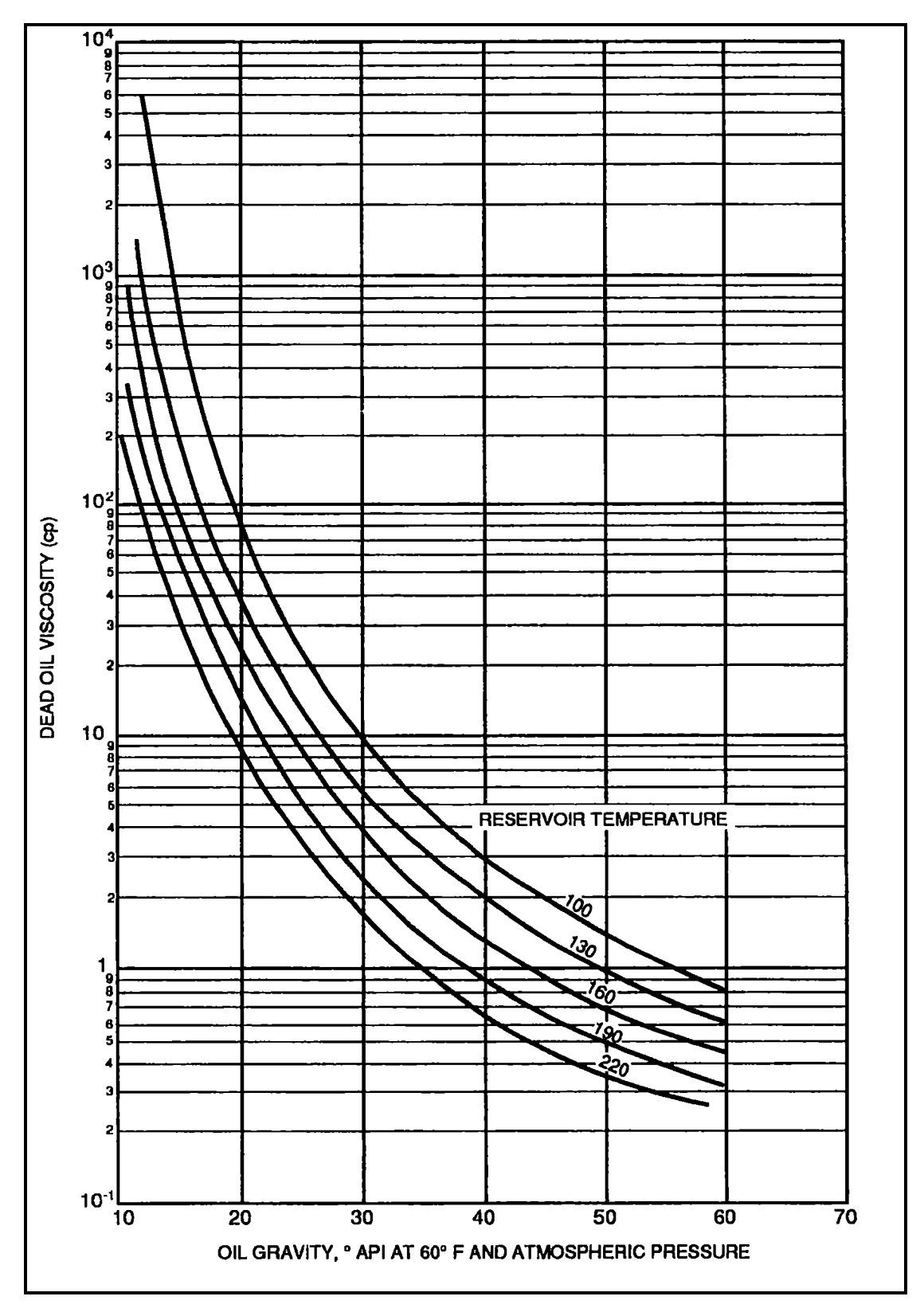


Fig. 70. Dead oil viscosity at reservoir temperature and atmospheric pressure (after Beal).

MATRIX ENGINEERING MANUAL

Well Performance

Section 200

July 1998

Page 133 of 168

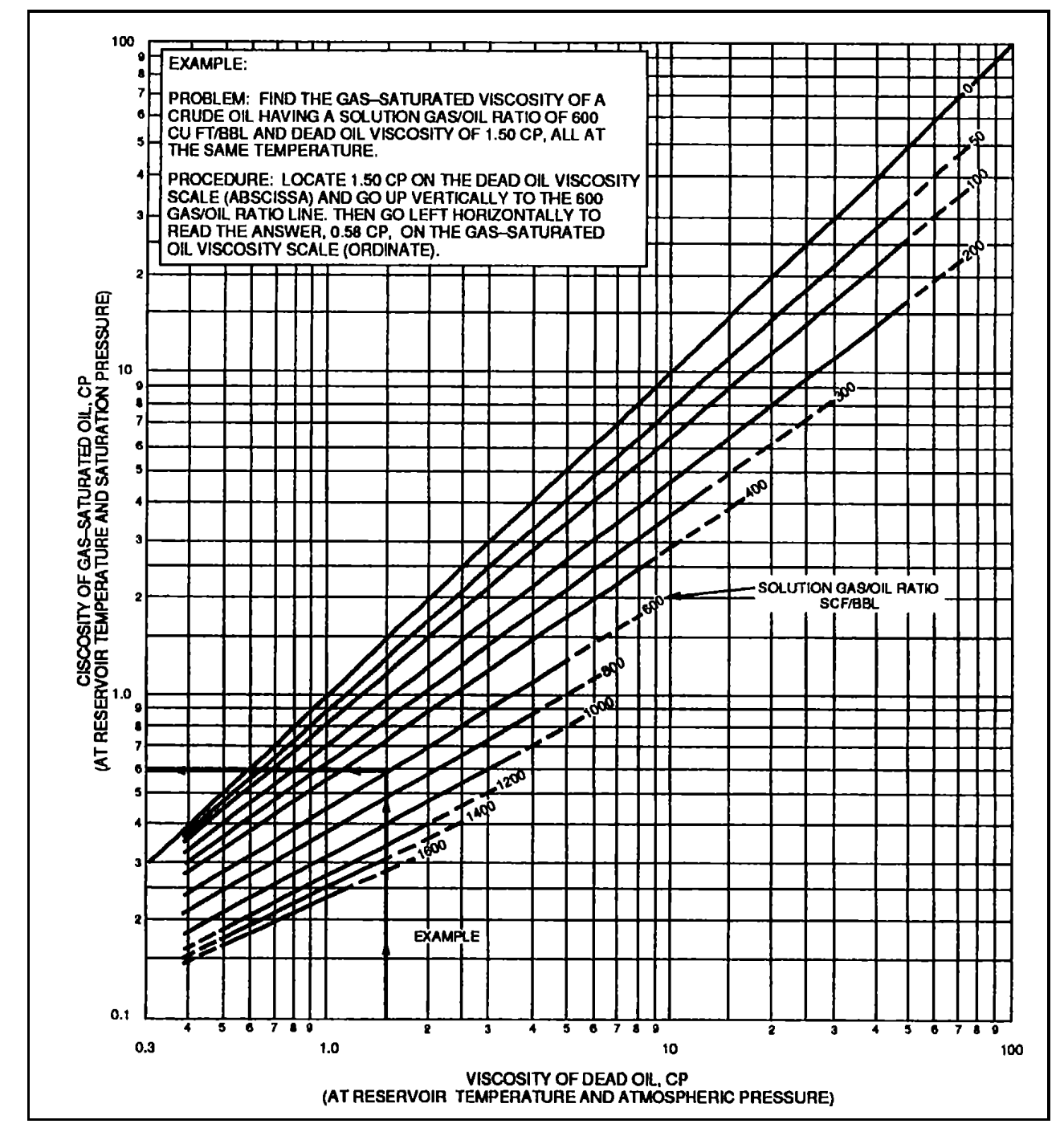
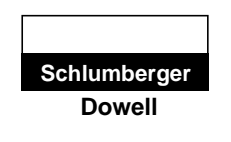


Fig. 71. Viscosity of gas-saturated crude oil at reservoir temperature and pressure. Dead oil viscosity from laboratory data, or from the previous figure (after Chew and Connally).

Section 200
July 1998
Page 134 of 168

Well Performance



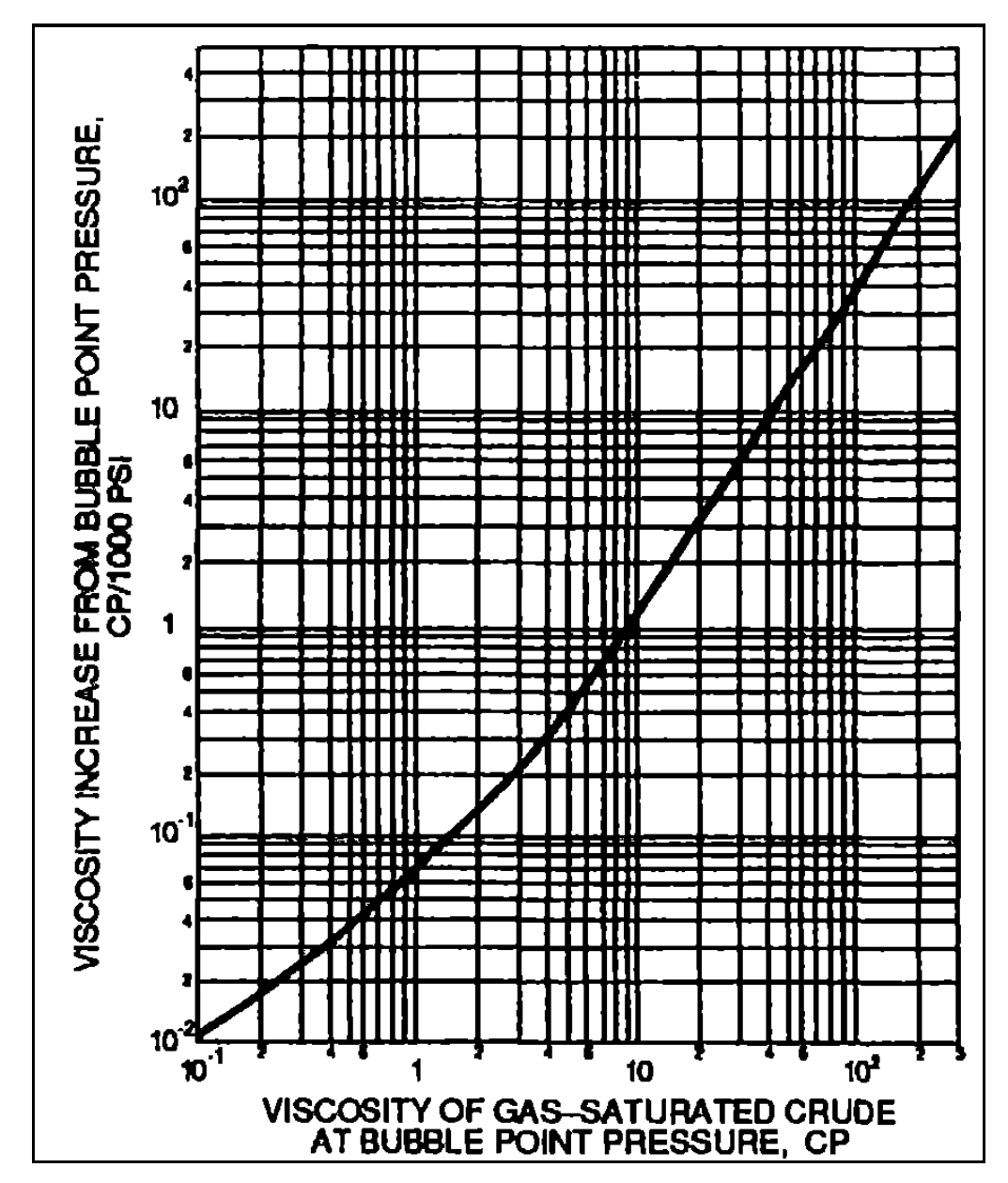


Fig. 72. Rate of increase of oil viscosity above bubble-point pressure (after Beal).

7.5 Gas Physical Properties

The specific gravity of gas is an important correlating parameter for the gas property evaluation. Normally, it can be easily determined in the laboratory. In the absence of a laboratory-determined value, the specific gravity of gas can be calculated from the following relationship knowing the molecular weight (M) of gas.

$$\gamma_g \approx \frac{M}{29}$$

where the molecular weight of air is 29. Thus, the specific gravity of air is 1.

MATRIX ENGINEERING MANUAL

Well Performance

Section 200 July 1998

Page 135 of 168

Gas density can be easily determined from the real gas law:

$$\rho_g = 0.0433 \ \gamma_g \frac{p}{ZT}$$

where,

 ρ_s = density of gas (g/cc),

 γ_s = specific gravity of free gas (air = 1),

p = pressure of gas (psia),

T = absolute temperature of gas (${}^{\circ}R$),

= 460 + temperature (°F),

Z = real gas deviation factor.

7.6 Real Gas Deviation Factor

The real gas deviation factor is an important variable used in calculating the gas density and gas formation volume factor. To determine this parameter, Standing used the law of corresponding states. This law states that at the same reduced pressure and reduced temperature, all hydrocarbon gases have the same gas deviation factor. The reduced pressure and reduced temperature are defined as follows:

$$p_{pr} = reduced \ pressure = \frac{p}{p_{pc}}$$

$$T_{pr} = reduced\ pressure = \frac{T}{T_{pc}}$$

where p and T are the absolute pressure and absolute temperature of gas.

 P_{pc} = pseudo-critical pressure,

 T_{pc} = pseudo-critical temperature.

Pseudo-critical pressure and pseudo-critical temperature are correlated by Brown et al. with the specific gravity of gas (Fig. 73).

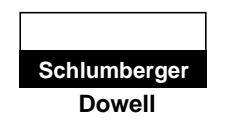
After determining the pseudo-critical pressure and pseudo-critical temperature from the correlation in Fig. 73, the reduced pressure and reduced temperature are calculated using the definition provided earlier. For these calculated reduced pressures and reduced temperatures, the gas deviation factor can be calculated using the appropriate correlations after Standing and Katz (Fig. 74).

The gas formation volume factor (B_s) can be calculated from:

$$B_g = \left(\frac{cf}{scf}\right) = -0.0283 \frac{ZT}{p}$$

Section 200
July 1998
Page 136 of 168

Well Performance



where,

p = pressure (psia),

T = absolute temperature (${}^{\circ}R$).

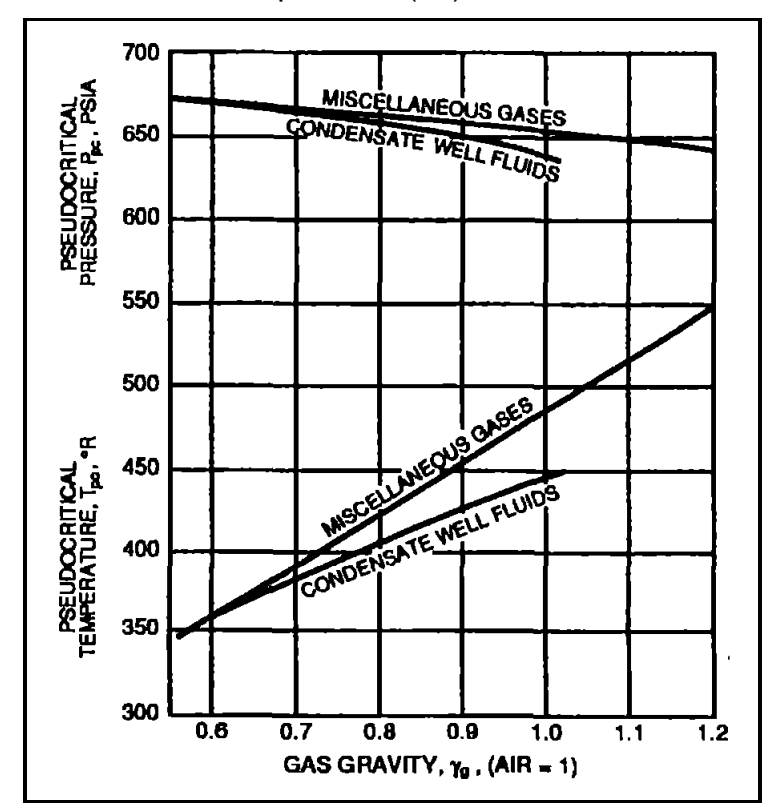


Fig. 73. Correlation of pseudocritical properties of condensate well fluids and miscellaneous natural gas with fluid gravity (after Brown et al.).

MATRIX ENGINEERING MANUAL

Well Performance

Section 200

July 1998

Page 137 of 168

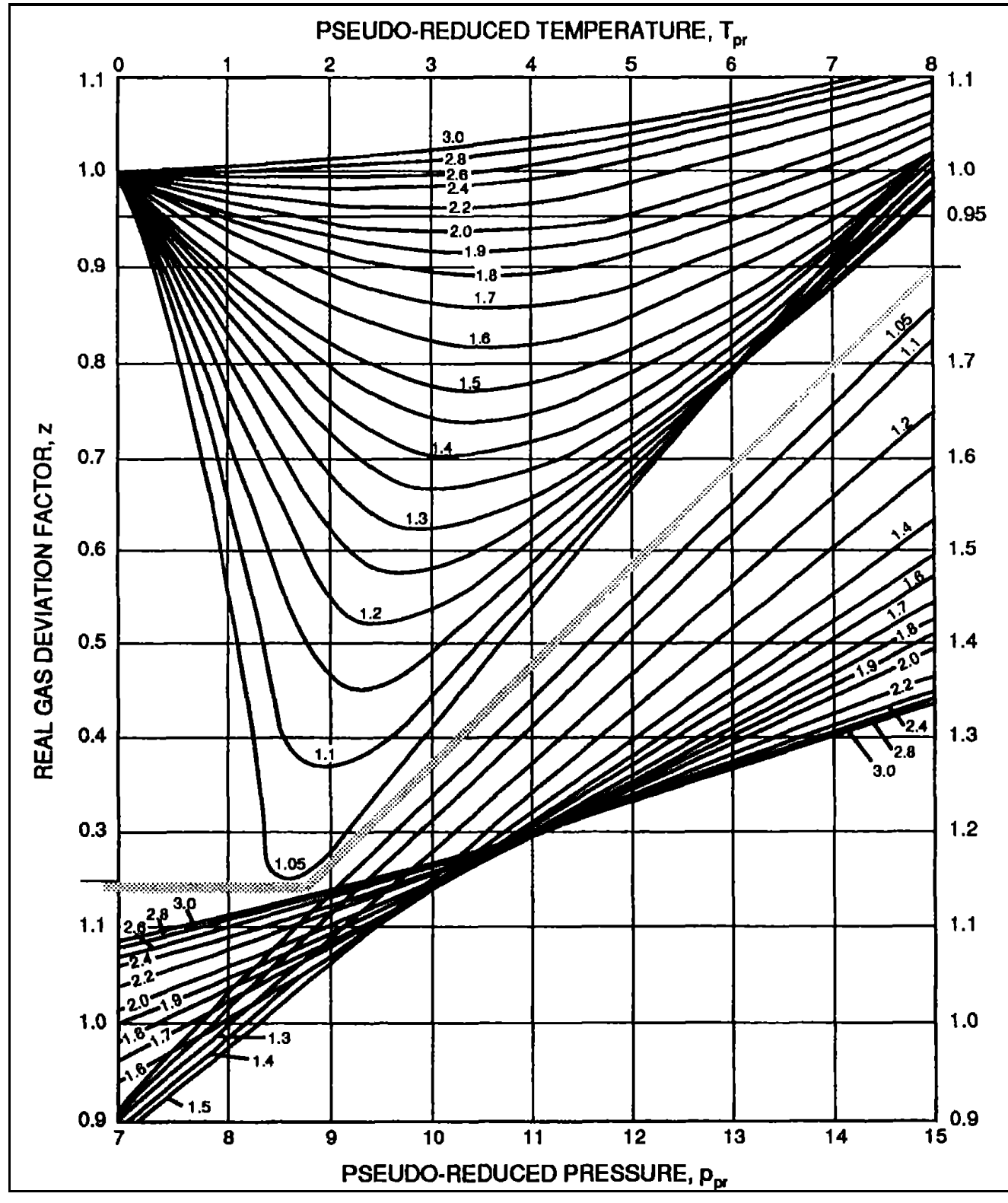
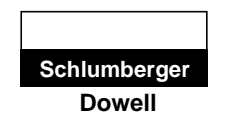


Fig. 74. Real gas deviation factor for natural gases as a function of pseudoreduced pressure and temperature (after Standing and Katz).

Section 200
July 1998
Page 138 of 168

Well Performance



7.7 Gas Viscosity

Carr, Kobayashi, and Burrows presented a correlation for estimating natural gas viscosity as a function of gas gravity, pressure and temperature. This correlation also includes correlations for the presence of nonhydrocarbon gases in the natural hydrocarbon gas. Carr et al. correlated the viscosity of natural gases at one atmospheric pressure with the specific gravity of gas and the temperature of gas (Fig. 75). The viscosity of natural gas at atmospheric pressure is then corrected for pressure using the second correlation (Fig. 76). To use Fig. 76, the pseudo-reduced pressure and pseudo-reduced temperature need to be calculated. This correlation presents the viscosity ratio of the viscosity of gas at the appropriate pressure and temperature to the viscosity of gas at atmospheric pressure and given temperature.

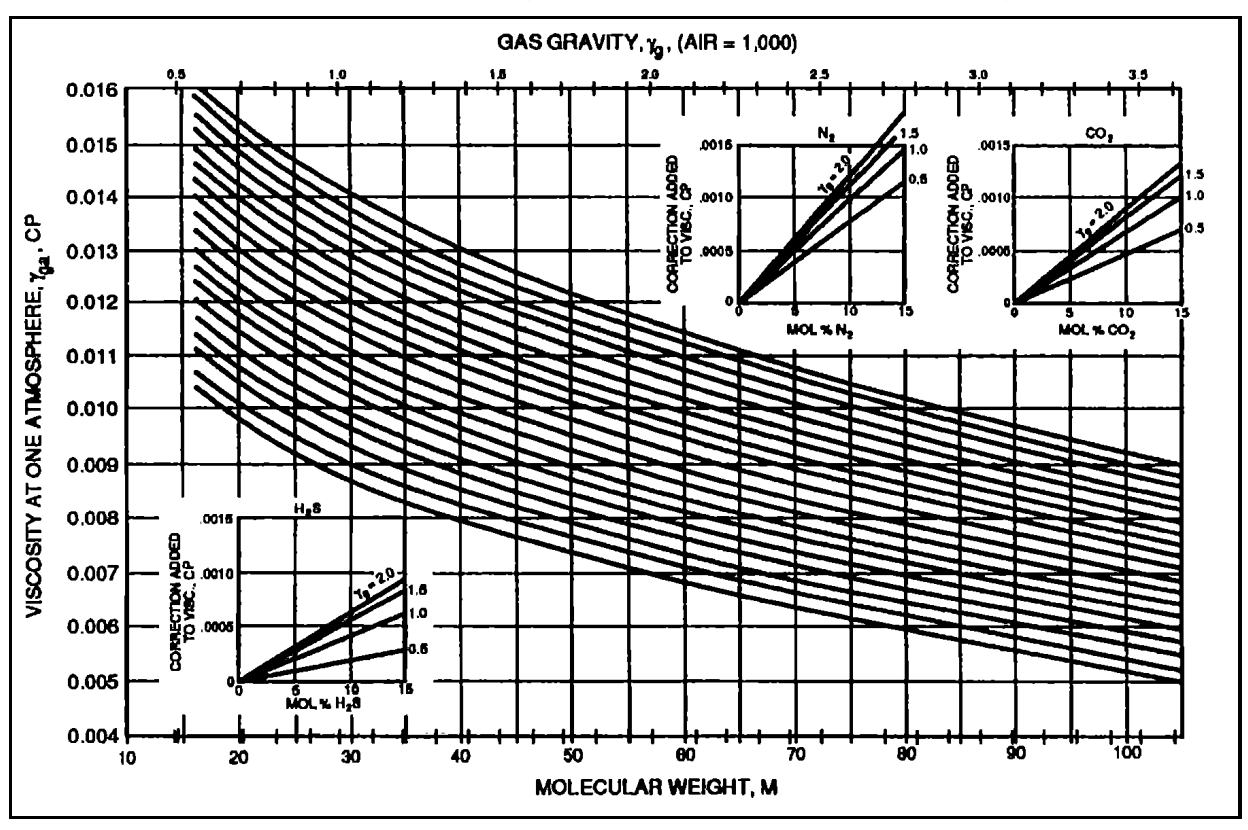
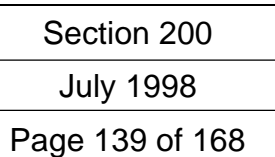


Fig. 75. Viscosity of natural gases at 1 atm (after Carr, Kobayashi, and Burrows).

MATRIX ENGINEERING MANUAL

Well Performance



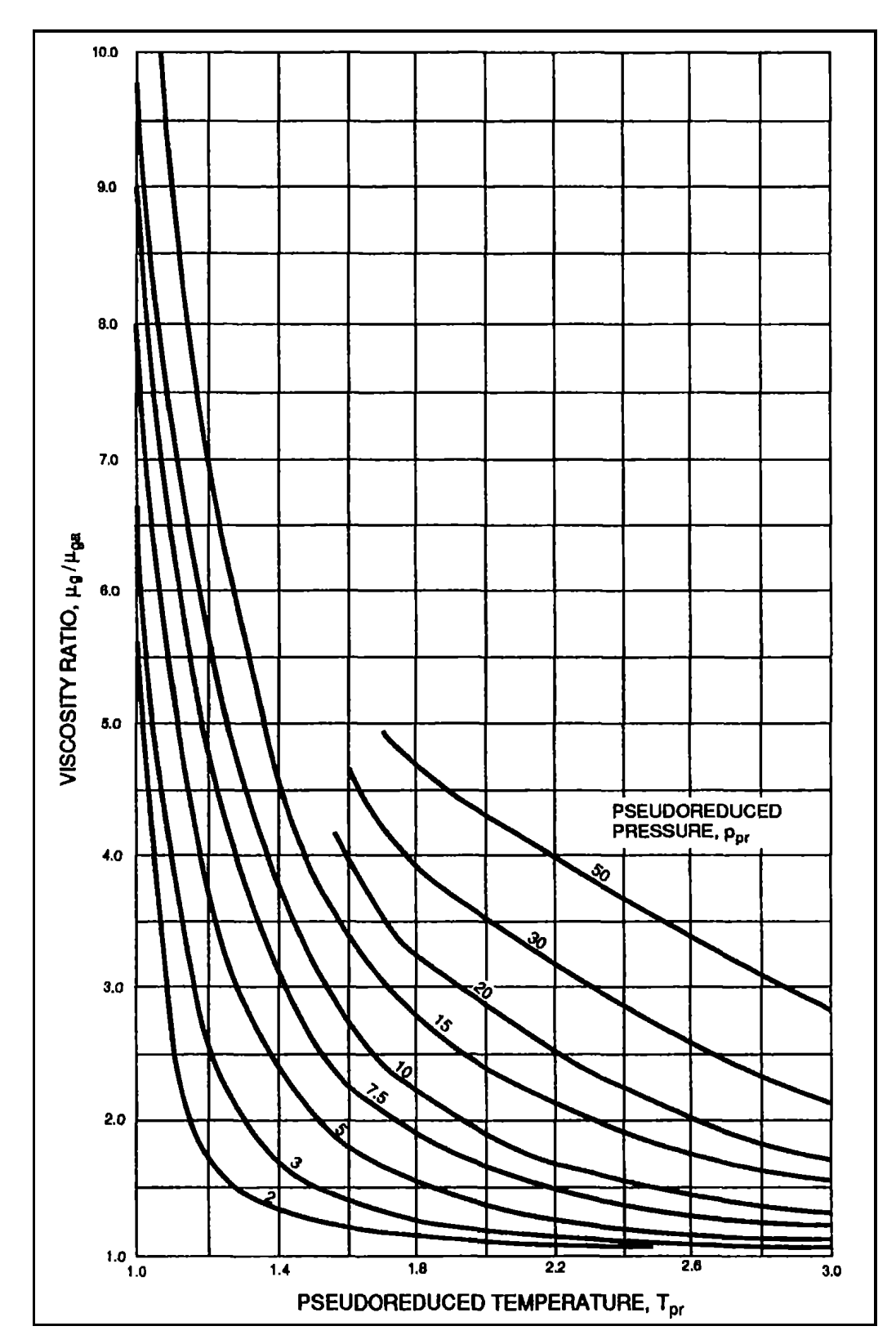


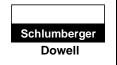
Fig. 76. Effect of temperature and pressure on gas viscosity: μ_{ga} (after Carr, Kobayashi, and Burrows).

July 1998

Page 140 of 168

MATRIX ENGINEERING MANUAL

Well Performance



7.8 Rock and Fluid Compressibility

Compressibility is defined as the change in volume per unit volume for unit change in pressure at constant temperature.

$$c = compressibility = \frac{1}{V} \left(\frac{dV}{dp} \right)_{T}$$

The unit of compressibility is reciprocal of pressure (1/psi).

7.9 Oil Compressibility (c_o)

The isothermal compressibility of an undersaturated oil (above the bubblepoint pressure) can be defined as:

$$c_o = -\frac{1}{V_o} \left(\frac{dV_o}{dp} \right)_T = \frac{1}{\rho_o} \left(\frac{d\rho_o}{dp} \right)_T = -\frac{1}{B_o} \left(\frac{dB_o}{dp} \right)_T$$

Oil compressibility is always positive as the volume of an undersaturated liquid decreases as the pressure increases. Oil compressibility can be determined from laboratory experiments. In the absence of laboratory data, oil compressibility can also be determined from the Trube correlation (Fig. 77). Trube correlated pseudo-reduced compressibility (c_{pr}) with the pseudo-reduced pressure (p_{pr}) and pseudo-reduced temperature (T_{pr}). The oil compressibility can then be estimated from:

$$c_o = \frac{c_{pr}}{p_{pc}}$$

where,

 p_{pc} = pseudo-critical pressure estimated from Fig. 78,

 T_{pc} = pseudo-critical temperature estimated from Fig. 78.

The apparent compressibility of oil (c_{oa}) below the bubblepoint pressure can be calculated taking into account the gas in solution by:

$$c_{oa} = c_o + \frac{R_s}{(0.83p + 21.75)} \times \frac{B_g}{B_o}$$

For an isothermal condition, the compressibility of oilfield water can be defined as:

$$C_w = -\frac{1}{B_w} \left(\frac{dB_w}{dp}\right)_T$$

where,

 B_{w} = formation volume factor of water.

Dodson and Standing presented a correlation for estimating the compressibility of water (Fig. 79). Since the gas solubility in water is low, the effect of gas solubility is ignored in this manual section.

MATRIX ENGINEERING MANUAL

Well Performance

Section 200

July 1998

Page 141 of 168

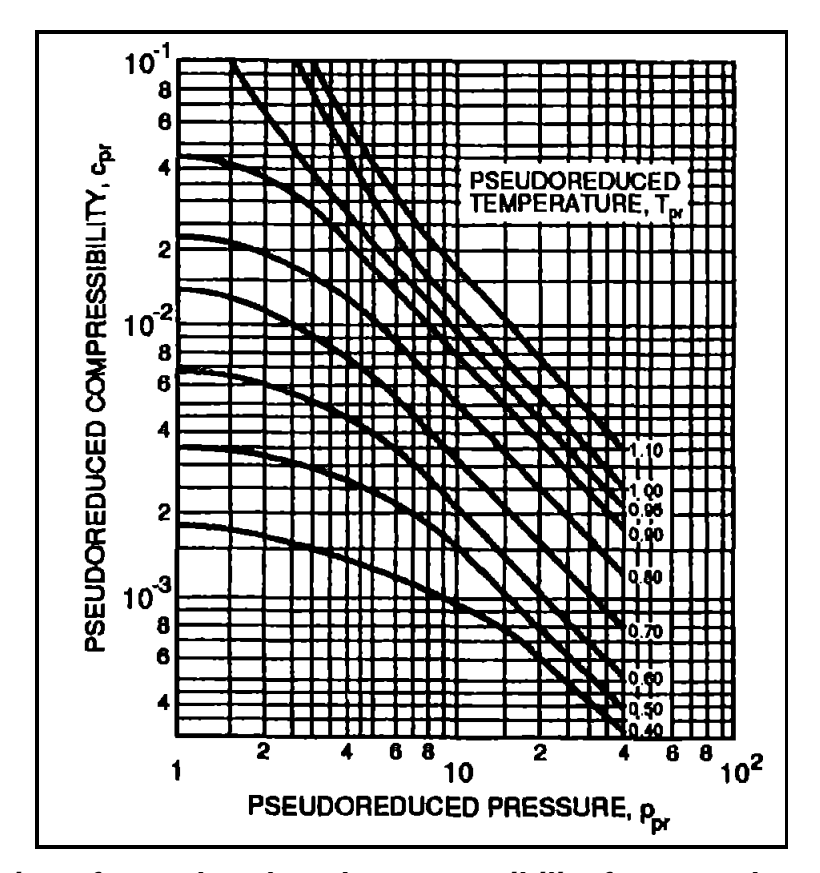


Fig. 77. Correlation of pseudoreduced compressibility for an undersaturated oil (after Trube).

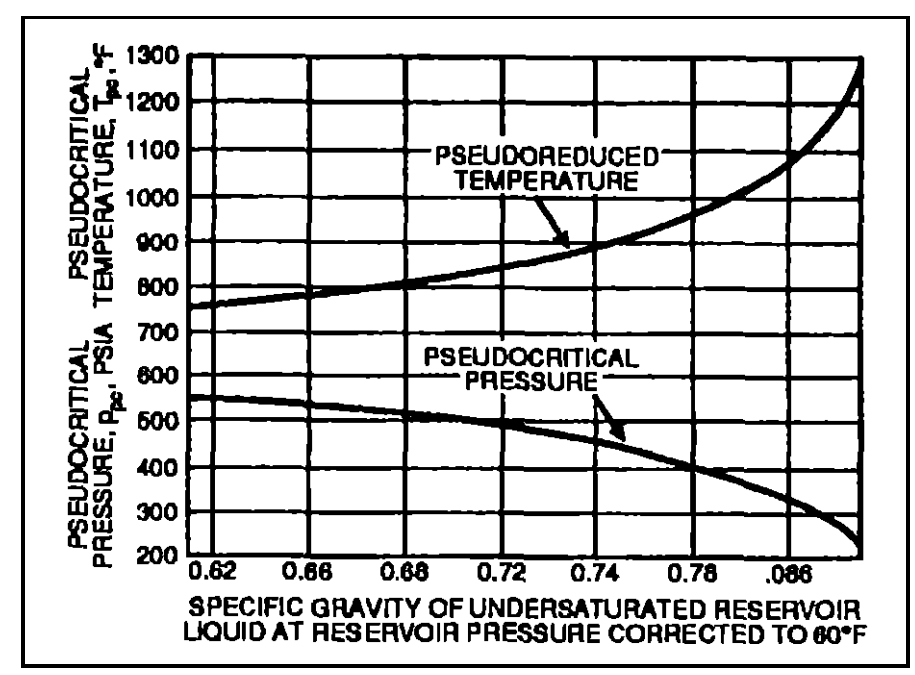
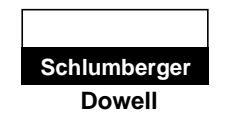


Fig. 78. Approximate correlation of liquid pseudocritical pressure and temperature with specific gravity (after Trube).

Section 200
July 1998
Page 142 of 168

Well Performance



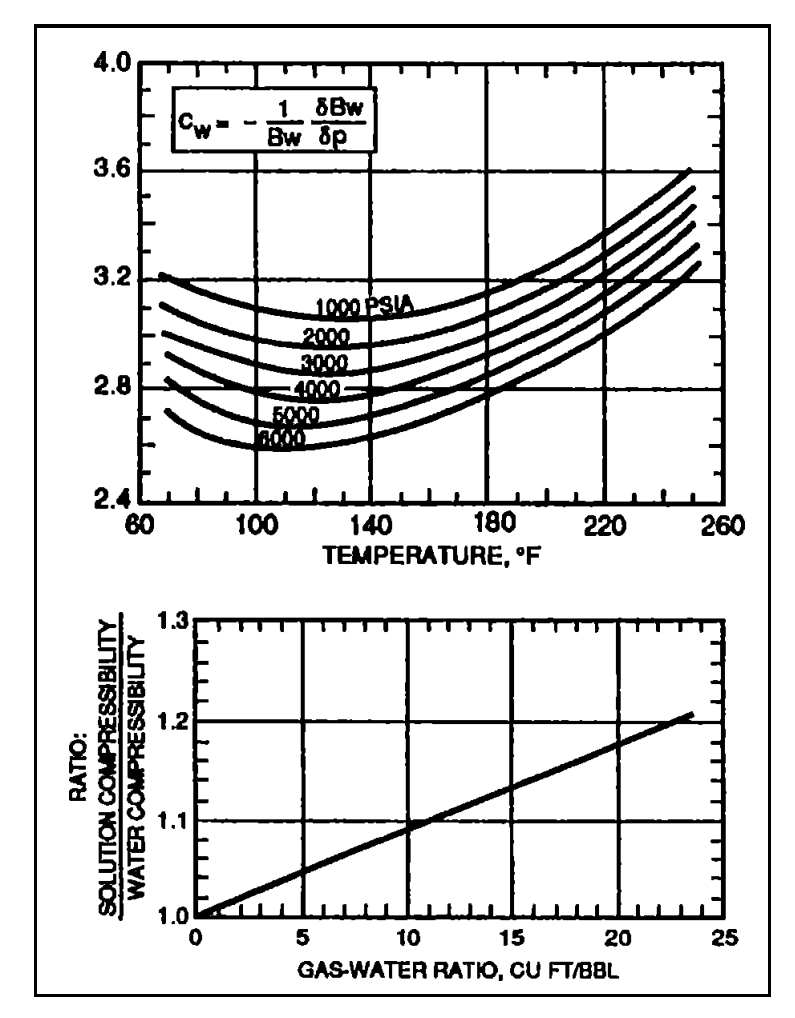


Fig. 79. Effect of dissolved gas on water compressibility (after Dodson and Standing).

7.10 Gas Compressibility

Gas compressibility under isothermal conditions can be defined as:

$$c_g = \frac{1}{p} - \frac{1}{Z} \left(\frac{dZ}{dP} \right)_T$$

where,

Z = gas deviation factor at absolute pressure p in psia and absolute temperature T in ${}^{\circ}R$.

Trube presented a correlation for the estimation of gas compressibility. Trube defined gas compressibility as the ratio of pseudo-critical compressibility to the pseudo-critical pressure as:

$$c_g = \frac{c_{pr}}{p_{pc}}$$

MATRIX ENGINEERING MANUAL

Well Performance

Section 200
July 1998
Page 143 of 168

To estimate the gas compressibility, Trube presented correlations to estimate the c_{pr} function of pseudo-reduced pressure and pseudo-reduced temperature (Fig. 80 and Fig. 81). Note that these two correlations are similar. They present pseudo-reduced compressibility at two different ranges of compressibility values.

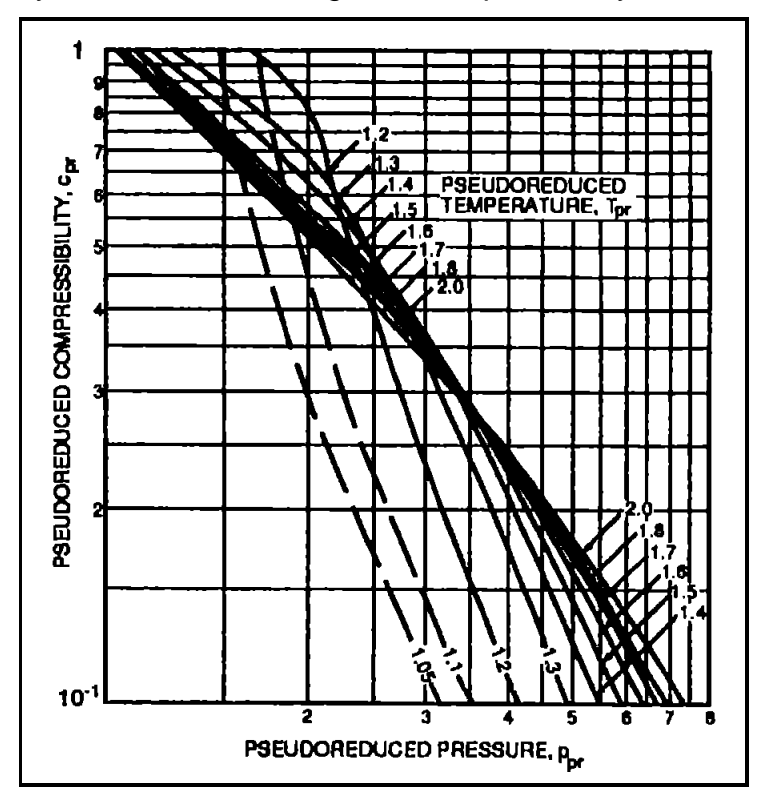


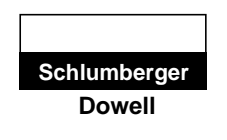
Fig. 80. Correlation of pseudoreduced compressibility for natural gases (after Trube).

Section 200	
July 1998	

Page 144 of 168

MATRIX ENGINEERING MANUAL

Well Performance



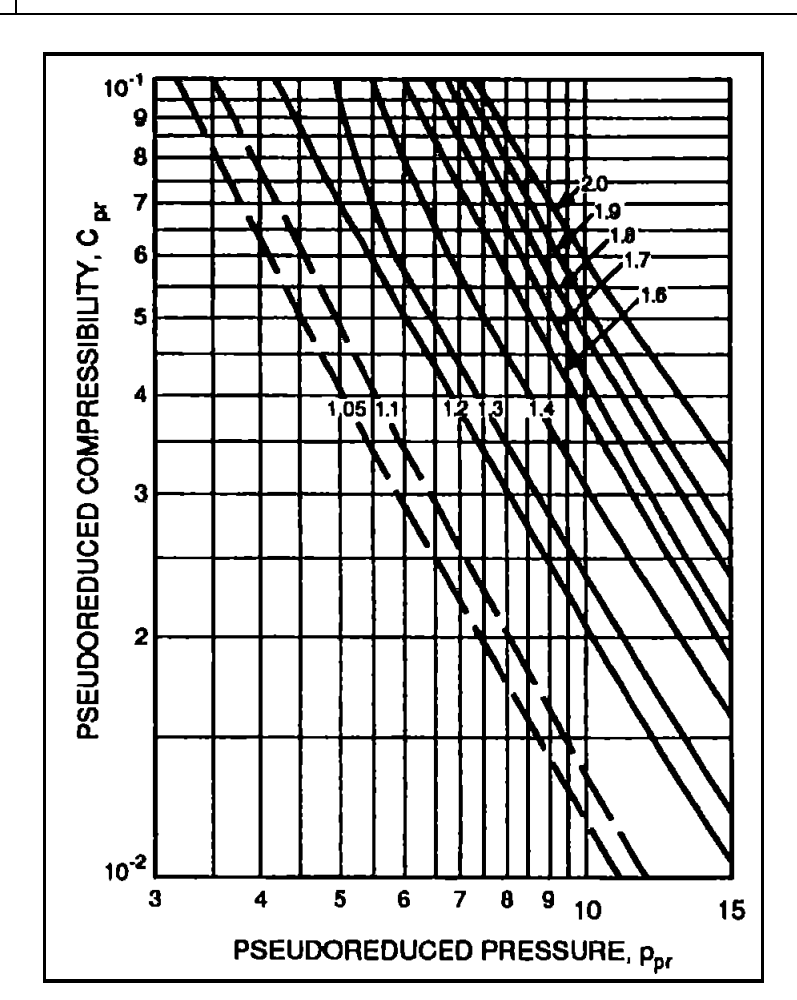


Fig. 81. Correlation of pseudoreduced compressibility for natural gases (after Trube).

7.11 Rock Pore Volume Compressibility

Rock compressibility under isothermal conditions can be defined as:

$$c_f = \frac{1}{V_p} \left(\frac{dV_p}{d_p} \right)_T$$

There are different correlations for rock compressibility, each for a fixed type of rock. Fig. 82 shows the rock compressibility correlation after Newman. It is strongly recommended to use laboratory data for this parameter wherever possible. From Fig. 82, it is clear that these correlations are questionable at best. However, for any well performance calculations, rock compressibility forms a minor component of the total compressibility (c_i) defined as:

$$c_t = C_o S_o + c_w S_w + c_g S_g + c_f$$

where,

S = saturation of fluid where subscript o is used for oil, g for gas and w for water.



MATRIX ENGINEERING MANUAL

Well Performance

Section 200	
July 1998	
Page 145 of 168	

$$S_o + S_w + S_g = 1$$

Gas compressibility is an order of magnitude higher than the rock or liquid compressibility. In gas reservoirs, it is often assumed that:

$$c_t \approx c_g$$

It may also be noted that whereas the gas compressibility is in the order of 10⁻⁴, the liquid or rock compressibilities are typically in the order of 10⁻⁵ or 10⁻⁶.

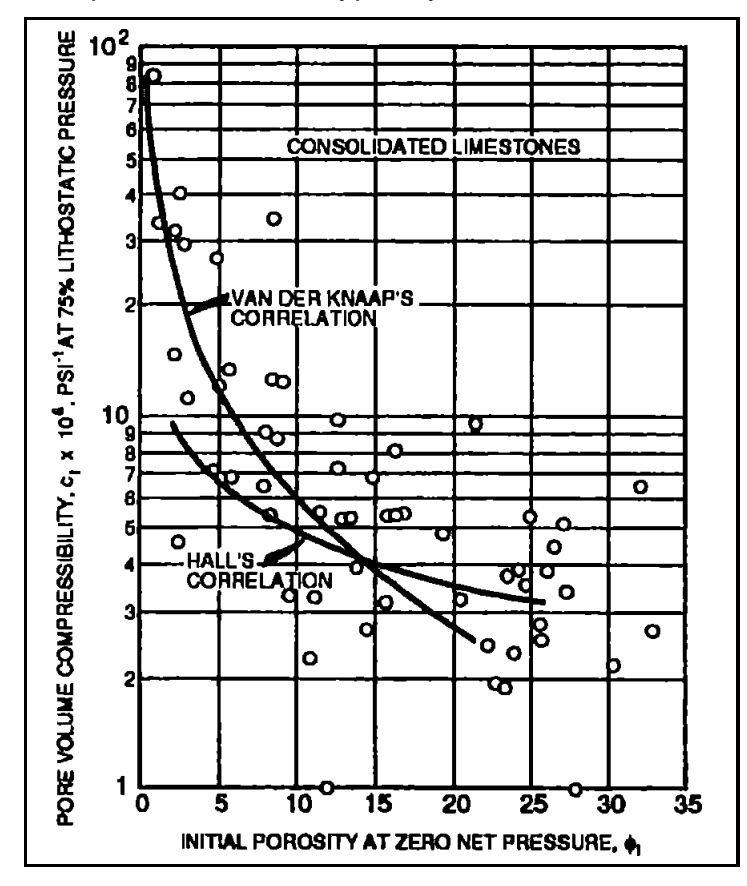
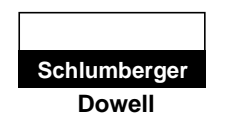


Fig. 82. Pore-volume compressibility at 75% lithostatic pressure versus initial sample porosity for limestones (after Newman).

Section 200
July 1998
Page 146 of 168

MATRIX ENGINEERING MANUAL



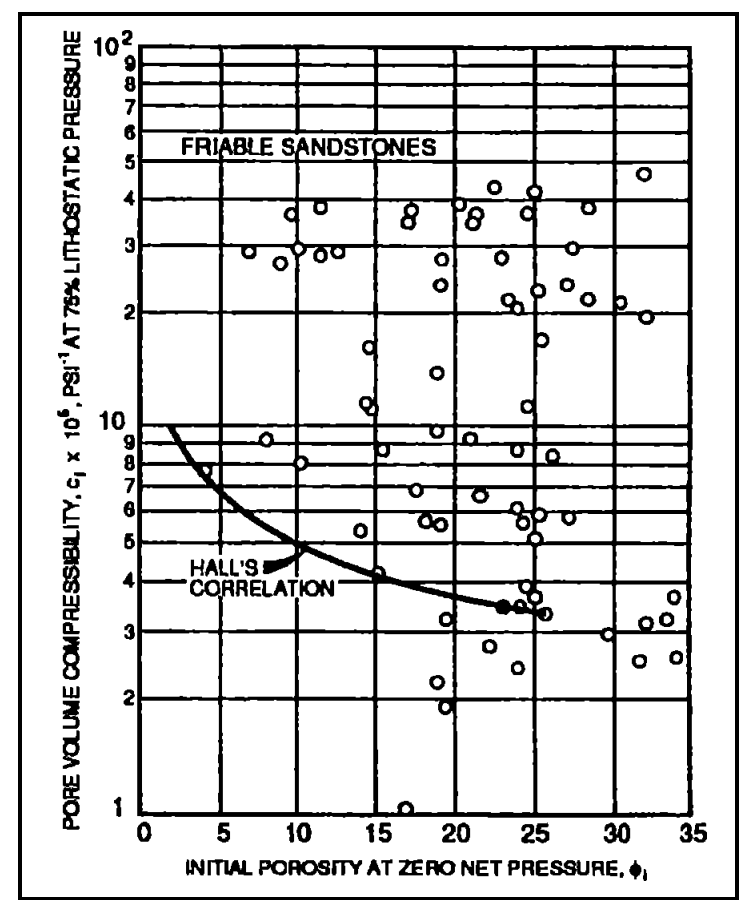


Fig. 83. Pore-volume compressibility at 75% lithostatic pressure versus initial sample porosity for fiable sandstones (after Newman).

MATRIX ENGINEERING MANUAL

Well Performance

Section 200

July 1998

Page 147 of 168

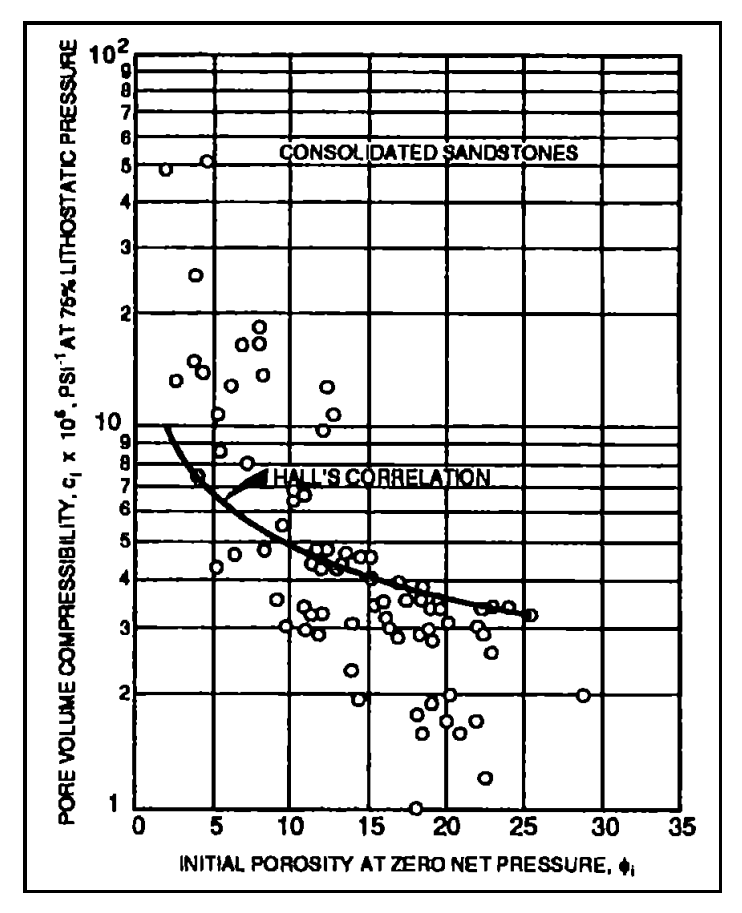


Fig. 84. Pore-volume compressibility at 75% lithostatic pressure versus initial sample porosity for consolidated sandstones (after Newman).

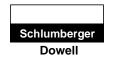
Section 200

July 1998

Page 148 of 168

MATRIX ENGINEERING MANUAL

Well Performance



8 Vertical Flowing Pressure Gradient Curves

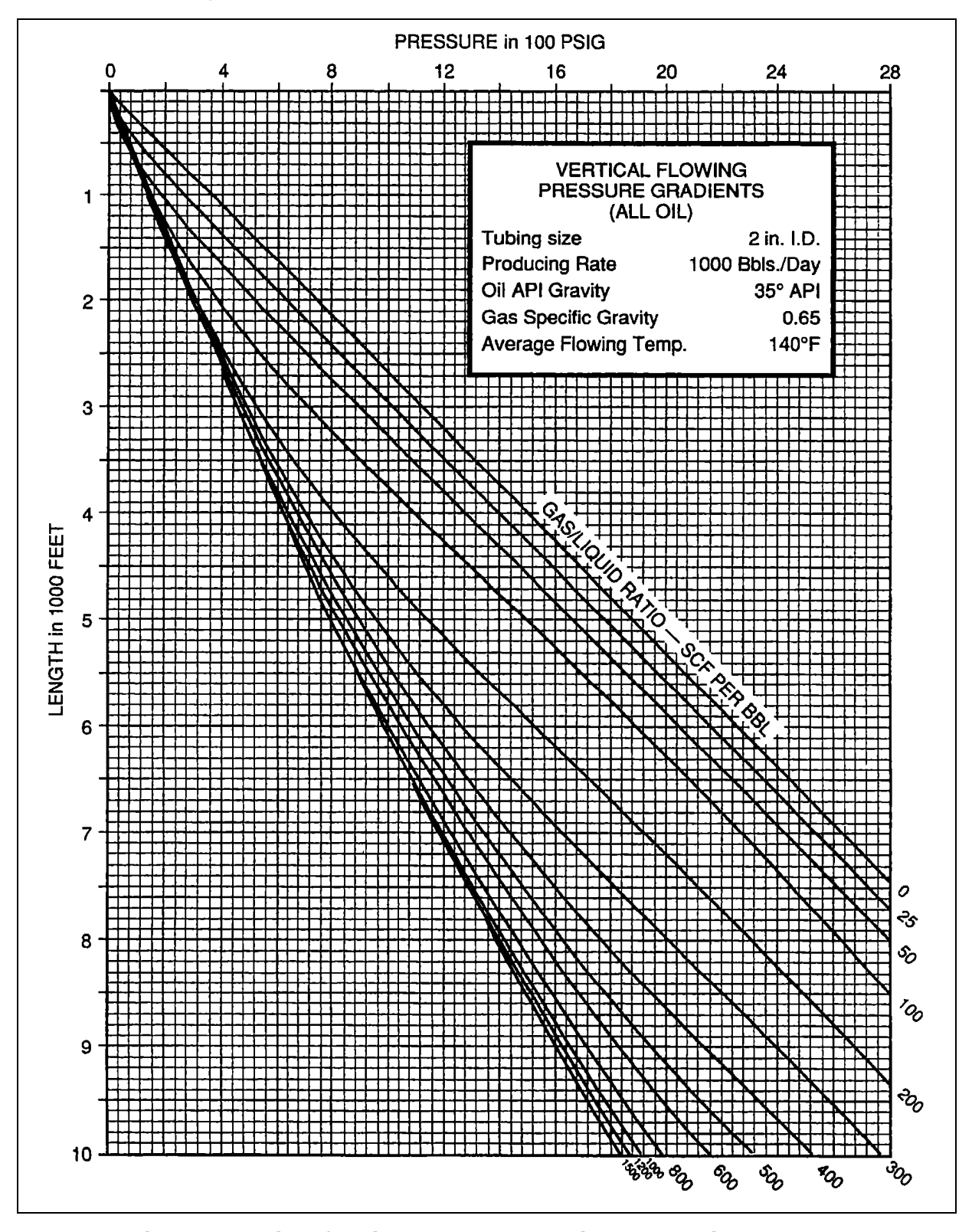


Fig. 85. Vertical flowing pressure gradients. All oil - 1000 BPD.

MATRIX ENGINEERING MANUAL

Well Performance

Section 200 July 1998

Page 149 of 168

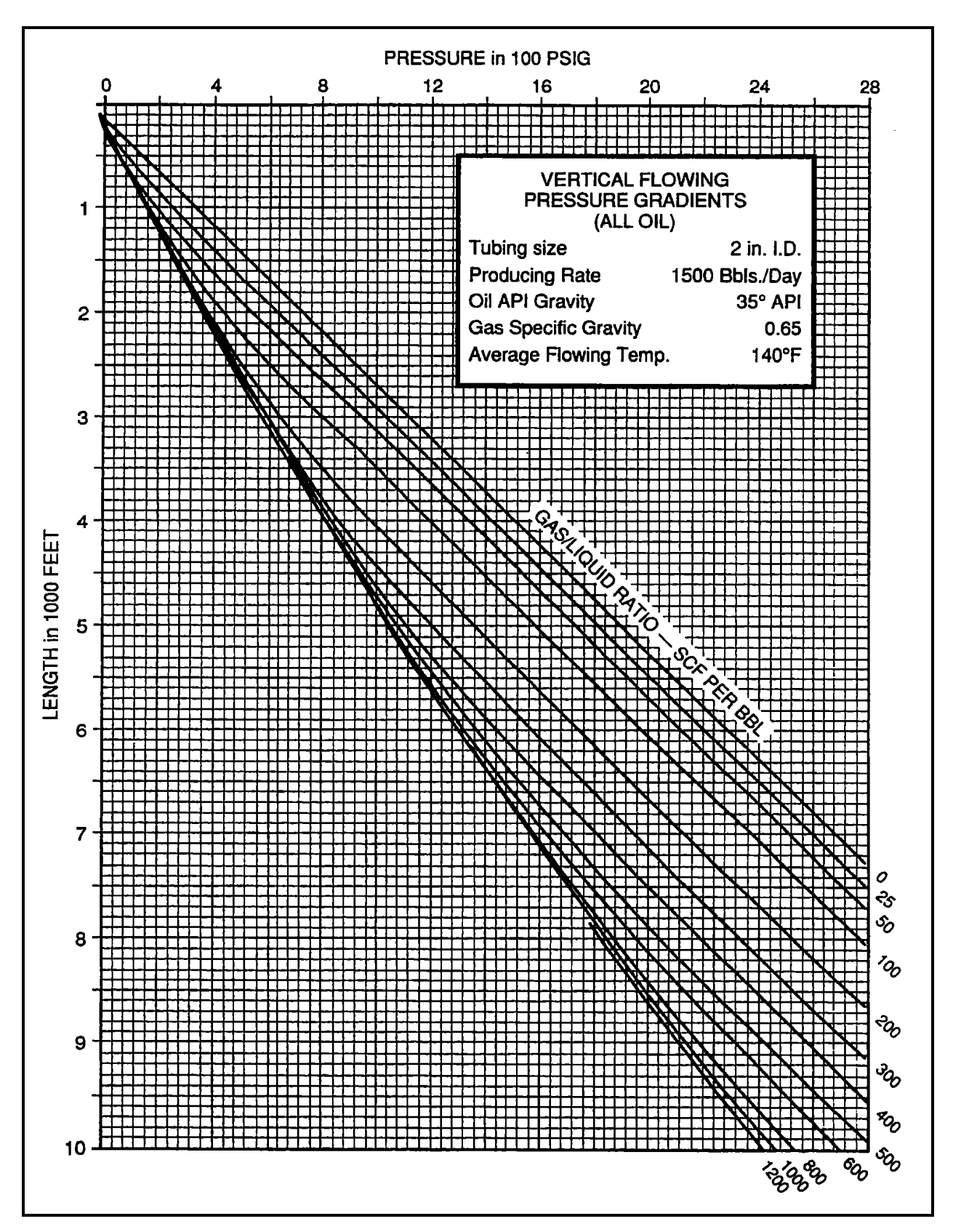


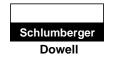
Fig. 86. Vertical flowing pressure gradients. All oil - 1500 BPD.

Section 200

July 1998

Page 150 of 168

MATRIX ENGINEERING MANUAL



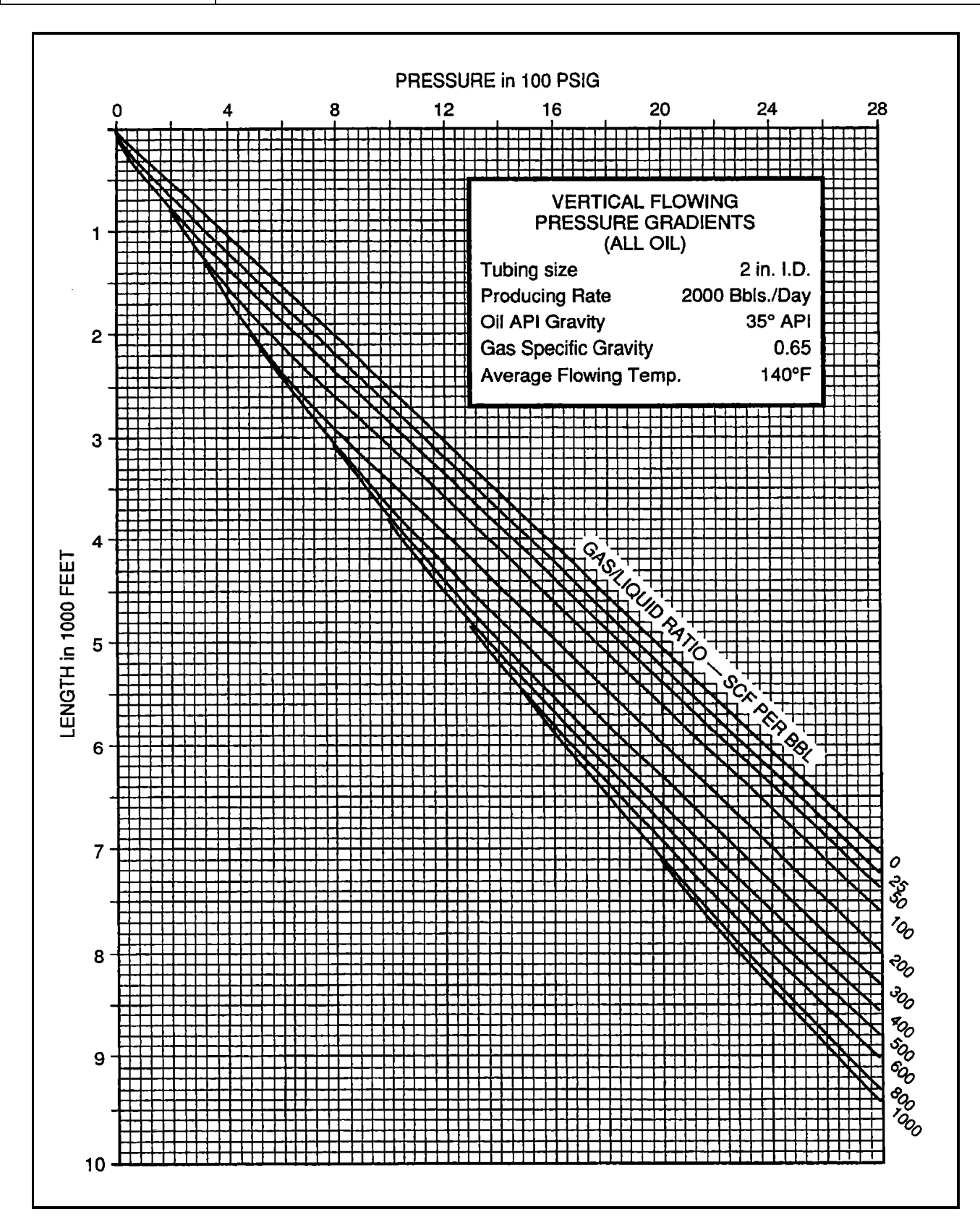


Fig. 87. Vertical flowing pressure gradients. All oil - 2000 BPD.

MATRIX ENGINEERING MANUAL

Well Performance

Section 200

July 1998

Page 151 of 168

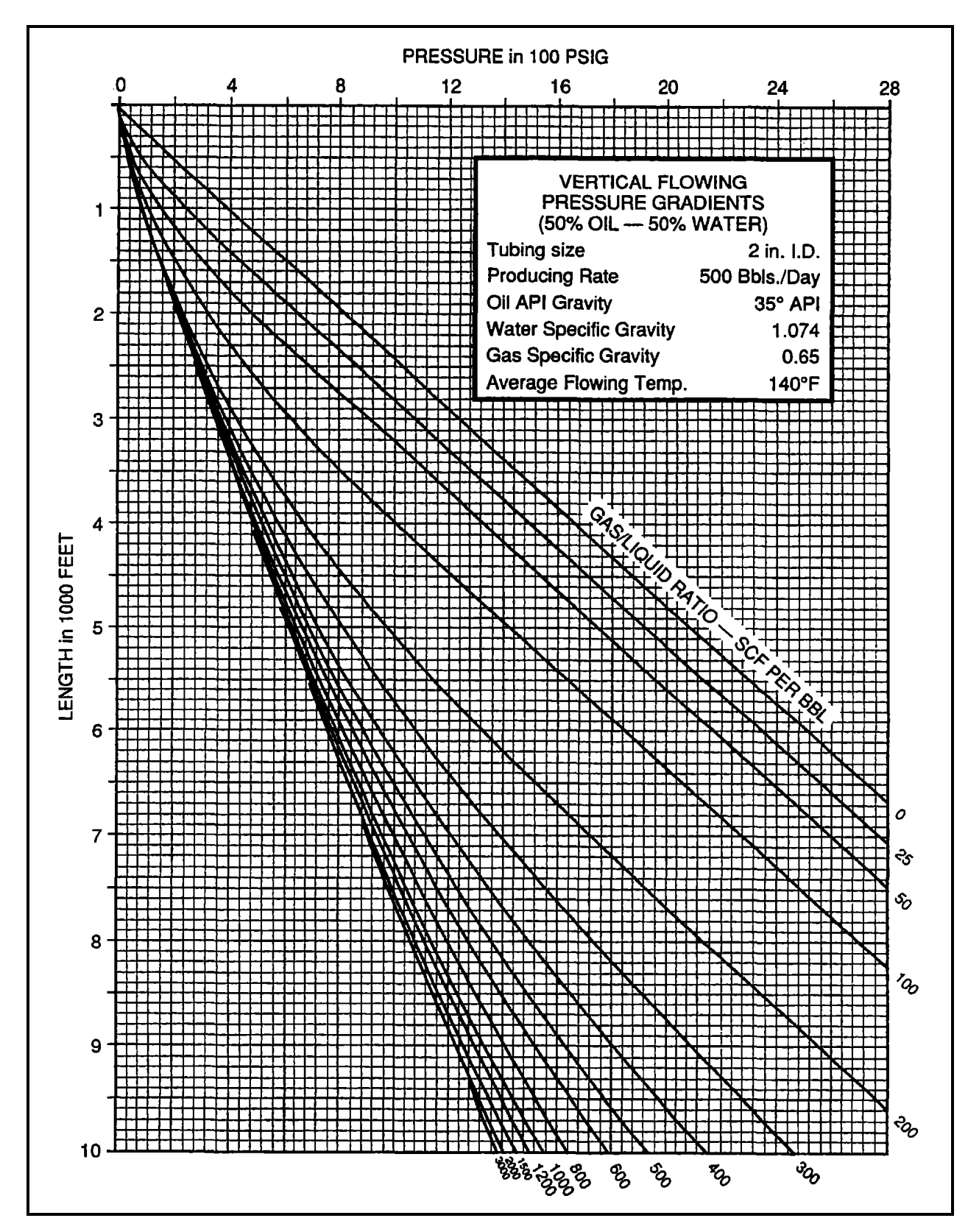
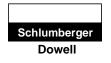


Fig. 88. Vertical Flowing pressure gradients. 50% oil - 50% water - 500 BPD.

MATRIX ENGINEERING MANUAL



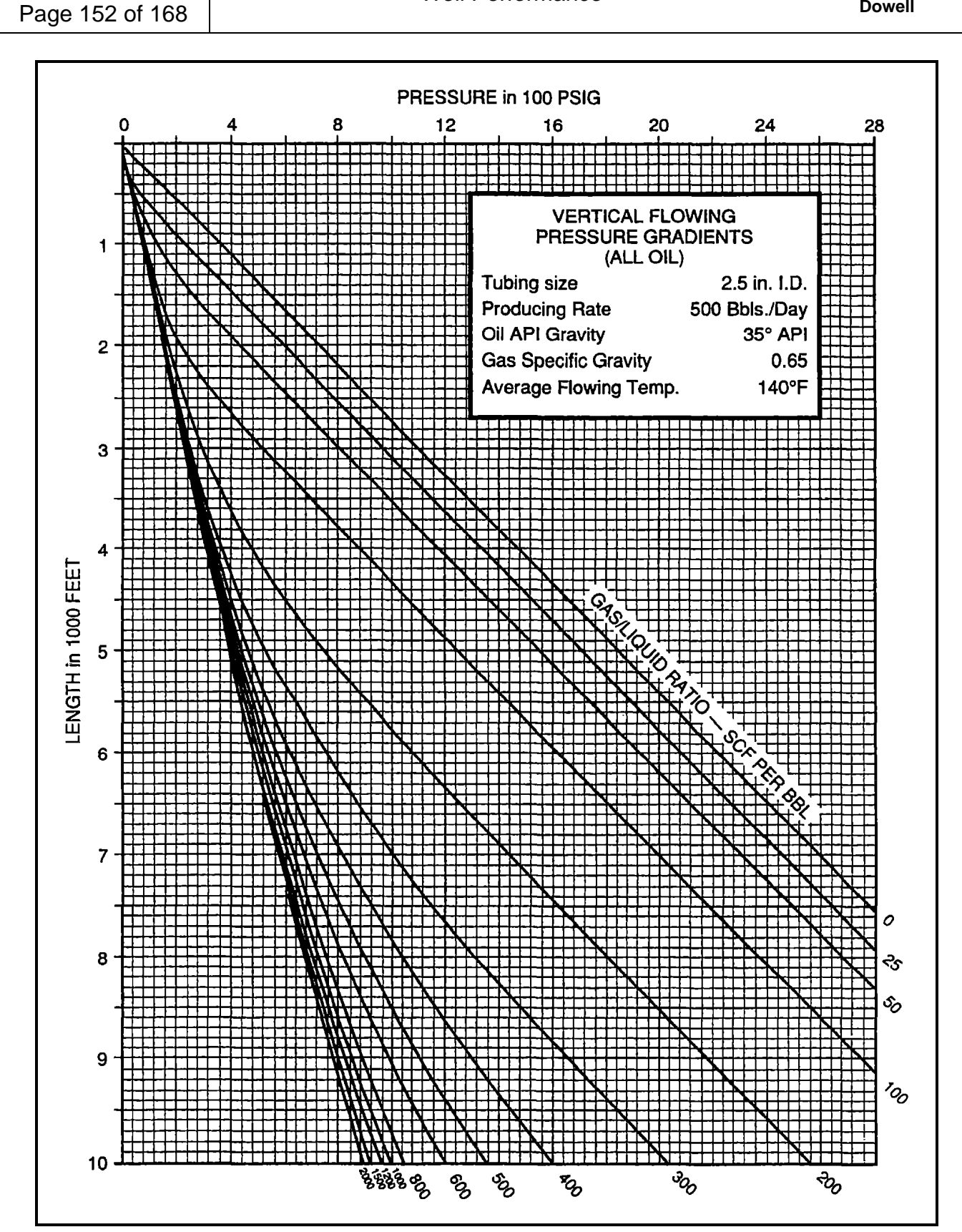


Fig. 89. Vertical fowing presssure gradients. All oil - 500 BPD.

MATRIX ENGINEERING MANUAL

Well Performance

Section 200

July 1998

Page 153 of 168

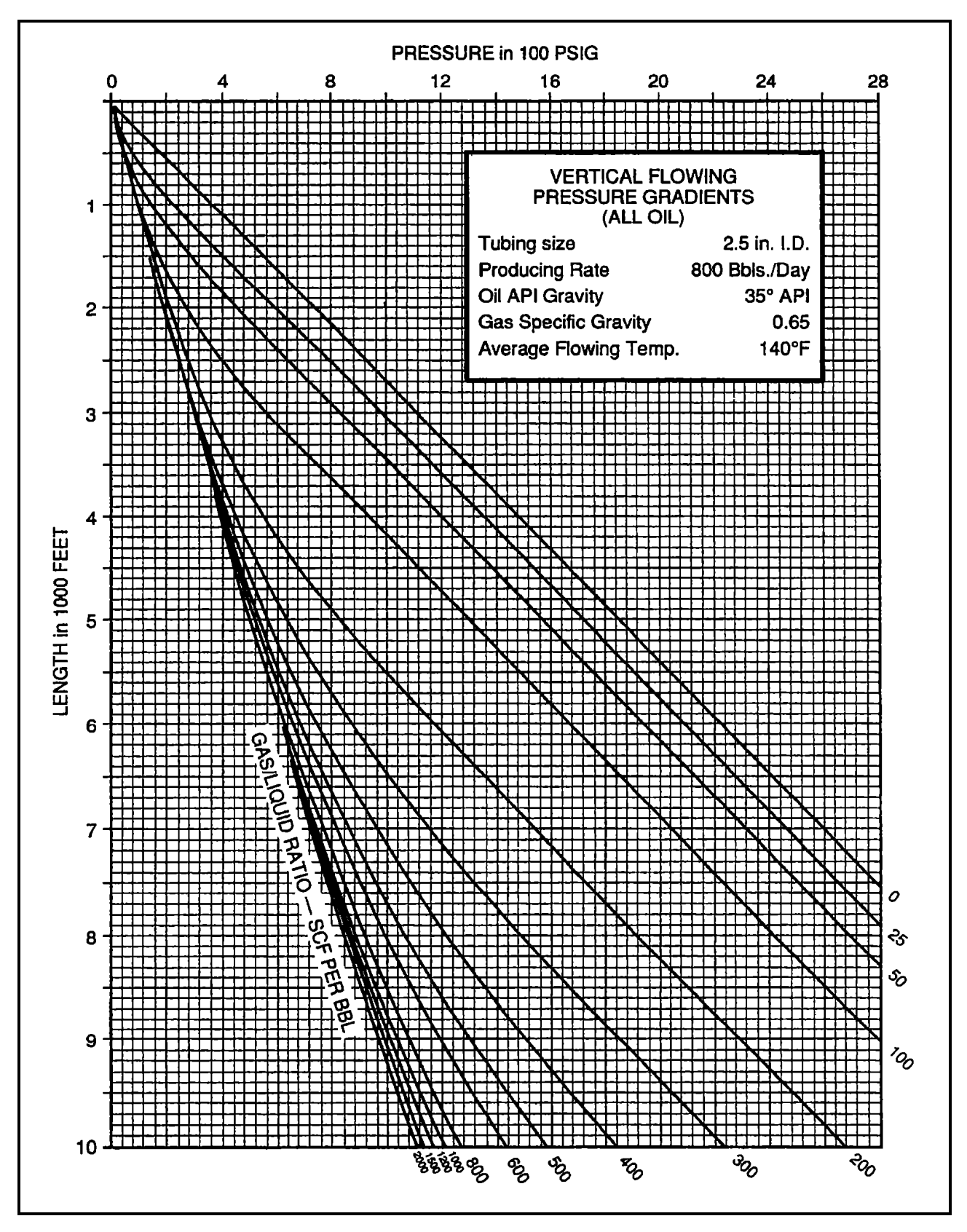
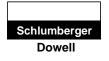


Fig. 90. Vertical flowing pressure gradients. All oil - 800 BPD.

Page 154 of 168

MATRIX ENGINEERING MANUAL



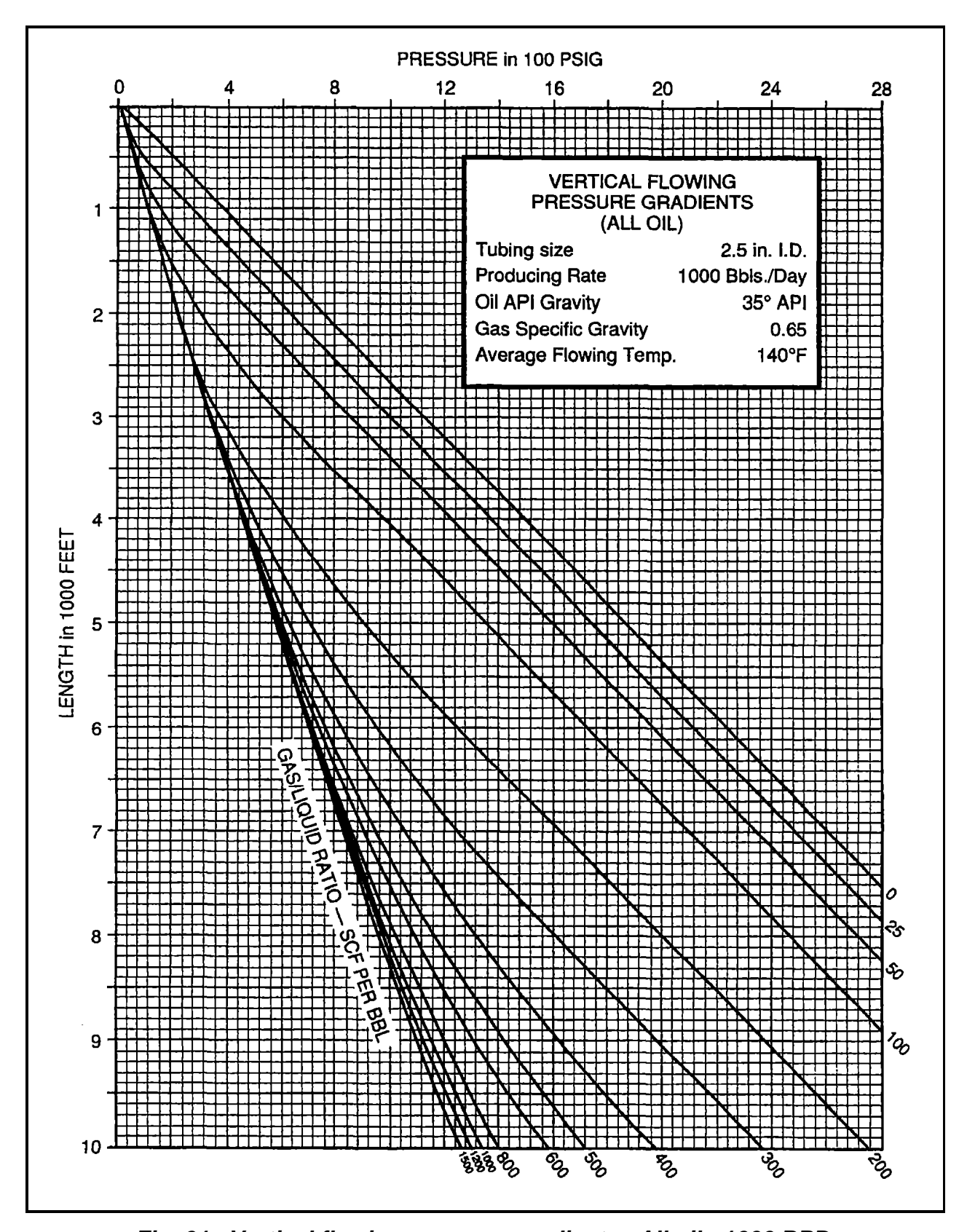


Fig. 91. Vertical flowing pressure gradients. All oil - 1000 BPD.

MATRIX ENGINEERING MANUAL

Well Performance

Section 200

July 1998

Page 155 of 168

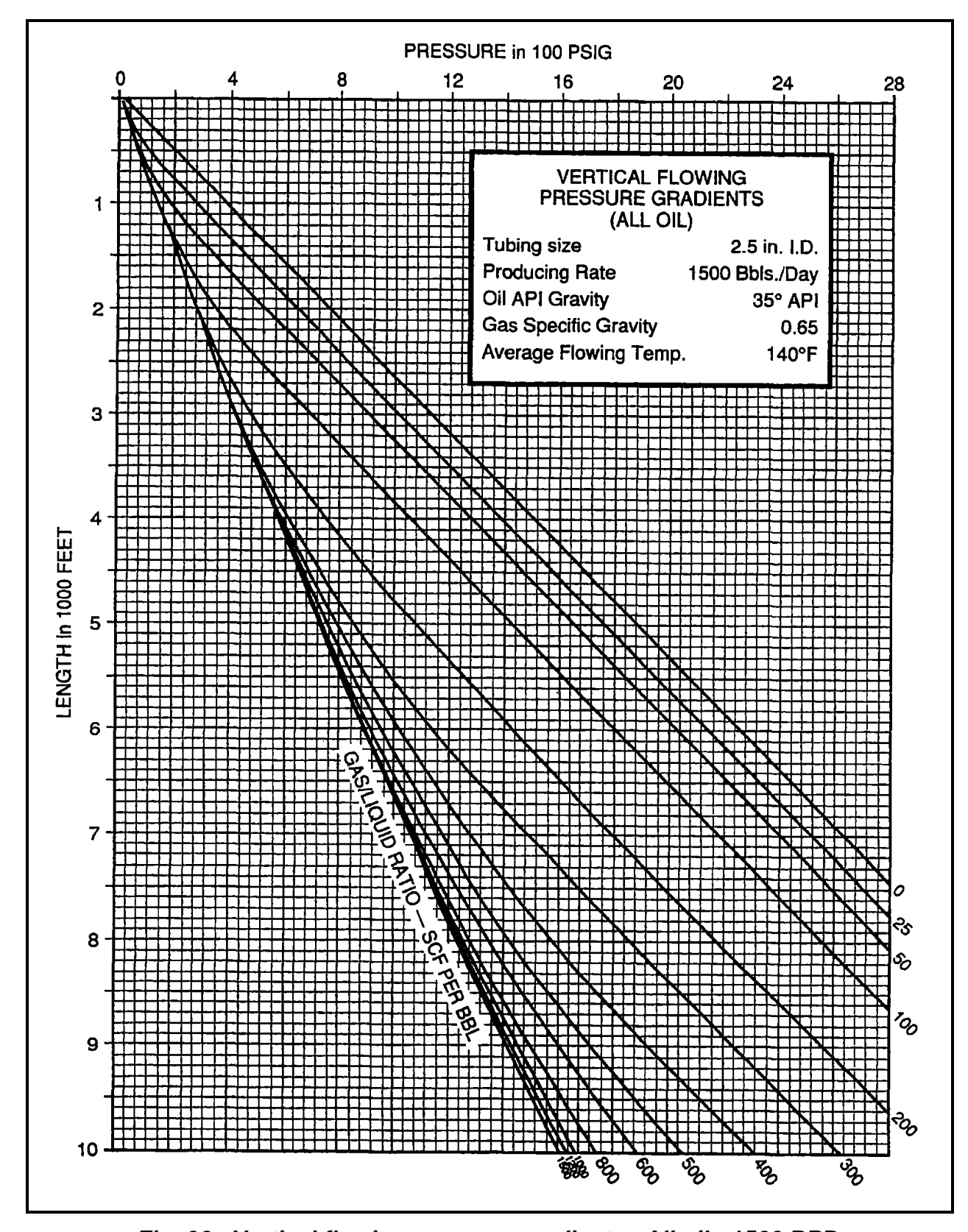


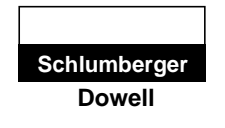
Fig. 92. Vertical flowing pressure gradients. All oil - 1500 BPD.

Section 200

July 1998

Page 156 of 168

MATRIX ENGINEERING MANUAL



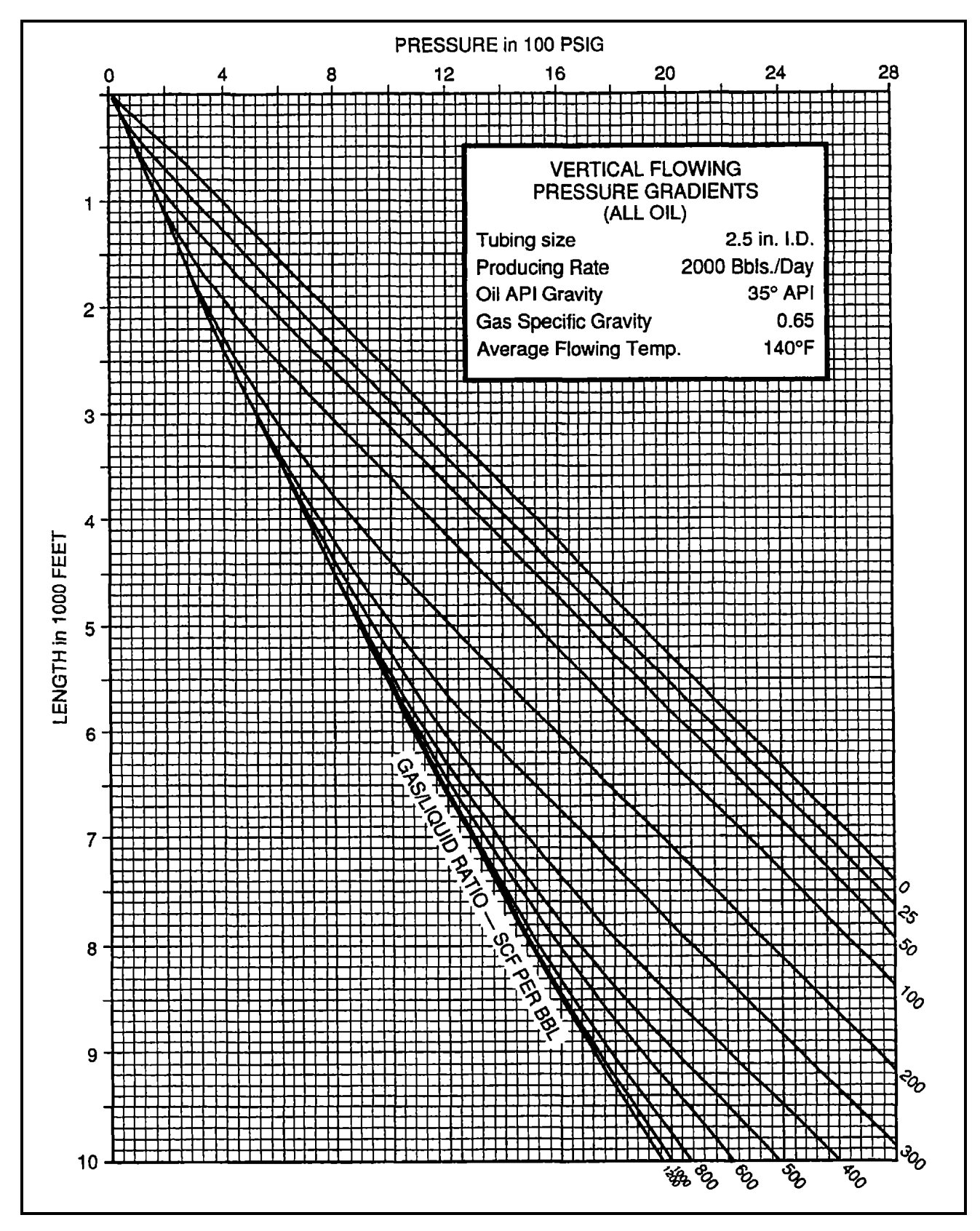


Fig. 93. Vertical flowing pressure gradients. All oil - 2000 BPD.

MATRIX ENGINEERING MANUAL

Well Performance

Section 200

July 1998

Page 157 of 168

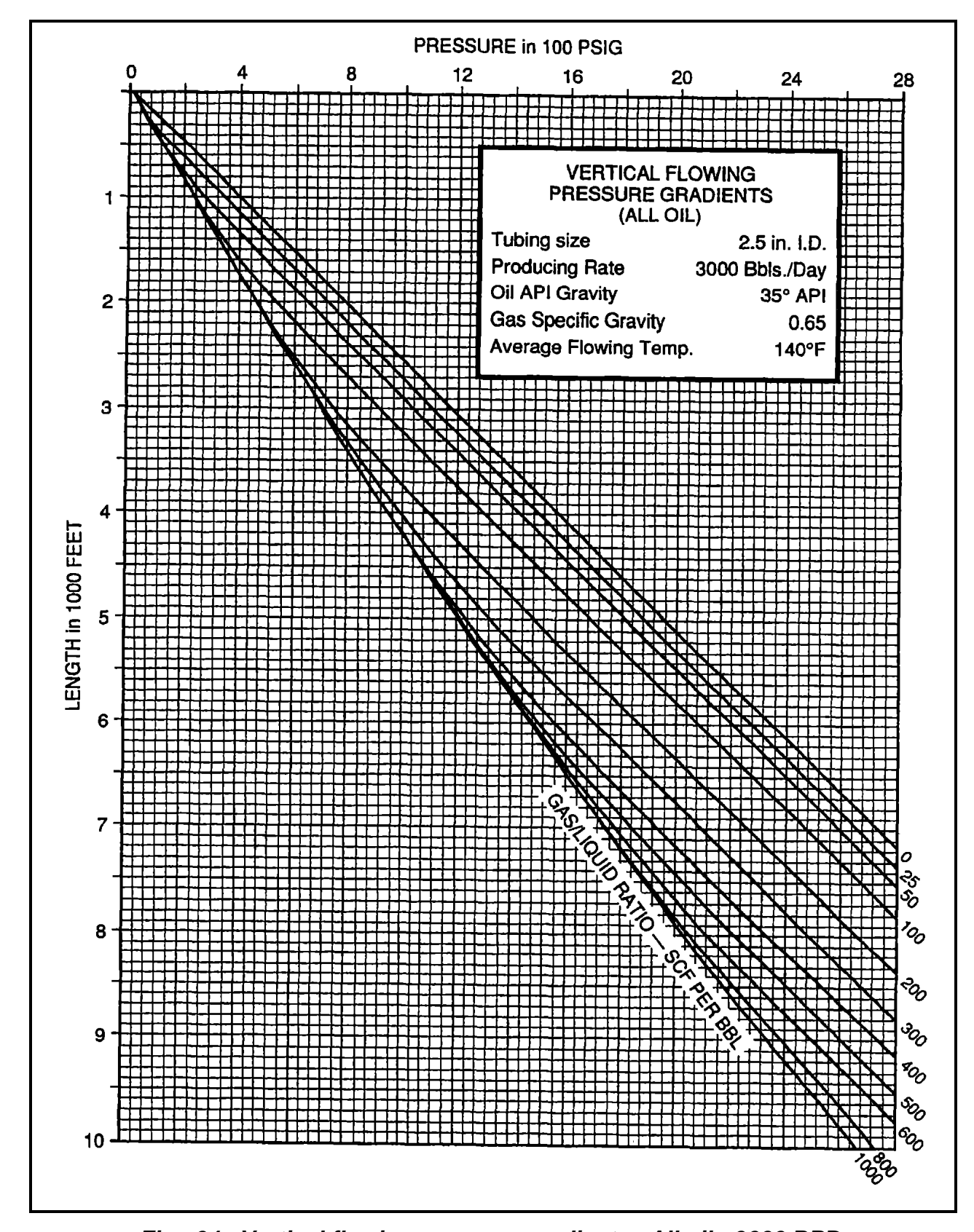
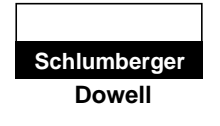


Fig. 94. Vertical flowing pressure gradients. All oil - 3000 BPD.

Page 158 of 168

MATRIX ENGINEERING MANUAL



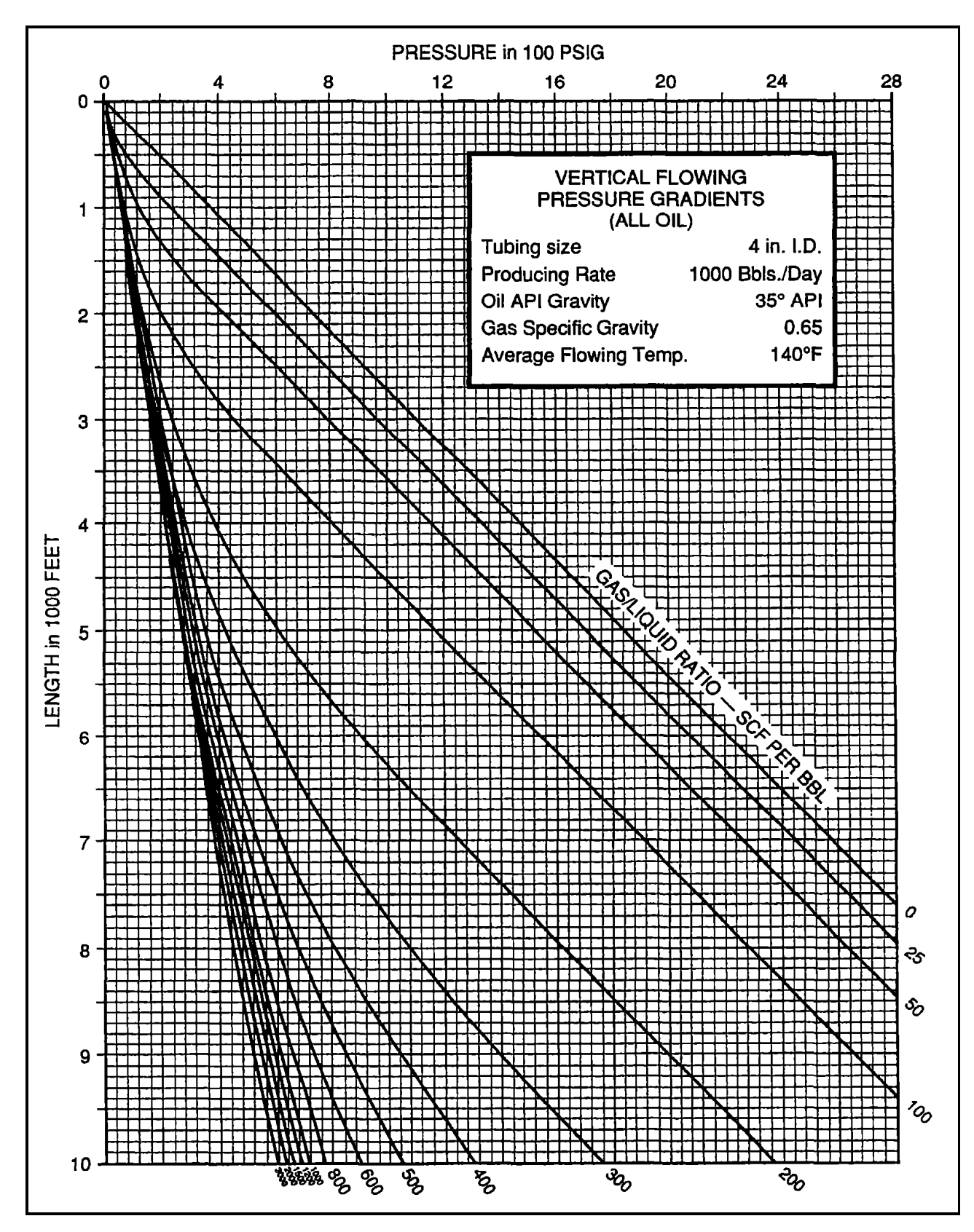


Fig. 95. Vertical flowing pressure gradients. All oil - 1000 BPD.

MATRIX ENGINEERING MANUAL

Well Performance

Section 200 July 1998

Page 159 of 168

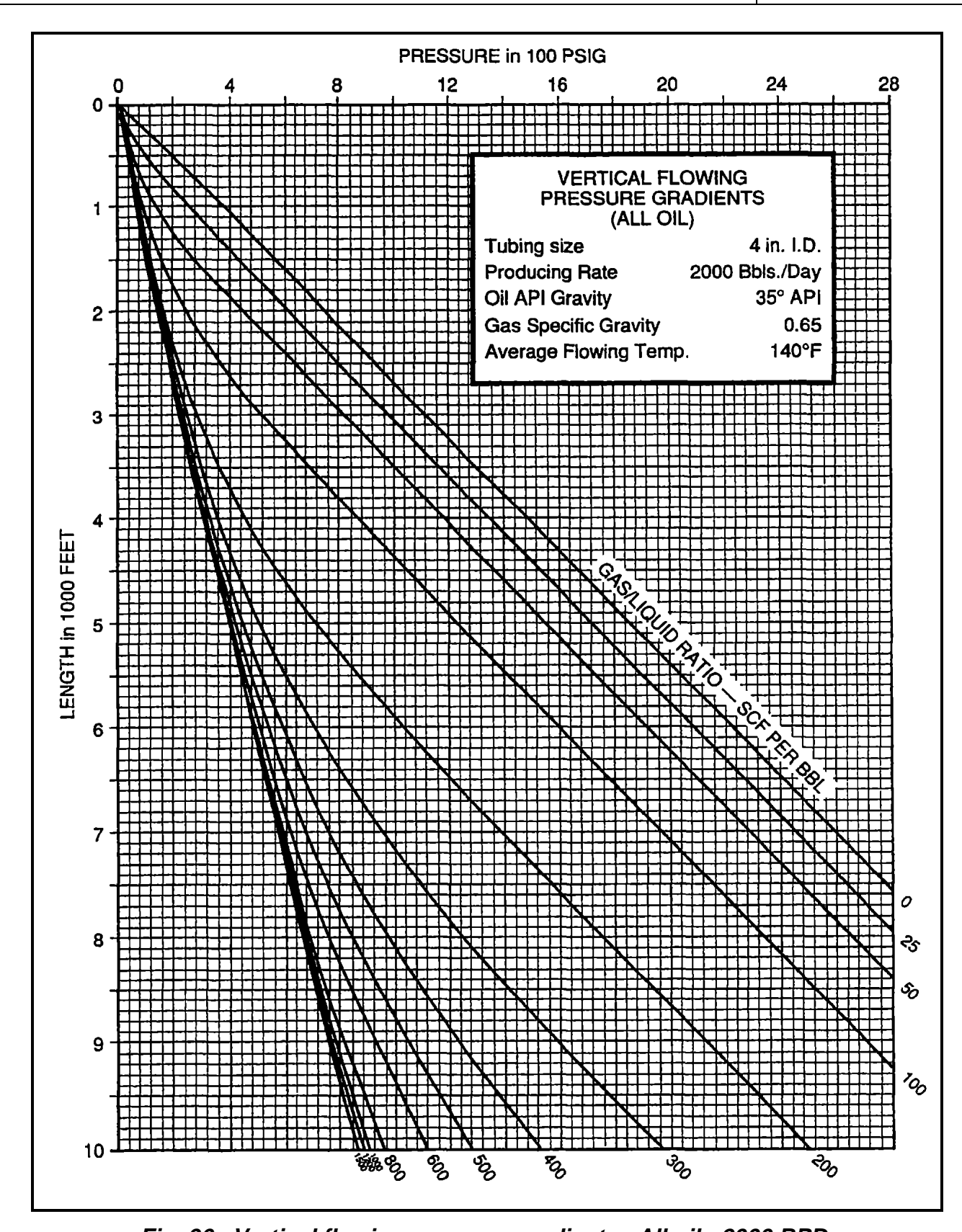
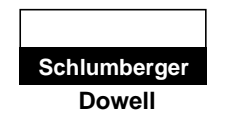


Fig. 96. Vertical flowing pressure gradients. All oil - 2000 BPD.

Page 160 of 168

MATRIX ENGINEERING MANUAL



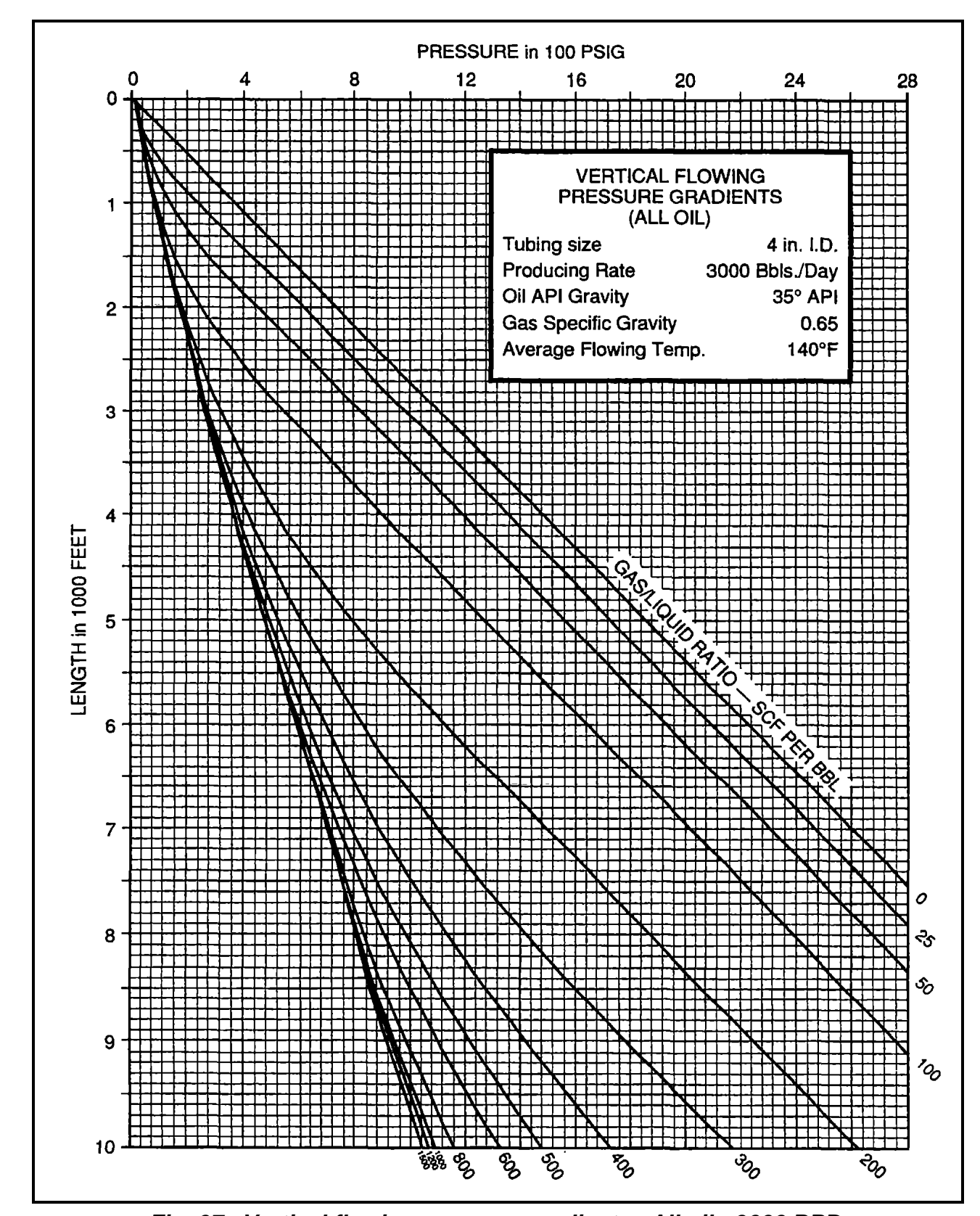


Fig. 97. Vertical flowing pressure gradients. All oil - 3000 BPD.

MATRIX ENGINEERING MANUAL

Well Performance

Section 200 July 1998

Page 161 of 168

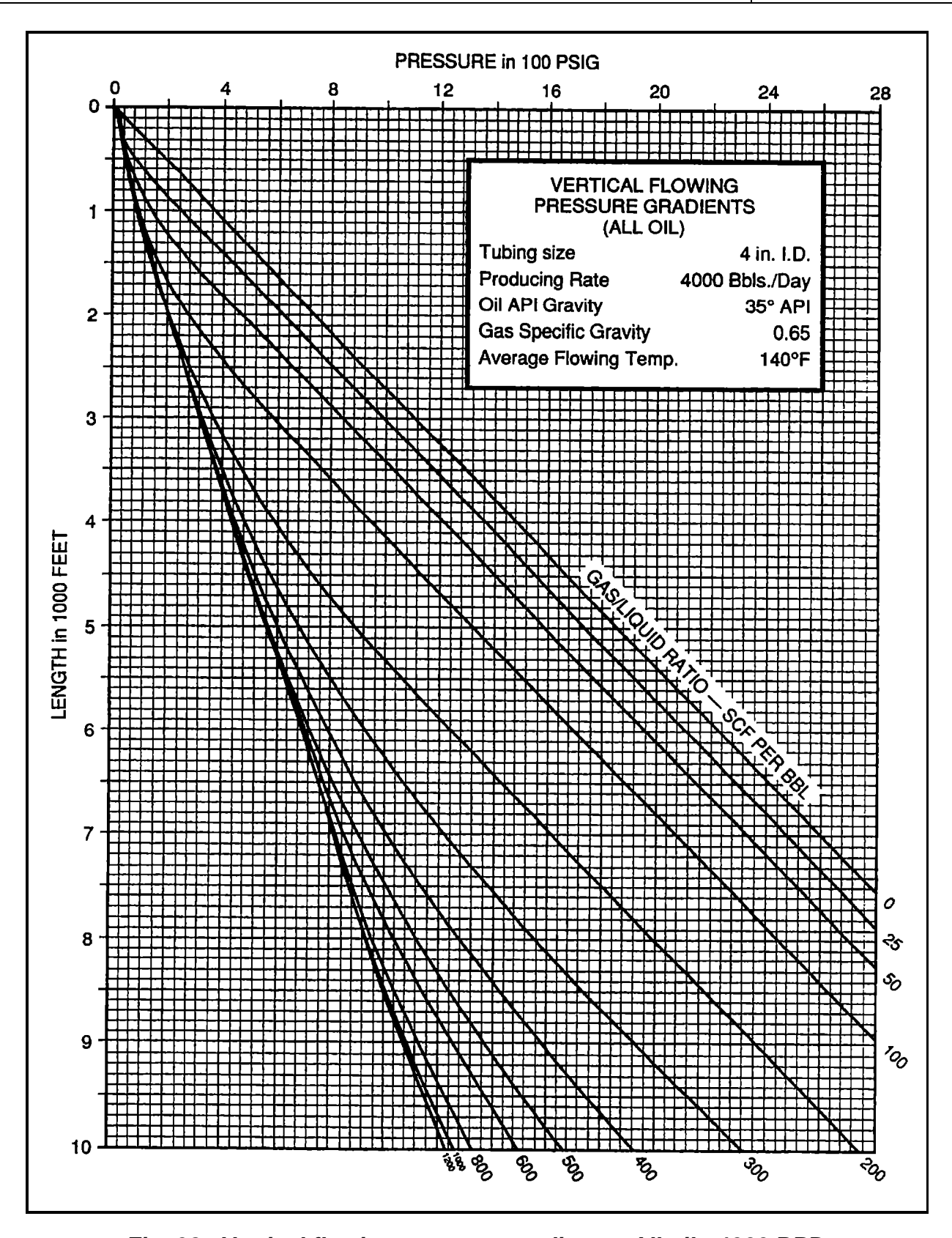
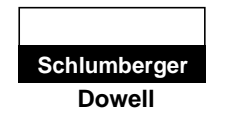


Fig. 98. Vertical flowing pressure gradients. All oil - 4000 BPD.

Page 162 of 168

MATRIX ENGINEERING MANUAL



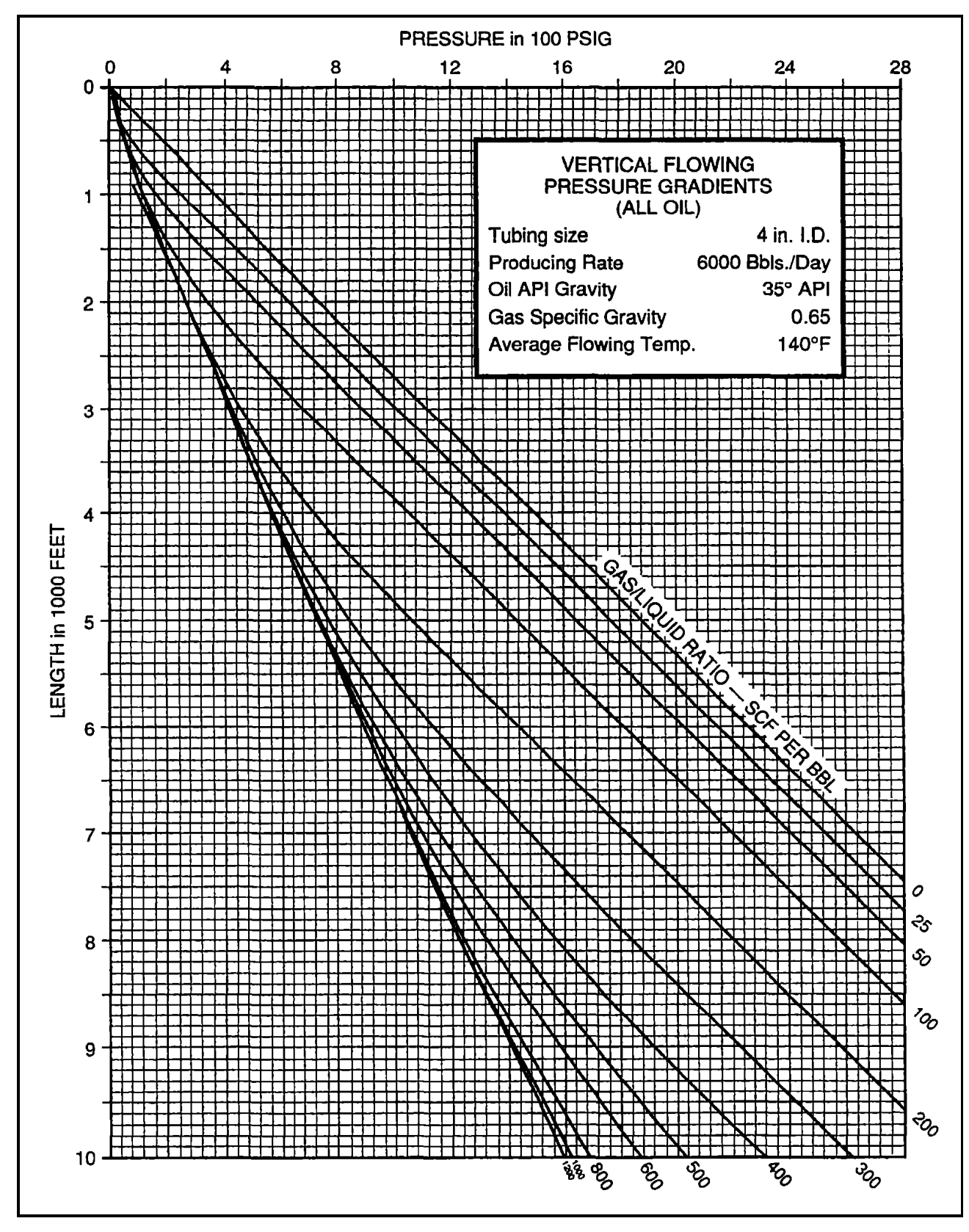


Fig. 99. Vertical flowing pressure gradients. All oil - 6000 BPD.

MATRIX ENGINEERING MANUAL

Well Performance

Section 200 July 1998

Page 163 of 168

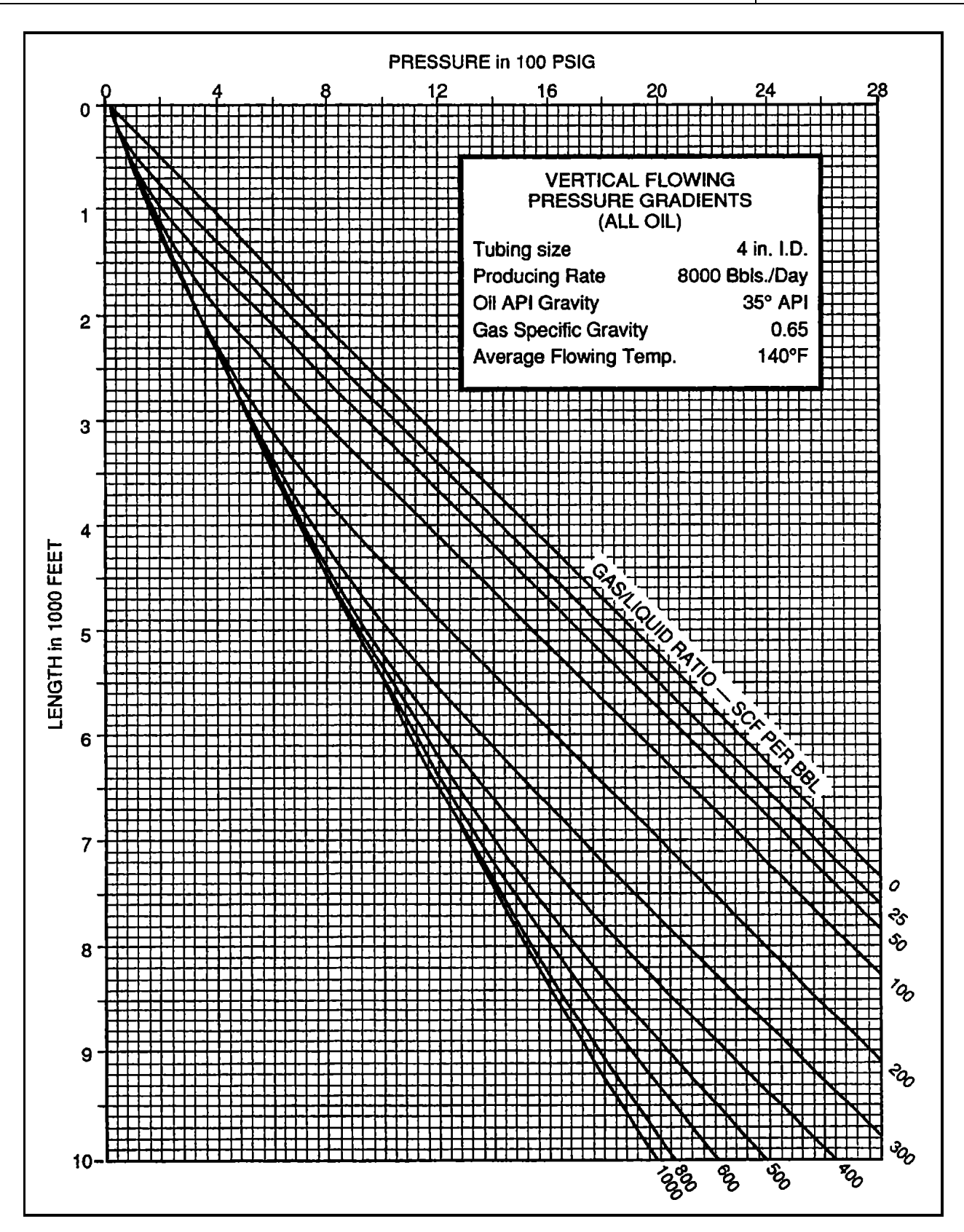


Fig. 100. Vertical flowing pressure gradients. All oil - 8000 BPD.

Section 200

July 1998

Page 164 of 168

MATRIX ENGINEERING MANUAL

Well Performance



9 Calculation Of Gas Velocity

$$\frac{qp}{zT} = \frac{q_s p_s}{T_s}$$

where,

 q_s =gas flow rate (MMscf/D)

q = gas flow rate (MMcf/D)

p = pressure (psia)

 $T = \text{Temperature } (\circ R)$

d = diameter (ft)

f = Moody friction factor.

Therefore,

$$q = \left(\frac{14.65}{520}\right) \left(\frac{q_s \ zT}{p}\right) = 0.028173 \ \frac{q_s \ zT}{p}$$

Velocity,
$$v(ft/sec) = \left(\frac{q}{A(ft^2)}\right) \left(\frac{10^6}{86,400}\right) = \left(\frac{q}{\frac{\pi d^2}{4}}\right) \left(\frac{10^6}{86,400}\right)$$
$$= \left(\frac{q}{d^2}\right) \left(\frac{4 \times 10^6}{\pi \ 86,400}\right) ft/sec$$
$$= 14.7365 \frac{q}{d^2} \ ft/sec$$

Therefore,

$$V(ft/sec) = 14.7365 \times 0.02873 \frac{q_s zT}{pd^2}$$
$$= 0.415273 \frac{q_s zT}{pd^2}$$

Calculation of Friction Loss Term

Friction term =
$$\frac{fdL \ v^2}{2 \ g_c \ d} = \left(\frac{(0.415173)^2}{2 \times 32.174}\right) \left(\frac{fq_s^2}{d^5}\right) \left(\frac{zT}{p}\right)^2 dL$$

= $0.002679 \left(\frac{f}{d^5}\right) \left(\frac{zT}{p}\right)^2 q_s^2 dL$

MATRIX ENGINEERING MANUAL

Well Performance

Section 200	
July 1998	

Page 165 of 168

Reynolds' Number

$$N_{Re}$$
 =1,488 $\frac{dv\rho}{\mu}$

d = diameter (ft)

v = velocity (ft/sec)

 ρ = density (lbm/ft³)

 μ = viscosity (cp)

 γ_{g} = specific gravity of gas (Air = 1)

that is,
$$\begin{split} N_{Re} &= \textit{1,488d} \left\{ \textit{0.415173} \ \frac{q_s \ zT}{pd^2 \mu} \right\} \left\{ \textit{2.7047} \ \frac{p \gamma_g}{zT} \right\} \\ &= \textit{1,671} \ \frac{q_s \ \gamma_g}{\mu d} \end{split}$$

Also reported in literature as 20,500 $\frac{q_s \gamma_g}{\mu_d}$ for diameter d of pipe in inches.

Cullender and Smith Modification

Divide Equation 17 by $(Tz/p)^2$ and obtain,

$$\left(\frac{53.24}{\gamma_g}\right)\left(\frac{p}{Tz}\right)dp + \left(\frac{p}{Tz}\right)^2\sin\theta \ dL + 0.002679\left(\frac{fq^2}{d^5}\right)dL = 0$$

that is,

$$dL\left\{ \left(\frac{p}{Tz}\right)^{2}\sin\theta + 0.002679\left(\frac{fq^{2}}{d^{5}}\right) \right\} = -\left(\frac{53.24}{\gamma_{g}}\right)\left(\frac{p}{Tz}\right)dp$$

that is,

$$\frac{\gamma_g L}{53.24} = \int_{pwh}^{pbh} \frac{\left(\frac{p}{Tz}\right) dp}{0.002679 \left(\frac{fq^2}{d^5}\right) + \left(\frac{p}{Tz}\right)^2 \sin\theta}$$

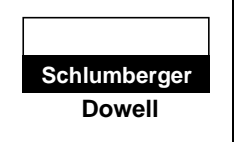
Section 200

July 1998

Page 166 of 168

MATRIX ENGINEERING MANUAL

Well Performance



10 Partial Penetration

Partial penetration occurs when the well has been drilled partially through the producing interval or when only part of the cased interval has open perforations (Fig. 101).

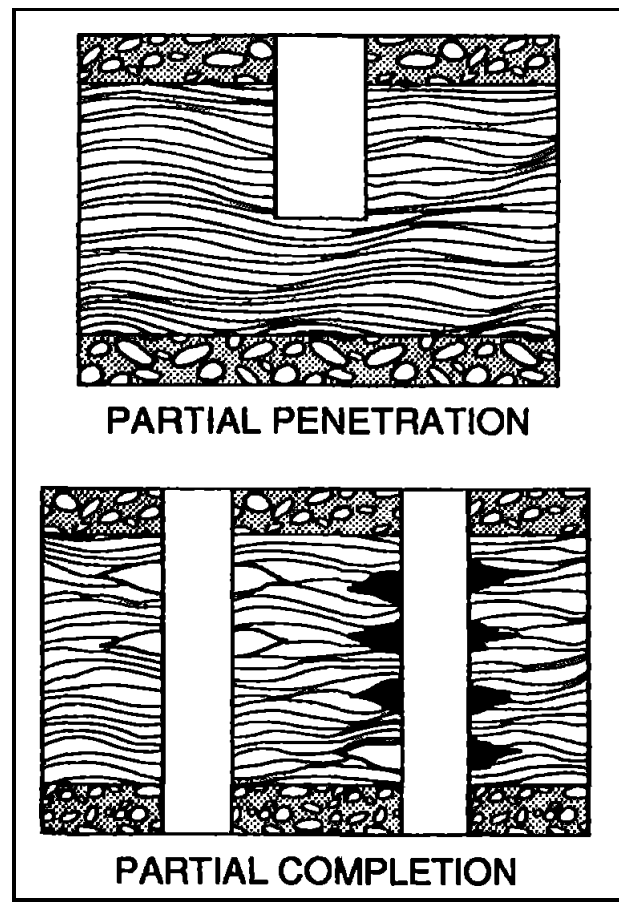


Fig. 101. Partial penetration.

MATRIX ENGINEERING MANUAL

Well Performance

Section 200
July 1998
Page 167 of 168

The pseudo-skin factor (s_R) due to partial penetration can be computed using the nomograph (Fig. 102).

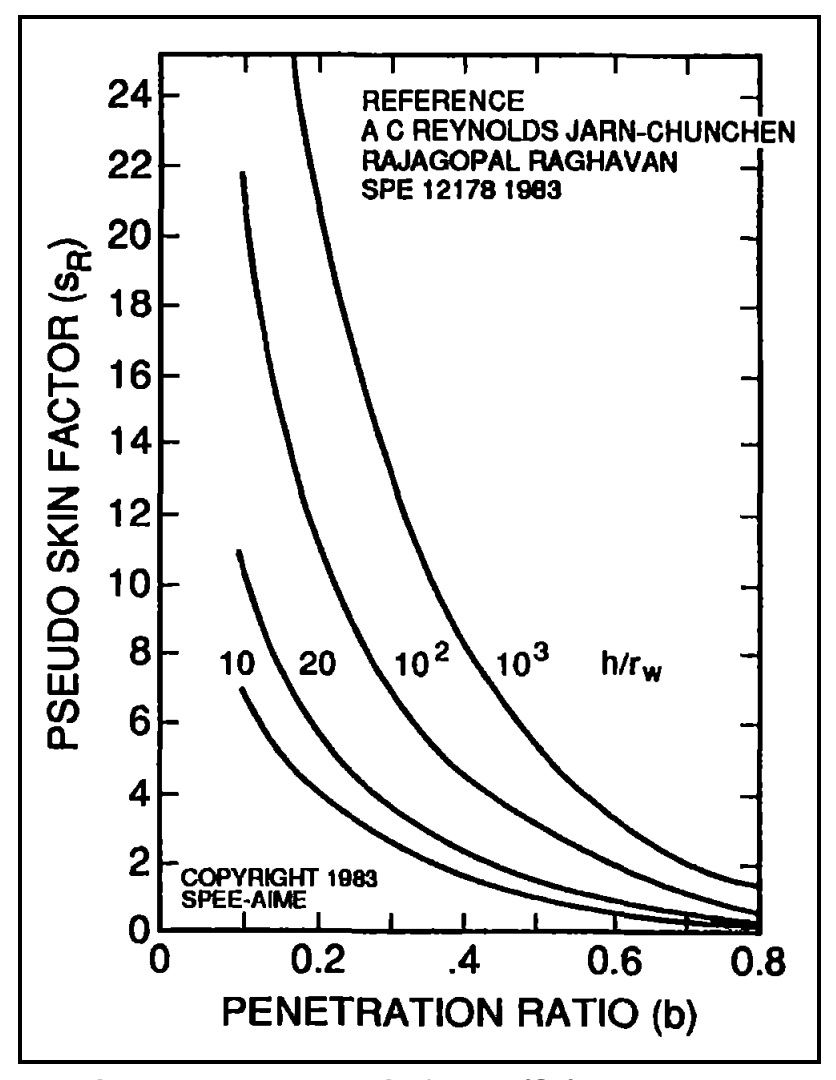
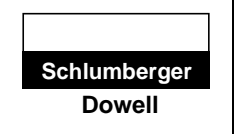


Fig. 102. Pseudo-skin factor (S_R) nomograph.

Page 168 of 168

MATRIX ENGINEERING MANUAL

Well Performance



11 Prats' Correlation

Prat (1961) defined a correlation between the dimensionless wellbore radius (r_{we}/x_f) and the dimensionless fracture conductivity. This is shown in Fig. 103.

Here,
$$C_{fD} = \frac{k_f w}{k x_f}$$

and $C_{fD} \ge 10$

$$\frac{r_{we}}{x_f} = 0.5$$

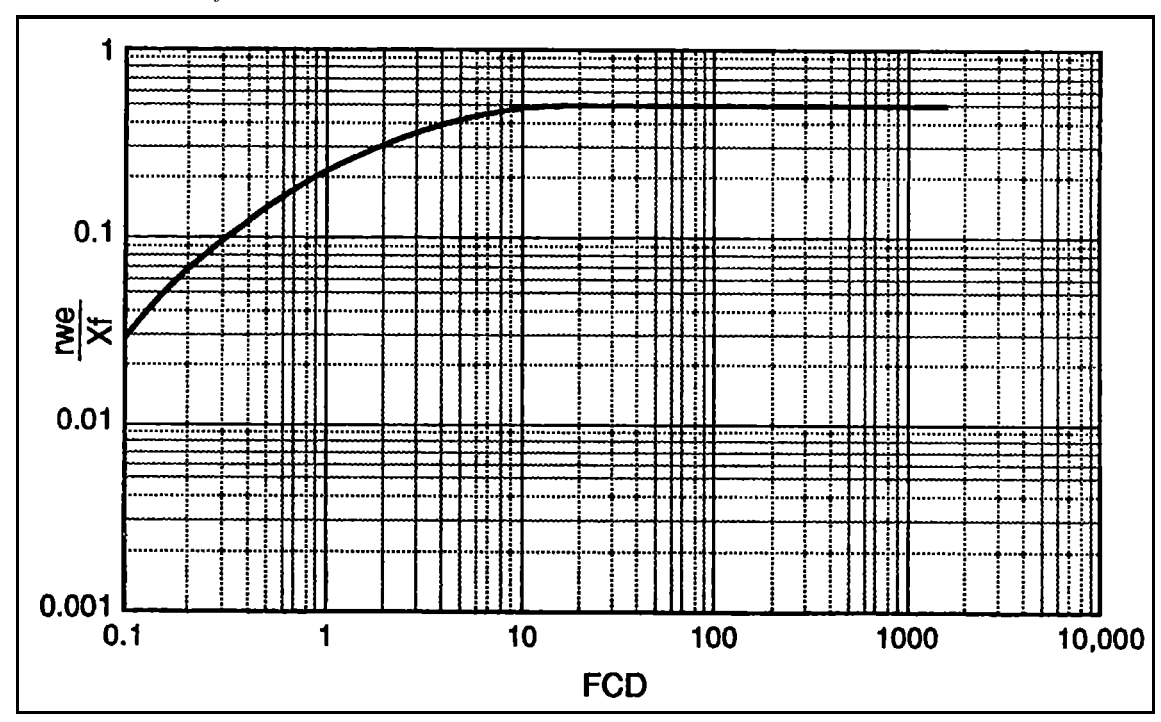


Fig. 103. Dimensionless wellbore radius versus C_{pp} .